

Bundesministerium für Forschung und Technologie

Forschungsbericht W 81-015

Luft- und Raumfahrt

– Weltraumforschung/Weltraumtechnologie –

**Die Instrumente des Plasmaexperiments
auf den HELIOS-Sonnensonden**

von

**H. Rosenbauer
R. Schwenn
H. Miggenrieder
B. Meyer
H. Grünwaldt
K.-H. Mühlhäuser
H. Pellkofer
J. H. Wolfe**

**Max-Planck-Institut für Aeronomie
Katlenburg-Lindau 3**

August 1981

This handbook contains a work report on a project funded by the Federal Ministry for research and technology.

The authors are responsible for the content of this report.

The Federal Ministry for research and technology assumes no liability for the correctness, the accuracy and completeness of the information, as well as respect private rights of third parties.

This is an English translation of the original German document.

The work was carried out by Imperial College London using computer translation with limited further copy editing, with the goal producing a technically useable English document for understanding the operations of the Helios E1 experiment. It is not intended to be a perfect translation; if you find errors however, please send corrections to Tim Horbury (t.horbury@imperial.ac.uk).

Our thanks to the original engineers, Eckart Marsch (provision of the document), U. Kiel (document scanning), Chadi Salem (provision of the PDF), Sophie Albosh (copy editing) and Ingo Muller-Wodarg and Christoph Larndorfer (German expertise).

Imperial College London does not claim the copyright of the original document or this translation.

Tim Horbury, Chris Chen, Lorenzo Matteini, David Stansby

Imperial College London, October 2016

Vertrieb:



Fach-
informations-
zentrum

Energie
Physik
Mathematik
GmbH
Karlsruhe

7514 Eggenstein-Leopoldshafen 2
Telefon 072 47 / 82 46 00 / 01
Telex 7 826 487 fize d

Als Manuskript gedruckt.

Preis: DM 39,10 + MwSt.

Printed in the Federal Republic of Germany

Druck: Engelhardt Offsetdruck GmbH, Himmelschlüsselstraße 39, 8000 München 50

ISSN 0170-1339

BMFT-FB-W 81-015

Federal Ministry for research and technology

research report W 81-015 air and space
-Space Exploration / Space Technology-

The instruments of the Plasma experiments on the HELIOS-Sun
probes

by

Dr. Helmut Rosenbauer

Dr. Rainer Schwenn

Dr. Hans Miggenrieder

Dr. Bernhard Meyer

Dipl.-Phys. Heiner Grünwaldt

Dipl.-Phys. Karl-Heinz Mühlhäuser

Dipl.-Ing. Heinz Pellkofer

Dr. John H. Wolfe

Max Planck Institute for Aeronomy

Katlenburg-Lindau 3

Managing Director

Prof. Dr. W.I. Axford

August 1981

1. Berichtsnr. BMFT-FB-W 81-015	2. Berichtsart Abschlußbericht	3. Weltraumforschung/ Weltraumtechnologie
4. Titel des Berichts Die Instrumente des Plasmaexperimentes auf den HELIOS-Sonnensonden		
5. Autor(en) (Name, Vorname(n)) Rosenbauer, Helmut; Schwenn, Rainer; Miggendorfer, Hans; Meyer, Bernhardt; Grünwaldt, Heiner; Mühlhäuser, Karl-Heinz; Pellkofer, Heinz; Wolfe, John H.		6. Abschlußdatum November 1980
8. Durchführende Institution (Name, Adresse) Max-Planck-Institut für Aeronomie Postfach 20 3411 Katlenburg-Lindau 3		7. Veröffentlichungsdatum August 1981
12. Fördernde Institution (Name, Adresse) Bundesministerium für Forschung und Technologie (BMFT) Postfach 200706 5300 Bonn 2		9. Ber.Nr./Auftragneher
		10. Förderungszeichen 01H30011/WRS01071
		11. Seitenzahl 226
		13. Literaturangaben 26
		14. Tabellen 43
		15. Abbildungen 68
16. Zusätzliche Angaben		
17. Vorgelegt bei (Titel, Ort, Datum)		
18. Kurzfassung (Gliederung s. Hinweise) Four independent instruments are grouped under the name "Plasma Experiment", whose shared responsibility is the investigation of the interplanetary plasma, the so-called solar wind. Primarily, the speed distribution functions of the different types of particles are measured. From this you can derive all hydrodynamic parameters of the solar wind plasma. Three instruments measure the positive component of the solar wind (protons and heavy ions with energy charge values between 0.155 and 15.32 keV). Two of them allow the determination of particle direction on both the angle of incidence. The fourth instrument analysed electrons in the energy range of 0.5 up to 1660 eV with one-dimensional direction resolution. The history of the mission shows that all instruments that are completely new to the part, fulfill the expectations.		
19. Schlagwörter Sonnensonden HELIOS 1/2, Plasmaexperiment, Protonen, Elektronen, Meßtechnik.		
20. ...	21. ...	22. Preis DM 39,10 + MwSt.

DOCUMENT CONTROL SHEET

1. Report No. BMFT-FB- W 81-015	2. Type of Report Final Report	3. Space Research/ Space Technology
4. Report Title The instruments of the plasma experiment aboard the HELIOS solar probes		
5. Author(s) (Family Name, First Name(s)) Rosenbauer, Helmut; Schwenn, Rainer; Miggenrieder, Hans; Meyer, Bernhard; Grünwaldt, Heiner; Mühlhäuser, Karl-Heinz; Pellkofer, Heinz; Wolfe, John H.		6. Report Date November 1980
		7. Publication Date August 1981
8. Performing Organization (Name, Address) Max-Planck-Institut für Aeronomie Postfach 20 3411 Katlenburg-Lindau 3		9. Originator's Report No.
		10. BMFT-Reference No. 01H3001I/WRS0107I
		11. No. of Pages 226
		12. No. of References 26
12. Sponsoring Agency (Name, Address) Bundesministerium für Forschung und Technologie (BMFT) Postfach 200706 5300 Bonn 2		14. No. of Tables 43
		15. No. of Figures 68
16. Supplementary Notes		
17. Presented at (Title, Place, Date)		
18. Abstract The "Plasma Experiment" aboard of the solar probe HELIOS consists of four independent instruments which are designed to investigate the interplanetary plasma, the so-called solar wind. Primarily the velocity distribution functions of the different kinds of particles are measured. All important hydrodynamic parameters of the solar wind plasma can then be derived. Three instruments analyze the positive component of the solar wind (protons and heavier ions with energy-per-charge values from 0.155 to 15.32 kV). Two of them permit an angular resolution in both directions of incidence. One instrument measures electrons in the energy range from 0.5 to 1660 eV with a one-dimensional angular resolution. Since the launch all the instruments, which are partially novel developments, have performed very well.		
19. Keywords HELIOS solar probes, plasma experiment, protons, electrons, measurement techniques.		
20.	21.	22. Price DM 39,10

Table of Contents

Summary.....	9
Preface.....	10
1. Overview.....	11
The HELIOS mission.....	11
Task of the plasma experiment.....	18
Historical overview.....	20
2. Construction of the experiment.....	25
The measuring methods used.....	25
The instruments for positive ions.....	29
The electron instrument.....	31
The electronics box.....	33
3. Technical description of the instruments.....	35
Instrument I1a (in box E1A)	35
Analyzer part of I1a.....	36
Stimulation in Inflight test.....	37
I1a energy channels.....	38
I1a direction channels.....	41
Electronic part of I1a.....	41
Instrument I1b (in box E1B)	45
Analyzer part of I1b.....	45
I1b measuring channels.....	46
Electronic part of I1b.....	46
Instrument I2 (in box E1B)	48
Analyzer part I2.....	49
Stimulation in Inflight test.....	50
I2 measuring channels.....	50
I2 direction channels.....	52
Electronics part I2.....	52

Instrument 13 (in box 11C).....	56
Analyzer part I3.....	56
Measurement Channels I3	59
Stimulation in the Inflight test.....	63
Electronic part of I3	63
Electronics box (in box E1D)	68
4. Organization of data generation and data transmission	77
Normal data mode (NDM)	77
High data mode (HDM)	80
The E1 data into the stream of telemetry data from HELIOS... ..	83
The probe telemetry system	83
Block structure of the E1 telemetry data	85
Forward words	101
Commands and checking the	109
Telemetry commands	109
Digital housekeeping channels (DHK)	112
Housekeeping analog channels (AHK)	112
Test cycle (Inflight test)	114
5. Description of key components and technologies	124
Channeltron amplifier	124
Electrometer	125
Analyzer high-voltage generation	130
Channeltronhochspannungserzeugung	133
Current controlled oscillator (CCO) to the	
Channeltron amplification measurement	133
High frequency generator	136
Counter	141
Reduce work	141
Memory	147
Memory control	150

	Maximum viewfinder and data control	152
	Control flow	154
	Construction technology of	155
	Electromagnetic compatibility.....	163
	Channeltrons.....	164
6.	Calibration of instruments	172
	The calibration system	172
	Trace of an instrument calibration	174
	Calibration data	178
	Calibration of I2	181
7.	Testing	185
	Test unit	185
	Qualification and acceptance tests	189
	Integration of E1 in the probe and system tests	194
	First turn on the instruments of	196
	Special tests later.....	199
8.	Flight experience with the E1 instruments	200
	Final word	218
	Literature	221
	List of abbreviations	225

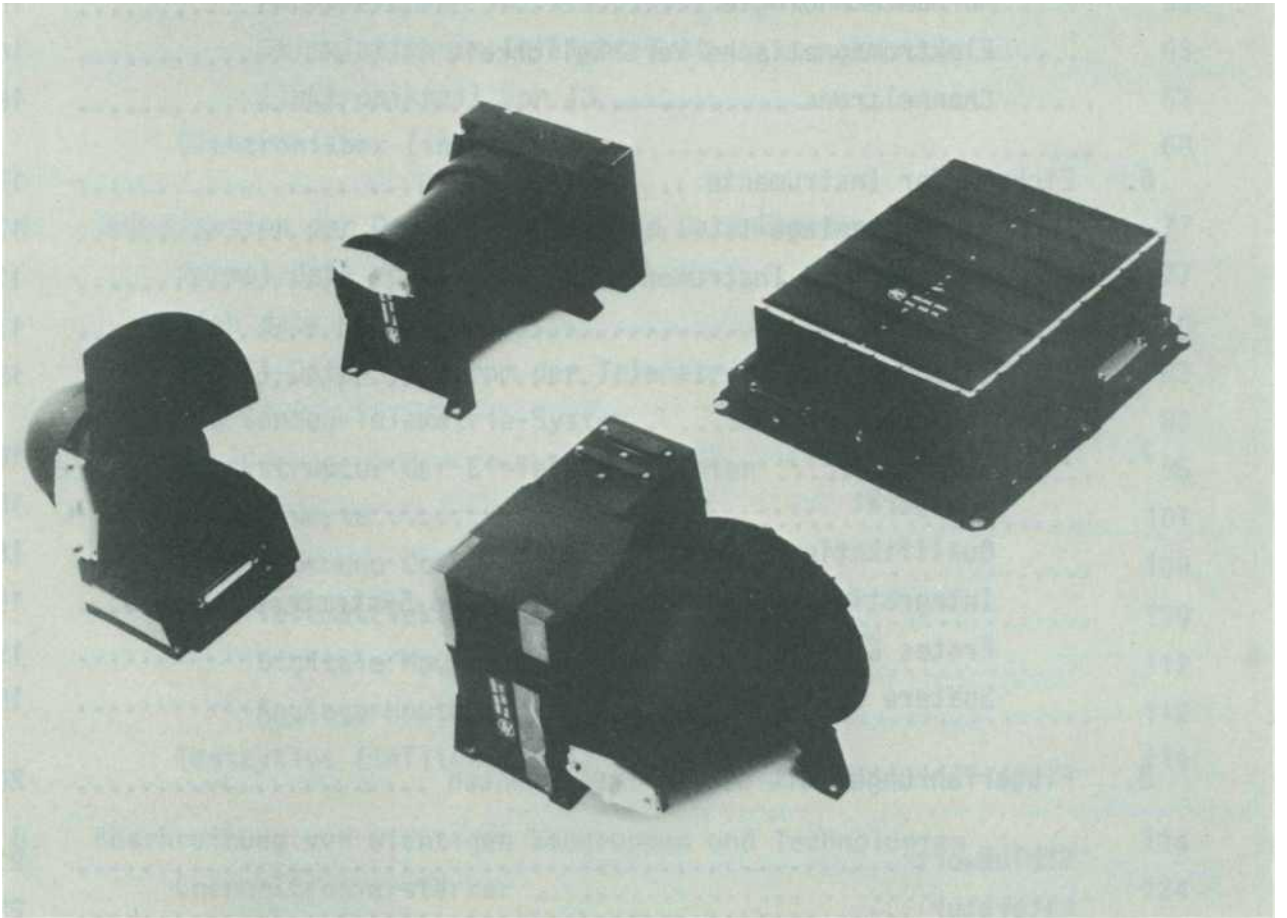


Figure 1: The tools of the Plasma experiments for the HELIOS-Sun probes.

The box E1A (center top) contains the two electrostatic instruments I1a and I1b, for positive ions, box E1B (left) the electron instrument I2, box E1C (center bottom) the dynamic mass spectrometer I3 for positive ions. The box E1D right contains the common power supply and control, as well as the digital electronics for preprocessing of measured data.

The devices shown here are on board Helios 2.

SUMMARY

Four independent instruments are grouped under the name "Plasma Experiment", whose shared responsibility is the investigation of the interplanetary plasma, the so-called solar wind. Primarily, the speed distribution of the different types of particles are measured. From this you can derive all hydrodynamic parameters of the solar wind plasma. Three instruments measure the positive component of the solar wind (protons and heavy ions with energy charge values between 0.155 and 15.32 keV). Two of them allow the determination of particle direction on both the angle of incidence. The fourth instrument analysed electrons in the energy range of 0.5 up to 1660 eV with one-dimensional direction resolution.

The two HELIOS first have each a set of these instruments on board. All - up on the electron instrument on HELIOS 2, where since August 1977 switching between the two fields of energy does not longer work properly - working since the beginning of the mission on the 10.12.74 and 15.1.76 completely trouble-free, far beyond the intended mission duration 18 months also. The concept laid down long before the launch has distinguished itself for the experiment - type of instruments, sensitivity, dynamics and measuring ranges, measurement programs, redundancies etc - during mission operation in almost all details proven.

PREFACE

This description of the instruments of the HELIOS plasma experiment based on the experiment descriptions that had been created as a basis for the industrial production of instruments. Largely the contractually agreed-upon final report delivered by the contract company Messerschmidt-Bölkow-Blohm was incorporated with, in particular its detailed technical part.

This report reflects some of our own experiences in addition throughout the project. These include the tests of Channeltrons carried out at the Institute and also continued after the start as "Endurance test". In addition, we report on preparations and implementation of instrument calibrations, which took place at the plant built at MPE. The topic data evaluation is not long since completed and remains here excluded. However, some general experiences due to the operation of the mission will be discussed, especially in comparison to the set several years earlier instrument concepts.

Such assessments from the perspective of today are all interspersed in the report in the form of comments - marked by a different font -.

The drafting of this report, we sought an accurate and complete collection of all details that could be ever important, passed all those who work with the data of these instruments, to the hand. This seems particularly important to us because the HELIOS mission has brought us an unexpected abundance of unique data and brought even further, many scientists for years to come are dealing with those, including also more and more those who have never seen the instruments.

The report presented the Federal Ministry for research and technology as a technical final report according to BEwF-Z/A-1969 for the funds as part of the promotion donations from chapter 3006, title 893.20 the BMFT for the development and production of the plasma experiment for the solar probe HELIOS with the mark WRS 10/7 had been granted.

1.Overview

The HELIOS mission

The German-American space program "Solar probe HELIOS" is supposed to contribute to the exploration of interplanetary space between 0,29 and 1 AU (1 AU = 150 Mill. km). Two nearly identical built spacecraft were placed highly eccentric elliptical orbits around the Sun, up to 0,3095 or 0,290 AU introduce on the Sun. The launch of HELIOS 1 was on the 10.12.1974, HELIOS 2 followed on the 15.1.1976. A full orbit around the Sun takes 186 days for HELIOS 2, 191 days for HELIOS 1. Figure 2 shows the orbit ellipses from HELIOS 1, HELIOS 2 and the Earth, with marks for the day number of the year 1976.

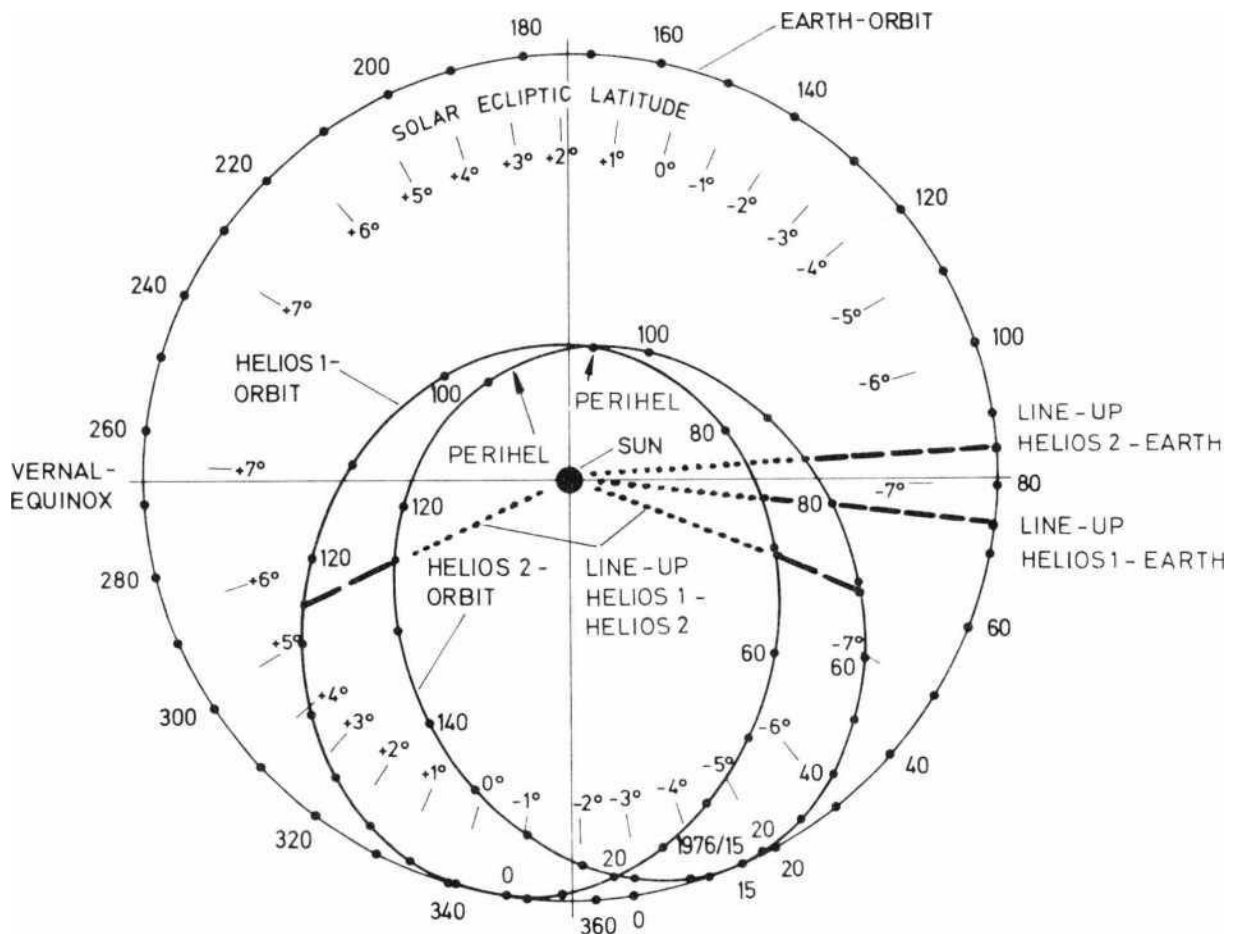


Figure 2: The orbit ellipses from HELIOS 1, HELIOS 2 and the Earth. The day numbers refer to the year 1976.

Due by the start dates - we had no better wish us the location of the ellipses -.The long axis of the HELIOS 1-orbit is located almost on the node line of the solar Equator, i.e.exactly perpendicular to the Sun axis, around $7,25^\circ$ to the ecliptic is inclined. Therefore, HELIOS 1 in terms of perihelion - flies over where his path speed is largest - in less than 20 days is a range of 12° in solar width. For this the Earth needs four months! So, we witnessed for the first time directly the width dependency of structures in the solar wind. The displacement of the HELIOS 2 starts from December 75 on January 76 we have to owe the torsion of the HELIOS 2 ellipse towards the HELIOS 1 ellipse.Only resulted in 1976/77 a total of 8 "line up" constellations (see fig. 2), where both probes of the Sun seen in a row stood.In some cases, there was also the Earth just nearby.So could here from the Sun away flowing plasma successively examined in several places in the area and radial changes directly detected.Due to the different orbital periods there was line up more no after 1977 unfortunately.

The distance between of the probes remain small enough that spatial and temporal structures in interplanetary space are often good to distinguish. In this respect, HELIOS is considered the first real interplanetary double mission.

The basic design of HELIOS is shown in the diagram in Fig. 3.

Figure 4 shows a view of HELIOS 2 shortly before the start.Due to the characteristic spool shape, temperatures will be anywhere bearable in spite of solar radiation fluctuating by a factor of 11.The figure axis, the HELIOS rotating at 60 revolutions per minute, is oriented perpendicular to the orbital plane and the ecliptic.But has the top at HELIOS 1 North, at HELIOS 2 South.

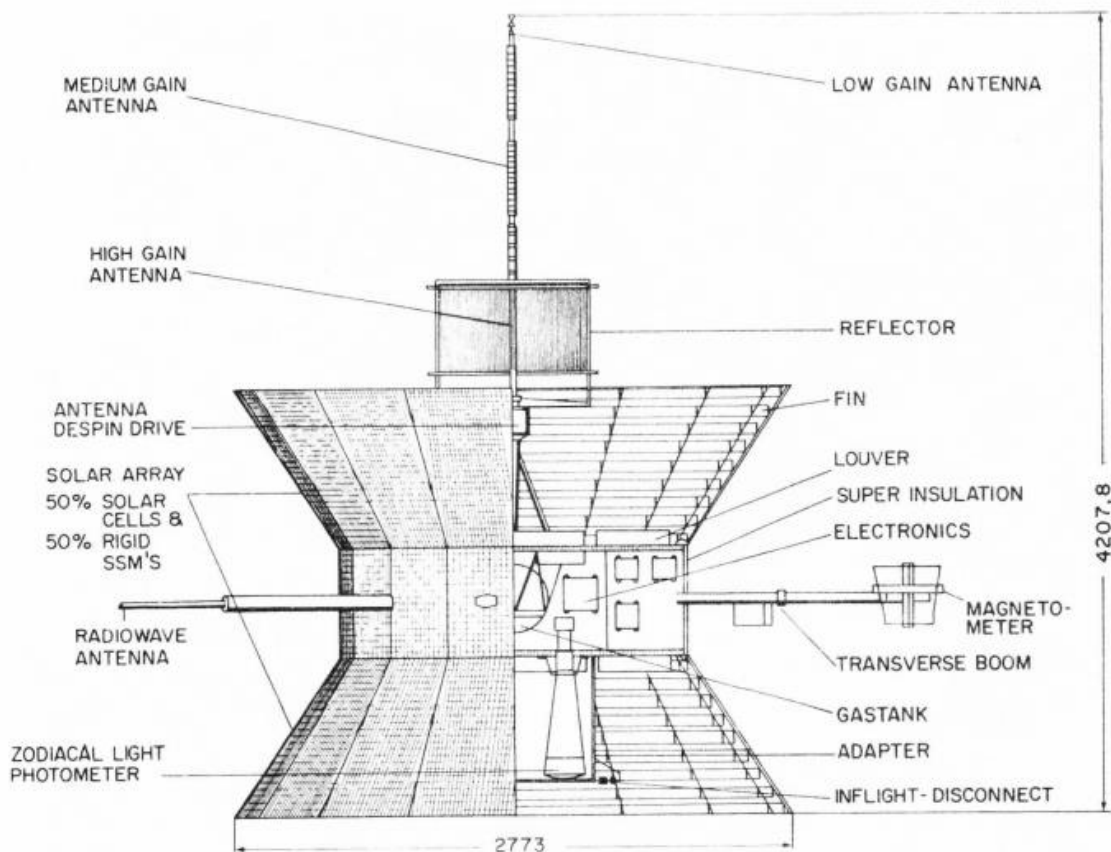


Figure 3: A diagram showing the construction of HELIOS

The main technical features of the two probes are summarized in table 1. Both probes are equipped with a nearly identical set of instruments for the implementation of in-situ measurements. These instruments are a total of 10 groups of instruments - called linguistically untidy "experiments" - which are maintained by different groups of researchers from the Federal Republic and the United States. Table 2 gives an overview of the experiments, their ranges, as well as the approximate order in the spacecraft. The experiment 1, the "plasma experiment", carried out under direction of Dr. Helmut Rosenbauer at the Max Planck Institute for Extraterrestrial physics in Garching, now at the Max Planck Institute for Aeronomy in Lindau, is the subject-matter of the present final report.

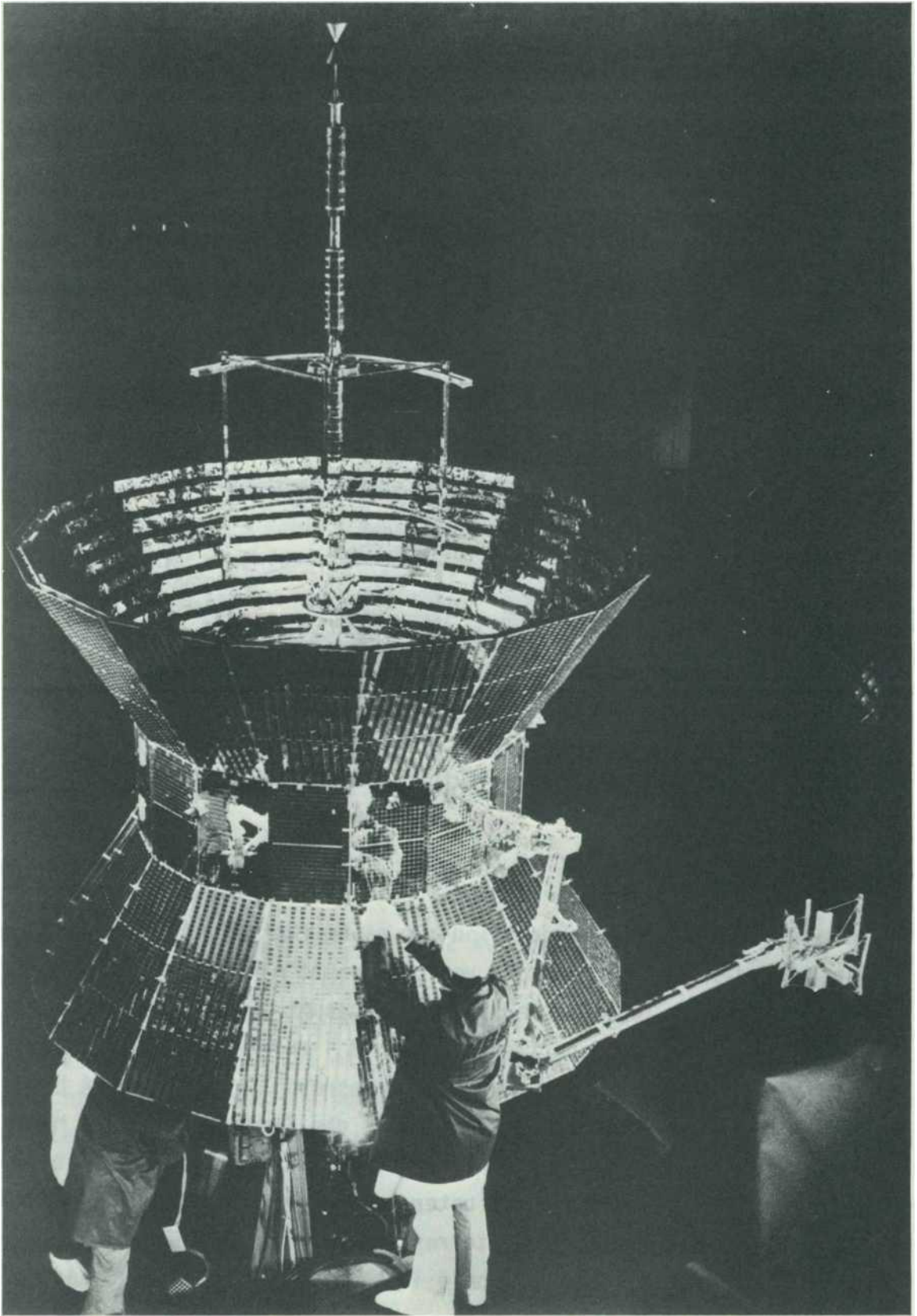


Figure 4: The solar probe HELIOS 2, just before the start

Mass	370.0 kg
Mass of experiments	74.2 kg
Largest diameter	2.773 m
Height including antenna	4.208 m
Magnetometer reeling expanded	9.20 m
Power supply	Solar cells
Maximum power of Aphelion/perihelion	229W / 238 W
Power consumption of the experiments	57.2 W
Telecommunication	S-band
Frequency of the transmitter	2297MHz (2295 MHz)
Frequency of the receiver	2115MHz (2113 MHz)
Bitrates, switchable	8 up to 4096 BPS
On-board memory	500 kBit
Number of telemetry formats	6
Max.Power of the transmitter	20W
Temperature heat shield	-60°C to +150°C
Solar cells	-60°C to +180°C
Antenna	-50°C to +220°C
Central part	-25°C to +35°C
Launcher Titan IIIE/Centaur D-1T/TE-M-364-4	
Perihelion distance	0.30958 AU (0.29038 AU)
Inclination	< 0.02 °
Orbital period	191 Days (186 days)
Spin rate	60 ± 1 RPM
Spin axis, perpendicular to the orbital plane	Tolerance ± 1 °
The first plans for project solar probe	1966
Mission definition	1968/69
Beginning the probe development at MBB	April 1970
Start date	10.12.1974 at 7.11 GMT (15.1.1976 at 5.34 GMT)
Total cost of the HELIOS project	695 Million DM
of which German share	465 Million DM

Table 1: Data of the HELIOS solar probe.
The numbers in brackets are valid
for HELIOS 2.

No.	Designation:	Experimenters: Head	Organization:	Scientific task: measurement.....
1	Plasma Experiment	H. Rosenbauer R. Schwenn J H. Wolfe	MPI for physics and Astrophysics, Institute for Extraterrestrial Physics, Garching / Munich NASA Ames Research Center, Moffett field, CAL.	of low-energy charged particles (solar wind), protons, α -particles, electrons
2	Förster-probes magnetometer I (Brunswick)	G. Musmann A. Maier F. M. Neubauer	Technical University of Braunschweig, Institute of geophysics and meteorology	the interplanetary quasi stationary magnetic field and of shock fronts
3	Förster-probes magnetometer II (Rom. GSFC)	N.F. Ness L.F. Burlaga F. Mariani	NASA-GSFC, Greenbelt, Md. Università degli Studi, istituto di Fisica "(G).Marconi".Rome	the interplanetary magnetic field and magnetic shock fronts
4	Induction coil - magnetometer	G. Dehmel F.M. Neubauer	Technical University of Braunschweig, Institute for telecommunications	by rapid changes of the magnetic field and magnetic shock waves
5	Plasma and Radio wave Experiment	D.A. Gurnett P.J. Kellogg R R. Weber	University of Iowa, DEP. of Physics & Astronomy, Iowa City, Iowa University of Minnesota, school of Physics & Astronomy, Minneapolis, Minnesota, NASA-GSFC, Greenbelt, Md.	by electrostatic and electromagnetic wave phenomena and shock waves
6	Experiment of cosmic rays I (Kiel)	H. Kunow G Green R. Müller G. Wibberenz	University of Kiel, Institute of pure and applied nuclear physics	Protons, α -particles and heavy nuclei of solar and Galactic origin.
7	Experiment of cosmic radiation II (GSFC)	J.H. Trainor K.G. McCracken E.C. Roelof B.J. Teegarden	NASA-GSFC, Greenbelt, Md. University of New Hampshire SCIRO, Melbourne/Australia	of medium - and high-energy particles, x-rays
8	Electron Detector	E. Keppler G. Umlauf B. Wilken Dr. Williams	Max Planck Institute for Aeronomy, Institute for Physics of the stratosphere, Lindau, Harz ESSA, Boulder, Colorado	of medium energy electrons. Protons and positrons
9	Zodiacal light photometer	C. Leinert H. Link E. Pitz	Max Planck Institute for astronomy, Heidelberg	the zodiacal light
10	Micrometeorites Analyser	E. Grün P. Gammel J. Kissel	Max Planck Institute for nuclear physics, Heidelberg	of dust particles

Table 2a: The "active" experiments on HELIOS

No.	Designation:	Experimenters: Head	Organization	Scientific task measurement
11	Celestial mechanics Experiment	W.Kundt O.Böhringer H. Ovenhausen J. Peyn W. G. Melbourne I. D. Anderson	University Hamburg, Institute for theoretical physics I JPL, Pasadena, Cal.	Test of general relativity (Einstein, Brans-Dicke) with the help of a precise orbit determination of the solar probe (exploitation of the "signal delay effect")
12	Faraday- Rotation- Experiment	H.Volland M. Bird G. S. Levy	University of Bonn, Radio-astronomical Institute JPL.Pasadena, CAL	By measuring the following errors: 1. Rotation of the polarization plane (Faraday effect), 2. Runtime change (run-time effect) of the signals by the plasma. 3. Line distribution of the telemetry carrier as a result of high plasma density and temperature, Determination of the Electron density and completion of scientific discovery, HELIOS-programme in terms of the dynamics of Solar Interplanetary events
12Z	Occultations Experiment	P.Edenhofer E.Lüneburg Fr.H. Stark	DFVLR Oberpfaffenhofen. Institute of aviation radio and microwaves	Determination of the Electron density distribution of the solar corona in the heliocentric distance of approx.5-25 solar radii based on analysis of distance and Doppler data during the three planned occultations through appropriate numerical inversion procedures
13	Additional study on the plasma experiment (E 1)	G. H. Voigt B. Könemann H. Schröder	Technical University of Braunschweig. Chair of theoretical physics B	By calculating the disturbance caused by the HELIOS spacecraft (as a result of the Special geometry and surface coating) and implementation of correction invoices allow the physical interpretation of particle measurements (E 1)

Table 2b: the 'passive' experiments on HELIOS

Task of the plasma experiment

Since L. Biermann in 1957 concluded from Comet observations, that constantly ionized gas in the interplanetary space must escape from the Sun, many theories have been developed about this phenomenon, and since the first interplanetary spacecraft flights it is also directly experimentally verified. It was called a "Solar wind", and the interest in his research has continued since then. Several reasons: firstly an astrophysical plasma, which probably is emitted in a similar way by a majority of all the stars, is directly accessible; us here on the other hand, the solar wind provides us information about operations on the Sun. He decisively influenced also the physical events in the Earth's magnetosphere and in the vicinity of other planets. In addition can be obtained by studying plasma physical findings, which are difficult or impossible to obtain in the laboratory.

Close to the Earth's orbit, the parameters of the solar wind are now fairly well known. It is known that he composed on average to about 95% of protons, 4% from α -particles and small amounts of heavier ions and a lot of electrons just compensate the ion charges. The particle density is located close to the Earth's orbit in the order of 10 cm^{-3} . This plasma flow with a mean speed of approx. 400 km s^{-1} about radially from the Sun out to the outside. The direction of movement of the individual protons scatters towards this direction slightly due to the "temperature" of the Proton component of about 10^5 K .

However, the average thermal energy predominates when the electrons (approx. 15 eV) opposite the translational energy ($\approx 1 \text{ eV}$), so that their Velocity distribution by a spacecraft out appears nearly isotropic. The numbers specified here are subject to fluctuations, which are taken of interest for themselves, because they either on structures on the Sun or on operations, E.g. point out wave propagation in plasma between the Sun and Earth.

Yet major questions for understanding of the underlying physical processes are open despite the apparently already very good study of the solar wind. This is because to a large extent, that virtually all previous measurements in the solar system beyond the orbit of Venus were made, that so about the development of the phenomenon between the place of origin and approx. 0.7 AU nothing is known.

The various theories differ but above all in the course of important plasma parameters in this field. Here, so just measurements of HELIOS from can provide insight into the accuracy of the various models. Due to the large approaching of HELIOS the Sun is also succeeding to correlate the observations in the solar wind much closer than was previously possible, with appearances on the Sun's surface and clarify important details not previously collected in the theories about the expansion of the solar wind. Finally, the plasma parameters measured at the location of the probe are also an important basic information for other HELIOS experiments, because the electric and magnetic fields (the 4 experiments deal with its measurement) are directly influenced by the solar wind, and the higher energy particles (3 experiments) are also influenced by him.

The plasma experiment is designed but not so that it gets its value only through the special orbit by HELIOS; instead attempted to allow for measurements, which have not yet been made so far even close to Earth's orbit through the development of new tools. Here, especially the analysis of plasma electrons are up to lowest energies and the complete separation of the distribution functions of protons and of α -particle to name a few.

The instruments have met each of these expectations so far fully and in detail. In addition there have been some other very important aspects mainly because of the unexpected length of the mission: on one of the years of "formation flying" the two probes provides new insights into the large-scale structure of the interplanetary medium. On the other hand a now closed record by end of 1974 - a year before the end of the solar cycle 20 - currently late in 1980, before where the activity maximum of cycle 21 is already exceeded. This record is unique therefore because by exceedingly skillful mission operation with the help of the onboard memory almost all gaps in the data received at the ground stations, also with a low data rate, could be bridged, which was not originally intended. Therefore, there are good prospects for new insights into changes of the solar wind with the solar cycle.

Historic overview

The HELIOS project started end of 1966. At the time, the Governments of the United States and the Federal Republic of Germany a bilateral project "Solar probe" decided as it was called at that time. In July the mission definition study was then begun. The result was definition until April 1969 the mission group report. Finally in July 1969 could with the signing of the memorandum of understanding the cooperative project HELIOS between the American space agency NASA and the Federal Ministry of scientific research are contractually agreed.

In parallel, the plans for the implementation of in-situ plasma measurements ripened up already at the Max Planck Institute for Extraterrestrial Physics (MPE) in Garching. Prof. Reimar Lüst and Prof. Klaus Pinkau, which are certainly among the fathers of the HELIOS project, were directors at the Institute. They commissioned Helmut Rosenbauer early in 1967 with the development of appropriate instruments. As a kind of exercise, he first designed a "dream"-instrument with all only conceivable finesse, he suggested then - again as an exercise - for the ESRO satellite HEOS-A2. Contrary to expectations, this proposal early 1968 was adopted and had to be built. Heiner Grünwaldt and Heinz Pellkofer, took over the care at MPE the instrument was developed to flight readiness and finally built by the company AEG-Telefunken. The novel concept of this instrument, as well as the characteristic size of the sensor part are identical with those of the later instruments I1a and I1b for HELIOS: 3D-resolution with the help of nine channeltrons behind a quarter sphere analyser, almost concentrically arranged hemisphere Analyzer with atomizing electrometer, vacuum concept, the location of the measurement channels, the principle of the selection according to the position of maximum of distribution etc. At that time began the first laboratory tests of channeltrons, who soon encouraged us in the hitherto unheard-of view that life of Channeltrons, through appropriate treatment, especially by consistently avoiding contamination with organic molecules (pump oil, plastic, epoxy, colors etc.), practically can be extended indefinitely.

When the HEOS instrument the Interior of the UHV suitable sensor principle was therefore introduced and held: exclusive use of materials such as glass, metal, ceramic, evacuable housing, operating only in the absolutely oil-free vacuum. As a result of which no degradation of channeltrons could be determined in fact during the HEOS Mission (from 31.1.72 to August 1974).

From the outset, separation and analysis of the heavier ions of the protons had regarded as desirable. Until early 1970 a principle as feasible turned out for various preparatory work and studies, which was later realized in the construction of the electrodynamic mass Analyzer (I3). The measurement of electrons was because of huge surplus of photoelectron in the surroundings of each spacecraft always considered nearly impossible and also appear as less interesting. Only at the direct instigation of Prof. Ludwig Biermann, Helmut Rosenbauer began with serious considerations, which finally culminated in the novel instrument I2.

After several attempts at various vacuum systems, in which first the flow characteristics were examined by spherical analyzers, the construction of the calibration facility began in 1970. She was in a container outside the actual laboratory building as clean room decorated specifically (a wooden shack about 100 m from the main building removed) built. This separation was our blessing in disguise: as on the 22.12.1970 the laboratory building reasons never clarified completely burned down, nothing could be saved literally, out of the container. This fire threw back far us, especially when the HEOS project, a year before the planned start. Luckily, here no flight unit was directly affected, more or less randomly, so that the calibration work could begin in the spring of 1971. There were at that time only on the paper, which however completely burned the HELIOS instruments. By a large part of the documents, there were copies of various project partners to happiness. Yet our already large backlog in the production of project papers was almost hopeless and long time could not be raised.

In May 1970 the company Messerschmitt-Bölkow-Blohm (MBB) in Ottobrunn was selected from the only two received offers from industry companies.

At that time, many interfaces to the probe were still completely unclear or have been amended several times.

In addition, we had also our ideas about the possibilities of the instruments constantly adapt to what is feasible and vice versa. This extremely constructive design phase until mid 1971 developed a fruitful, very open community in the literal sense that formed a sound basis for further work, from which emerged then finally sophisticated instruments, working excellently and correctly from the start and even after years. In this initial phase, on MBB site except the project manager Jochen Brauer, in particular the gentlemen Stiller and Nogai and Friedrich (electronics), as well as H. Wagner (mechanics) involved, at the MPE H. Rosenbauer, the project manager H. Pellkofer and (since 1971) Rainer Schwenn, who took over the role after the resignation of H. Pellkofer 1972. He conducted also the long-term and selection tests of the channeltrons, supported by the assistants Erna Kusser and later Edith Wantosch. Bernhard Meyer calculated form and flow characteristics of the mass Analyzer (I3). Then in 1972 still Hans Miggenrieder came as the last of the co investigators, who prepared the first of all the special calibration system for the low-energy electrons. The entire UHV vacuum systems were in supervised by Hans Ludwig, who later played with the sensor integration in support of MBB. Konrad Müller oversaw all experiment - and system tests. Together with H. Ludwig, H. Miggenrieder and R. Schwenn, he was instrumental in the launch preparations.

The probe system on the experiment, the constant deadline pressure, long time unclear requirements but also the productive functioning of close cooperation between MBB and MPE were all in all an unwanted side effect: the determination of the volume of work for the contract between MPE and MBB was extremely difficult, simply because the scope is constantly changed. The main treaty was signed only on the 13.12.71. In six additional contracts later 32 were "Change proposals", i.e. collects technical, cost-effective amendments.

First, the electrical integration model (EM) was completed. In January, 72 started the first measurements of the calibration system. Some problems were uncovered here and part before delivery of the EM to the prime contractor (HAN) in May 72 fixed. In April, 72 MBB provided the so-called sensor Kit

consisting of the sensor parts without any electronics and completely identical with the EM. Because all details could be, measured on the calibration system exactly regardless of the schedules of the project. These surveys served especially as preparation for the upcoming always under great time pressure calibrations of the flight instruments. To automate the calibration, Matthias Bechly in the framework of a thesis developed a fully automated control and data acquisition unit, the "pacemaker" and later to redundant "Green step machine".

The prototype instruments (P type) were passed in August 1973, the flight unit 1 (F1 type) in November 1973, the flight spare unit (F2 type) in April 1974. It's not the place, all the many names, acts, problems, almost catastrophes, last-minute project quarrels and speciality Affairs to enumerate rescues who kept us in this time in breathing. Facilitating sounds 10 seconds after starting out from the set of an employee is telling: "Thank God, thing we need do no more what...".

Turn on of the experiment by the JPL out ran without problems. K. Müller and R. Schwenn monitored the work of the instruments by the JPL out and led still up in January 1975, mission control to the GSOC of the DFVLR in Oberpfaffenhofen was transferred several tests. Some of the experiences of this first weeks could be used for changes in HELIOS 2, etc. Reduction of microphony of I1b, displacement and reduction of the Azimut channels I2 and move the azimuth channels with a new command at I1a.

Particularly dramatic was the so-called "Multipacting" to the high-gain antenna: electron avalanches trained in narrow slots of the dipole of antenna is apparently in the strong electric field through a kind of resonance effect. This our I2 interference electron instrument was almost flooded, and also the wave experiments received bad data. After rigorous testing, it was decided at regular intervals on the medium-gain antenna switch, without the highest bit rates, to help those affected at least temporarily to achieve results. Also, laboratory tests for clarification and possible elimination of the fault for HELIOS 2 were immediately started. This could be achieved by an appropriate modification, in fact. A similar modification must have set up probably by itself aboard Helios 1 the first perihelion approach; because of the disruptive effect ceased completely after the first perihelion for unknown reasons and has never occurred.

In addition to the mission control HELIOS 1 and beginning to review preparations for the HELIOS 2 1975 ran start at full speed. This included the conversion of the P instruments in a set of full-featured flight spare units. All changes carried out for HELIOS 2 proved to be great success; all instruments were flawless. Only in August 1977, the switch-off time of the mercury relay in the electron instrument began to increase, so that since September '77 electrons practically only in the low-energy part of the program can be measured. This is the only change that occurred in all our instruments on both probes since the start. Regular tests show that all functions are completely unchanged, that all power supplies have remained stable and that the channeltrons not degrade. None of the provided cold redundancy must be used so far.

Now is already a wealth of scientific results before (see the bibliography). May be not reported here.

It was however pointed out that the results from 1974 to 1980 at many places in sometimes startling ways justify the design considerations of the years 1967 to 1971. Of course now working on a new generation of instruments, 1985 flying and much more detailed measurements with the ISPM mission. Apart from that, there are very few, almost insignificant points, which from today's perspective, improvements to HELIOS instruments would be desirable. Stated in the technical chapters each.

2. Construction of the

experiment used measuring

methods

Known under the name "Plasma experiment", in following with "E1", summarizes four independent instruments, their shared responsibility is the study of the solar wind plasma. Three of the instruments (I1a, I1b and I3) measure the positive component, a (I2) the electrons of the solar wind.

Primarily, the speed distribution of the different types of particles are measured. The low density of the interplanetary plasma allows to a basically simple process: the particles are sorted according to their energies and incident directions and counted individually.

All E1 instruments work on the same basic principle: the charged particles pass through static or dynamic deflection systems; but only particles that come from certain directions, and which is located, the ratio of energy to charge (E/q) in a limited area of suitable can happen and be counted.

As an example, an Analyzer with ball-shaped baffle plates (medium-RADIUS R , distance d), where the voltage up, was called. As a condition for the middle of the passband is:

$$\frac{E}{q} = U_p \cdot \frac{1}{2} \frac{R}{d}$$

By changing the plates voltage the permeability range can be shifted and therefore gradually become an energy spectrum. Such used spherical analyzers in I1a, I1b, and I2. The plate voltage is switched up here in 32 steps from revolution to Revolution (according to the spin of HELIOS).

The E1 instruments are assembled in the vicinity of the Equator by HELIOS look with their entrance funnels through gaps in the heat shields radially outward. Due to the orientation of the spin axis of the HELIOS, the middle of the fields is always in the plane of the ecliptic. The rotation is taken to the Azimuthal direction resolution (angle in the plane of the ecliptic, see fig. 5) the measurements of HELIOS directly to help; by spin-synchronous sector pulse, measurement time is divided into each rotation in azimuth appropriate, channels, which cover the range of the expected particle incident direction.

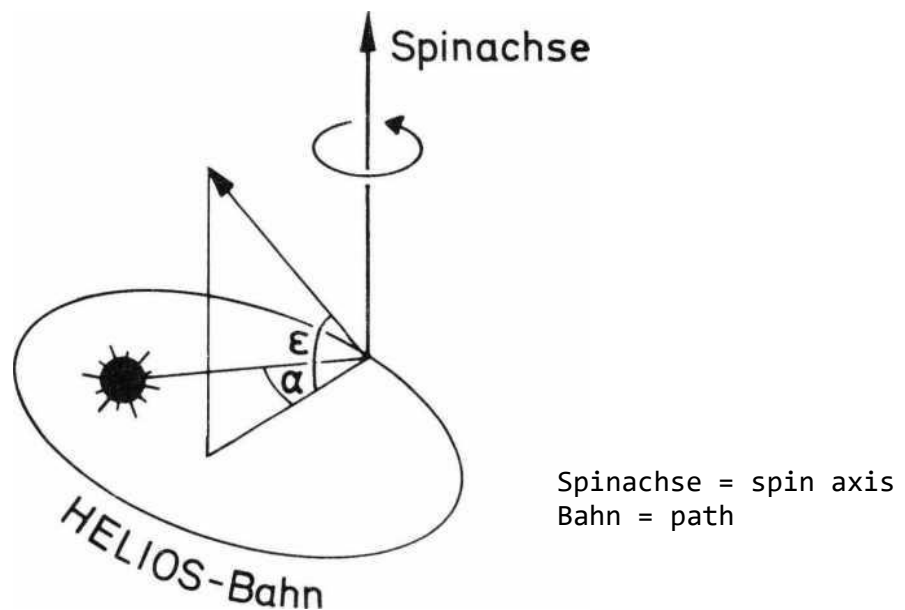
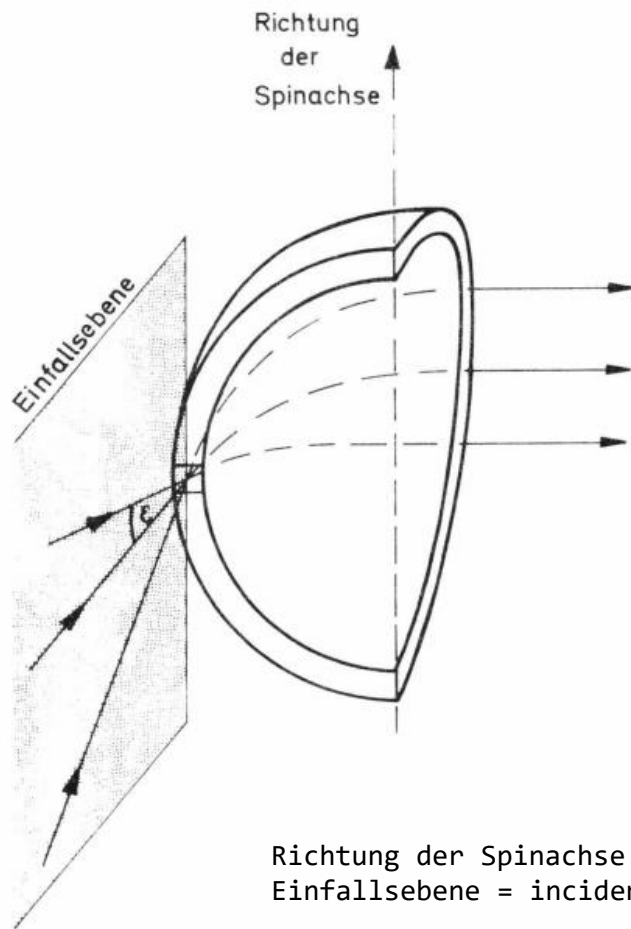


Figure 5: Definition of the angle (α) azimuth and elevation (ϵ) of the particle incident direction.

The ion instruments I1a and I3 is also a resolution with regard to the second angle of incidence, the elevation (angle perpendicular to the ecliptic); This allows a "three-dimensional" measurement of the velocity distribution. As shown schematically in Figure 6, particles covered by different elevation angles ϵ through the inlet to escape after traversing a quarter spherical Analyzer at different points of the border and can be registered by separate detectors. From this scheme can be also derived, that hemispherical



Richtung der Spinachse = Direction of the spin axis
Einfallsebene = incident plane

Figure 6: scheme of a quarter sphere electrostatic analyser. Particles with different incidence angles ϵ emerge at various points of the Analyzer and then detected with single detectors.

shaped Analyzer all particles of the implied plane of incidence on a point opposite the inlet be focused. So, a detector at this point provides a measurement result integrated over all the angles of elevation. I1b and the electronic instrument I2 use this principle.

A highly sensitive electrometer, which directly measures the incident ion current is used for detecting particles in I1b. In the other instruments, the particles with the help of open "channeltrons" (continuous electron multiplier) are counted separately.

The most important data of the individual instruments are in table 3 compiled.

Instrument 1 a für positive Ionen				Kanäle
– Energie pro Ladung	0,155	bis 15,32 kV		32 · 2
– Azimut				
– (bezogen auf Sonne)	–54,5	bis 32,7		16 · 2
– Elevation	–20	bis +20		9
Analysator:	Viertelkugel mit R = 60 mm, d = 1,2 mm			
Detektoren:	9 Channeltrons.			
Instrument 1 b für positive Ionen				Kanäle
– Energie pro Ladung	0,145	bis 14,32 kV		32 · 2
– Azimut	–56,25	bis +118		1
– Elevation	–40	bis +40		1
Analysator:	Halbkugel mit R = 54 mm, d = 4,5 mm			
Detektor:	Elektrometer mit Quantisierungseinheit $1,6 \times 10^{-16}$ As.			
Instrument 2 für Elektronen				Kanäle
– Energie pro Ladung	0,5	bis 15,5 V (A)		16
	10,7	bis 1660 V (B)		16
– Azimut	360			8 · 2
– Elevation	–9	bis +9		1
Analysator:	Halbkugel mit R = 40 mm, d = 5 mm			
	Ebene Ablenkplatten mit d = 33,6 mm			
Detektor:	1 Channeltron.			
Instrument 3 für positive Ionen				Kanäle
– Geschwindigkeit	199	bis 767 km/s		16
– Azimut	–53,2	bis 30,8		16 · 2
– Elevation	–20	bis +20		9
– M/q-Werte (bezogen auf H ⁺)	1	bis 5,33		15
Analysator:	Sinusähnliche Platten mit d = 2 mm, l = 135 mm			
	Frequenzen von 1,058 bis 4,088 MHz			
Detektoren:	9 Channeltrons.			

Translation Key:

- Für = for
- Ionen = ion
- Kanäle = Channel
- Energie pro Ladung = Energy per charge
- Bis = to
- Azimut = Azimuth
- Bezogen auf Sonne = based on Sun
- Analysator = Analyser
- Viertelkugel mit = quarter sphere with
- Detektoren = Detectors
- Halbkugel mit = Hemisphere with
- Elektrometer mit Quantisierungseinheit = Electrometer with quantization unit
- Elektronen = Electrons
- Ebene Ablenkplatten mit = level deflection plates with
- Geschwindigkeit = speed
- M/q-werte = M/q values
- Bezogen auf = based on
- Sinusähnliche Platten mit = Modified sine wave panels with
- Frequenzen von = Frequencies of

Table 3: Main data of E1 instruments

The instruments for positive ions

The main task of the plasma experiment is the measurement of the three-dimensional Velocity distribution of protons in the solar wind. On board Helios, there is no redundancy for these measurements; Therefore the instruments were designed equivalent I1a and I3 in relation to the Proton measurements as largely, in the sense of a "cold" redundancy; Only one of the two instruments is in operation and fills the entire data provided for three dimensional Proton measurements with its data share.

In the phases of the perihelion, where I3 due to its high power consumption and its approx. 30-fold lower sensitivity can only be operated routine switching of I3 after I1a has kept about every hour for each 10 min very.

The instruments I1a and I1b are housed in a common box (E1A). Their spherical analyzers are almost concentric. The 32 energy channels have 17% distance from each other and are almost exactly the same for both instruments. Every second measuring cycle moves the energy channels by half a channel spacing, the azimuth channels as well. For quiet solar wind then two spectra can be used together which substantially improves the resolution in two dimensions.

Nevertheless, there are still gaps in the grid of channels. This leads in cases of extremely cold plasma - especially after shocks - to that sometimes the entire Proton flow in a single channel meets and falls right then so to speak "through the grate". A really complete overlapping of the range would be desirable therefore at least for the measurement of cold plasma. It is necessary but also mentioned that in speed space almost "punctate" measurements very facilitate the evaluation of results in not too cold plasma. A complete solution of the problem would be possible only through transmission of results also from the gaps of the current measurement grid, what but a much higher data rate would be necessary.

The relatively large opening and the wide plate distance of I1b together with the integral effect of the hemisphere allows to measure the flow of ions of the solar wind as ion power. Here, charged ions repeatedly deliver a correspondingly higher contribution than in I1a, where each particle is simply counted regardless of its charge. So, the combination of both measurements provides information about the charge level of heavy ions in the solar wind. At the same time, I1b has a certain redundancy function due to its simplicity.

This concept has confirmed shining through the unambiguous identification of previously not in the solar wind of suspected ions.

Also the novel instrument I3, housed in box E1C, should reveal something about the composition of the positive component of the solar wind. It contains a "electrodynamic Analyzer" as the core. Its deflection plates have a roughly sinusoidal curve, so that an applied sinusoidal alternating voltage get through only particles with a corresponding speed can be. It is determined by the frequency of the applied alternating voltage and the geometry of the Analyzer. On the other hand, the amount of the plate voltage as in the electrostatic Analyzer provides also for the curvature of the particle paths and for the excretion of all particles with wrong E/q values. The two independent criteria of speed and energy per charge lead to a selection of particles according to their mass-per-charge ratio (M/q). A total of 15 fixed M/q values can be set for each of 16 speed values. The highest value of 767 km / sec corresponds to Proton of energies of 3.08 keV compared to 15.31 keV at I1a. In its azimuth and elevation channels but this instrument resembles exactly the instrument I1a.

Unfortunately, the sensitivity of I3 is so low that the already rare heavy ions only in exceptional cases to prove really are. The home value consists in the complete separation of α -particles are the Proton, whose distributions often completely overlap in perihelion in the pure range of E/q .

The electron instrument

An increasing importance in all theoretical models the electrons of the plasma of the solar wind. But the measurement of such electrons in the energy field of a few electron volts is generally difficult and therefore until today not properly managed: a photo electrons, their density is higher than that of plasma electrons; several magnitude caused by the sunlight on the surface of the probe on the other hand, even the energy areas overlap.

Thus we must distinguish the electrons according to their origin. This is possible; because photoelectron are invading the detector vertically, have - with some simplifying assumptions - always a lower energy than the electric potential ϕ of the entire probe, if ϕ is positive; Photo electrons with higher energy than $e \cdot \phi$ can not return to the probe and to the detector. Solar electrons reaching the detector, have always a higher energy than $e \cdot \phi$, because you to are accelerated by this amount. Because now the spectra of photo-electrons and plasma electrons will vary in General, you will measure a discontinuity in the measured energy spectrum of electrons at the point of the probe potential.

To do this, one must avoid above all that that photo electrons, only produced within the instrument and hence higher energies $e \cdot \phi$ can have, this moving blur.

You can achieve this by such a geometry which basically makes it impossible for the reaching of the detector all photo electrons generated in the sensor interior. The HELIOS electron instrument I2, housed in box E1B, therefore consists of two consecutive deflection systems: the first serves only the electrons to be analyzed from the cone of light out - and to the actual energy Analyzer, which is always in the shade, to draw into.

It is also provided that the probe potential is positive, and that does not distract in the Visual field of the Inhomogeneities of the electric field sensor the incident electrons. Unfortunately, a complete coating of HELIOS with a conductive layer to achieve a uniform positive potential for various reasons has been impossible to achieve. Only the central part of HELIOS is covered with two wide conductive rings are electrically connected with the probe structure. They provide enough large photo electron emission, and thereby compensate for the strong flow of plasma electrons falling from the top and bottom of the shaded surfaces of HELIOS. These surfaces must be also conductive and "grounded". This potential can

be kept most of the time about positive by HELIOS. The interference as a result of electrostatic charging of non-conductive surfaces by plasma and photo electrons however remain and must be taken into account in the evaluation.

When you first turn of I2, all with great excitement waited whether this novel instrument really works as expected. In fact - from the first range of the predicted buckling about 3eV was to see clearly. However, he is usually slightly smeared by the aforementioned interference and for direct measurement by ϕ not suitable. The total area of the senior rings turns during approximately 80% of the time sufficient, to keep ϕ positive. Only in solar wind streams with a high Electron density is ϕ negative. This is pretty much the estimates.

The experimenters had campaigned for the first-time implementation of "electrostatic purity" in an interplanetary probe with all his strength. With the success of this concept at HELIOS - even if it not entirely kept out - has led that "electrostatic purity" has become the standard by space probes, which are to measure low-energy particles and fields.

The electronics box

All E1 instruments are of a common electronics box (E1D) of supplies. It contains all of the interfaces between the instrument and the probe systems:

- o The electrical supply current is led on a 28 V line of the "nonessential bus", in the E1 main converter galvanically from the input pipe decoupled, on the different supply voltages (+ 5V, - 5V, + 28 V, + 33 V) transformed and distributed to the instruments.
- o E1D is electrically connected to the probe structure and contains the star point for the grounding of the entire E1 system. All other E1 boxes are electrically isolated mounted structure.
- o of telemetry commands are transferred in the E1 command register, evaluated and converted into appropriate control signals for the instruments. Both the arrival of commands as carried out execution according to feedback from the instruments is summarized in the form of individual bits to "digital housekeeping words" and transferred to the engineering data system of the probe.
- o the program system controls the switching of plate voltages and the situation and length of the azimuth with the help of clock pulses offered by the probe.
- o the data system prepares the data, stores it and passes it to the HELIOS telemetry. The data system
 - the counter for the preamplified detector pulse from the instruments,
 - the encoder for the count rates,.
 - a logic for the selection of the significant measurement channels,
 - two magnetic core memory with a capacity of 4096 bits each.

o the measurement data of a cycle are read synchronous spin in one of the store, while the other time-synchronous emits the data previously stored on the telemetry. The memory switches after the slower of these processes, and a new cycle begins. If this memory readout time of less than half or a quarter of the time is, is a cycle twice or read four times. In the reverse case, so at low bit rates, the switching moves so long until the current meter reading is finished. The time distance of two spectra can be between 40.5 sec and 43 min 12 sec.

o the data system is redundant in its main parts. In case of emergency can be toggled via command on the intact part.

So far, no change has been necessary.

o the engineering data system to collect important data about the technical condition of the instruments (input currents, high voltages, command State, temperatures). The probe transmits these data in the context of the engineering format (FM4). In the control center via screen can be monitored in real time.

o an automatic test cycle can be used with a command, which is controlled by the electronics box. Instead of the data of two measurement cycles appear then test data to the Control Board voltages, Channeltron reinforcements, zero count advise and the function of digital electronics.

3. Technical description of the instruments

instrument I1a (in box E1A)

A quarter spherical electrostatic Analyzer is the heart of this high-resolution instruments for positive ions. The spherical shells are almost concentrically arranged on the half spherical shells of I1b (see Figure 7). The scoops are close so close together in a common "funnel", who looks through a hole in the wall of the spacecraft outward radial. Along the edge of the outlet of the quarter balls (see Fig. 6) 9 channeltrons are attached, which correspond to an average distance of angle of incidence directions of 5° .

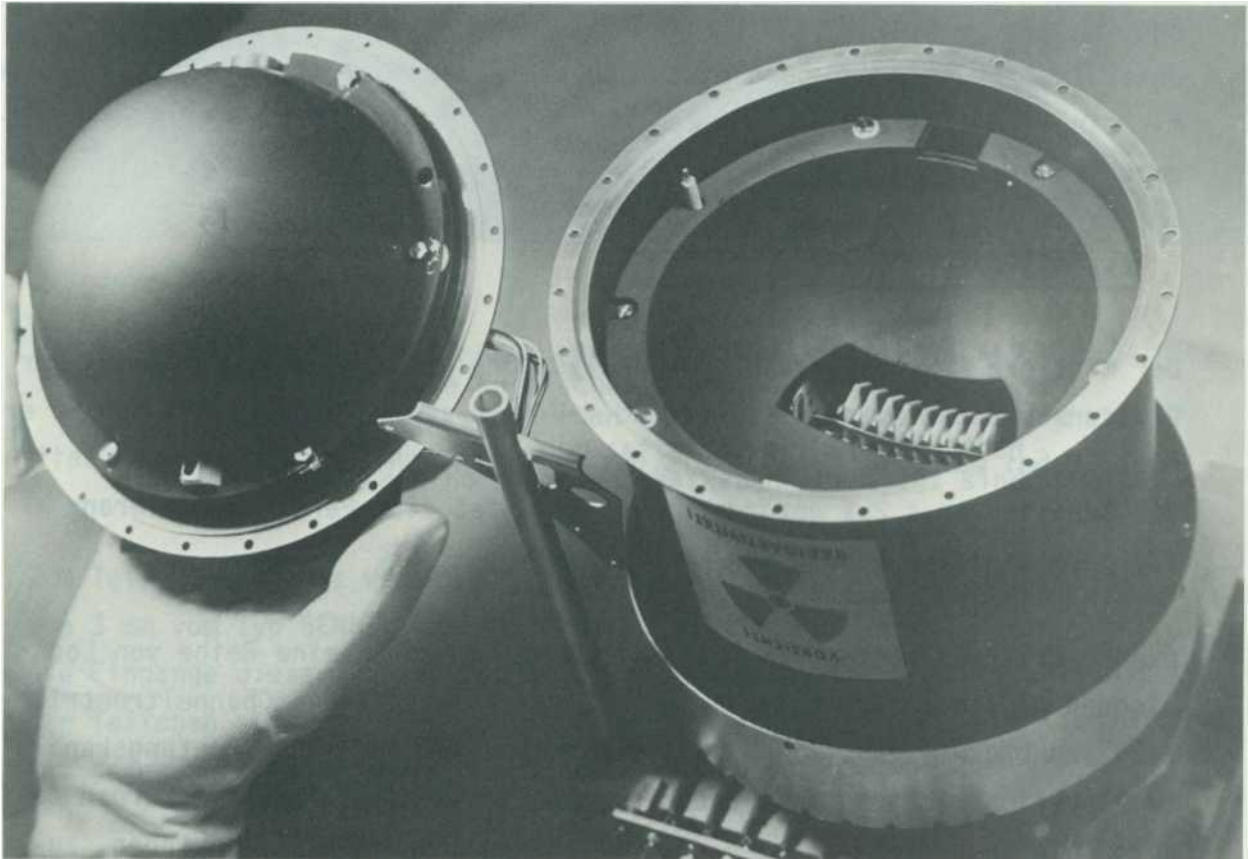


Figure 7: Look in the open instrument I1a/I1b.
Right the Analyzer shells of the quarter sphere instruments I1a with the aperture and the channeltrons at the edge of the outlet. The inlet is front (face-down). Left hemisphere cups of I1b.

The instrument is mounted in the solar probe that the field level of the Analyzer is a Meridian plane. Then matches the direction resolution of a resolution reached by the 9 detectors in the elevation (see Fig. 5). The azimuth resolution can be achieved now electronically subdivision in succession measurements during rotation of the probe.

The used electrostatic Analyzer analyzes the positive ions in the solar wind energy per charge (E/q , dimension: Volt). Since particles of various kinds have usually about the same average speed, the interpretation of a range is not completely clear: so you can for example ${}^4\text{He}^+$ particles not of equal fast ${}^{16}\text{O}^{4+}$ Distinguish particles, because in two varieties is $E/q = 4$, where $E/q = 1$ for protons. Because you know that the first and greatest maximum must match the protons in the spectrum, one can conclude from the other maxima on the content and the nature of the remaining components.

Using the above direction resolution, you can measure so the full three-dimensional Velocity distribution of the positive particles of the solar wind with a such on analyser.

Analysing Part by I1a

The average radius of curvature of Analyzer plates R_m is 60 mm. The plate distance d is 1.2 mm to give an R/d ratio of 50. Accuracy of the R/d ratio in the "active part" of the shells of $\pm 2\%$ was required. This means for each individual bowl of $\pm 10\mu$ a manufacturing tolerance.

The outlet of the Analyzer are formed by a series of aperture, which facilitate between the spherical shells and the Channeltron funnels attached (fig. 8). The aperture set elevation towards the channels of direction of and limit the channels. Also, the electrons that arise in the Channeltron funnel, withheld this, because this aperture with a fine mesh grid are covered.

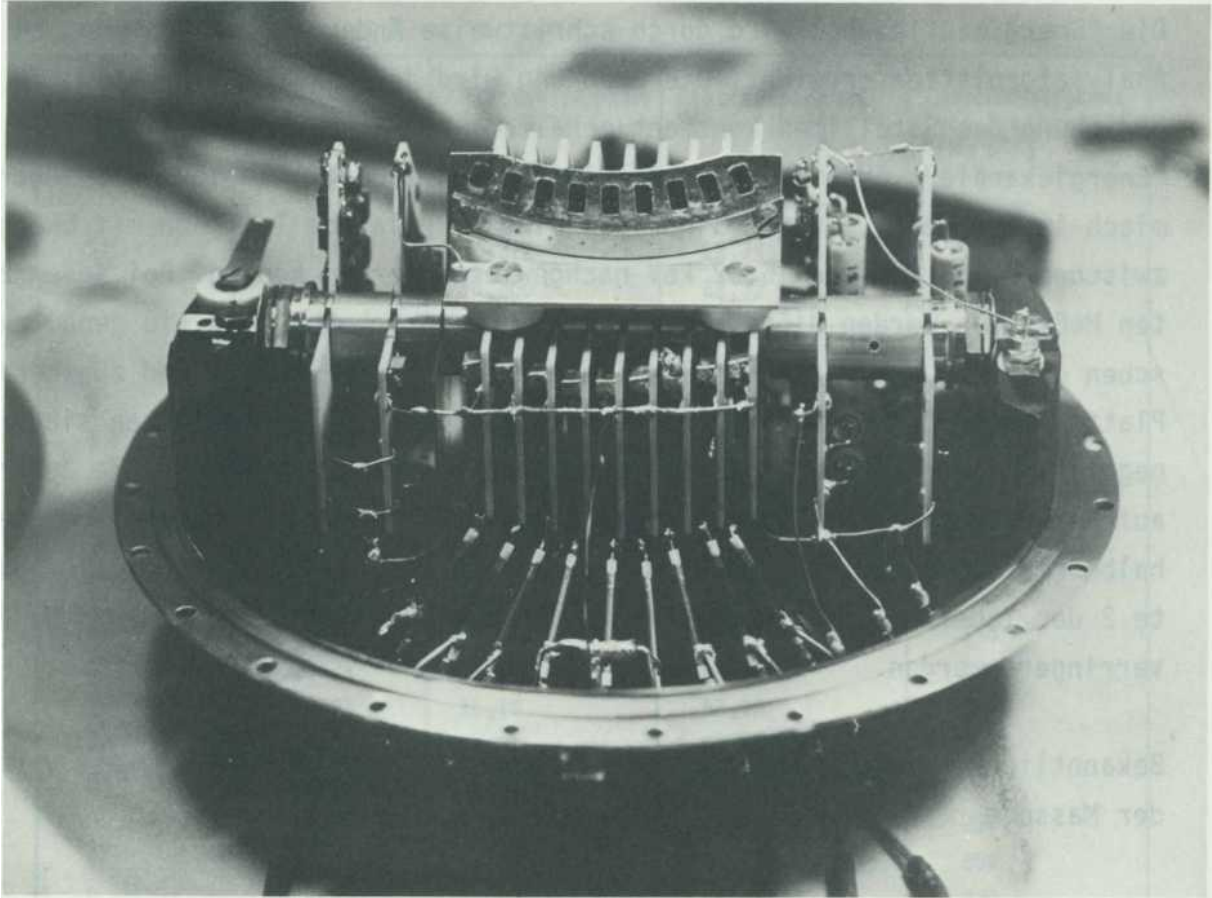


Figure 8: Here also the cylinder part of the housing, as well as the spherical shells by I1a are removed. The channeltrons are carried by a common shaft, on which side the boards with the high voltage cascade are attached.

Channeltrons used for detecting particles funnel diameter by 3 mm type BENDIX CEM 4013 M.

The inputs of this channeltrons are sufficient for acceleration of particles on negative voltage. The aperture with the bars has a potential of 200 V compared to the Channeltron funnels.

Stimulation in Inflight test

To stimulate the channeltrons with the so called "Inflight Test" serves light a UV glow lamp; It is mounted near the Channeltron funnel, so that all channeltrons are lit correspondingly. The intensity of this UV glow lamp is, lit with a high voltage of approximately 550 V and operated at 350 V is set so that Channeltrons emit workable and meaningful count rates.

I1a energy channels

The "energy" resolution is achieved by gradual change of voltage to the plates of the Analyzer. The voltage is kept constant each of the measurements per revolution of the satellite. The instrument has 32 "energy channels", more precisely said "Energy-per-charge channels", which logarithm-mixing are considered way, that simply charged particles with energies between 0,158 keV and 15.62 keV can be detected. Every second measuring cycle, these energy channels are moved so that they are exactly between these channels. All energy channels and associated plate voltages are given in table 4. The voltages are negative and are attached to the inner Bowl, while the outer housing potential lies. This means that the ions in the medium to the half plate voltage U_p to be speeded up. So, the values specified in column 2 of table 4 for the channel centers by $U_p/2$ must be reduced.

It is known that the energy of a particle with velocity v and mass m is

$$E = \frac{m}{2} v^2$$

For protons with $m_p = 1.6724 \times 10^{-24} g$ results in a formula for v_p as a function of E

$$v_p = 437.4 \cdot \sqrt{E}$$

where E in keV to use is. The values of v_p to the energy channels from column 2 in table 4 are also specified in column 5, for the data analysis, these values by using the calibration results are modified anything.

The accuracy of the plate voltage is better than $\pm 1\%$.

The deviations from these values is in the range of temperature to be expected during the mission not more than $+ 1\% \pm 50$ mV. The ripple voltage is 2% ss.

Energiekanal	Energie zu Ladung (keV)	Plattenspannung Sensor 1a (V)	Plattenspannung Sensor 1b (V)	Geschwindigkeit von Protonen (km s ⁻¹)
1'	0,1580	6,322	26,34	172
1	0,1700	6,800	28,33	178
2'	0,1829	7,314	30,48	185
2	0,1967	7,867	32,78	192
3'	0,2116	8,462	35,26	199
3	0,2276	9,102	37,93	206
4'	0,2448	9,791	40,80	214
4	0,2633	10,53	43,88	222
5'	0,2832	11,33	47,20	230
5	0,3046	12,18	50,77	239
6'	0,3277	13,11	54,61	248
6	0,3524	14,10	58,74	257
7'	0,3791	15,16	63,18	266
7	0,4078	16,31	67,96	276
8'	0,4386	17,54	73,10	287
8	0,4718	18,87	78,63	297
9'	0,5074	20,30	84,57	308
9	0,5458	21,83	90,97	320
10'	0,5871	23,48	97,85	331
10	0,6315	25,26	105,3	344
11'	0,6793	27,17	113,2	357
11	0,7306	29,23	121,8	370
12'	0,7859	31,44	131,0	384
12	0,8453	33,81	140,9	398
13'	0,9093	36,37	151,5	413
13	0,9780	39,12	163,0	428
14'	1,052	42,08	175,3	444
14	1,132	45,26	188,6	460
15'	1,217	48,69	202,9	477
15	1,309	52,37	218,2	495
16'	1,408	56,33	234,7	513
16	1,515	60,59	252,5	532

Table 4: Energy per charge channels and Plate voltages of instruments I1a and I1b

Energiekanal = Energy channel

Energie zu Ladung = Energy to charge

Plattenspannung = Plate Voltage

Geschwindigkeit von Protonen = Speed of protons

Energiekanal	Energie zu Ladung (keV)	Plattenspannung Sensor 1a (V)	Plattenspannung Sensor 1b (V)	Geschwindigkeit von Protonen (km s ⁻¹)
17'	1,629	65,17	271,5	552
17	1,753	70,10	292,1	573
18'	1,885	75,40	314,2	594
18	2,028	81,11	337,9	616
19'	2,181	87,24	363,5	639
19	2,346	93,84	391,0	663
20'	2,523	100,9	420,6	687
20	2,714	108,6	452,4	713
21'	2,919	116,8	486,6	739
21	3,140	125,6	523,4	767
22'	3,378	135,1	563,0	795
22	3,633	145,3	605,5	825
23'	3,908	156,3	651,3	855
23	4,204	168,1	700,6	887
24'	4,521	180,9	753,6	920
24	4,863	194,5	810,6	954
25'	5,231	209,3	871,9	989
25	5,627	225,1	937,8	1026
26'	6,052	242,1	1009	1064
26	6,510	260,4	1085	1104
27'	7,003	280,1	1167	1145
27	7,532	301,3	1255	1187
28'	8,102	324,1	1350	1231
28	8,715	348,6	1452	1277
29'	9,374	374,9	1562	1325
29	10,08	403,3	1680	1373
30'	10,85	433,8	1808	1425
30	11,67	466,6	1944	1478
31'	12,55	501,9	2091	1533
31	13,50	539,9	2249	1590
32'	14,52	580,7	2420	1648
32	15,62	624,6	2603	1710

Table 4: (continued)

Energiekanal = Energy channel

Energie zu Ladung = Energy to charge

Plattenspannung = Plate Voltage

Geschwindigkeit von Protonen = Speed of protons

I1a direction channels

The rotation (spin) probe to help will be taken to the angular resolution of the Azimuth: it is as simple as temporal Division of the measurement.

The instrument has 16 channels, each 3.5 ° azimuth channels width and 5.6 ° distance. The middle of the azimuth angle range used to measure so that they involved a certain suspension of the viewing direction of the instrument before the Sun line, based on the spin of the probe is situated, is equivalent to. It reflects the fact, that the plasma particles - although almost radially from the Sun flying away - no longer meet because of the significant ground speed of HELIOS from the direction of the Sun on the probe. At HELIOS 2, the hold-back angle via tele command can be toggled in two stages.

This time derivative to the half channel spacing, so 2.8 ° is reduced at any second cycle. This creates a second grid 16 channels of azimuth, which is offset by 2.8 °. This shift of the Azimuth channels is performed simultaneously with the aforementioned shift of energy channels. The exact location of the Azimuth channels is provided in tables 9 and 10 on pages 71 and 72.

The angular resolution in the elevation is achieved through the use of 9 channeltrons in conjunction with quarter spherical analyser. The distance of these channels is approx. 5 °, the width 2.8 °. These 9 elevation channels are symmetrical to the equatorial plane of the probes.

Electronic part of I1a (see block diagram fig. 9)

Instrument I1a becomes supplied by the electronics box (E1D) only control signals, that determine the end of the program, as well as with a voltage of 28 V direct from the main current transformer (main-converter), which is also located in the electronics box. The sensor electronics delivers the preamplified Channeltron pulse on the electronics box for the registration, evaluation, and storage. All electronics for assistance and control of the instrument, as well as for data processing is located with the exception of the high voltage cascade in the electronic part of the sensor box. The electronics of the sensor consists of the following units (see Figure 10):

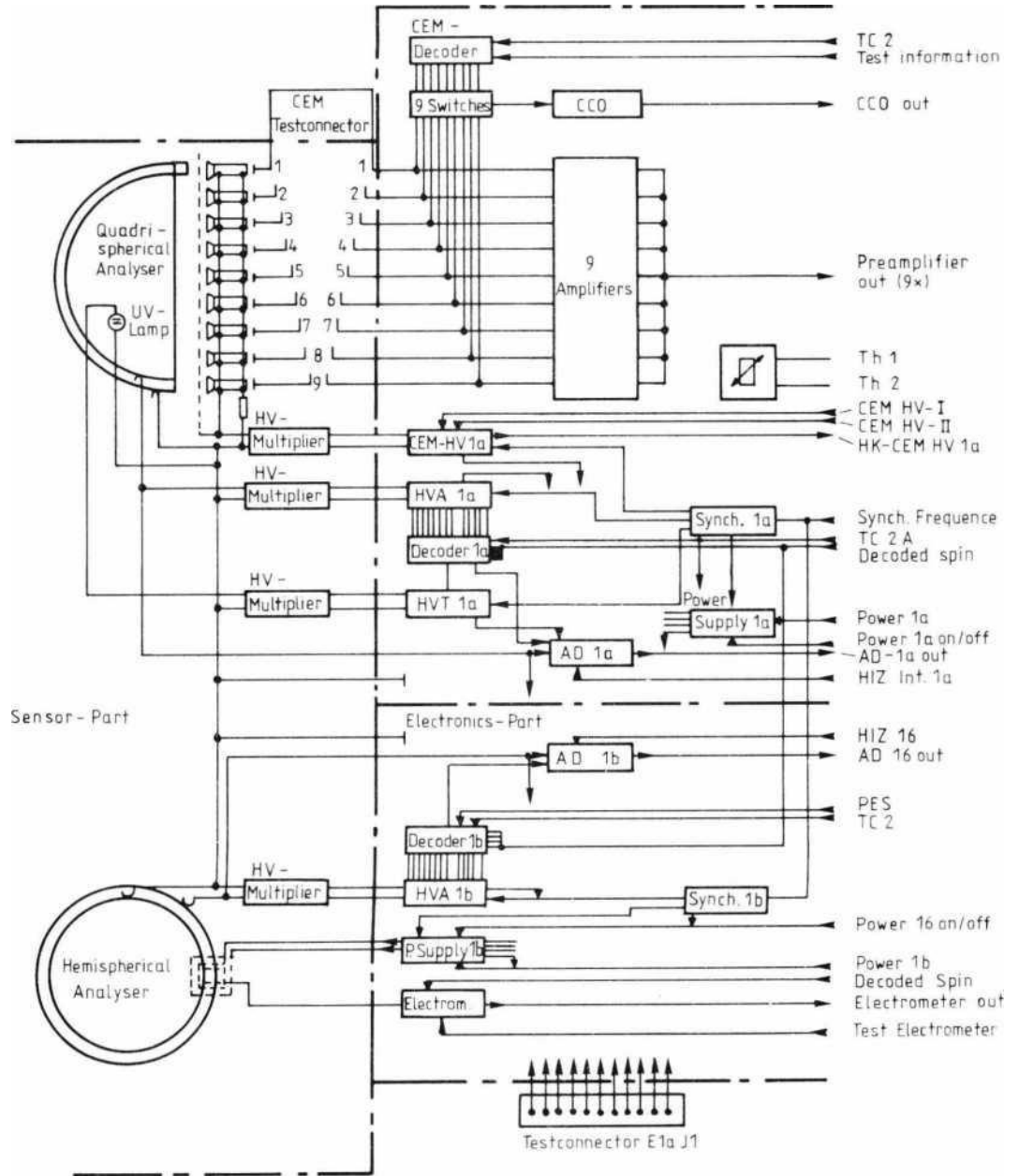


Figure 9: Instrument I1a/I1b, block diagram. The sensor part in the vacuum sealed package contains all parts carrying high voltage, the electronics part analog and digital electronics.

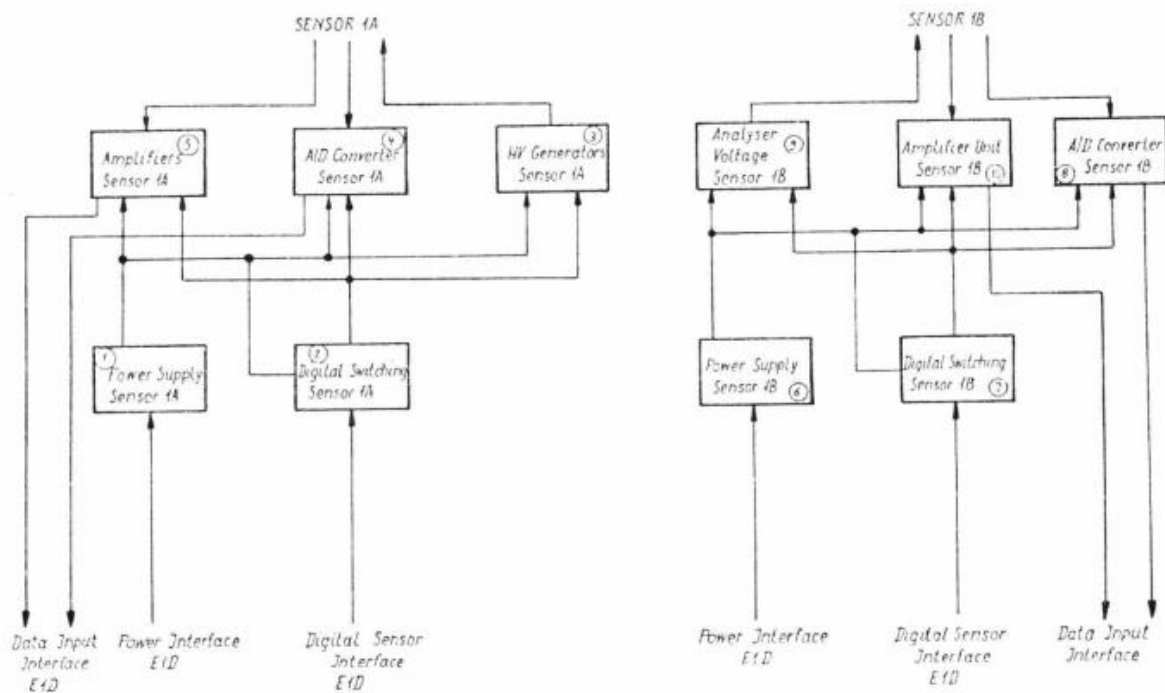


Figure 10: Instrument I1a/I1b Block diagram of the electronic part

- Sensor power supply (power supply)
- Channeltron amplifier unit (amplifiers)
- Analyzer of power generation, power generation for UV - Glow lamp and Channeltron supply voltage - procreation (HV generator)
- Analog - to-digital converters (A/D-converter)
- Digital control unit (digital switching)

The sensor power supply generates all voltages required to operate of the electronics from the 28V-supply of the main power transformer. It is activated and deactivated using the appropriate command. The Channeltron amplifier unit includes 9 Channeltron amplifier which reinforce the output given by the channeltrons and give further processable form. Furthermore, this unit belongs to a so called CCO (current controlled oscillator), which during the Inflight test quantises an ejected charge from a randomly selected Channeltron. This allows the determination of the current amplification of a Channeltron.

The Analyzer power generation is a gradually switchable high-voltage generator with very little input and decay time constant.

The high voltage generator for the UV glow lamp is used only during the Inflight test and supplied the necessary ignition and ARC voltage the lamp. The electronics for the production of Channeltron-is a controlled high-voltage generator that works with a twelve-stage multiplier cascade supply voltage. He is on and off and has three power settings for three different output voltages (3,3 kV, 3.7 kV, 4.1 kV).

All high voltage cascade are housed together with the plates of the Analyzer and the channeltrons in the vacuum-tight part of the sensor and get only their control voltages from the electronics section through soldered unions.

The analog - to-digital converter is used to convert analog voltages to digitally processed readings and is used only for checking the Analyzer voltages during the Inflight test.

The digital control unit prepares the program control signals of the electronics box, (decodes the state of the so-called Energy channel meter) and thus controls the analyser voltage generation.

Instrument I1b (in box E1A)

The instrument I1b will supply energy Spectra by current measurement without any direction resolution in a simple way, so that even in case of failure of the data reduction logic or contamination of channeltrons still the most important plasma parameters speed, temperature and density can be determined.

Here, it used a hemispherical analyser which integrates over approximately 80 ° in elevation. The integration of the azimuth is achieved that is the entire ion flow, over about a half of probe turn the direction of the Sun around, summed up.

Analyzer part of I1b

The hemispherical analyser panels have the following dimensions:

Medium-RADIUS: $R = 54 \text{ mm} \pm 1\%$

Plate distance: $d = 4,5 \text{ mm} \pm 2\%$ $R/d = 12$

Inlet opening: $4.5 \times 10 \text{ mm}$

The outer plate is connected to the housing potential, the inner plate is at negative potential.

A super-insulated collector located in the focus area of the hemispherical analyser acts as a particle catcher. Between Analyzer plates and particle collector, a grid is attached to decouple of the Analyzer voltages or used to hold back the electrons. It is biased to -36 V against the collector.

The trapped positive charge is fed into a highly sensitive electrometer amplifier, which emits a standard pulse to the digital electronics at the output a digitization level per unit of quantization. The following data are for the electrometer amplifier:

Quantization unit (QE): $1.6 \times 10^{-16} \text{As}$, i.e. 1000 Elementary charges

Dynamic range: $1.6 \times 10^{-16} \text{As}$ up to $3.2 \times 10^{-12} \text{As}$

Time constant: 60 ms

Accuracy: $\pm 10\%$ for $Q \geq 1.6 \times 10^{-14} As$ $\pm 8\%$ for $Q \geq 1.6 \times 10^{-13} As$

Set zero count rate: 20 ± 5 QE/Measurement

Long-term constancy zero count rate: ± 10 QE

Measuring Channels of I1b

The number and the distribution of energy channels is identical to I1a (tab.4), where here is a translation of the half plate voltage have to consider. The range switch-over from one cycle to another is the same as for I1a. The voltages are correspondingly higher due to the greater distance of plates. For the accuracy or Tolerance is the same with the following exceptions:

Temperature stability of DC voltage: $\pm 1\% \pm 250mV$

Drop-out time from the highest to the lowest

Channel : < 200 ms

Electronic part of I1b (see block diagram fig. 9)

Instrument I1b is supplied by the electronics box with control signals, and a voltage of 28 V direct from the main current transformer (main-converter) to determine program flow. The sensor electronics delivers the processed measurements to the electronics box. All electronics to the care and control of the instrument, as well as for data processing is located with the exception of the high voltage cascade in the electronic part of the sensor box. The electronics of the sensor consists of the following units (see Figure 10):

- Sensor power supply (power supply)
- Analyzer voltage generation (analysis of voltage)
- Electrometer amplifier unit)
- Analog - to-digital converters (A/D-converter)
- Digital control unit (digital switching)

The sensor power supply generates all voltages required for the operation of the electronics. It is activated and deactivated using the appropriate command. The Analyzer power generation is a gradually switchable high-voltage generator with very little input and decay time constant.

The electrometer consists basically of a low-noise high-stability power amplifier and an electronic unit for the quantization of the measured load with the appropriate control circuitry.

The analog - to-digital converter is used to convert analog voltages to digitally processed readings and is only for the validation of Analyzer voltages during the so called "do test" used.

The digital control unit prepares the program control signals of the electronics box, decoded the stand of the so called Energy channel meter and controls so the analyser voltage generation.

The set zero count rate of approx. 20 counts remained stable during the mission remarkably although was been charged with slow drifting due to the strong temperature differences. The short term stability proved problematic: HELIOS-1 were suddenly large fluctuations of the zero count rate, as the motor of the despun high-gain antenna was switched on. Apparently "heard" the electrometer which is very similar to a highly sensitive capacitor microphone is, the structure-borne sound emanating from the bearings. This disorder was not occur during ground tests, probably because the store were differently loaded under the influence of gravity.

Instrument I2 (in box E1B)

This instrument is used for the investigation of the electrons of the solar wind.

A hemisphere is used for the analysis of energy also here - like at I1b - Analyzer. A flat disk Analyzer is used however, which hides the electrons in the beam of sunlight and serves as light swamp. The arrangement is designed so that no photoelectrons generated on the entrance Panel or in the Interior of the sensor, can reach the Channeltron at the output of the Analyzer; in addition, only at least dual reflected light between the hemisphere Analyzer cups can reach (see Figure 11).

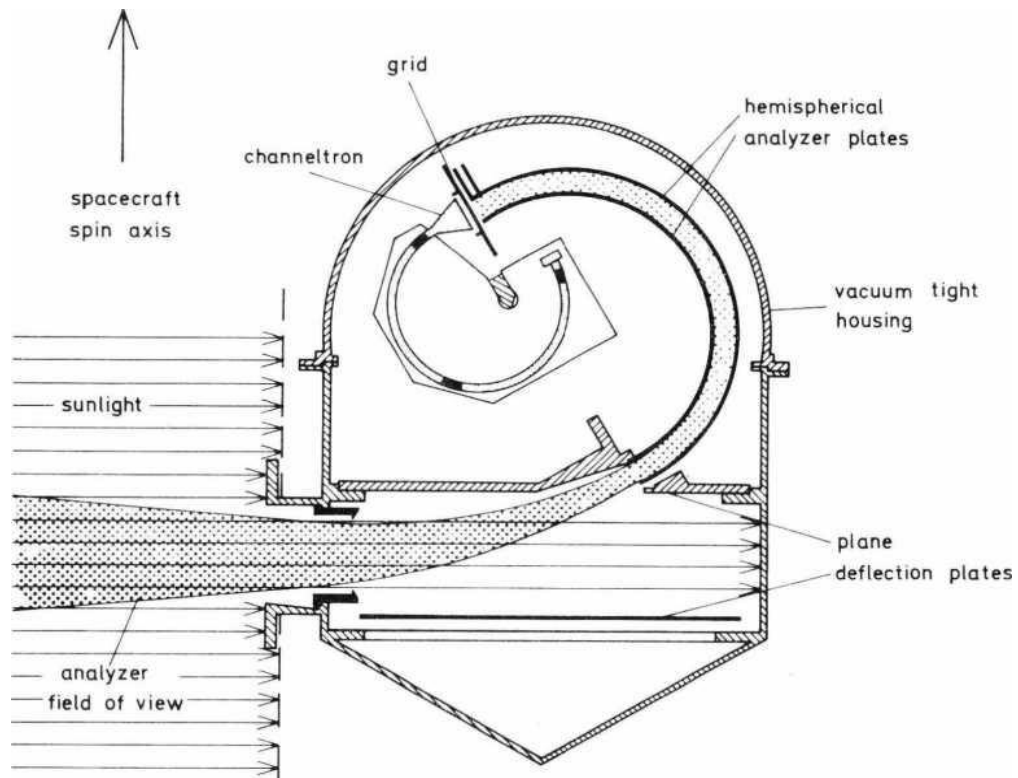


Image 11: Function image of the electron instrument I2

An elevation resolution is omitted here, so that only a single particle detector is required. The azimuth resolution is reached by the spin of the probe. The power range is from 0.5 eV to 1445 eV.

Analyzer part of I2

Following dimensions have the hemisphere shaped Analyzer plates:

Medium Radius $R = 40\text{mm} \pm 1\%$

Plate distance $d = 5\text{mm} \pm 2\%$ $\frac{R}{d} = 8$

The inner Bowl is connected to the housing potential, as well the subsequent plate plates analyser; the outer panels are placed on negative potential. In order to reduce inhomogeneities in the field, a metallic border runs along the edge of the voltage carrying plate of the plate analyser, reaching roughly half way to the other plate. Close to the entry-opening, this border runs higher to simultaneously act as light aperture.

A Channeltron is for detecting particles used funnel diameter of 8 mm (type CEM 4018 M the company BENDIX). There is a pinhole with 8 mm in diameter, on which, much like at I1a - a mesh is soldered between Analyzer plates and Channeltron. This aperture prevents the funnel of the Channeltron from attracting electrons from a wider area when the funnel is at +200 V potential. You at the same time forms the outlet aperture of the Analyzer and acts as another Light baffle. This aperture is in the measuring program B (for electrons from 9 eV) on a potential of - 6 V put, to hold back photo electrons.

Flight experience with HELIOS 1 and subsequent laboratory tests proved} this is not necessary. That's why this aperure has been connected with mass in HELIOS 2.

Stimulation in Inflight test

To stimulate the channeltrons with the Inflight-Test, a UV glow lamp; is mounted near the channeltrons. The intensity of this UV glow lamp which is ignited and operated with high voltage is adjusted by appropriate coating of its surface, that a workable and meaningful the Channeltron count rate is down.

I2 measuring channels

Sensor 2 can run two different measurement programs, telecommands are toggled by (S2A- and S2B program).

In the program A electrons measured in 16 channels with energies between 0.5 eV and 13.3 eV, the required relatively low plate voltages (see table 5) are generated directly in the electronic part of I2 by means of a vacuum-tight implementation in the sensor part.

In program B electrons are measured in also 16 channel with energies between 9.28 eV and 1445 eV. The necessary plate voltages are generated up to 850 V with HV-cascades in the sensor area. Analyzer power supply units different for the two programs are switched by a relay inside the sensor.

The switch from one energy channel to the next higher is done in every turn of HELIOS before azimuth channel facing away from the Sun. The new value of the plate voltage is reached within the allowed tolerances in 3 ms. For the switching time program A to B downtime must be brought because of the switching time of the relay 100ms in purchase (program B is always connect to A; tele command controls only the transfer of one or the other data blocks). This means that the values in the first 4 azimuth channels in the lowest energy channel of program

Programmteil	Kanalnummer	Kanalmitte (eV)	Kanalabstand (eV)	Spannung am Kugelanalysator (V)	Spannung am Plattenanalysator (V)
A	1	0		0	0
	2	0,5	0,5	0,125	0,294
	3	1	0,5	0,250	0,588
	4	1,5	0,5	0,375	0,882
	5	2	0,5	0,500	1,18
	6	2,7	0,7	0,675	1,59
	7	3,4	0,7	0,850	2,0
	8	4,1	0,7	1,03	2,41
	9	4,8	0,7	1,20	2,82
	10	4,8	1,0	1,45	3,41
	11	6,8	1,0	1,70	4,00
	12	7,8	1,0	1,95	4,59
	13	8,8	1,0	2,20	5,18
	14	10,3	1,5	2,58	6,06
	15	11,8	1,5	2,95	6,94
	16	13,3	1,5	3,33	7,82
B	1	9,28		2,32	5,456
	2	13,0		3,25	7,639
	3	18,2		4,55	10,69
	4	25,48		6,37	14,97
	5	35,67		8,92	20,96
	6	49,94		12,48	29,33
	7	69,92	Faktor	17,48	41,08
	8	97,89	1.4	24,47	57,50
	9	137,1		34,26	80,51
	10	191,9		47,96	112,7
	11	268,6		67,15	157,8
	12	376,1		94,01	220,9
	13	526,5		131,6	309,3
	14	737,1		184,3	433,0
	15	1032,0		258,0	606,3
	16	1445,0		361,2	848,8

Table 5: energy channels and plate voltages of sensor 2.
To get the real location of the channel centers by adding the half voltage on the ball Analyzer.

Programmteil = Program part
 Kanalnummer = Channel Number
 Kanalmitte = Channel middle
 Kanalabstand = Channel spacing
 Spannung am Kugelanalysator = Voltage at the ball analyser
 Spannung am Plattenanalysator = Voltage on the plates analyser
 Faktor = Factor

B for data analysis, particularly in continuous flow (normal-data mode), may not be used to evaluate. The ratio of the voltage on the plates analyser to the on the ball Analyzer should be nominally about 2.35. The final value was set for the respective sensor calibration and then by attaching trim resistors hardwired. The absolute values of the voltages on the capacitor of the ball are $\pm 1\%$ exactly, with a maximum ripple voltage of $\pm 2\%$ ss.

I2 direction channels

The 2 sensor is mounted in the probe so that the two plates of the first Analyzer of parallel to the equatorial plane and the ecliptic are (see Figure 11). The Analyzer on the top plate, ensuing would integrate due to its hemispherical shape about a significant azimuth angle range (unlike sensor 1B, whose integrated hemispherical about the elevation angle). To make a subdivision in single azimuth channels using the probe rotation, the passband of the hemispheres should be limited. This is done by an isolated overlapping aperture arrangement between the plates of the ball that let only an about 15 mm wide strip in the plane of the Analyzer.

There are 8 azimuth channels with 45 degrees distance and 28.1° width (or 11.2° width at HELIOS 2) they are limited with the opening time of the counter. Due to the geometry of sensor 2, the width of the elevation angle - range is designed with about 10° , symmetrical to the equatorial plane of the probe. So, this instrument measures virtually a cut through the electron distribution.

Electronics part I2 (see block diagram in Fig. 12)

Instrument I2 is powered only by the electronics box with control signals which determine the programme sequence of the sensor, as well as a supply voltage 28 V directly from the main current transformer (main converter). The sensor

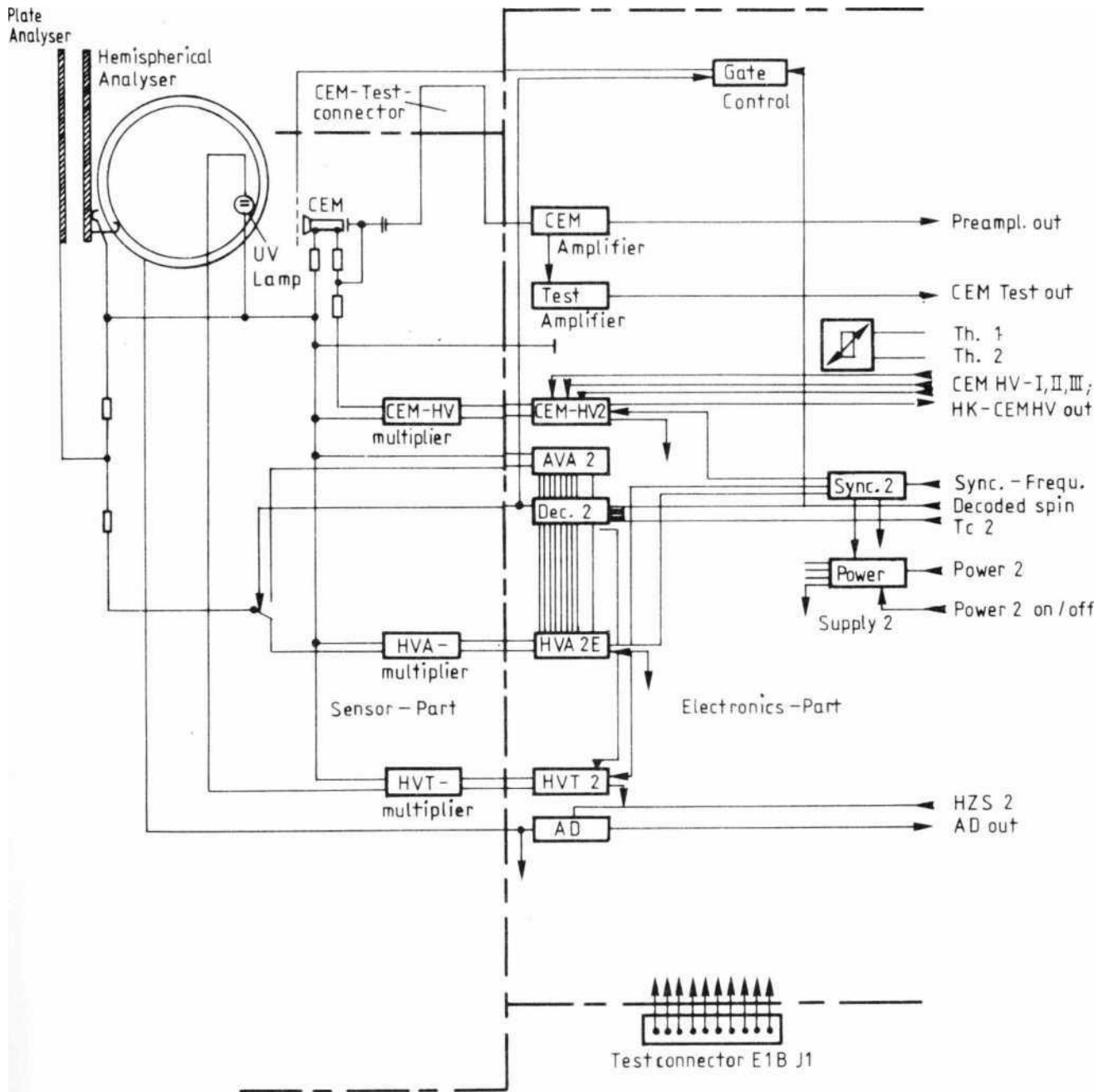


Figure 12: Instrument I2 Block diagram

electronics delivers the preamplified counting pulses to the electronics box on the registration and further processing. All electronics for assistance and control of the sensor and data processing is located with the exception of the high voltage cascade in the electronic part of the sensor box. The electronics of the sensor consists of the following units (see Figure 13):

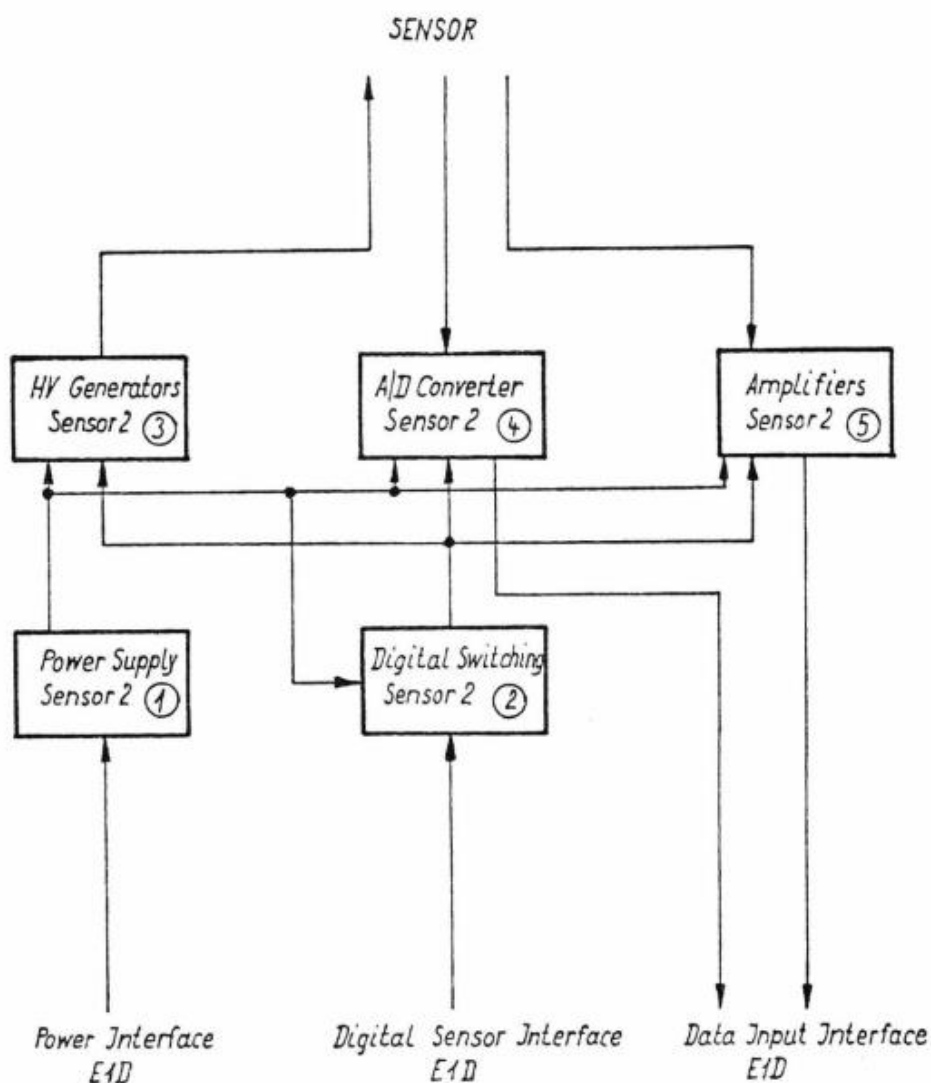


Image 13: Instrument 2 electronics part (block diagram)

- Sensor power supply (power supply)
- Channeltron amplifier unit (amplifiers)
- Analyzer voltage generation, power generation for UV
Glow lamp and Channeltron supply voltage generation
(HV-generator)
- Analog - to-digital converters (A/D-converter)
- Digital control unit (digital switching)

The Sensor power supply produces all the operation of the electronics required voltages. It is activated and deactivated using the appropriate command. The Channeltron amplifier unit consists of a Channeltron-amplifier, which amplifies the impulses emitted by the Channeltron and is in processable form; also from a second such amplifiers with a higher "threshold". This amplifier is used during the Inflight test to verify the adequate reinforcement of channeltrons; As long as the count rates of two amplifiers around are equal and independent of the height of the threshold, the reinforcement of the channeltrons is sufficient.

The Analyzer voltage generation consists of two parts. One part is the production of low voltage of the program part of A and presents itself as gradually switchable reference voltage source; the other part to the generation of the Analyzer voltages of program part B is a gradually switchable high-voltage generator with very little input and decay time constant. The high voltage generator for the UV glow lamp is used only during the Inflight test and supplied the necessary ignition and ARC voltage the lamp. The electronics for the production of Channeltron supply voltage is a controlled high-voltage generator that works with a twelve-stage multiplier cascade. He is on/off and has three power settings for three different output voltages (3,3 kV, 3.7 kV, 4.1 kV).

The analog - to-digital converter is used to convert analog voltages to digitally processed readings and is used only for checking the Analyzer voltage during the Inflight test.

The digital control unit prepares the program control signals from electronics box, decodes the energy channel counter State and controls accordingly both Analyzer power generations.

Instrument I3 (in box E1C)

The energy and direction of distributions of different ions in the solar wind should be measured with this instrument separately.

An angle-resolved, electrodynamic particle path Analyzer is used for the analysis. It consists of two circular segment plates, which are nearly cosine-shaped wavy along the RADIUS (see Figure 14). By applying an electrical alternating voltage manages to separate positively charged particles speed and mass per charge.

Analyzer part I3

The exact shape of the Analyzer plates was calculated on the basis of the following considerations:

The equation of motion for a particle with mass m , charge q and the velocity \vec{w} in an electric field \vec{E} is

$$q \cdot \vec{E} = m \cdot \vec{w}$$

In a narrow channel of the vector of the electric field with good approximation is vertical on the vector of speed, i.e.

$$\vec{E} \cdot \vec{w} = 0$$

This condition is met, if \vec{w} and \vec{E} in component display have the following form

$$\vec{w} = \{u, v\}$$

$$\vec{E} = \{v, -u\} \frac{E}{w}$$

E is an alternating field with the angular frequency ω

$$E = E_0 \cdot \cos \omega t$$

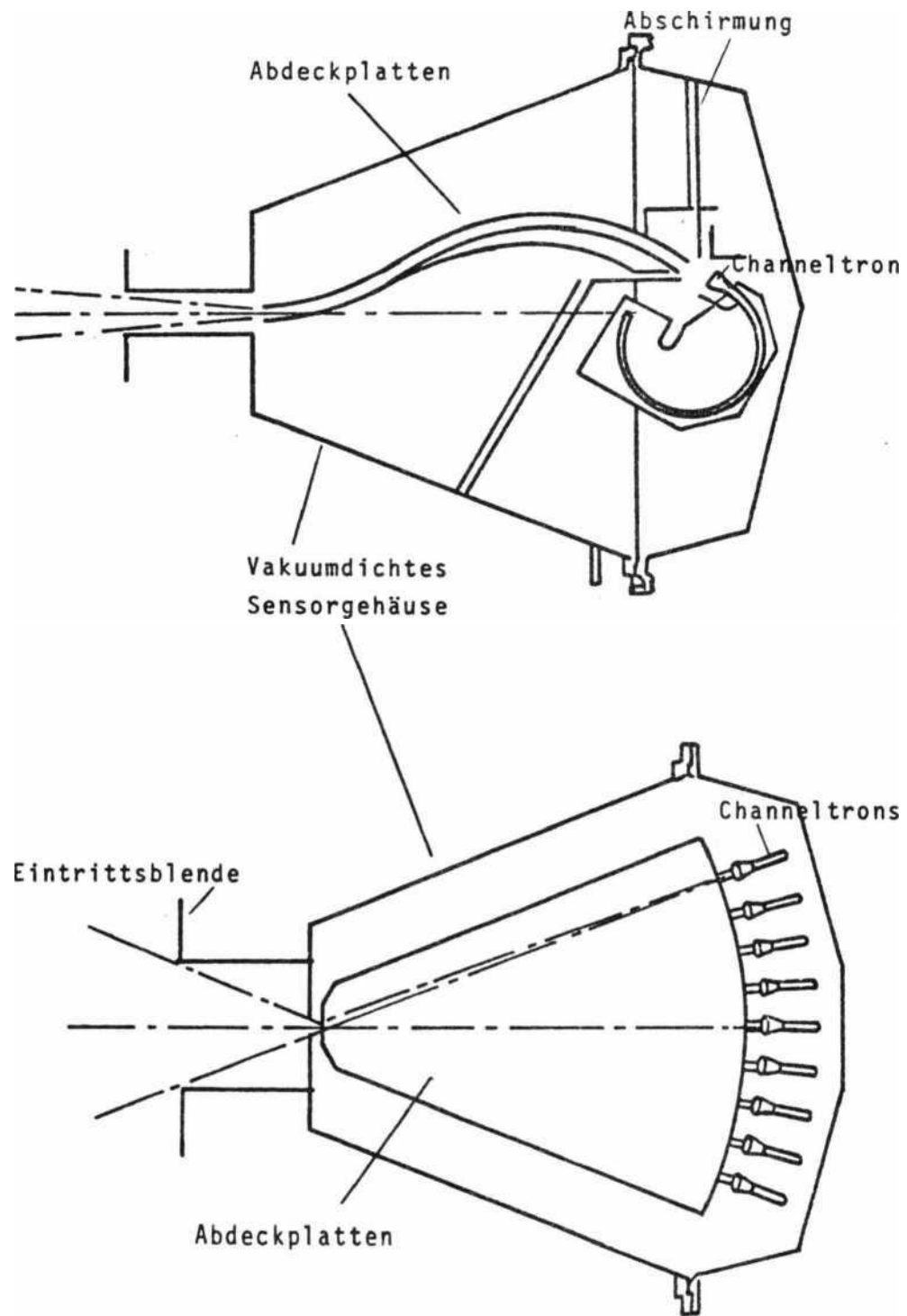


Image 14: Instrument 3 Function image

- Abschirmung = Shielding
- Abdeckplatten = Cover plates
- Vakuumdichtes = Vacuum-tight
- Sensorgehäuse = Sensor housing
- Eintrittsblende = Entrance aperture

The components of the motion equation is then

$$u = \frac{q}{m} \cdot \frac{v}{w} E_0 \cos(\omega t + \phi)$$

$$v = -\frac{q}{m} \cdot \frac{u}{w} E_0 \cos(\omega t + \phi)$$

with ϕ is a possible phase shift of the particle opposite to the electrical field.

Along with the differential equations for the location coordinates

$$\dot{x} = u \text{ and } \dot{y} = v$$

It has a system of four differential equations 1. All right, this method was solved numerically with the Runge-Kutta.

From the variety of solutions of this system, a solution was selected mainly practical according to the realization in the instrument. This curve was at the same distance of 2 mm with deflection plates "cased". We opted for a period length L of $\frac{3}{2}\pi$ with a total path length S through the Analyzer of 133.4 mm. Parallel curves in this rotation by an angle of 45° about an axis through the channel entrance creates a pair of surfaces. At the outlet edge of this plate 9 channeltrons are fitted with the angular distance of the 5° , allowing a determination of particle direction of incidence regarding the elevation, such as when I1a. Also the subdivision in azimuth channels are just like at I1a.

For a particle with the speed w (based on a full period length 2π) to occur the Analyzer with the length L , it so to speak 'in time' must the electric voltage (frequency $f = \omega/2\pi$), i.e.

$$w = f \cdot L$$

If the amplitude U_m thereby obeys still the condition

$$U_m = \frac{m}{q} \cdot \omega^2 \cdot A \cdot d$$

(A is the half amplitude, d the plate distance of the Analyzer, both in cm), can only particles with a fixed mass per charge-value m/q in this speed w just get through. Of course there are many particles that do meet these conditions all but arrive at the wrong time on the Analyzer, i.e. so out of phase with the AC voltage. This restriction leads to the mentioned reduction of sensitivity of I3 to I1a by approximately a factor of 30, despite the slightly larger inlet.

In particular, the following values were chosen:

$$A = 1.5 \text{ cm} \quad d = 0.2 \text{ cm}$$

$$S = 13.34 \text{ cm for } \frac{3}{2} \pi \text{ period length.}$$

Measurement Channels I3

The frequency of the plate voltage is switched from turn to turn in 16 steps of 1,058 MHz to 4,088 MHz high. This corresponds to particle velocities from 199 to 769 km s^{-1} (see table 6). Here the Amplitude between 10,15 and 256,05 V is so varied, so that M/q values of 1 (Proton) up to 5.3 ($^{16}\text{O}^{3+}$) can be recorded (see table 7). You can extract the values of the plate voltages for each combination of speed and mass per charge table 8. In the lower part, some values are specially marked. At high frequencies because the voltages required for large M/q values can not be realized for performance reasons. That's why the voltage that is outside the marked limits or the M/q value is kept for an appropriate period of time. In the M/q -channel 16, the voltage is set to zero.

Frequencies and voltages be adhered to $\pm 1\%$.

The angular resolution in elevation and azimuth is completely analogous to sensor 1a.

Kanal-Nr.	Geschwindigkeit (km/sec)	Frequenz (MHZ)
1	198,9	1,058
2	217,5	1,157
3	238,0	1,206
4	260,6	1,386
5	286,2	1,517
6	312,1	1,660
7	341,6	1,817
8	373,8	1,988
9	409,1	2,176
10	447,7	2,381
11	489,8	2,605
12	536,0	2,851
13	586,6	3,120
14	641,9	3,414
15	702,4	3,736
16	768,6	4,088

Table 6: speed channels and corresponding frequencies
of Analyzer voltages in instrument I3.

Geschwindigkeit = speed

Kanal-Nr.	Ionenart	m/q
1	${}^4\text{He}^{2+}$	2,00
2	${}^3\text{He}^{2+}$	1,50
3	${}^1\text{H}^+$	1,00
4		1,35
5		1,65
6	${}^{12}\text{C}^{5+}$	2,40
7	${}^{16}\text{O}^{6+}$	2,62
8		3,00
9	${}^{16}\text{O}^{5+}$	3,20
10	${}^{14}\text{N}^{4+}$	3,50
11	${}^{16}\text{O}^{4+}$	4,00
12		4,40
13	${}^{14}\text{N}^{3+}$	4,66
14		4,90
15	${}^{16}\text{O}^{3+}$	5,33
16		0

Table 7: m/q channels instrument I3.

Ionenart = ion

M/q-Kanal		1	2	3	4	5	6	7	8	9	10	11	12	13	14	15
Atom		He	He	H	-	-	C	O	He	O	N	O	-	N	-	O
Masse M		4.0026	3.0160	1.0078	1.3505	1.6505	12.0000	15.9949	3.0160	15.9949	14.0031	15.9949	4.4005	14.0031	4.9005	15.9949
Ladung q		2	2	1	1	1	5	6	1	5	4	4	1	3	1	3
M/q		2.0013	1.508	1.0078	1.3505	1.6505	2.4000	2.6658	3.0160	3.1990	3.5008	3.9987	4.4005	4.6677	4.9005	5.3316
f [MHz]	v [kms ⁻¹]															
1.058	198.9	20.16	15.19	10.15	13.60	16.62	24.17	26.85	30.38	32.22	35.26	40.28	44.33	47.02	49.36	53.70
1.157	217.5	24.10	18.16	12.14	16.26	19.88	28.91	32.11	36.33	38.53	42.17	48.17	53.01	56.23	59.03	64.23
1.266	238.0	28.86	21.74	14.53	19.47	23.80	34.61	38.44	43.50	46.14	50.49	57.67	63.47	67.32	70.68	76.90
1.386	260.6	34.59	26.06	17.41	23.34	28.53	41.48	46.08	52.13	55.30	60.51	69.12	76.07	80.69	84.71	92.17
1.517	285.2	41.44	31.22	20.86	27.96	34.17	49.69	55.20	62.45	66.24	72.49	82.81	91.13	96.66	101.48	110.41
1.660	312.1	49.62	37.38	24.98	33.48	40.92	59.51	66.10	74.78	79.32	86.80	99.15	109.12	115.74	121.52	132.21
1.817	341.6	59.45	44.79	29.93	40.11	49.03	71.29	79.19	89.60	95.03	104.00	118.80	130.73	138.67	145.59	158.40
1.988	373.8	71.16	53.62	35.83	48.02	58.69	85.34	94.80	107.25	113.76	124.50	142.21	156.50	166.00	174.28	189.62
2.176	409.1	85.26	64.24	42.92	57.53	70.31	102.25	113.58	128.50	136.30	149.16	170.38	187.50	198.88	208.81	208.81
2.881	447.7	102.08	76.91	51.39	68.88	84.18	122.42	135.98	153.85	163.19	178.58	203.99	224.49	238.12	250.00	250.00
2.605	489.8	122.19	92.06	61.52	82.45	100.77	146.54	162.77	184.16	195.34	213.77	213.77	213.77	213.77	213.77	213.77
2.851	536.0	146.36	110.27	73.68	98.75	120.70	175.52	194.97	220.59	233.97	256.05	256.05	256.05	256.05	256.05	256.05
3.120	586.6	175.28	132.06	88.24	118.27	144.55	210.21	233.49	233.49	233.49	233.49	233.49	233.49	233.49	233.49	233.49
3.414	641.9	209.87	158.13	105.66	141.61	173.08	173.08	173.08	173.08	173.08	173.08	173.08	173.08	173.08	173.08	173.08
3.736	702.4	251.32	189.36	126.53	169.58	207.26	207.26	207.26	207.26	207.26	207.26	207.26	207.26	207.26	207.26	207.26
4.088	768.6	226.72	226.72	151.49	203.04	248.16	248.16	248.16	248.16	248.16	248.16	248.16	248.16	248.16	248.16	248.16

Table 8: speed and m/q-channels as the analyser voltages (in V/eff) and frequencies (in MHz). At high frequencies, not all m/q channels can be passed through from performance reasons. Here, standing outside the marked areas each m/q value is then persisted. In the m/q-channel 16, the voltage is reset to zero.

Ladung = charge

Stimulation in Inflight test

A UV glow lamp, helps to stimulate the channeltrons Inflight test It is mounted near the Channeltron funnel, so that it illuminates all channeltrons accordingly. Its intensity is so that meaningful count rates arise.

Electronics part I3 (see block diagram fig. 15)

Instrument I3 is supplied by the electronics box with control signals, and a voltage of 28 V direct from the main current transformer (main converter) to determine program flow. The sensor electronics delivers the preamplified counting pulses on the electronics box for the registration, evaluation, and storage. All electronics to the care and control of the instrument, as well as for data processing is located with the exception of the high voltage cascade in the electronic part of the sensor box. The electronics of the sensor consists of the following units (see Figure 16):

- Sensor power supply (power supply)
- Channeltron amplifier unit (amplifiers)
- Power generation for UV glow lamp and Channeltron - supply generation (HV generator)
- Analog - to-digital converters (A/D-converter)
- Digital control unit (digital switching)
- High frequency generator to the plate voltage generation (RF power generator) with decoding device (digital control unit)

The sensor power supply generates all voltages required for the operation of the electronics. It is activated and deactivated using the appropriate command. The Channeltron amplifier unit consists of 9 Channeltron amplifiers core, which reinforce the emitted pulses given by the channeltrons and leave in the processable form. Furthermore, this unit also includes a so called CCO (current controlled oscillator), that quantises the charge given by the individual channeltrons during the in-flight tests and thus permits a determination of the instantaneous amplification of channeltrons.

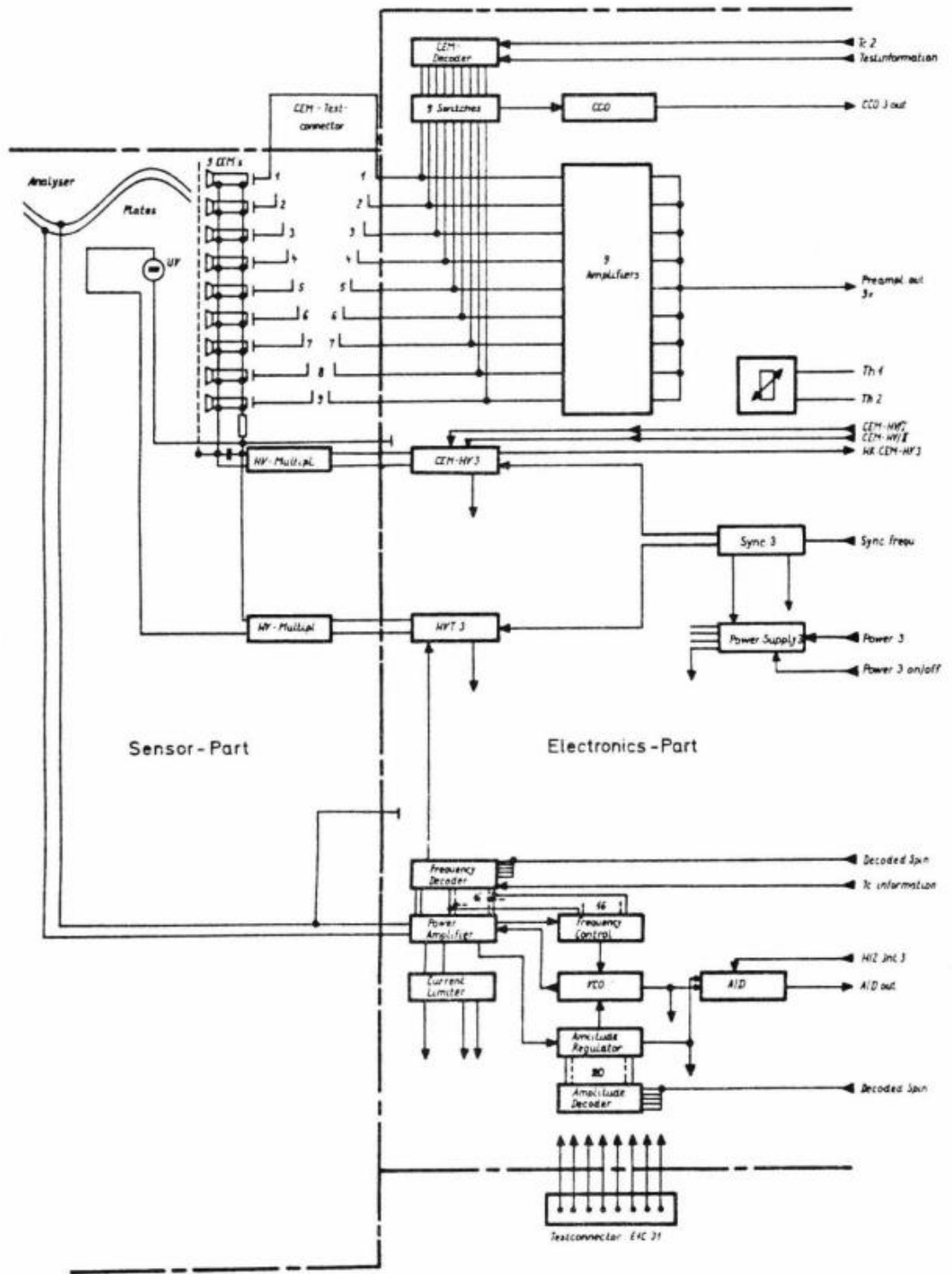


Image 15 Instrument I3 Block diagram

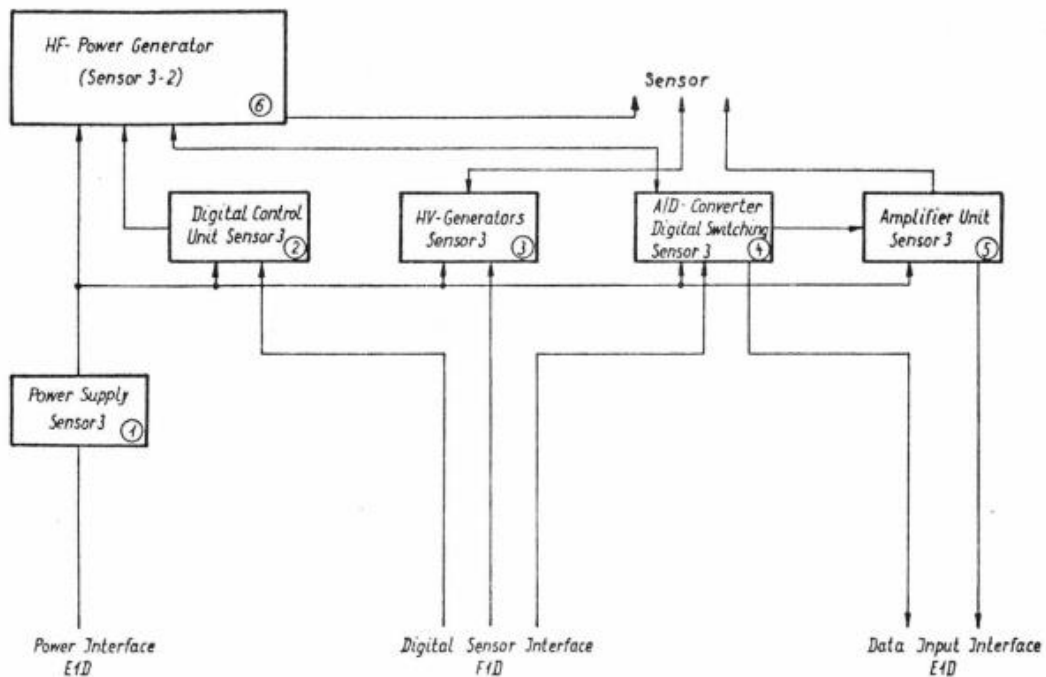


Figure 16: Instrument I3, electronics block diagram

The high voltage generator for the UV glow lamp is used only during the Inflight test and supplied the necessary ignition and ARC voltage the lamp. The electronics for the production of Channeltron supply voltage is a controlled high-voltage generator that works with a twelve-stage multiplier cascade. He is on and off and has three power settings for three different output voltages (3,3 kV, 3.7 kV; 4.1 kV).

The analog - to-digital converter is used to convert analog voltages to digitally processed readings and is used only for checking the amplitude of the high frequency voltage during flight test.

The digital control unit is greatly simplified compared to sensor 1a for this sensor. She assumes here only control the selection of channeltrons which is switched during flight test on the CCO.

The Analyzer voltages and frequencies is a separate decoding device, which works directly with the frequency generator here (as much more complicated). The high-frequency generator (fig. 17) for producing the plates voltage works as

a resonant circuit, with the capacity of the panels together with stray capacity and a coil forming the circle. The resonance frequency is designed to realize the highest frequency, so the F16. The other lower frequencies are matched this that the capacity of the disk capacity are connected in parallel. At the same time, the control frequency of 16 of course appear voltage-controlled oscillators according to. This control frequency will be adjusted via a control loop of the resonance frequency of the amplifier. The output amplitude of high-frequency voltage is set by a reference generator (DC) and compared with the rectified output voltage in a comparison circuit, and adjusted by means of a control circuit. Selecting the frequency and the desired voltage is performed by the above mentioned decode body that selects the desired channel affiliations from the information supplied by the electronics box.

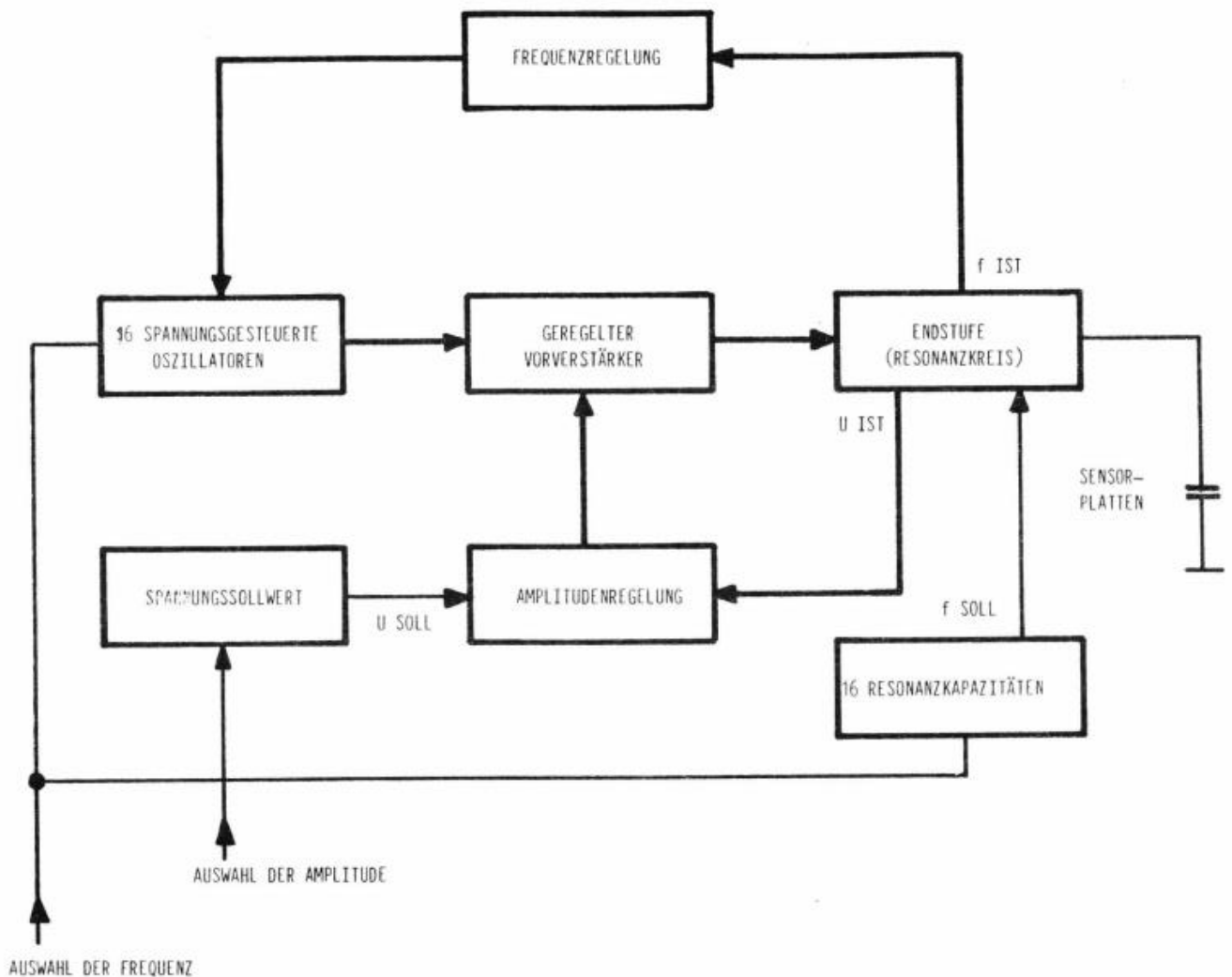


Figure 17: high frequency generator (principle) for instrument I3

Frequenzregelung = frequency control
Spannungsgesteuerte = voltage controlled
Geregelter Vorverstärker = Regulated preamp
Endstufe (Resonanzkreis) = Amplifier (resonant circuit)
Spannungssollwert = Voltage setpoint
Amplitudenregelung = amplitude control
Resonanzkapazitäten = resonance capacitances
Auswahl = selection

Electronics box (in box E1D)

The units of the electronics box have the following main tasks:

- Power supply of the four sensors
- Power supply of units of the electronics box
- Processing of the data from the sensors
- Save the selected data
- Transfer the stored data to the telemetry
- Production of the measurement time grid (spin-synchronous)
- Generation of the signals to control flow and program control of the sensors
- Processing of the tele-commands
- Transfer of housekeeping data, temperatures.

As can be seen from images 18 and 19, run the counting pulses from the sensors via a corresponding switching logic in one of the two redundant digital electronics units. The pulses are counted in the applicable associated counters. The control unit of the counter, i.e. the formation of the corresponding azimuth angle is worried by the control flow.

The Azimuthal measuring ranges of all instruments are specified in tables 9 and 10. HELIOS 2 differs in several respects from HELIOS 1:

- HELIOS 2 is "on its head", i.e. the spin vector is facing South therefore the direction of E1 in HELIOS 2 from East to West over the Sun swings, just vice versa like in HELIOS 1.
- The location of the middle of the ranges is different (different "suspension").
- At HELIOS 2, the suspension can be moved through a tele command 7.03 degrees.
- The width of the Azimut channels of I2 is only 11.25° at HELIOS 2, instead of 28.1° at HELIOS 1.
- The shift of the I2 channels in each 2nd Range of HELIOS 2 is 22.5° . As a result, two consecutive measurements form a grid of 16-equidistant channel.

The flow of control also ensures the temporally coordinated readout of the counter and the transfer of data to the reducing plant. After the

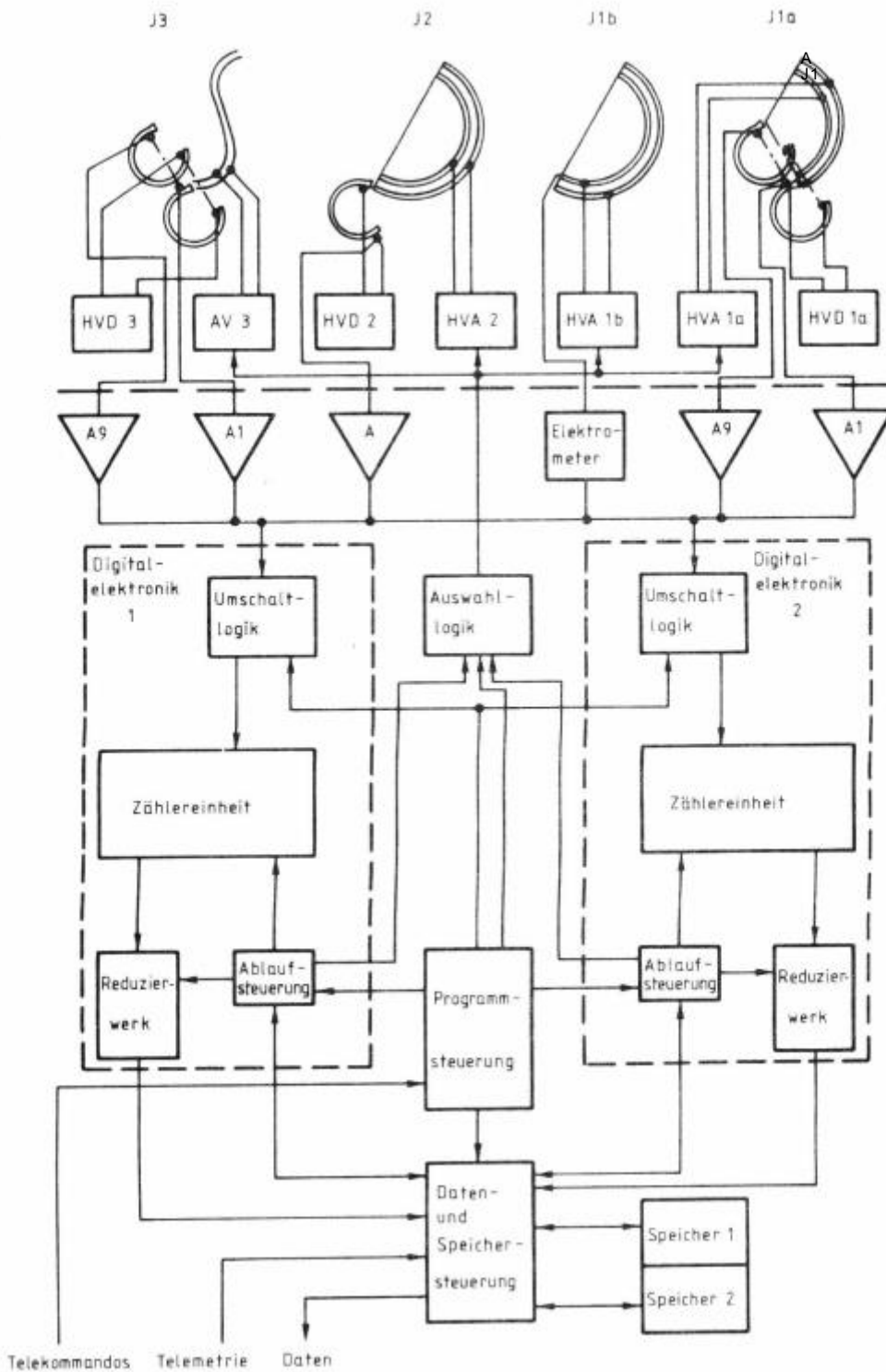


Figure 18: Electronics box, function diagram

Digitalelektronik = Digital Electronics

Umschaltlogik = switching logic

Auswahllogik = selection logic

Zählereinheit = counter unit

Reduzier-werk = Reducing plant

Ablaufsteuerung = flow control

Programmsteuerung = program control

Daten- und Speichersteuerung = Data and storage control

Speicher = memory

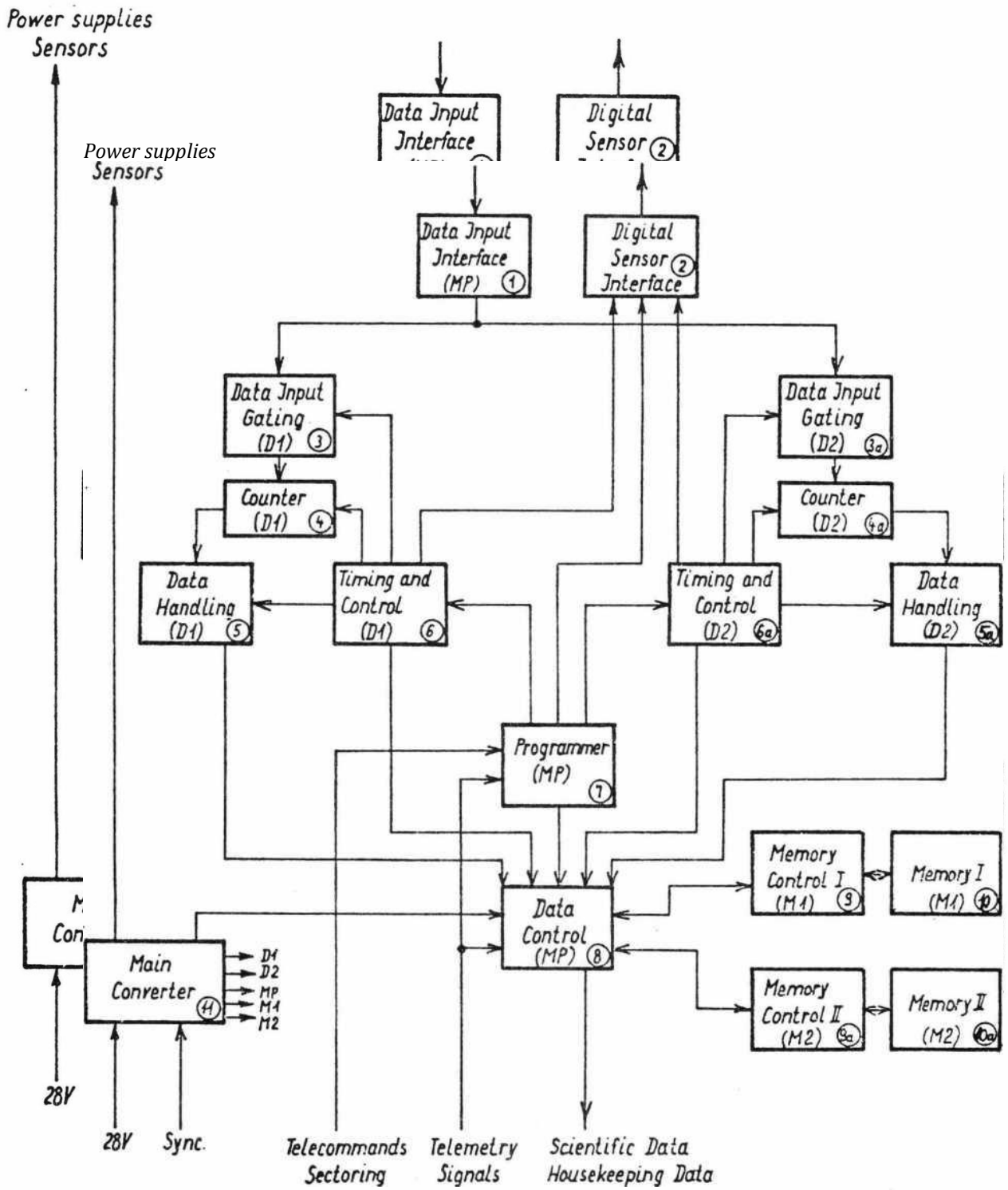


Figure 19: electronic box, block diagram

SENSOR	MESSWINKEL	OHNE VERSCHIEBUNG		MIT VERSCHIEBUNG	
		ANFANG	ENDE	ANFANG	ENDE
Sensor 1a und Sensor 3	1. Azimut	- 56,36 ⁰	- 52,84 ⁰	- 53,55 ⁰	- 50,03 ⁰
	2. Azimut	- 50,74 ⁰	- 47,22 ⁰	- 47,93 ⁰	- 44,41 ⁰
	3. Azimut	- 45,12 ⁰	- 41,60 ⁰	- 42,31 ⁰	- 38,79 ⁰
	4. Azimut	- 39,50 ⁰	- 35,98 ⁰	- 36,69 ⁰	- 33,17 ⁰
	5. Azimut	- 33,88 ⁰	- 30,36 ⁰	- 31,07 ⁰	- 27,55 ⁰
	6. Azimut	- 28,26 ⁰	- 24,74 ⁰	- 25,45 ⁰	- 21,93 ⁰
	7. Azimut	- 22,64 ⁰	- 19,12 ⁰	- 19,83 ⁰	- 16,31 ⁰
	8. Azimut	- 17,02 ⁰	- 13,50 ⁰	- 14,21 ⁰	- 10,69 ⁰
	9. Azimut	- 11,40 ⁰	- 7,88 ⁰	- 8,59 ⁰	- 5,07 ⁰
	10. Azimut	- 5,78 ⁰	- 2,26 ⁰	- 2,97 ⁰	+ 0,55 ⁰
	11. Azimut	0,00 ⁰	+ 2,81 ⁰	+ 3,51 ⁰	+ 6,32 ⁰
	12. Azimut	+ 5,62 ⁰	+ 9,13 ⁰	+ 8,43 ⁰	+ 11,94 ⁰
	13. Azimut	+ 11,24 ⁰	+ 14,75 ⁰	+ 14,05 ⁰	+ 17,56 ⁰
	14. Azimut	+ 16,86 ⁰	+ 20,37 ⁰	+ 19,67 ⁰	+ 23,18 ⁰
	15. Azimut	+ 22,48 ⁰	+ 25,99 ⁰	+ 25,29 ⁰	+ 28,80 ⁰
	16. Azimut	+ 28,10 ⁰	+ 31,61 ⁰	+ 30,91 ⁰	+ 34,42 ⁰
Integrations- Zähler	Öffnungszeit ist identisch mit AZ 1 bis AZ 16	- 56,36 ⁰	+ 31,61 ⁰	- 53,55 ⁰	+ 34,42 ⁰
Sensor 1b	Meßphase	- 56,36 ⁰	+ 137,54 ⁰	- 53,55 ⁰	+ 140,35 ⁰
	Nullp. korr.	- 87,27 ⁰	- 84,46 ⁰	- 84,46 ⁰	- 81,65 ⁰
Sensor 2	1. Azimut	+ 154,40 ⁰	- 177,19 ⁰	+ 157,21 ⁰	- 174,38 ⁰
	2. Azimut	- 160,33 ⁰	- 132,23 ⁰	- 157,52 ⁰	- 129,42 ⁰
	3. Azimut	- 115,37 ⁰	- 87,27 ⁰	- 112,56 ⁰	- 84,46 ⁰
	4. Azimut	- 70,41 ⁰	- 42,31 ⁰	- 67,60 ⁰	- 39,50 ⁰
	5. Azimut	- 25,45 ⁰	+ 2,65 ⁰	- 22,64 ⁰	+ 5,62 ⁰
	6. Azimut	+ 19,67 ⁰	+ 47,77 ⁰	+ 22,48 ⁰	+ 50,58 ⁰
	7. Azimut	+ 64,63 ⁰	+ 92,73 ⁰	+ 67,44 ⁰	+ 95,54 ⁰
	8. Azimut	+ 109,59 ⁰	+ 137,69 ⁰	+ 112,40 ⁰	+ 140,50 ⁰

Table 9: Azimuthal angle of sensors for F1, in relation to the HELIOS-Sun line. Negative sign refer to Western directions. The order of the channels is equivalent to the rotation of HELIOS 1 from West to East, i.e. against the clockwise direction when viewed from the North.

Messwinkel = measuring angle
 Ohne verschiebung = Without shift
 Mit verschiebung = with shift
 Anfang = Beginning
 Integrations-Zähler = Integrations counter

SENSOR	MESSWINKEL	KEIN VORHALT			
		OHNE VERSCHIEBUNG		MIT VERSCHIEBUNG	
		ANFANG	ENDE	ANFANG	ENDE
Sensor 1a und Sensor 3	1. Azimut	- 40,78 ⁰	- 37,26 ⁰	- 43,59 ⁰	- 40,07 ⁰
	2. Azimut	- 35,16 ⁰	- 31,64 ⁰	- 37,97 ⁰	- 34,45 ⁰
	3. Azimut	- 29,53 ⁰	- 26,01 ⁰	- 32,34 ⁰	- 28,82 ⁰
	4. Azimut	- 23,91 ⁰	- 20,38 ⁰	- 26,72 ⁰	- 23,20 ⁰
	5. Azimut	- 18,29 ⁰	- 14,77 ⁰	- 21,10 ⁰	- 17,58 ⁰
	6. Azimut	- 12,67 ⁰	- 9,15 ⁰	- 15,48 ⁰	- 11,96 ⁰
	7. Azimut	- 7,05 ⁰	- 3,53 ⁰	- 9,86 ⁰	- 6,34 ⁰
	8. Azimut	- 1,43 ⁰	+ 2,09 ⁰	- 4,24 ⁰	- 0,72 ⁰
	9. Azimut	+ 4,19 ⁰	+ 7,71 ⁰	+ 1,38 ⁰	+ 4,90 ⁰
	10. Azimut	+ 9,81 ⁰	+ 13,33 ⁰	+ 7,00 ⁰	+ 10,52 ⁰
	11. Azimut	+ 15,43 ⁰	+ 18,95 ⁰	+ 12,62 ⁰	+ 16,14 ⁰
	12. Azimut	+ 21,05 ⁰	+ 24,57 ⁰	+ 18,24 ⁰	+ 21,76 ⁰
	13. Azimut	+ 26,67 ⁰	+ 30,19 ⁰	+ 23,86 ⁰	+ 27,38 ⁰
	14. Azimut	+ 32,29 ⁰	+ 35,81 ⁰	+ 29,48 ⁰	+ 33,00 ⁰
	15. Azimut	+ 37,91 ⁰	+ 41,43 ⁰	+ 35,10 ⁰	+ 38,62 ⁰
	16. Azimut	+ 43,53 ⁰	+ 47,05 ⁰	+ 40,72 ⁰	+ 44,24 ⁰
Integrations- Zähler	Öffnungszeit ist identisch mit AZ 1 bis AZ 16	- 40,78 ⁰	+ 47,05 ⁰	- 43,59 ⁰	+ 44,24 ⁰
Sensor 1b	Meßphase	- 40,78 ⁰	+ 153,28 ⁰	- 43,59 ⁰	+ 150,47 ⁰
	Nullp. korr.	- 68,20 ⁰	- 65,38 ⁰	- 71,00 ⁰	- 68,20 ⁰
Sensor 2	1. Azimut	- 172,97 ⁰	- 161,72 ⁰	+ 164,53 ⁰	+ 175,78 ⁰
	2. Azimut	- 127,97 ⁰	- 116,72 ⁰	- 150,47 ⁰	- 139,22 ⁰
	3. Azimut	- 82,97 ⁰	- 71,72 ⁰	- 105,47 ⁰	- 94,22 ⁰
	4. Azimut	- 37,97 ⁰	- 26,72 ⁰	- 60,47 ⁰	- 49,22 ⁰
	5. Azimut	+ 7,03 ⁰	+ 18,28 ⁰	- 15,47 ⁰	- 4,22 ⁰
	6. Azimut	+ 52,03 ⁰	+ 63,28 ⁰	+ 29,53 ⁰	+ 40,78 ⁰
	7. Azimut	+ 97,03 ⁰	+ 108,28 ⁰	+ 74,53 ⁰	+ 85,78 ⁰
	8. Azimut	+ 142,03 ⁰	+ 153,28 ⁰	+ 119,53 ⁰	+ 130,78 ⁰
MIT VORHALT: 7,03 ⁰ zeitlich später					

7. Azimut

97,03°

108,28°

- 74,53°

85,78°

Table 10: Azimuthal angle of sensors for F2 and P, in relation to the HELIOS-Sun line.

Negative sign refers to Eastern directions. The order of the channels is equivalent to the rotation of HELIOS 2 from East to West, i.e. in a clockwise direction when viewed from the North.

Messwinkel = measuring angle
 Kein vorhalt = No derivative action
 Ohne verschiebung = Without shift
 Mit verschiebung = with shift
 Anfang = Beginning
 Integrations-Zähler = Integrations counter
 Mit vorhalt = with derivative action
 zeitlich später = later in time

reducing the data in the data and storage control run. Here those data to be passed to the memory to be selected. At the same time, this unit concerned - controlled by the control flow - that the respective data in the prescribed space are written. Another part of this Unit ensures - controlled by the satellite telemetry that the memory content is delivered to the telemetry bit - and Word-serial.

Those signals are obtained from the control flow at the same time, which control the sensors, i.e. the energy channels, etc. set. These signals are routed to the sensors with control signals from the control unit of the program selection logic of each switched on digital electronics. Figure 18 is also clearly which parts of the electronics box are redundant, namely:

- Data switching logic
- all counters
- Reduce plant
- Control of flow.

It seems as if the data and storage control unit would constitute a bottleneck regarding the reliability of data processing. That is not the case, is from Figure 19 clearly showing the units of the electronics box slightly clearer.

The control of data contains only the maximum viewfinder for the data of sensor 1a and sensor 3. Also associated with each memory (functionally limited - a memory is written a spin-synchronous with experiment data, the other is read synchronously from the telemetry) its own disk controller. Thus a data control is, i.e. Selection of the data to be stored, performed only in the normal data mode of this unit. In data-mode, this unit virtually represents a short circuit as the data selection in this program directly from control flow, which is redundant.

This means that in Normal-Data-Mode-operation in case of failure of Maximum

finder (data control) that are not to use the data under certain circumstances. In this case can immediately on high-data-mode program be switched, because here the maximum viewfinder while running, but is not required, because the data control is performed by the redundant control of flow in this program. The failure of a storage controller or a memory, however, has more serious consequences. While in the above case, no data is lost, only the half time resolution is given in this case in the normal data mode operation, i.e. only every second data block is evaluated. In the high data mode operation, only every second block of data is transmitted when a storage controller or a memory failure, i.e. that only you are transferred half of the energy channels. In this case, the switch over to the normal-data-mode program can help immediately.

Such emergencies did not occur until late 1979. The redundant digital electronics D2 (see Figure 18) was tested in each case after the start, but since then no longer to be used.

In the program control unit is also the command of tele reception - register. Here, all the received commands are stored and raised their execution at the appropriate time.

The power supply of the experiment is done via a main voltage converter (main converter), which by the probe supplied to so called "power ground"-related 28 VDC main bus voltage converts and refers to "signal ground". This is done in a converter that is synchronized with the 120 kHz synchronization frequency of the probe. The switching on and off of the experiment is done by switching on or off the voltage of 28 V on the side of the probe.

This main power converter provides for the following units separate voltages, which are permanently present, as soon as the experiment is turned on

- Memory 1 memory control 1 (M1)
- Memory 2 memory control 2 (M2)
- Data control
- Program Control (MP)
- Data interface

The separate voltages for the Digital electronics are switchable via tele command.

Also provides the main transformer yet another + 28 V voltage, switch led to the individual sensors via separate, to be controlled, with tele-commands. Figure 20 shows the voltage distribution within the experiment and the single - switch-off possibilities.

The unit selection logic (digital sensor interface) is supplied with voltage by the individual sensors. This means that only those components in operation are actually used, i.e. If the associated sensors, which the control signals are sent, are turned on.

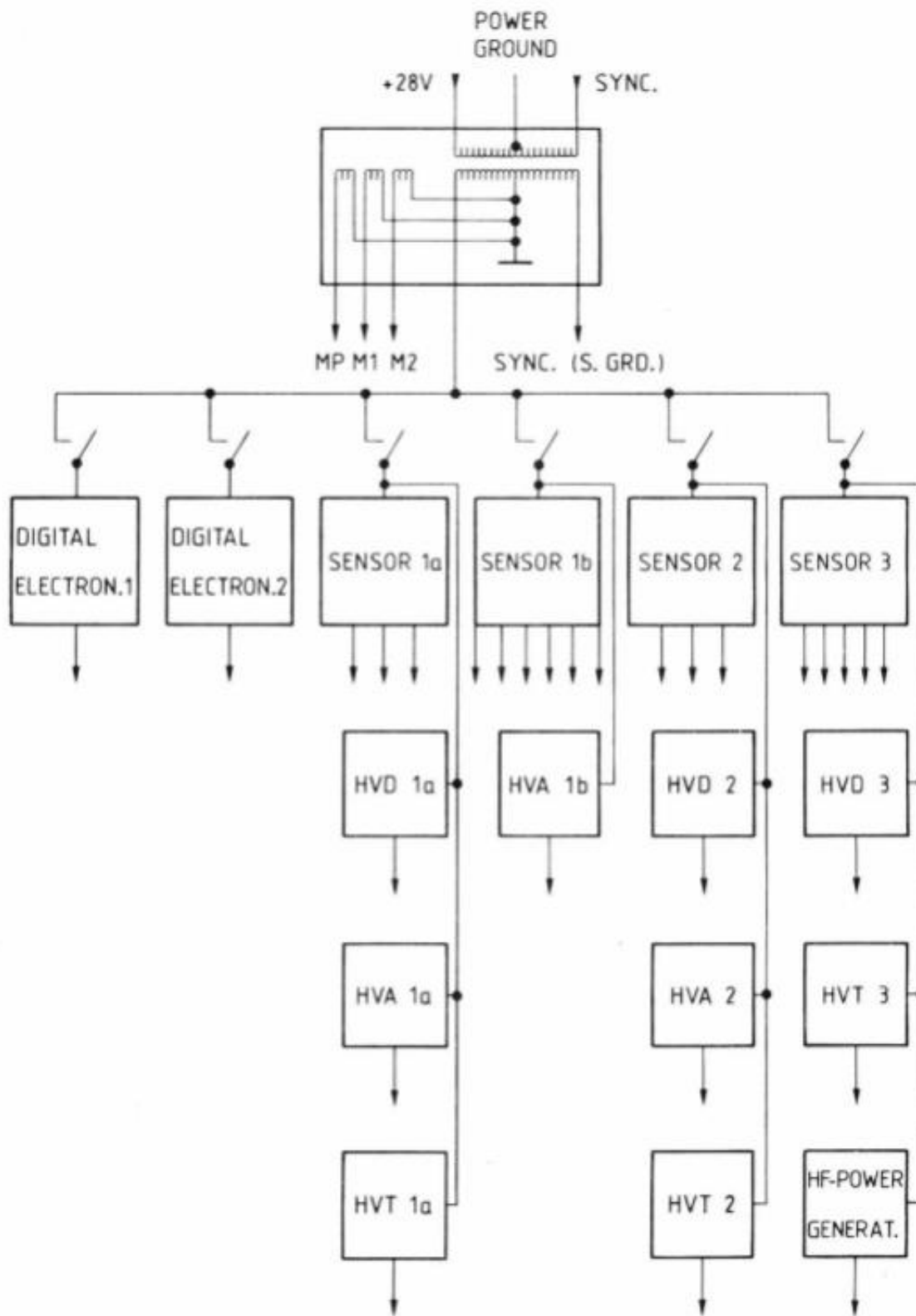


Fig. 20: voltage distribution in the experiment

4. Organization of data generation and data transmission

The instrument 1a produced in every HELIOS turn, so per second in 9 elevation and 16 azimuth channels together 144 readings in the form of a 16-bit counter. That alone exceeds already the maximum upper transmission rate of HELIOS. There must occur a pre-evaluation and reducing the data still on board. Initially all data - converted as described later - in 8 bit words. Still, two different measuring programs were provided to reduce data that allow even a certain adaptation to the strongly varying bitrates of the probe.

Normal data mode (NDM)

The most interesting part of the spectrum of ion - protons and α -particle - meets most of the time only a fraction of the entire measuring range, but shifted due to the known fluctuations of solar wind all the time. The "normal data mode" measurement program (NDM) for medium and low bitrate is adapted. Here first look up the maximum of the intensity of Proton experiment internal logic, i.e. the address of the measuring channel in energy (EN), azimuth (AZ) and elevation (EL), in which the highest count rate occurred. In the next measuring cycle only a limited number of measuring channels around this maximum is registered, namely $9 \times 5 \times 5$ (EN x AZ x EL), 225 so values. The nine energy channels are designed that even the helium ions - such as the double E/q ratio of protons - are yet covered. Meanwhile, already a new maximum for the next cycle is determined over the whole measuring range.

In addition, the "integration counter" for I1a and I3 in each energy channel provides a count rate which is created by summing all azimuth and elevation channels - also those are just not transferred on the basis of the selected maximum -. This allows for the estimation of the marginal areas occasionally cut off the three-dimensional measurement and also a direct comparison with the instrument that is also an integral and directly measuring the ion current 1B. Also its 32 results per cycle are always transferred.

When I3 instead of I1a is turned on, applies a similar selection process, with some differences in the NDM: in the first 16 turns of a cycle the full speed range is searched again a maximum of Proton distribution (so for $M/q = 1$). This is then used as at I1a as Centre for the 225 readings from the first 16 Revolutions of the next cycle. In each case during the revolutions 17 - 32 only works the integration counter. With a fixed "speed channel", where the protons previously had the highest intensity, all M/q -values are sequentially set. This program is based on the observation that the average speed of different ions is always pretty much equal to that of the proton. The integration over the angle makes sense due to the very low density of heavy ions.

So we knew it until 1974. Meanwhile, just the HELIOS-have measurements shown that α -particles are often much faster than Protons: especially in fast solar wind streams (sometimes in slow), and particularly dramatically close to perihelion.

When operating in the NDM, I3 here must almost inevitably miss the α -particles. On the other hand, the Proton Spectra completely purified by α -particles are particularly interesting here.

Operation of I3 the NDM can enter a special case: if the maximum channel is higher than in channel V_{10} , at the end of the 16th Revolution still not 225 results measured. In this case, in turn 17, 18, etc. will also in each 5×5 direction channels measure, until filled up the store with the 225 data values. Following the program-sequence valid from rotation 17 onwards, the maximum speed channel is thereby set and after each rotation the M/q channel is advanced. Thereby, one obtains in addition to the integrated M/q spectrum from rotation 17 to 32 the spatial orientation of some M/q channels. To make this effect well to exploit, the somewhat unusual order of M/q channels (see table 7) was elected. From I2 all 16 energy channels transmitted by either part A or part B in 8 azimuth channels, altogether 128 values per cycle. Part A or B are selected by command. Figure 21 shows the arrangement of the data of the individual instruments in the data frame.

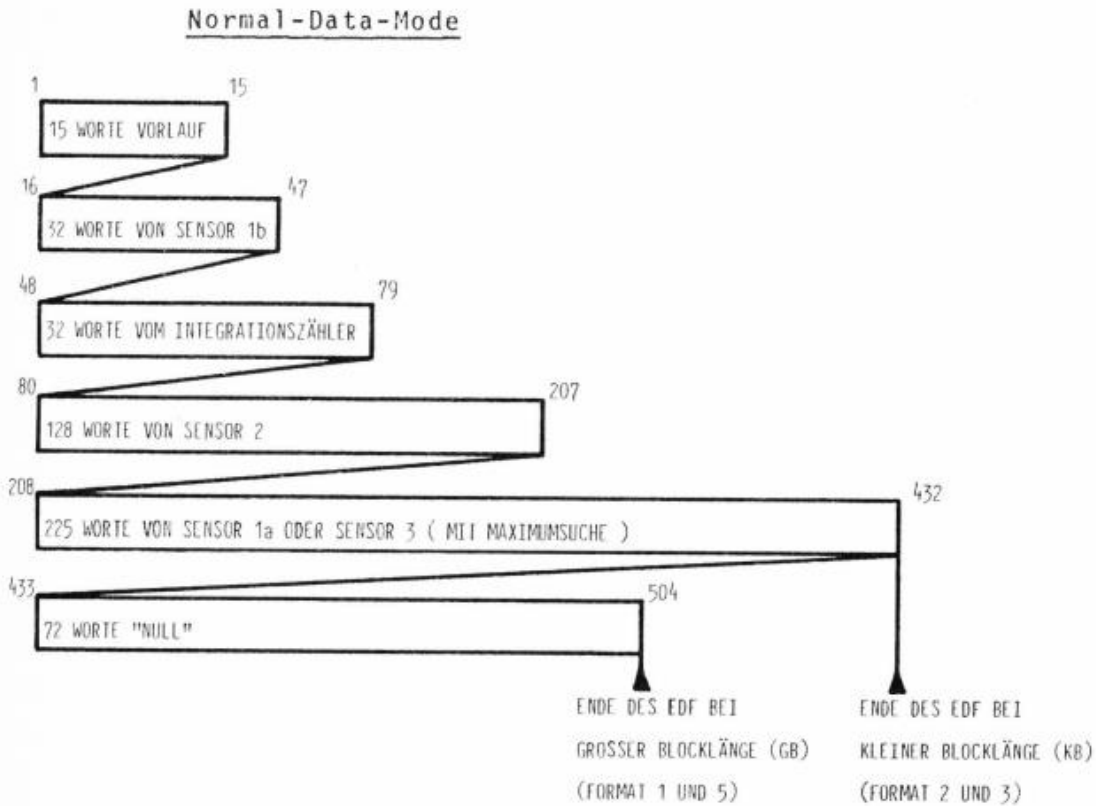


Figure 21: Structure of the experiment data frame (EDF) at normal data mode (NDM).

Translation from top to bottom, left to right:

- 15 words preceding
- 32 words from sensor 1b
- 32 words from integrations counter
- 128 words from sensor 2
- 225 words from sensor 1a or sensor 3 (with maximum search)
- 72 Words ''zero''
- End of the EDF at large block length (GB) (Format 1 and 5)
- End of the EDF at smaller block length (KB) (Format 2 and 3)

High data mode (HDM)

In the case of high bit rates "High-Data-Mode" (HDM) can be toggled to a command and on the measurement program. Here, the range selection by maximum provision is eliminated. I1a and I3, a fixed grid of 7 x 7 angle channels is transferred for 8 energy channels. These are the channels AZ 5 to AZ 11 or EL 2 to EL 8. When HDM going despite low bit rate and correspondingly shorter block length of 432 instead of 504 words, also EL 8 is still omitted.

Unfortunately, the solar wind is blowing sometimes from an other direction, as for the selection of AZ 5 until AZ 11 accepted. We had us and also the election of the "hold-back angle" by 11.2° at the slow Wind is oriented in terms of perihelion. At $v \approx 300 \text{ km s}^{-1}$ and a HELIOS ground speed of 60 km s^{-1} occurs a radial flowing wind under $\alpha \approx -12^\circ$ to HELIOS 1. More often we found however fast wind ($v > 600 \text{ km s}^{-1}$) in the aphelion, where the ground speed is only 25 km s^{-1} . There is the "declination" only 2° , nearly 2 azimuth channels in addition to the selected middle of the measuring range (see table 9). In the HDM so unfortunately sometimes important parts of the distribution were cut off. In extreme cases, we were forced even despite the availability of a high-bitrate to operate in the NDM, where this designation is so irrelevant. This justifies belated decision to control the choice of NDM and HDM not automatically by the bit rate but by ground command.

Due to this experience we made a change at HELIOS 2: we introduced an additional command, with the entire range of instruments can be moved around 7.03° . In this position, the "declination" due to the high line speed in the perihelion phases in the middle is compensated fairly well (see table 10).

The 32 energy channels are divided into 4 blocks (HDM1 to HDM 4) each with 8 channels. Each of these groups is filling a whole data frame (EDF) for himself. At the highest data rate of 2048 BPS can all 10,125 s

a block of HDM are sent, so after 40.5 seconds all 4 blocks of a measuring cycle energy full-resolution each with 7 x 7 direction channel are available. Again, the result is the highest time resolution can be achieved already with 256 BPS in the NDM. If the bit rate is lower than 2048 BPS (for example 1024, 512, etc. BPS), correspondingly long pauses between the HDM-blocks are inserted in the HDM (10.25 s; 20.25 s; 40.5 s etc.).

If this breaks longer than 20.25s operation in HDM is often meaningless because no longer match the HDM blocks due to faster temporal changes in the solar wind. Therefore, mission control was reliant always to switch from HDM to NDM if the breaks are longer than 10.125 s.

At I3 during the second part of the cycle the speed channels are again saved and the angle-resolved mass channels are cycled through. However, the speed channel is advanced after each cycle, irrespective of the proton maximum. After 16 cycles you have got for each of the 16-M/q values a three dimensional spectra as well as 16 additional proton spectra. I2 both parts of the program are transferred to the HDM always completely, as well by I1b and by the I1a/I3 integration counter.

The arrangement of the data of a HDM block in the data frame shown in Figure 22.

High-Data-Mode

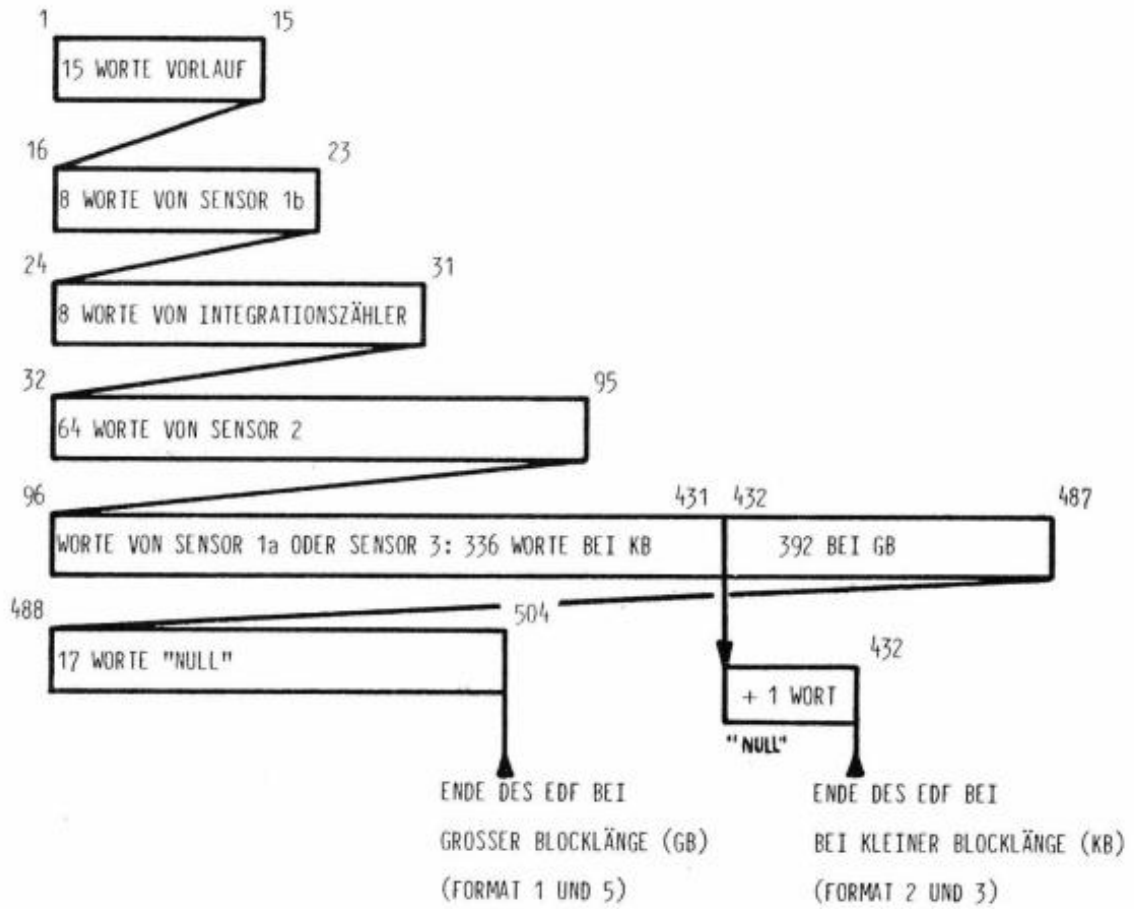


Figure 22: Structure of the experiment data frame (EDF) at high-data mode (HDM).

Translation from top to bottom, left to right:

- 15 words preceding
- 8 words from sensor 1b
- 8 words from integrations counter
- 64 words from sensor 2
- Words from sensor 1a or sensor 3: 336 words in KB
392 in GB
- 17 Words ''zero''
- + 1 Word ''zero''
- End of the EDF in large block length (GB) (Format 1 and 5)
- End of the EDF in small block length (KB) (Format 2 and 3)

The E1 data into the stream of telemetry data from HELIOS

First, it is explained how the E1 data are inserted in the telemetry data from. Due to the highly variable telemetry conditions according to the distance of HELIOS - Earth, between 0 and 2 AU varies, there are many variations. By Tele-command operation can be adapted each external conditions by E1.

The probe telemetry system

Due to the strongly changing during the HELIOS mission telemetry conditions (to be bridged distance 2 AU i.e. 300 million km, 3 different on-board antennas, 3 different power levels, 3 different antenna systems on Earth) the transmission bit rate of the probe between 8 BPS up to 4096 BPS. At certain times, even no telemetry connection is possible ("blackout" before and behind the Sun); data in the large 500 k-board - memory inscribed and later transmitted to Earth.

The table 11 shows all potential telemetry conditions and their consequences for E1.

Some explanations to do this:

- A "word" (word) of HELIOS telemetry consists of 8 bits.
- A 'framework' (s/c-frame) contains 155 words (1142 bit), which are divided on the experiments and include also housekeeping-data.
- The six "formats" (format, FM1, FM2... FM6), regulate the distribution of words of a framework for individual experiments.
(FM4 contains only Housekeeping data, and FM6 E1 is not involved in. Both are therefore not listed in table 11.)
- A "main frame" (main frame) contains 72 frames, regardless of format and bit rate.
- An "experiment data frame" (experiment data frame, EDF) includes a self-contained block of data of an experiment, i.e. a complete measurement cycle in the NDM, or a quarter of a cycle in the HDM.

FORMAT	FM 1	FM 2	FM 3	FM 5
	HIGH RATE	NORMAL RATE	REDUCED RATE	VERY HIGH RATE
BITRATEN (bps)	512 1024 2048	32 64 128 256 512	8 16 32 64	4096
BLOCKLÄNGE: 8 BIT-WORTE BITS	504 4032	432 3456	432 3456	504 4032
WORTE/RAHMEN	28	48	24	14
SUBKOMMUTIERUNGSRATE	18	9	18	36
AUSLESEZEIT FÜR 1 SPEICHER	10,125 s at 2048 bps	40,5 s at 256 bps		10,125 s
DATENANTEIL DES EXPERIMENTS %	20,6 %	35,3 %	17,6 %	9,7 %

Table 11: Overview of the data formats and the shares of E1.

Bitraten = BIT rate

Blocklänge = Block Length

Worte/ Rahmen = Words/Frame

Subkommütierungsrate = Sub Communication Rate

Auslesezeit für 1 speicher = Selection time for 1 store

Datenanteil des Experiments = Data portion of the experiment

- The "sub commutation rate" (subcommrate) refers to how many frames an EDF is divided.
- The "elite"TimeFor 1 EDF is given by

$$\frac{\text{Sub commutation rate} \times \text{frame length (bits per frame)}}{\text{Bit rate}}$$

The block length provided to E1 is dependent on the format. In FM1 and FM5 is 504 words (big block length, GB), FM2 and FM3 432 words (small block length, KB).

In table 12, the selection times for 1 EDF are put together for the different formats and bit rates. You can see here, that for example by 32 BPS the read-out time in FM2 with 364 s only half as long is like in FM3 at the same bitrate. The same applies for 512 BPS between the FM1 and FM2. FM2 for E1 is also better.

Of course, the high proportion of E1 on the total data rate of 35.3% is in FM2 at the expense of other experiments. That is why this compromise was negotiated between the experimenters: for the Time, where at all between the FM2 and FM1 or FM3 can be selected, FM2 used to 50%. Usually shuts alternately depending on a whole passage (over a ground station) in one or the other format.

Block structure of the E1 telemetry data

First 21 and 22 refers to the images, which show the block construction of the data framework of E1.

Tables 13 and 14 show the structure of the experiment data frames again separately for normal data mode and high data mode. Both data frames differ only by the data units of each instrument. Each EDF begins with 15 words (W) "Advance"-data that indicate the operating status of the experiment for the following data in the digital encoding.

The number of real experiment data is not fully adapted for technical reasons of length of EDF. This can be seen from the following list:

Format	Bit rate (bit / s)	Elite time for 1 EDF (s)	Measuring time (s) $\pm 1.7\%$	Distance two blocks of data (s)	Program
Format	Bitrate (bit/s)	Auslesezeit für 1 EDF (s)	Meßdauer (s) $\pm 1,7 \%$	Abstand zweier Daten- blöcke (s)	Programm
3	8	2592	32	2592	NDM
	16	1296	32	1296	NDM
	32	648	32	698	NDM
	64	324	32	324	NDM
	(64)	324	$(9+311)x3+9$	$324x4$	HDM)
2	64	162	32	162	NDM
	(64)	162	$(9+151)x3+9$	$162x4$	HDM)
	128	81	32	81	NDM
	(256)	81	$(9+ 71)x3+9$	$81x4$	HDM)
	256	40,5	32	40,5	NDM
	(256)	40,5	$(9+ 31)x3+9$	$40,5x4$	HDM)
	512	20,25	32	40,5	NDM
512	20,25	$(9+ 11)x3+9$	$20,25x4$	HDM	
1	512	40,5	32	40,5	NDM
	(512)	40,5	$(9+ 31)x3+9$	$40,5x4$	HDM)
	1024	20,25	32	40,5	NDM
	1024	20,25	$(9+ 11)x3+9$	$20,25x4$	HDM
	2048	10,125	32	40,5	NDM
	2048	10,125	$(9+ 1)x3+9$	$10,125x4$	HDM
5	2048	20,25	32	40,5	NDM
	2048	20,25	8	$20,25x4$	HDM
	4096	10,125	32	40,5	NDM
	4096	10,125	8	$10,125x4$	HDM

Table 12: time resolution and program opportunities depending on format and bit rate.

Note: In the HDM, a measurement consists of 4 EDFs. Therefore, HDM is not used if the distance between the EDFs is greater than 20,25 s (bracketed values).

Normal-Data-Mode

WORT-Nr.	INFORMATION	ANZAHL DER WORTE
1 ⋮ 15	VORLAUF	15
16 ⋮ 47	DATEN SENSOR 1b	32
48 ⋮ 79	DATEN INTEGRATIONSZÄHLER	32
80 ⋮ 207	DATEN SENSOR 2	128
208 ⋮ 432	DATEN SENSOR 1a ODER SENSOR 3	225
----- EDF - ENDE BEI KB -----		
433 ⋮ 504	"NULL"	72
----- EDF - ENDE BEI GB -----		

Table 13: Layout of the experiment data frame (EDF) at normal data mode.

- Wort-Nr. = Word no.
- Anzahl der worte = Number of words
- Vorlauf = leader
- Daten = data
- Integrationszähler = integration counters
- Oder = or
- Ende bei = end with
- Null = Zero

High-Data-Mode

WORT-Nr.	INFORMATION	ANZAHL DER WORTE
1 ⋮ 15	VORLAUF	15
16 ⋮ 23	DATEN SENSOR 1b	8
24 ⋮ 31	DATEN INTEGRATIONSZÄHLER	8
32 ⋮ 95	DATEN SENSOR 2	64
96 ⋮ 431	DATEN SENSOR 1 ODER SENSOR 3 BEI KB + 1 WORT	336
----- EDF - ENDE BEI KB -----		
487 ⋮ 504	DATEN SENSOR 1 ODER SENSOR 3 BEI GB "NULL"	56 (392) 17
----- EDF - ENDE BEI GB -----		

Table 14: Layout of the experiment data frame (EDF) in high data mode.

Wort-Nr. = Word no.
 Anzahl der worte = Number of words
 Vorlauf = leader
 Daten = data
 Integrationszähler = integration counters
 Oder = or
 Bei = at/with/in
 Ende bei = end with
 Null = Zero

	available EDF-length	generated data per NDM	EDF HDM
Format 2 and 3 (KB)	432W	432W	431W
Format 1 and 5 (GB)	504W	432W	487W

Those words of EDF which are not filled with data, are also encoded by "Zeros" - filled.

As you can see from the above list, the HDM program on the formats 1 and 5 (GB) is aligned with the high bit rates. This program is applicable also at the lower bitrates of the formats 2 and 3 (KB). Then 56 less words transmitted in the data block from I1a or I3, compared to the normal data block of 487 words. This is done by omitting the channel EL 8 in all 7 azimuth channels at all 8 energy channels of the respective HDM block.

The tables 15 to 25 can exactly detect the formation of each individual reading of all instruments in the different modes of E1.

Normal-Data-Mode

WORT-Nr.	KANAL	BEDEUTUNG
16	EN 1	ZÄHLERGEBNIS
17	EN 2	ZÄHLERGEBNIS
⋮	⋮	⋮
47	EN 32	ZÄHLERGEBNIS

High-Data-Mode

WORT-Nr.	KANAL				BEDEUTUNG
	HDM 1	HDM 2	HDM 3	HDM 4	
16	EN 1	EN 9	EN 17	EN 25	ZÄHLERGEBNIS
17	EN 2	EN 10	EN 18	EN 26	ZÄHLERGEBNIS
⋮	⋮	⋮	⋮	⋮	⋮
23	EN 8	EN 16	EN 24	EN 32	ZÄHLERGEBNIS

Table 15: Structure of the data from sensor I1b

Translation key:

Wort-Nr. = Word no.

Kanal = Channel

Bedeutung = Importance

Zählergebnis = Counting results

Normal-Data-Mode

INTEGRATIONSZÄHLER SENSOR 1a

WORT-Nr.	KANAL	BEDEUTUNG
48	EN 1	ZÄHLERGEBNIS
49	EN 2	ZÄHLERGEBNIS
⋮	⋮	⋮
79	EN 32	ZÄHLERGEBNIS

High-Data-Mode

WORT-Nr.	KANAL				BEDEUTUNG
	HDM 1	HDM 2	HDM 3	HDM 4	
24	EN 1	EN 9	EN 17	EN 25	ZÄHLERGEBNIS
25	EN 2	EN 10	EN 18	EN 26	ZÄHLERGEBNIS
⋮	⋮	⋮	⋮	⋮	⋮
31	EN 8	EN 16	EN 24	EN 32	ZÄHLERGEBNIS

Table 16: Structure of the data of the integration counter of I1a

Translation key:

Integrationszähler = Integration counter

Wort-Nr. = Word no.

Kanal = Channel

Bedeutung = Importance

Zählergebnis = Counting results

Normal-Data-Mode

INTEGRATIONSZÄHLER SENSOR 3

WORT-Nr.	KANAL	BEDEUTUNG
48	F1 M3	ZÄHLERGEBNIS
49	F2 M3	
...	...	
63	F16 M3	
64	F(z) M1	
65	F(z) M2	
79	F(z) M16	

High-Data-Mode

WORT-Nr.	KANAL				BEDEUTUNG
	HDM 1	HDM 2	HDM 3	HDM 4	
24	F1 M3	F9 M3	F(1-16) M1	F(1-16) M9	ZÄHLERGEBNIS
25	F2 M3	F10 M3	F(1-16) M2	F(1-16) M10	
...	
31	F8 M3	F16 M3	F(1-16) M8	F(1-16) M16	

Legend: $F(z)$ = frequency channel (speed channel) the maximums

$F(1-16)$ = Frequency canal (speed channel) the HDM counter sensor 3 (speed channel counter)

Table 17: Structure of the data of the integration counter I3.

Translation key:

Integrationszähler = Integration counter

Wort-Nr. = Word no.

Kanal = Channel

Bedeutung = Importance

Zählergebnis = Counting results

Normal-Data-Mode

SENSOR 1a

WORT-Nr.	KANAL	BEDEUTUNG	
208	EL (x-2)	ZÄHLERGEBNIS	
209	EL (x-1)		
210	EL (x)		
211	EL (x+1)		
212	EL (x+2)		
213	EL (x-2)		
214	EL (x-1)		
215	EL (x)		
216	EL (x+1)		
217	EL (x+2)		
218	EL (x-2)		
222	EL (x+2)		
223	EL (x-2)		
227	EL (x+2)		
228	EL (x-2)		
232	EL (x+2)		
233	EL (x-2)		
257	EL (x+2)		
258	EL (x-2)		
432	EL (x+2)		
	Az (y-2)		
	Az (y-1)		EN (z-2)
	Az (y)		
	Az (y+1)		
	Az (y+2)		
	Az (y-2)		EN (z-1)
	Az (y+2)		
	Az (y-2)		EN (z)
	Az (y+2)		EN (z+6)
			ZÄHLERGEBNIS

Legend: EL (x) = MAXIMUM ELEVATION channel
 AZ (y) = MAXIMUM azimuth channel
 EN (z) = MAXIMUM energy channel

Table 20: Structure of the data of I1a, normal data mode.

Translation key:
 Wort-Nr. = Word no.
 Kanal = Channel
 Bedeutung = Importance
 Zählergebnis = Counting results

High-Data-Mode und große Blocklänge

SENSOR 1a

WORT-Nr.	KANAL				BEDEUTUNG
	HDM 1	HDM 2	HDM 3	HDM 4	
96	EL 2 } EL 3 } EL 4 } EL 5 } Az 5 EL 6 } EL 7 }	} } } } EN 9 }	} } } } EN 17 }	} } } } EN 25 }	ZÄHLERGEBNIS
97					
98					
99					
100					
101	EL 8 } EN 1 EL 2 } EL 8 } Az 6	} } EN 10 }	} } EN 18 }	} } EN 26 }	
102					
103	EL 2 } EL 8 } Az 7	} } EN 11 }	} } EN 19 }	} } EN 27 }	
109					
110	EL 2 } Az 11 EL 8 }	} } EN 16 }	} } EN 24 }	} } EN 32 }	
144					
145	EL 2 } Az 5 } EN 3 EL 8 } Az 11 }	} } EN 16 }	} } EN 24 }	} } EN 32 }	
193					
194	EL 2 } Az 5 } EN 3 EL 8 } Az 11 } EN 8	} } EN 16 }	} } EN 24 }	} } EN 32 }	
487					

Table 21: Structure of the data of I1a, high data mode and large block length.

Translation key:
 Wort-Nr. = Word no.
 Kanal = Channel
 Bedeutung = Importance
 Zählergebnis = Counting results
 Und = and
 Große = large
 Blocklänge = Block length

High-Data-Mode und kleine Blocklänge

SENSOR 1a

WORT-Nr.	KANAL				BEDEUTUNG			
	HDM 1	HDM 2	HDM 3	HDM 4				
96	EL 2	}	}	}	ZÄHLERGEBNIS			
97	EL 3							
98	EL 4							
99	EL 5 } Az 5							
100	EL 6							
101	EL 7							
102	EL 2 } EN 1					EN 9	EN 17	EN 25
...	... } Az 6							
107	EL 7							
108	EL 2 } Az 7							
...	...							
137	EL 7 } Az 11							
138	EL 2 } Az 5	EN 10	EN 18	EN 26				
...	...							
179	EL 7 } Az 11							
180	EL 2 } Az 5	EN 11	EN 19	EN 27				
...	... } EN 3				
431	EL 7 } Az 11	EN 16	EN 24	EN 32	ZÄHLERGEBNIS			

Table 22: Structure of the data of I1a, high data mode and small block length.

Translation key:
 Wort-Nr. = Word no.
 Kanal = Channel
 Bedeutung = Importance
 Zählergebnis = Counting results
 Und = and
 Kleine = small
 Blocklänge = Block length

Normal-Data-Mode

SENSOR 3

WORT-Nr.	KANAL			BEDEUTUNG
208	EL (x-2)	}	Az (y-2)	ZÄHLERGEBNIS
209	EL (x-1)			
210	EL (x)			
211	EL (x+1)			
212	EL (x+2)			
213	EL (x-2)	}	Az (y-1)	
214	EL (x-1)			
215	EL (x)			
216	EL (x+1)	}	F (z-2), M3	
217	EL (x+2)			
218	EL (x-2)			
222	EL (x+2)			
223	EL (x-2)			
227	EL (x+2)	}	Az (y+1)	
228	EL (x-2)			
232	EL (x+2)			
233	EL (x-2)	}	Az (y-2)	
257	EL (x+2)			
258	EL (x-2)			
432	EL (x+2)	}	Az (y+2)	
		}	F (z-1), M3	
		}	F (z), M3	
		}	F (z+6), M3	
			ZÄHLERGEBNIS	

Legend: EK (x) MAXIMUM ELEVATION channel
 AZ (y) = Maximum azimuth channel
 F (z) = MAXIMUM FREQUENCY-(speed) Channel
 M = mass channel number

Table 23: Structure of the data of I3, normal mode data

Translation key:
 Wort-Nr. = Word no.
 Kanal = Channel
 Bedeutung = Importance
 Zählergebnis = Counting results

High-Data-Mode und große Blocklänge

SENSOR 3

WORT-Nr.	KANAL				BEDEUTUNG
	HDM 1	HDM 2	HDM 3	HDM 4	
96	EL 2	}	}	}	ZÄHLERGEBNIS
97	EL 3				
98	EL 4				
99	EL 5 } Az 5				
100	EL 6				
101	EL 7				
102	EL 8 } F1, M3				
103	EL 2 } Az 6				
109	EL 8				
110	EL 2 } Az 7				
144	EL 8 } Az 11				
145	EL 2 } Az 5				
193	EL 8 } Az 11				
194	EL 2 } Az 5 F3, M3				
487	EL 8 } Az 11 F8, M3				
		F9, M3	F(1-16), M1	F(1-16), M9	
		F10, M3	F(1-16), M2	F(1-16), M10	
		F11, M3	F(1-16), M3	F(1-16), M11	
		F16, M3	F(1-16), M8	F(1-16), M16	
				ZÄHLERGEBNIS	

LEGEND: F(1-16) = Frequency channel ACCORDING TO HDM-COUNTER SENSOR 3 (SPEED CHANNEL COUNTER)

Table 24: Structure of the data of I3, high data mode and large block length

Translation key:
 Wort-Nr. = Word no.
 Kanal = Channel
 Bedeutung = Importance
 Zählergebnis = Counting results
 Und = and
 Große = large
 Blocklänge = Block length

WORT-Nr.	KANAL				BEDEUTUNG
	HDM 1	HDM 2	HDM 3	HDM 4	
96	EL 2 EL 3 EL 4 } Az 5 EL 5 EL 6 EL 7	F 9, M3	F(1-16), M1	F(1-16), M9	ZÄHLERGEBNIS
97					
98					
99					
100					
101	F 1, M3	F(1-16), M1	F(1-16), M9		
102					
103					
104					
105					
106	EL 2 } Az 6 ... EL 7	F 9, M3	F(1-16), M1	F(1-16), M9	
107					
108					
109					
110					
111	EL 2 } Az 7 ... EL 7	F 9, M3	F(1-16), M1	F(1-16), M9	
112					
113					
114					
115					
116	EL 2 } Az 11 ... EL 7	F 9, M3	F(1-16), M1	F(1-16), M9	
117					
118					
119					
120					
121	EL 2 } Az 5 ... EL 7	F 10, M3	F(1-16), M2	F(1-16), M10	
122					
123					
124					
125					
126	EL 2 } Az 11 ... EL 7	F 10, M3	F(1-16), M2	F(1-16), M10	
127					
128					
129					
130					
131	EL 2 } Az 5 ... EL 7	F 11, M3	F(1-16), M3	F(1-16), M11	
132					
133					
134					
135					
136	EL 2 } Az 11 ... EL 7	F 11, M3	F(1-16), M3	F(1-16), M11	
137					
138					
139					
140					
141	EL 2 } Az 5 ... EL 7	F 16, M3	F(1-16), M8	F(1-16), M16	
142					
143					
144					
145					
146	EL 2 } Az 11 ... EL 7	F 16, M3	F(1-16), M8	F(1-16), M16	
147					
148					
149					
150					
151	EL 2 } Az 5 ... EL 7	F 3, M3	F(1-16), M3	F(1-16), M11	
152					
153					
154					
155					
156	EL 2 } Az 11 ... EL 7	F 8, M3	F(1-16), M8	F(1-16), M16	
157					
158					
159					
160					
161	EL 2 } Az 5 ... EL 7	F 8, M3	F(1-16), M8	F(1-16), M16	
162					
163					
164					
165					
166	EL 2 } Az 11 ... EL 7	F 8, M3	F(1-16), M8	F(1-16), M16	
167					
168					
169					
170					
171	EL 2 } Az 5 ... EL 7	F 8, M3	F(1-16), M8	F(1-16), M16	
172					
173					
174					
175					
176	EL 2 } Az 11 ... EL 7	F 8, M3	F(1-16), M8	F(1-16), M16	
177					
178					
179					
180					
181	EL 2 } Az 5 ... EL 7	F 8, M3	F(1-16), M8	F(1-16), M16	
182					
183					
184					
185					
186	EL 2 } Az 11 ... EL 7	F 8, M3	F(1-16), M8	F(1-16), M16	
187					
188					
189					
190					
191	EL 2 } Az 5 ... EL 7	F 8, M3	F(1-16), M8	F(1-16), M16	
192					
193					
194					
195					
196	EL 2 } Az 11 ... EL 7	F 8, M3	F(1-16), M8	F(1-16), M16	
197					
198					
199					
200					
201	EL 2 } Az 5 ... EL 7	F 8, M3	F(1-16), M8	F(1-16), M16	
202					
203					
204					
205					
206	EL 2 } Az 11 ... EL 7	F 8, M3	F(1-16), M8	F(1-16), M16	
207					
208					
209					
210					
211	EL 2 } Az 5 ... EL 7	F 8, M3	F(1-16), M8	F(1-16), M16	
212					
213					
214					
215					
216	EL 2 } Az 11 ... EL 7	F 8, M3	F(1-16), M8	F(1-16), M16	
217					
218					
219					
220					
221	EL 2 } Az 5 ... EL 7	F 8, M3	F(1-16), M8	F(1-16), M16	
222					
223					
224					
225					
226	EL 2 } Az 11 ... EL 7	F 8, M3	F(1-16), M8	F(1-16), M16	
227					
228					
229					
230					
231	EL 2 } Az 5 ... EL 7	F 8, M3	F(1-16), M8	F(1-16), M16	
232					
233					
234					
235					
236	EL 2 } Az 11 ... EL 7	F 8, M3	F(1-16), M8	F(1-16), M16	
237					
238					
239					
240					
241	EL 2 } Az 5 ... EL 7	F 8, M3	F(1-16), M8	F(1-16), M16	
242					
243					
244					
245					
246	EL 2 } Az 11 ... EL 7	F 8, M3	F(1-16), M8	F(1-16), M16	
247					
248					
249					
250					
251	EL 2 } Az 5 ... EL 7	F 8, M3	F(1-16), M8	F(1-16), M16	
252					
253					
254					
255					
256	EL 2 } Az 11 ... EL 7	F 8, M3	F(1-16), M8	F(1-16), M16	
257					
258					
259					
260					
261	EL 2 } Az 5 ... EL 7	F 8, M3	F(1-16), M8	F(1-16), M16	
262					
263					
264					
265					
266	EL 2 } Az 11 ... EL 7	F 8, M3	F(1-16), M8	F(1-16), M16	
267					
268					
269					
270					
271	EL 2 } Az 5 ... EL 7	F 8, M3	F(1-16), M8	F(1-16), M16	
272					
273					
274					
275					
276	EL 2 } Az 11 ... EL 7	F 8, M3	F(1-16), M8	F(1-16), M16	
277					
278					
279					
280					
281	EL 2 } Az 5 ... EL 7	F 8, M3	F(1-16), M8	F(1-16), M16	
282					
283					
284					
285					
286	EL 2 } Az 11 ... EL 7	F 8, M3	F(1-16), M8	F(1-16), M16	
287					
288					
289					
290					
291	EL 2 } Az 5 ... EL 7	F 8, M3	F(1-16), M8	F(1-16), M16	
292					
293					
294					
295					
296	EL 2 } Az 11 ... EL 7	F 8, M3	F(1-16), M8	F(1-16), M16	
297					
298					
299					
300					
301	EL 2 } Az 5 ... EL 7	F 8, M3	F(1-16), M8	F(1-16), M16	
302					
303					
304					
305					
306	EL 2 } Az 11 ... EL 7	F 8, M3	F(1-16), M8	F(1-16), M16	
307					
308					
309					
310					
311	EL 2 } Az 5 ... EL 7	F 8, M3	F(1-16), M8	F(1-16), M16	
312					
313					
314					
315					
316	EL 2 } Az 11 ... EL 7	F 8, M3	F(1-16), M8	F(1-16), M16	
317					
318					
319					
320					
321	EL 2 } Az 5 ... EL 7	F 8, M3	F(1-16), M8	F(1-16), M16	
322					
323					
324					
325					
326	EL 2 } Az 11 ... EL 7	F 8, M3	F(1-16), M8	F(1-16), M16	
327					
328					
329					
330					
331	EL 2 } Az 5 ... EL 7	F 8, M3	F(1-16), M8	F(1-16), M16	
332					
333					
334					
335					
336	EL 2 } Az 11 ... EL 7	F 8, M3	F(1-16), M8	F(1-16), M16	
337					
338					
339					
340					
341	EL 2 } Az 5 ... EL 7	F 8, M3	F(1-16), M8	F(1-16), M16	
342					
343					
344					
345					
346	EL 2 } Az 11 ... EL 7	F 8, M3	F(1-16), M8	F(1-16), M16	
347					
348					
349					
350					
351	EL 2 } Az 5 ... EL 7	F 8, M3	F(1-16), M8	F(1-16), M16	
352					
353					
354					
355					
356	EL 2 } Az 11 ... EL 7	F 8, M3	F(1-16), M8	F(1-16), M16	
357					
358					
359					
360					
361	EL 2 } Az 5 ... EL 7	F 8, M3	F(1-16), M8	F(1-16), M16	
362					
363					
364					
365					
366	EL 2 } Az 11 ... EL 7	F 8, M3	F(1-16), M8	F(1-16), M16	
367					
368					
369					
370					
371	EL 2 } Az 5 ... EL 7	F 8, M3	F(1-16), M8	F(1-16), M16	
372					
373					
374					
375					
376	EL 2 } Az 11 ... EL 7	F 8, M3	F(1-16), M8	F(1-16), M16	
377					
378					
379					
380					
381	EL 2 } Az 5 ... EL 7	F 8, M3	F(1-16), M8	F(1-16), M16	
382					
383					
384					
385					
386	EL 2 } Az 11 ... EL 7	F 8, M3	F(1-16), M8	F(1-16), M16	
387					
388					
389					
390					
391	EL 2 } Az 5 ... EL 7	F 8, M3	F(1-16), M8	F(1-16), M16	
392					
393					
394					
395					
396	EL 2 } Az 11 ... EL 7	F 8, M3	F(1-16), M8	F(1-16), M16	
397					
398					
399					
400					
401	EL 2 } Az 5 ... EL 7	F 8, M3	F(1-16), M8	F(1-16), M16	
402					
403					
404					
405					
406	EL 2 } Az 11 ... EL 7	F 8, M3	F(1-16), M8	F(1-16), M16	
407					
408					
409					
410					
411	EL 2 } Az 5 ... EL 7	F 8, M3	F(1-16), M8	F(1-16), M16	
412					
413					
414					
415					
416	EL 2 } Az 11 ... EL 7	F 8, M3	F(1-16), M8	F(1-16), M16	
417					
418					
419					
420					
421	EL 2 } Az 5 ... EL 7	F 8, M3	F(1-16), M8	F(1-16), M16	
422					
423					
424					
425					
426	EL 2 } Az 11 ... EL 7	F 8, M3	F(1-16), M8	F(1-16), M16	
427					
428					
429					
430					
431	EL 2 } Az 5 ... EL 7	F 8, M3	F(1-16), M8	F(1-16), M16	
432					
433					
434					
435					
436	EL 2 } Az 11 ... EL 7				

Forward words

Each EDF begins with a set of 15 8-bit words, which contain a variety of information about the operating condition of the whole experiment in addition to some code words. The code words are called

L L L L 0 0 0 0.

This pattern is easy to recognize, and is in fact used in any form of data analysis to identify the beginnings of EDF. If one were to interpret a code word as count rate and decode this bit pattern would prove as illegal.

The meaning of all words of flow emerges from the tables 26 and 27. In the test cycle, the last 5 words have a different meaning; in particular, the swapping of code words makes easily identifiable test cycles.

Some notes on the tables 26 and 27

- For safety, the maximum address is transmitted twice.

Not much help. Data failure almost always whole telemetry frame are affected by E1 so at least 14 words (see table 11). Today we would like a duplicate of the lead words in the middle of each EDF.

- The S/C-time refers to the first measurement channel of the spectrum. So can each measurement to 2^{-3} s i.e. 1/8s are precisely arranged.

It was very in the identification of some shock events helpful. But the "size" of the clock with 2^{12} s: is insufficient. She starts all 68 min 16 sec from scratch to count. It is useless for the classification of data that were written during station gaps in the on-board memory. An extension of time words to 8 bit would have been beneficial.

- Word 5 / bit 1 shows, (MV) or not (KV) are whether the energy and azimuth channels moved.
- The flow of words reveal nothing about the status of the channeltrons.

The data analysis somewhat more difficult, especially in the common switching at Perihelion between I1A and I3, that require a change of Channeltron voltages. From 4.1 kV to 3,3 kV get only about a "reset"-command that would first put the CEM-HV zero. So, it is possible that counting rates are zero for a short time in the middle of a cycle up to turn back on unless the reason is easily recognizable. As also the Housekeeping data from which the CEM-HV were to recognize, be queried only at larger intervals. Another difficulty arises from the fact that the instruments in the middle of the measurement cycle will be switched. Desirable, therefore delaying the switch until the end of the current cycle and also a new set of would control words at the end of each measurement.

WISSENSCHAFTLICHER ZYKLUS		TESTZYKLUS	
WORT-Nr.	BEDEUTUNG	WORT-Nr.	BEDEUTUNG
1	CODEWORT	1	CODEWORT
2	S/C TIME WORT 1	2	S/C TIME WORT 1
3	S/C TIME WORT 2	3	S/C TIME WORT 2
4	CODEWORT	4	CODEWORT
5	MAXIMUM REGISTER 1	5	MAXIMUM REGISTER 1
6	MAXIMUM REGISTER 2	6	MAXIMUM REGISTER 2
7	CODEWORT	7	CODEWORT
8	PROGRAMM-WORT 1	8	PROGRAMM-WORT 1
9	PROGRAMM-WORT 2	9	PROGRAMM-WORT 2
10	CODEWORT	10	CODEWORT
11	MAXIMUM REGISTER 1	11	CODEWORT
12	MAXIMUM REGISTER 2	12	CODEWORT
13	CODEWORT	13	ZUFALLSGENERATOR WORT 1
14	CODEWORT	14	ZUFALLSGENERATOR WORT 2
15	CODEWORT	15	CODEWORT

Table 26: Building of the forward words

Wissenschaftlicher Zyklus = Research Cycle

Testzyklus = Test cycle

Bedeutung = Importance

Zufallsgenerator = Random

Wort Nr. 1

Codewort

Bit 1 L
Bit 2 L
Bit 3 L
Bit 4 L
Bit 5 Ø
Bit 6 Ø
Bit 7 Ø
Bit 8 Ø

Wort Nr. 2

S/C-Time Wort 1

Bit 1	2^{12}	sec
Bit 2	2^{11}	sec
Bit 3	2^{10}	sec
Bit 4	2^9	sec
Bit 5	2^8	sec
Bit 6	2^7	sec
Bit 7	2^6	sec
Bit 8	2^5	sec

Wort Nr. 3

S/C-Time Wort 2

Bit 1	2^4	sec
Bit 2	2^3	sec
Bit 3	2^2	sec
Bit 4	2^1	sec
Bit 5	2^0	sec
Bit 6	2^1	sec
Bit 7	2^2	sec
Bit 8	2^{-3}	sec

Table 27: Meaning of the lead words (Word 1 with 3)

Wort Nr. 4

Word no.4

Codewort

Code word such
wie Wort Nr. 1
as Word no.1

Wort Nr. 5

Word no.5

Maximum-Register Wort 1

Bit 10 = KV, MV = MV

Bit 20 = 0

Bit 30 = NDM, HDM, L = HDM

Bit 4 ENRB1

Bit 5 ENRB2

Bit 6 ENRB3

Bit 7 ENRB4

Bit 8 ENRB5

Verschiebung
Shift constant
konstante Null
null data mode
Data Mode

Maximumadresse
address energy
(= 00000 EN1)

Energy channel B2⁴
Energiekanal B2⁴
Energy channel B2³
Energiekanal B2³
Energy channel B2²
Energiekanal B2²
Energy channel B2¹
Energiekanal B2¹
Energy channel B2⁰
Energiekanal B2⁰
channel B2
energy channel
B2 °

Wort no.6 6

Maximum-Register Wort 2

Bit 1 ELRB1

Bit 2 ELRB2

Bit 3 ELRB3

Bit 4 ELRB4

Bit 5 AZRB1

Bit 6 AZRB2

Bit 7 AZRB3

Bit 8 AZRB4

Maximumadresse
address
Elevation
elevation
(0001 = EL1)

Maximumadresse
Maximum
address
Azimuth
(0000 = AZ1)
azimuth (0000 =
AZ1)

Elevation channel B2³
Elevationskanal B2³
Elevation channel B2²
Elevationskanal B2²
Elevation channel B2¹
Elevationskanal B2¹
Azimuth channel B2³
Azimutkanal B2³
Azimuth channel B2²
Azimutkanal B2²
Azimuth channel B2¹
Azimutkanal B2¹
Azimuth channel B2⁰
Azimutkanal B2⁰

Table 27 (continuation): Meaning of leading words (word 4 with 6)

- Codewort wie Wort Nr.1 = code word as word No.1
- Verschiebung = Shift
- konstante null = constant zero
- Kanal = channel
- Maximumadresse = Maximum address

Wort Nr. 7

Codewort
wie Wort Nr. 1

Wort Nr. 8

Programm-Wort 1

Bit 1	∅ = Sp 2, L = Sp 1	Auslesespeichernummer
Bit 2	∅	konstante Null
Bit 3	ENZ B1	} HDM-Blocknummer HDM 2 ¹
Bit 4	ENZ B2	
Bit 5	HDMZS3 B1	} HDM-Massenka-
Bit 6	HDMZS3 B2	
Bit 7	HDMZS3 B3	Sensor 3 2 ²
Bit 8	HDMZS3	(∅∅∅∅ = MK 1) 2 ¹

Wort Nr. 9

Programm-Wort 2

Bit 1	L = S1A on, ∅ = off	Sensor 1a ein/aus
Bit 2	L = S1B on, ∅ = off	Sensor 1b ein/aus
Bit 3	L = S2 on, ∅ = off	Sensor 2 ein/aus
Bit 4	L = S3 on, ∅ = off	Sensor 3 ein/aus
Bit 5	L = D1 on, ∅ = off	Digitalelektr. 1 ein/aus
Bit 6	L = D2 on, ∅ = off	Digitalelektr. 2 ein/aus
Bit 7	L = AYL off, ∅ = on	Vorhaltewinkelverschiebung ein/aus
Bit 8	L = S2A, ∅ = S2B	Programmart Sensor 2

Table 27 (continuation): Meaning of leading words (word 7 with 9)

Codewort wie Wort Nr.1 = code word as word No.1
 Auslesespeichernummer = Readout memory number
 konstante null = constant zero
 Massenkanalzähler = Mass channel counter
 Ein/aus = on/off
 vorhaltewinkel verschiebung = lead angle offset
 Programmart = Program Type

Word no.10

Code word such as Word no.1

Word no.11 scientific cycle

Maximum register Word 1 as Word no.5

Word no.11 test cycle

Code word such as Word no.1

Word no.12 scientific cycle

Maximum register Word 2 as Word no.6

Word no.12 test cycle

Code word such as Word no.1

Word no.13 scientific cycle

Code word such as Word no.1

Table 27 (continuation): Meaning of leading words (word 10 with 13)

Wort Nr. 13 bei Testzyklus

Zufallsgenerator Wort 1

Bit 1	∅	konstante Null	
Bit 2	ELZG B1	} Zufallsgenerator Elevationskanal (000 = El 1)	2 ²
Bit 3	ELZG B2		2 ¹
Bit 4	ELZG B3		2 ⁰
Bit 5	AZZG B1	} Zufallsgenerator Azimuthkanal (0000 = Az1)	2 ³
Bit 6	AZZG B2		2 ²
Bit 7	AZZG B3		2 ¹
Bit 8	AZZG B4		2 ⁰

Wort Nr. 14 bei wissenschaftlichem Zyklus

Codewort
wie Wort Nr. 1

Wort Nr. 14 bei Testzyklus

Zufallsgenerator Wort 2

Bit 1	L = Tc2, ∅ = Tc1	Testzyklusnummer	
Bit 2	∅	Konstante Null	
Bit 3	∅	Konstante Null	
Bit 4	ENZG B1	} Zufallsgenerator Energiekanal (0000 = EN1)	2 ⁴
Bit 5	ENZG B2		2 ³
Bit 6	ENZG B3		2 ²
Bit 7	ENZG B4		2 ¹
Bit 8	ENZG B5		2 ⁰

Wort Nr. 15

Codewort
Wie Wort Nr. 1

Table 27 (continued): Meaning of the words of the lead
(Word 13 with 15)

Testzyklus = test cycle
 Zufallsgenerator = Random
 konstante null = constant zero
 bei wissenschaftlichem Zyklus = in scientific cycle

Commands and checking the execution

The operation of the instruments by telemetry commands from the Mission control central is remote control. The execution of commands, as well as other important functions are monitored continuously with the help of "housekeeping" data on the screen from mission control. An optional command automatic test cycle ("Inflighttest") allows in addition a detailed review of the status of the instruments.

Telemetry commands

There are 19 commands on separate lines from the satellite as the so called "low-power-commands" available.

In addition to the input and switching off of the entire experiment, all switching of individual instruments, the digital electronics, the channeltron high voltages and the measuring programs using these commands performed.

The commands are listed in table 28. The command numbers and names (E.g. 374-1S0F) are the names used in the operation of the mission.

Some commands are executed immediately after arrival, others only after the end of the current cycle (X marked by).

With command 004-E10N, the 28 V power supply for E1 is switched on by the probe system. This throws the main converter and transferred the whole experiment in a working condition, through the automatic execution of all commands that are marked in table 30 "Coercion". So all the instruments as well as the Digital electronics and also the Channeltron high voltages are switched off. The two stores are already active and can be read out. But while no digital electronics, storage and program control does not work. Therefore the same memory is read out in this state again and again.

This sometimes resulted in misunderstandings. After switching command 004-E10N, the store contain mostly recognizable worthless information – they had been de-energised beforehand. If however the normal operation of E1 command 374-1S0F is canceled, from then on again the last meaningful measurement cycle. This

Table 28: E1 command list

NR.	KOMMANDO-NR.	FUNKTION	ZWANG	AUSFÜHRUNG	VERIFIKATION (DHK)	RÜCKSETZEN DURCH KOMMANDO-NR.
1	003-1S1A	I1a on, I3 off		direkt	W2 B5, B6	4; 7
2	024-1S1B	I1b on		direkt	W2 B4	7
3	353-1SE2	I2 on		direkt	W2 B3	7
4	045-1SE3	I3 on, I1a off		direkt	W2 B6, B5	1; 7
5	066-1DE1	Dig. 1 on, Dig. 2 off		direkt	W2 B7, B8	6; 7
6	311-1DE2	Dig. 2 on, Dig. 1 off		direkt	W2 B8, B7	5; 7
7	374-1S0F	All off	Zwang	direkt		
8	332-1TCY	Tc on (autom. reset)		X	W1 B3	7; autom.
9	107-1V11	CEM HV 1a/3 I		direkt	} W1 B5, B6 XX	(9);7
10	270-1V12	CEM HV 1a/3 II		direkt		10; 7
11	151-1V1R	CEM HV 1a/3 off	Zwang	direkt	} W1 B7, B8 XX	9; 10
12	172-1V21	CEM HV 2 I		direkt		(13);10
13	205-1V22	CEM HV 2 II		direkt	} W1 B7, B8 XX	12; 7
14	226-1V2R	CEM HV 2 off	Zwang	direkt		12;13
15	122-1HDM	High-Data-Mode		X	} W1 B1	16; 7
16	213-1NDM	Normal-Data-Mode	Zwang	X		15
17	234-1PGA	I2A Programm		X	} W1 B2	18; 7
18	247-1PGB	I2B Programm	Zwang	X		17
19	130-1AVL	Perihel/Azim. (HELIOS-2)		direkt	W1 B4	7
		SONDEN-KOMMANDOS				
	004-E10N	E1 on		direkt		
	277-E10F	E1 off		direkt		

X = NACH ABLAUF DES LAUFENDEN MESSZYKLUS

XX = CODIERUNG SIEHE TABELLE

X = At the end of the current measuring cycle
 XX = coding see table

Let alone considered to not realize that everything has been turned off, because all the code words, status bits, and count rates are apparently fine.

Only the command 066-1DE1 or 311-1DE2 makes sure that also the memory reading works. That's why only then, if no instruments are running, zeros are generated and therefore the rest of the memory is erased. Now the code words, time words and status bits of the initial run will be set correctly and you can see what is really on or off.

130-1AVL command does not work with HELIOS 1. At HELIOS 2, it serves for switching the hold-back angle to the perihelion position. Again, it may be withdrawn only by 374-1SOF.

The instrument can not be switched off individually but only together with 374-1SOF.

This proved awkward. In the late phase of the mission, temporarily single instruments must be switched off for performance reasons. That also the non-relevant instruments, as well as the Digital electronics must be with switched off and switched on again until then, certainly increases the risk.

Three commands to get the circuit of Channeltron high voltages.

With command 107-1V11 (or 172-1V21) the CEM-HV is set to 3.3 kV. Only then you can with 270-1V12 (or 205-1V22) switch up to 3.7 kV.

4,1 kV can be achieved by again sending 107-1V11 through (or 172-1V21). Direct switching down to 3.3 or 3.7 kV is not possible. To do so must with 151-1V1R (or 226-1V2R) to zero and then shift up again.

The CEM HV commands are ineffective, if not also the corresponding sensors are switched on. When switching from I1a to I3 or vice versa automatically also the respective CEM-HV is with on or off.

The commands 234-1PGA and 247-1PGB control the measuring program I2. This affects only in the NDM because anyway both parts of the program be transferred to the HDM.

Digital housekeeping channels (DHK)

Digital housekeeping channels are used for the monitoring of command execution in the instruments. There are 4 words with each 8 bits available, parallel offered the probe system, adopted by the telemetry bit-serial, and sub-commutes in the format 4 (engineering-format) with 4 lines. There they are called B016-B019. B016 and B017 represent the State of the command register (i.e. They show have sent commands to the experiment). The words B018 and B019 reveal whether the experiment has run the commands. The importance of all the bits is broken down in table 29. Each bit has an acronym as "Name", which eases the detection. These names also appear on the screens of the Mission Control Center, where the function of all units is routinely monitored.

Housekeeping analog channels

There are nine channels of analog measurement of input streams (with sensors and electronics, words B020 to B023, C020, C021) and by the CEM - high voltages (words C022-C024). The individual measured data are shown in table 30. Also, this data is passed the satellite from the electronic box on separate lines, where they are also queried at specific time intervals and queued in the "engineering data" of the FM4.

In addition, temperatures are measured with Thermistors at all 4 devices. The analog values of the Thermistors are passed on additional lines on the telemetry of the satellite and processed there.

The digital and analog Housekeeping data, as well as the temperatures be transferred depending on the mode - approximately every second cycle.

S/C Wd Nr. S/C WD No.	Bit no.	Acronym	Meaning
B016 B016	1	NORMDM	Normal data Mode (0)
	2	12PROA	12Program A (L)
	3	CREGTC	Testcycle on (L)
	4	11BLIM	Meaning no. 3 I } 0 LOL
	5	I13CEM	CEM HV I1A/3 3 II } > 0 L L
	6		CEM HV I1A/3 I } 0
	7	I2HCEM	CEM HV 12 II } 0 3.7 3.7 4.1
	8		CEM HV 12 (L)
B017 B017	1	CREGM2	Memory 2 on (L)
	2	ZERO	Must be zero 0
	3	CREGI2	12 on (L)
	4	CREGIB	11b on (L)
	5	CREGIA	I1a on (L)
	6	CREGI3	13 on (L)
	7	CREGD1	D1 on (L)
	8	CREGD2	D2 on (L)
B018 B018	1		-i number of j { 2 ⁴
	2		\ energy /. { 2 ³
	3	ENCHAN	rchannel J { 2 ²
	4		/\ { 2 ¹
	5		1 { 2 ⁰
	6	STATTC	Testcycle on (L)(L)
	7	STATC2	Testcycle PArt 2 (L)
	8	PRENDS	Program end signal (L)(L)
B019 B019	1	STATIA	11 a on (L)
	2	DUST	I1b on (L)
	3	STATI2	12 on (L)
	4	STATI3	13 on (L)
	5	STATD1	D1 on (L)
	6	STATD2	D2 on (L)
	7	CONPOW	Power for CM MD-register on (L)
	8	STATM1	Memory 1 on (L)

Table 29: Digital housekeeping data (DHK)

Figure 23 shows an example of the practical use of the Housekeeping data at the mission control. Here is monitored on the screen, whether currents, voltages or temperatures move within allowable limits. That exceed by "soft limits" - marked by a S+ or S- behind the numerical value - is usually not critical. The two S+ in image 23 about are merely due to too tight ranges. Exceedances reported by H+ or H- by "hard limits", means the alarm, which requires immediate clarification by the party concerned for the mission control. Also, verified the arrival of commands with this screen format, and monitors their execution.

In practice we have can pull little benefit from the analog - housekeeping data. This is of course because, in part that never critical phases or even failures occurred. But the values not representative are enough. Because the current recordings E.g. vary during the measuring cycle quite sharply, due to the varying plate voltages, so that random snapshots have little significance.

Test cycle (Inflight test)

The test cycle is to provide information about the technical condition of the entire experiment. This test cycle consists of two consecutive parts and is executed instead of measuring cycles. The experiment remains in previously existing on-State.

The test cycle is started with the command of 332-1TCY. The command is reset automatically after the end of the second part.

The Declaration of expiration of a test cycle is appropriately based on a practical example. Figures 24 and 25 show a paper copy of a test cycle generated in real time in the Mission control center in the NDM. You will find all necessary explanations to do so in the comments. The HDM, a test cycle is accordingly modified.

KANAL-Nr.	ACRONYM	LEITUNG	BEDEUTUNG
1	CURRIA	ASE SA +	Eingangsstrom Sensor 1a
2	CURRIB	ASE SB +	Eingangsstrom Sensor 1b
3	CURRI2	ASE S2 +	Eingangsstrom Sensor 2
4	CURRI3	ASE S3 +	Eingangsstrom Sensor 3
5	CURRD1	ASE E1 +	Eingangsstrom Digitalelektronik 1
6	CURRD2	ASE E2 +	Eingangsstrom Digitalelektronik 2
7	CEMI1A	ASE V1 +	Channeltronhochspannung Sensor 1a
8	CEMHI2	ASE V2 +	Channeltronhochspannung Sensor 2
9	CEMHI3	ASE V3 +	Channeltronhochspannung Sensor 3

Table 30: Analog housekeeping channels
 The least significant bit means 20 mV. These voltages are directly proportional to measuring currents and voltages.

Leitung = Line
 Bedeutung = Importance
 Eingangsstrom = input current
 Digitalelektronik = Digital electronics
 Channeltronhochspannung = Channeltron high voltage

```

H-91 DSS-63  77 105 07:53:00  FORMAT 13: PAYLOAD1-E1
  B/R:2048   FM 1      DM 3-0          FN: 103

CURRIA MA +.1360E+01          STATUS  E1PWR  ON
CURRIB MA +.1240E+01
CURRI2 MA +.9800E+00        CREGM2  ON    STATM1  ON
CURRI3 MA +.4000E-01        ZERO    0    CONPOW  ON
CURRD1 MA +.3120E+01        CREGI2  ON    STATI2  ON
CURRD2 MA +.0000E+00        CREGIB  ON    STATIB  ON
CEMI1A KV +.4080E+01 S+    CREGIA  ON    STATIA  ON
CEMHI2 KV +.3640E+01        CREGI3  OFF   STATI3  OFF
CEMHI3 KV +.2800E+00 S+    CREGD1  ON    STATD1  ON
ENCHAN      25              CREGD2  OFF   STATD2  OFF

TEMPERATURES
E1ELEC  C +.1295E+02        NORMDM  HIG    STATTC  OFF
E1SEN1  C +.1540E+02        I2PROA  B     STATC2  OFF
E1SEN2  C +.2700E+02        CREGTC  OFF   PRENDS  OFF
E1SEN3  C +.1540E+02        AZSHFT  PER
                                I13CEM  4.1
                                I2HCEM  3.7
    
```

Figure 23: Representation of the digital and analog Housekeeping data from E1 in the screen format of the mission control.

UFVLR GPOC 3031 OBE PFAIFENHOFE GERIRH SPACE OPERATION CENTER
MISSION HT LIOS-A OUTPUT «BUFFERED»

5. 7.80 GMT 17H 53M 20 163MS PAGE-NO. 18
DM 3-0 5.7.0C 'G F' T 17 H 5 3 M 163Mbf: it 7 /, : cxp PAGE-NO. 11

H-90 OSS--6'.30 137 06 : 4 0 : 4 n / A 12.3F".2
ST STATUS: KL NW TIME 10:42:1 <?. 3M; M2 D1-0N

OM 3-0 FN : 21 16 1E-1 < 11R
I2-OFF I1A-ON I2-UN I1B-ON WS 15-OFF (10)

INITIAL DATA: II 11110000 10011110 01G00111 11110000 10001000 01001010 11110000 F = F 0 / 2
f-9- 111 r, n 1 o 11110000 1 1 1 1 0000 11110000

CW: 5 11 fl
I1H 15 00001011 0.0001111 11110000 1344 1536 1792 2048 2304 2560 2816 3072 3328 3584 4096 4864
< + 4.) 0.3 0
I1A INTENT: > 3 06 772 3081 * 1 r * OO 5 4 L 6 4 0 746 864 992115? 13 4 1 5 1 792 2048 243 2
RN 7-32 7316 32 0 0 3 712 4 5 5 2 * . s ö 5 0 3 2 6 6 5 6 7 ft 7 ft 5 C 0 6 1 0240 1 17 76 1 7 7 2 1 5 2 £ 7 16432 21504 2 4 5 7 ©

I1A INTENT: > 3 06 772 3081 * 1 r * OO 5 4 L 6 4 0 746 864 992115? 13 4 1 5 1 792 2048 243 2
RN 7-32 7316 32 0 0 3 712 4 5 5 2 * . s ö 5 0 3 2 6 6 5 6 7 ft 7 ft 5 C 0 6 1 0240 1 17 76 1 7 7 2 1 5 2 £ 7 16432 21504 2 4 5 7 ©

I2H
r "oi 0" 1 0 0 1 5 0 20 g 272 IFT*. 5, (-3-71 6 1 0.5 8 1472 2'4 8 294W 4096 5888 8192
0 (D 7-) ? 1 0 0 15 0 15 20 g 2 5 * i + 7 2 j) 1 0 6 8 1 53.1 7 3 '2 2944 4 0 9 6 5888 8192
100 6 : oo 77-272 47 * 5 4 4 7 3 0 1 0 6 65 3 c. * 4.) 9o 81 92
100 1 0 1 io 1 47 0 02 72 24d 4 5 4 4 7 7: - > 1 0 0 6 153c.1 2 2 4 2944 4 u 9 6 5888 5 6192
7: " 3 0 7? 0 0 200 72 564 544 763 1 0 6 8 5 3 6 * 4 0 9 6 888 8192
A/n 5 1 (15 ü 1.0 A/c 200 27? 3 * 4 5 4 4 7 6 n 1 u 8 8 15 3 n 2 14 294 4J96 5888 8192
7 ft 5 0 7? 1 0 0 1 4 0 2 au 272 5 6 f +. 544 7 6 PI 1 U 8 6 1536 7 0 4 794 4 g 9 6 5888 6192
1 0 0 1 4 0 2 au 272 3 4 4 5 * . «1» 1 53u ^ 43 2 9 * 4 0 9 6 5888 8192

II / 5
A A A T: EU 9 EL 4 47 11 L O.: I * < M T EU 1 6 ICE A 2 1 2 (?) t N 9
E L 2 L I. 3 F L 4 FL *. f. Lo E L 2 EL. 3 E L 4 EL5 E L 6 E L 2 E L 3 F L 4 E L 5 E L 6
1 5 3 1 5 3 n 1 5 13 56 1 5 3 6 1536 1336 1 5 5 6 1 5 7 53o 1 1 5 3 1 536 1 536 1536 1536
1 5 3 1334 1 5 3 3 1 3 3 0 1 5 3 0 1536 1336 1 5 3 1 5 3 f 1 53c. ' 5 c 6 1536 1 5 3 0 1536 1536
1 5 1334 1 5 1 6 1 5 2 6 1 5 3 0 1536 1536 15 3 (c) 1 576 1 536 15 3 6 1 536 1 53 0 1536 1 536 1 536
1 5 3 6 13 5 1. 153 6 15 3 c. 1 5 5 0 1536 1 5 3 0 1536 1 5 3 0 1 526 1 5 3 r 1 5 3 1536 1 5 3 0 1536 1536
53o 1 15 3 6 1 5 io 1 5 2 ü 1 5 3 0 1 5 3 1536 1 5 5 6 1536 1 5 3 0 1 5 3 0 1536 15-3o 1536 1536
t, N 1
7 ft 1 336 15 3 0 1536 15 3 6 1 5 3 0 15 3 6 1536 E N 11 15 3 6 1 5 3 1 5 3 oi 1536 1 53c. 1 536 1536 1536
1 5 T 53o 1 153 4 1 5 5 6 1 5? o 1 5 3 6 1536 15 3 6 1 3 3 6 153N 1 5 3 1536 153 6 1536 1 536
11 153 6 1 5 2 * 15 3 * 1 5 5 c 1 5 3 0 53o 1 1536 1 5 5 6 15 3 c. 1 5 3 6 1 5 3 6 1 5 3 6 15 3 6 15 3 6 1536 1536
1? «1 3 1 3 3 n 1530 1 3 1.» 153 c, «1 1536 15 3 6 1 5 3 1 53c... 1 5 3 1336 1536 1536 1 536
AZ 1 153 6 1 3 3 6 1530 1534 1 5 3 0 15 5 6 1536 1 336 153.: 1 536... 1 53 4 1 536 53o 1 1536 1 536
EM!
E N 1 4 E N 1 5
2r 1 5 3 1 33- 15 3 6 1 j 5 6 1 5 3 o 1 536 1536 15 3 6 1 5 3 6 1 53 u 15:4 1 536 53o 1 1 536 1 536
A 2 1 5 3 15 3 7 15 3 * 15 5 6 1 5 J 0 1 5 3 o 1536 1536 1 536 153 c. 1 5 3 1 536 153 6 1536 1 536
A 1 1 536 1536 1 5 3 6 15 5 6 53o 1 155c. 1536 153. 1 536 1 536 15 3 6 1 536 1 5 3 o 1536 1536
12 15 3 6 15 3 c. 1 5 5 0 1 5 5 6 1 5 3 0 1530 1536 153 6 1576 1 5 3 D 1 5 3 1536 1 536 1536
213 153. 153 6 15 3 6 1536 1 5 3 0 1 5 3 1536 1536 15 3 6 1 5 3 6 1 536 1 5 3 1 536 53o 1 1536 1536

Fig. 24: Inflight test in the NDM, first part (explanations on p. 117).

Image 24Inflight-Test in the NDM, first part

- (1) The status of E1 for this TC is decoded ("initial data") from the 15 words of flow (see table 27).
- (2) This count rates are proportional to the plate voltages of I1b.
- (3) the same for I1a.If I3 instead of I1a, applies the encoding as specified in table 32.
- (4) the same for I2.
- (5) In the NDM not the correct voltage due to long changeover time from the low energy range A to high energy sector B in the first 4 AZ-channels.
- (6) Similarly for EN25 in AZ1 and AZ2.These channels are to be omitted so when evaluating data.In the HDM this problem does not occur, because before EN17 orEN25 break are (at least) 2 s; because for each block of HDM of 8 EN channels 10 rotations available.
- (7) ZGMax returns the address of a channel invented by a random number generator in the I1a/I3 grid in an increased rate is now fed.So will the maximum searcher who must find this artificial maximum, tested, and also the corresponding shift of the measurement grid in the entire grid.The address of this artificially generated maximum is in the words of 13 and 14 of the initial run (see table 27).The encoding of the address is different for I1a and I3 (tables 31 and 32).
- (8) These are the 5 x 5 x 5 channels of I1a/I3, which are used here with a fixed frequency, so that the function of the counter can be tested. Would ZGMax happen to fall in this grid, would be at this point to see just the artificial maximum a counting rate of 3072.

Fig. 25 Inflight test in the NDM, second part

- (1) The counter of I1b is tested here from EN1 to EN16 using a test frequency.
- (2) From EN 17 to EN32 is the electrometer with a test load applied, so that the consistency of the quantization unit (1000 charges) in flight can be checked (see Figure 23).
- (3) Here the I1a integration counter with a fixed frequency will be tested.
- (4) EN15 - that is in the place of the artificial maximum - the count rate of the CCO will be shown there, corresponding to the output current of the tested CEMs (from CEM6 to ZGMax) by I1a/I3.
- (5) The I2-counter with a fixed frequency will be tested in the first four turns (EN17 - 20).
- (6) After it is hung CEM again from I2 to the counter and the UV - Glow lamp switched on. The plate voltage is switched off.

The flight showed that apparently still some Residual voltages (from a few mV) are on the plates, so solar wind electrons can penetrate. Is the only way to explain that a strong dependency on the test count rate of the AZ channel is observed, quite similar to the way they occur in the lowest EN channel. This complicates some evaluation of the test cycle. This residual voltage increases slightly at each rotation. This repeats every 8 rotations in correspondence with the voltage generation at the plates which are subdivided into 4 groups of 8. That is why the counting rate of channels EN21-24 are pretty much the same as those of EN29-32.

- (7) From here on, the threshold of the CEM-amplifier from the normal value of 5×10^5 is raised for the remainder of the test to 1×10^7 charges. If the test count rates are about the same for both thresholds, proves that the CEM still has sufficient gain.

If count rates are lower at elevated threshold, does mean that a part of the pulse contains less than 10^7 charges. Then care must be taken, and it is advisable to raise the CEM voltage. In the present case, we find: 39936 is the sum of all counts of EN21 until EN24, the comparable total of EN29 until EN32 is 31872, so 25% lower. This result should be slightly distorted by temporal variations in the intensity of the UV-Lamps and not exactly known influence of plasma electrons. Long-term trends are certainly accurate enough to realize.

- (8) The maximum seeker has detected so really the artificial maximum.
- (9) Also in I1a/I3 now burns the UV-Lamp, and the plate voltages are suspended. The count rates are different in the individual EL channels, because the illumination of channeltrons through the UV lamp is not uniform.
- (10) A fixed frequency is entered at the ZGMax address. The average count rate of the concerned channeltrons (here 268) along with the number of CCO 10752 results according to the formula of p. 134 the average amplification $\bar{G} = 1.248 \times 10^6 \times 10752/268 = 5.0 \times 10^7$.

ENERGIE EN ZG

(Vorlaufwort 14,
bit 4 - 8)

BIT					BEDEUTUNG
B1	B2	B3	B4	B5	
∅	∅	∅	∅	∅	EN-Kanal 1
∅	∅	∅	∅	L	EN-Kanal 2
⋮	⋮	⋮	⋮	⋮	⋮
L	L	L	L	L	EN-Kanal 32

AZIMUT Az ZG

(Vorlaufwort 13,
bit 5 - 8)

BIT				BEDEUTUNG
B1	B2	B3	B4	
∅	∅	∅	∅	Az-Kanal 1
∅	∅	∅	L	Az-Kanal 2
⋮	⋮	⋮	⋮	⋮
L	L	L	L	Az-Kanal 32

ELEVATION EL ZG

(Advance-Word
13-bit, 2-4)
bit 2 - 4)

BIT			IMPORTANCE
B1	B2	B3	
0	0	0	EL Kanal 5
0	0	L	EL-channel 2
0	L	0	EL channel 3
0	L	L	EL-Channel 4
L	0	0	EL Kanal 5
L	0	L	EL-channel 6
L	L	0	EL-channel 7
L	L	L	EL-channel 8

Table 31: Decoding the random number generator for I1a

Bedeutung = Importance
Vorlaufwort = Advance word

AZIMUT Az ZG

(Vorlaufwort 13
bit 5 - 8)

BIT				BEDEUTUNG
B1	B2	B3	B4	
∅	∅	∅	∅	Az-Kanal 1
∅	∅	∅	L	Az-Kanal 2
∅	∅	∅	∅	∅
∅	∅	∅	∅	∅
L	L	L	L	Az-Kanal 32

ELEVATION EL ZG

(Vorlaufwort 13
bit 2 - 4)

BIT			BEDEUTUNG
B1	B2	B3	
∅	∅	∅	EL-Kanal 5
∅	∅	L	EL-Kanal 2
∅	L	∅	EL-Kanal 3
∅	L	L	EL-Kanal 4
L	∅	∅	EL-Kanal 5
L	∅	L	EL-Kanal 6
L	L	∅	EL-Kanal 7
L	L	L	EL-Kanal 8

FREQUENZ

Da bei Sensor 3 die Energiekanäle durch Frequenzkanäle ersetzt werden und ein Maximum nur in den ersten 16 Kanälen gesucht wird, wird der betreffende Frequenzkanal nach der nebenstehenden Tabelle dekodiert:

(Vorlaufwort 6
bit 1 - 3 und
Vorlaufwort 5
bit 7)

EL-ZG			EN ZG	ZUSAMMENSETZUNG
B1	B2	B3	B4	
∅	∅	∅	∅	F 1
∅	∅	∅	L	F 2
∅	∅	L	∅	F 3
∅	∅	L	L	F 4
∅	L	∅	∅	F 5
∅	L	∅	L	F 6
∅	L	L	∅	F 7
∅	L	L	L	F 8
L	∅	∅	∅	F 9
L	∅	∅	L	F 10
L	∅	L	∅	F 11
L	∅	L	L	F 12
L	L	∅	∅	F 13
L	L	∅	L	F 14
L	L	L	∅	F 15
L	L	L	L	F 16

Table 32: Decoding the random number generator for sensor 3

Translation of text to the left:

Frequenz

As sensor 3 the Energy channels will be replaced by frequency channels and a maximum only in the first 16 channels is sought, the frequency Channel in question is decoded according to the adjacent Table:

Bedeutung = Importance
Vorlaufwort = Advance word
Zusammensetzung = Composition

Test cycles were used even before the start for precise control the function of the entire experiment. Qualification and acceptance testing experiment level were the four boxes of each E1-unit connected together, as later in the probe. Their tasks such as power supply, Sun pulse, different pulse of telemetry, data acquisition, housekeeping - words etc., were taken over by a special test device. Here, oversaw a small calculator the data generated and reported unacceptable deviations from the nominal values. The computer simulated also commands that gradually offset the experiment in the various switching States, where it was then tested. A similar test program was also always went with the experiment that is integrated in the probe. These system tests, the test program by the "HELIOS test set" (HTS) was controlled and evaluated.

After starting, a similar test program was commanded initially, as when the functional tests on the ground. Since then is commanded in routine operation only once per day a test cycle, recorded in real-time as a paper copy, then sent with the post and evaluated "by hand".

This is entirely sufficient; a transition to tape recording and computer analysis was planned for some time, then it was allowed to be dropped again . Still, the sharp eye of a savvy connoisseur of instruments is irreplaceable...

5. Description some important assemblies

Channeltron Amplifier

The Channeltron amplifier is a charge sensitive amplifier, which produces an exit voltage proportional to the charge. Within certain limits, the exit voltage is independent of the stray capacitance found at the entrance of the device. The Channeltron amplifier (see Figure 26) have a protective circuit at the entrance, Prevent damage to the entry level at any high voltage excess shock at the Channeltron. This is followed by the charge amplifier,

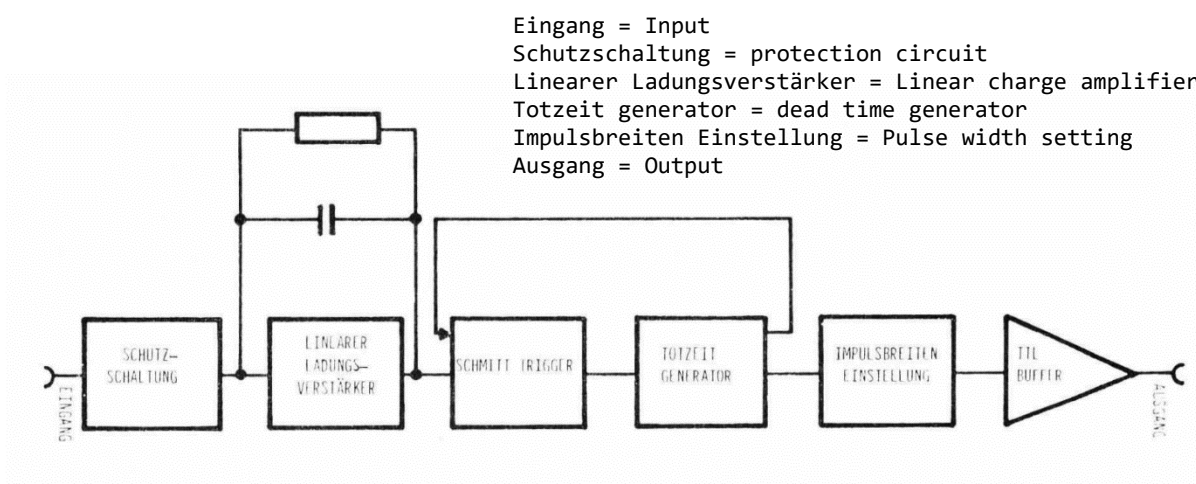


Figure 26: Channeltron amplifier, block diagram

Resistance is parallel to its recovery capacity. The time constant is designed for the highest frequency of 2 MHz.

The following circuit is a threshold discriminator which sets the input sensitivity. It is uniformly 8×10^{-14} As, corresponding to a minimum reinforcement of channeltrons of 5×10^5 . With the subsequent dead time stage the entrance of the discriminator for a period of time - so called "Dead time" - is blocked. This should amount to at all amplifiers 5×10^{-7} s \pm 10%. The subsequent pulse Shaper stage ensures a defined output pulse width at different heights of the charge pulses. The subsequent TTL fitting circuit finally ensures the required decoupling, as well as the TTL - compatibility of the output pulses.

Alongside the invariance of the time constant to threshold and temperature, a particular emphasis in the design of the amplifier was to obtain a high overloading threshold since the circuit is considerably overloaded at full Channeltron amplification.

Unfortunately, the amplifier not all fulfilled requirements to it. We would like the dead time now even shorter.

Because in some extreme cases, up to 75% measurement time of the individual channels through dead time was blocked, so that an extrapolation to the real particle flows can be just inaccurate. Although the dead time of the amplifier with the help of artificial pulse from the pulse generator was measured and adjusted. These values were also controlled at the calibration in the realistic interaction of Analyzer, channeltron, amplifiers and counters. Today a more accurate measurement in the finished instrument is desirable us but, with a possible tour of the temperature and the influence of modified Channeltron amplification - both occurs in the course of the mission - should be investigated.

Electrometer

The block diagram of the Elektrometers is shown in Figure 27. The circuit as it can be seen, divided into two parts: the actual electrometer amplifier and a quantizer facility on the basis of a CCO (current controlled oscillator). The signal current from the catcher flows to the entrance of the electrometer amplifier and there compensates with the power supplied across the feedback resistor. A corresponding current in the Integrator flows proportional to output voltage arising depending on the size of the input current. The output voltage of the Integrator exceeds a threshold value of the discriminator, the quantizer is appealing and is a counter-pole charge stored in a capacitor in the Integrator, which resets the output voltage of the Integrator to zero. At the same time with the activity of the quantizer a pulse is generated at the output led to a counter. The each output Pulse associated quantization unit QE amounts to 1.6×10^{-16} Asec, are 1000 elementary charges .

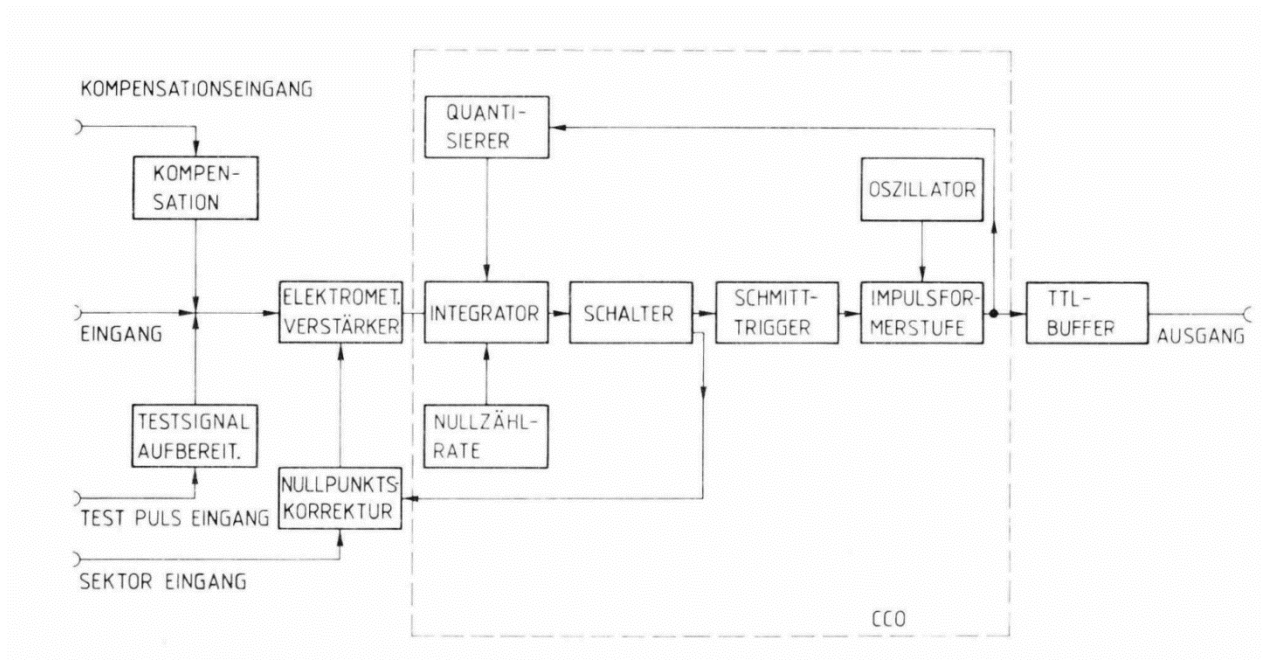


Fig. 27: Electrometer for I1b, block diagram

Kompensationseingang = Compensation input
 Quantisierer = Quantiser
 Eingang = Input
 Verstärker = amplifier
 Schalter = switch
 Impulsformerstufe = pulse shaper
 Ausgang = Output
 Aufbereitet = processed
 Null zähl rate = Zero count rate
 Nullpunktskorrektur = Zero point correction

A larger influx of false interferes with at a logarithmic presentation of results, as she here must be applied, even if it is temporally constant, since small measures are then no longer. For this reason one is so called "zero point correction" is provided. It exploited the fact that only during approximately a half of probe rotation is measured, while in the remaining time, no particles reach on the collector, because of the Sun facing direction occur no particles in the Analyzer. In this phase, an additional feedback when switched on via the switch forces the amplifier output to zero. Thus the second amplifier input input correction voltage remains effective through the store property of the capacitor during the subsequent test phase.

The calibration of the Electrometers is possible with the help of a linearly increasing voltage across a capacitor as a constant influx in the amplifier input and generates a certain count rate at the output.

There a certain capacitive penetration of to the Analyzer plates; the plate voltage on the collector cannot be avoided, the inverted and

steamed history of Analyzer voltage is applied via the compensation input. This compensates the charge created when switching the plate voltage on the collector.

To achieve integration over the amplifier noise - in particular for small count rates - a so called zero count rate of approx. 20 per measurement channel is set on the electrometer.

The electrometer works in a manner similar to a capacitor microphone: before the Ion collector a grid with negative potential must be cocked, driving back electrons to the catcher. If this mesh is shaken mechanically, capacitively couples it to the collector and deceptive charges. It is here of course undesirable. But soon after the start of HELIOS 1 the motor for the high-gain antenna in motion was used as "heard"

I1b unfortunately very clearly the apparently through friction arising structure-borne sound: the set zero count rate of 22 counts, which previously ranged on average only about 1-2 counts, now jumped between 5 and 40 counts. Later these spread declined somewhat, but it remained an uncertainty for each measured value of about ± 5 counts. This means nothing other than a reduction in sensitivity, and approximately by a factor of 5. For HELIOS 2, hastily made some changes to the I1B amplifier. The fluctuation of the count rates is here less than 1 count. As a result, the high sensitivity of the Electrometers by I1B can be exploited fully.

A temperature dependence was measured by the manufacturer for the size of the test charge fed into the flight test. During flight it is however found that the coupled test charges don't decrease with increasing temperature, but the sensitivity of the amplifier does. This is clear from comparison of the measured plasma concentrations of I1a and I1b. Of course, the instrument I1A counting particles has no temperature response. Therefore can from the ratio V_D of the densities, which has a value of 1 at 1 AU and decreases in perihelion to approximately 0.6, the

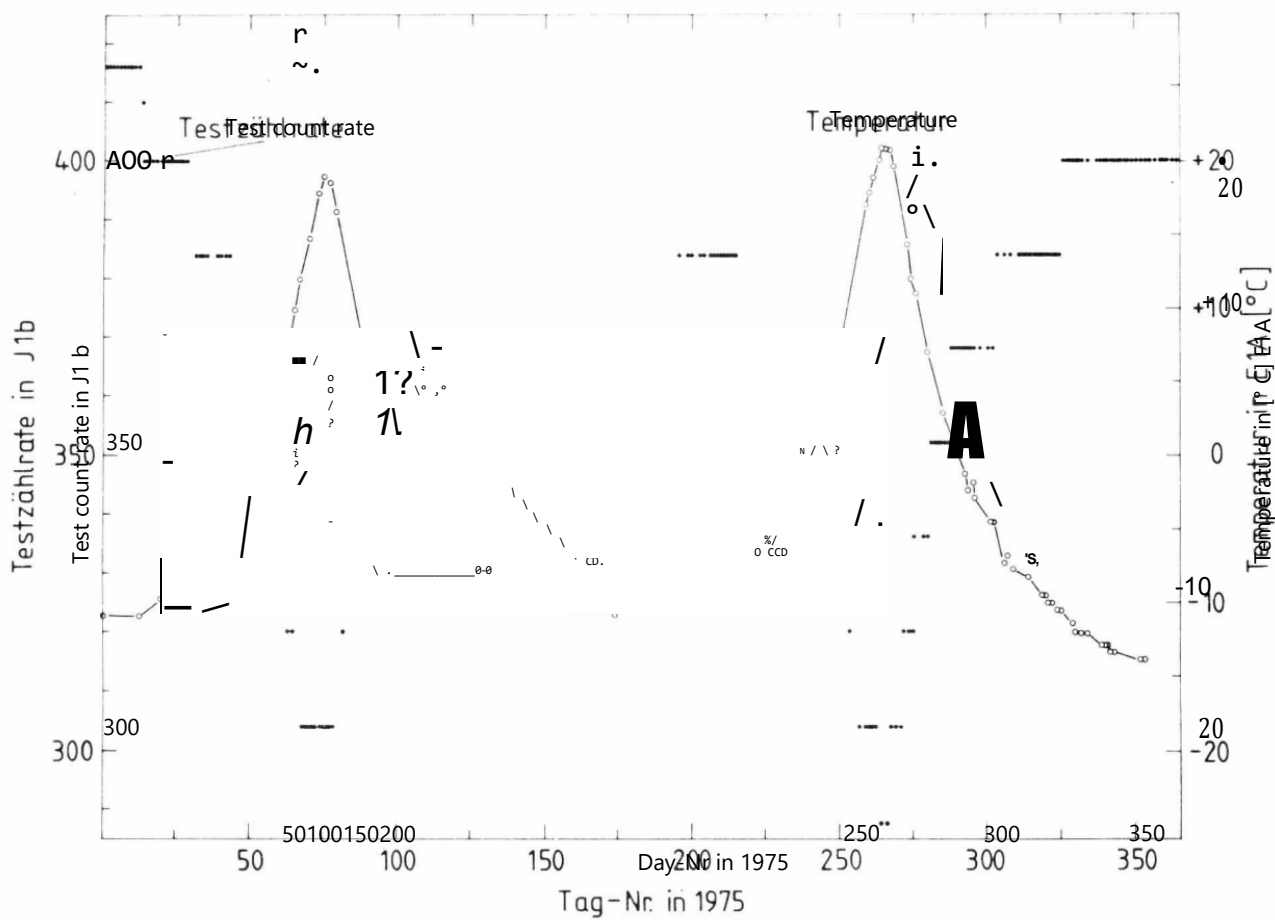
Changing the I1b sensitivity with the temperature directly derive. It showed view, that V_b (see fig. 28) follows exactly the change the test count rate in relation to their value at 1 AU. Since the test count rate at the inflight tests is regularly measured, one can derive easily the actual sensitivity of the electrometer for I1B. Therefore, this weakness of the instrument has no serious consequences.

To find this effect before the launch, we had also realistic operating with particle - temperature tests other than assessing the technical function E.g. need to perform the calibration system -.

Some characteristics of the Electrometers:

Input sensitivity	Eingangsempfindlichkeit	: $1,6 \cdot 10^{-15} \text{As}$
Dynamic range	Dynamikbereich	: $1,6 \cdot 10^{-15} \text{As} \dots 4 \cdot 10^{-11} \text{As}$
Output frequency range	Ausgangsfrequenzbereich	: 10 Hz ... 250 kHz
Quantization unit (QE)	Quantisierungseinheit (QE)	: $1,6 \cdot 10^{-16} \text{As}$
time constant	Zeitkonstante	: < 60 ms
Accuracy	Genauigkeit	: $\pm 10 \%$ für Q $1,6 \cdot 10^{-14} \text{As}$
		: $\pm 8 \%$ für Q $1,6 \cdot 10^{-13} \text{As}$
Set zero count rate	Eingestellte Nullzählrate	: 15 - 20 QE/Messung
zero point consistency	Nullpunktskonstanz	: 1 QE

Messung = Measurement



Test zählrate = Test count rate

Tag = Day

Fig. 28: Changes in test counting rates of I1b, the ratio of the measured per-proton density I1a/I1b and the I1b-temperature during the first year of the mission by HELIOS 1.

Analyzer high-voltage generation

This high-voltage generators work according to the principle of the operational amplifier (see block diagram of Fig. 29). The connection type is not inverting. This means that the transfer function is

$$U_a = U_e \cdot \left(1 + \frac{R_f}{R_e}\right)$$

Thus, the circuit works as follows:

A reference voltage U_e (switchable for operation cases "shift" and "without") is applied to the noninverting input of the differential amplifier using a voltage divider.

The output operates an actuator, which controls the amplitude of the voltage of a resonant converter. The sinusoidal output voltage transforms up into a multiplier cascade. The output voltage U_a is now fed back via high-impedance resistance R_f to the inverting input of the differential amplifier, where the single feed resistance is to ground. It is switched on the 32 logarithmically scaled output voltages such that for each a group of eight consecutive channels a certain reference voltage is applied (by switching on a specific divider resistor). So that means:

- U_{e1} for channels 1 - 8
- U_{e2} for channels 9 - 16
- U_{e3} for channels 17 - 24
- U_{e4} for the channels 25 - 32
- and 0V for 0V output voltage.

The respective 8 individual channels within the 4 groups are set by adjusting 8 different amplifications (switching of R_e). This should now be made clear with an example: it should be e.g. Channel 12 will be set. U_{e2} is applied and R_e No.4 switched on. Through this type of connection the decoding effort for the channels simplified considerably, since only $8 + 3 = 11$, information must be decoded yet another "Shift" or "without". The voltage U_{e4} is the full reference voltage, thereby saving a switch.

Some characteristics of the Analyzer high-voltage generation:

- 64 switching stages logarithmic ranked
- Output voltage accuracy : better than 1%
- Temperature dependence of the output voltage for sensor 1a and sensor 2 : $\pm 1\% \pm 50 \text{ mV}$ (-30°C ./ . $+60^\circ\text{C}$)
- Temperature dependence of the output voltage at sensor I1b : $\pm 1\% \pm 250\text{mV}$ (-30°C ./ . $+60^\circ\text{C}$)
- Output ripple voltage : 2 % ss
- Waste time constant of K32 after K1 : 200 ms
- Settling time : 3 ms

In the part of the program A I2, the maximum plate voltage is only 3.33 V (see table 5). The reference voltage is applied directly for these low voltages. To the HV cascade will be shut down via a relay. The Mercury thread relay used has typical switching times of less than 100 ms and is characterized primarily by, that it contains no magnetic components. The relay consists of a glass capillary tube, where a mercury thread by heating a small volume of gas is moving and this connects switching contacts or separates. The reset after shut-down of the filament is due to cooling of the heating volume. The cut-off speed depends only on the degree of cooling, what is normally sufficient the air. For operation in vacuum the glass tubes in a metal sheet sleeve must be matched exactly. This made unexpected difficulties of various kinds. Just a few keywords to name a few: changing heavy thermal loads, extreme requirements for components in the Interior of the sensor and finally the sudden death of the manufacturer of this relay shortly before completion. That's why we eventually had to do the assembly. While still an Indium-ring was squashed for improving the heat transfer between glass and metal. In the rest position of the relay, runs I2 in program part B, when not connected heaters in part A.

This old was declared so as fully to explain the failure of I2 on HELIOS 2. Here the heat transition described deteriorated after approx. 18 months of Mission so that the switch from program of A to B, i.e. the switch-off of the relay always

went slower. In each measurement cycle, the relay switch is independent of measurement program and data rate. Therefore, more and more energy channels of part B were now missing in all cycles. Finally, the contact was so bad that the idle state of the relay is probably at all never achieved. Therefore works since that time (about September 77) I2 HELIOS-2 in the A program only.

Channeltron high voltage generation

Therefore here only a few characteristics:

- 4 gears : 0 V; 3,3 kV; 3,7 kV; 4,1 kV
- Accuracy : ± 50 V
- Internal resistance : $1\text{ M}\Omega$
- Nominal load at I1a and I3 : $1,6 \cdot 10^8 \Omega$
- Nominal load at I2 : $1,5 \cdot 10^9 \Omega$
- Temperature dependence of the output voltage at nominal load : $\pm 1\%$ (-30°C ./ $+60^\circ\text{C}$)
- Output ripple voltage at nominal Load : $1,5 V_{SS}$

Current controlled oscillator (CCO) to the Channeltron Amplification Measure

This circuit is used together with the Channeltron amplifier during the Inflight test to measure the Channeltron amplification. The operational principle of the amplification measurement is as follows: output pulses of a channeltrons (stimulated by the calibration sources) are registered on the one hand about the Channeltron amplifier and counted in the following counters, on the other hand, the charge contents of Channeltron impulse will be transformed into a proportional number of pulses. The charge pulses of channeltrons by the catcher run to first an integrator, whose integration capacitor, as soon as the output voltage exceeds a certain threshold, again will be emptied.

At the same time a pulse is generated at the output, which can be counted. Thus, a current / frequency conversion occurs so.

The relationship between reinforcement of channeltrons and the input current of the CCO is

$$\bar{G} = \frac{i}{e \cdot f_{CEM}}$$

with \bar{G} Channeltron amplification, i the generated electricity, e the electron charge ($e = 1.6 \times 10^{-19}$ As) and f_{CEM} the number of Channeltron impulse per second. The conversion of the current i in a frequency f_{CCO} on the output of the CCO in accordance with the transfer constant

$$1 \text{ Hz} \cong 5 \text{ pA}.$$

Thus

$$\bar{G} = \frac{5 \cdot 10^{-12} \text{ Asec} \cdot f_{CCO}}{1,6 \cdot 10^{-19} \text{ Asec} \cdot f_{CEM}} = 3,12 \times 10^7 \cdot \frac{f_{CCO}}{f_{CEM}}$$

By replacing each 1 sec-related frequencies occurring during Inflight-test with count results n_{CCO} and n_{CEM} , this is the formula

$$\bar{G} = 1,248 \times 10^6 \cdot \frac{n_{CCO}}{n_{CEM}}$$

During the inflight test, depending on the value of the random generator, a Channeltron of number 2 to 8 is switched onto the CCO via a multiplexer. This multiplexer includes management while still a DC limiter. The connection of the CCO in conjunction with the channeltron amplifier is shown in Figure Figure 30. The temperature dependence of the implementation of current in frequency of the CCO is low ($\sim 4\%$ between $- 40^\circ$ and $+ 50^\circ$ C).

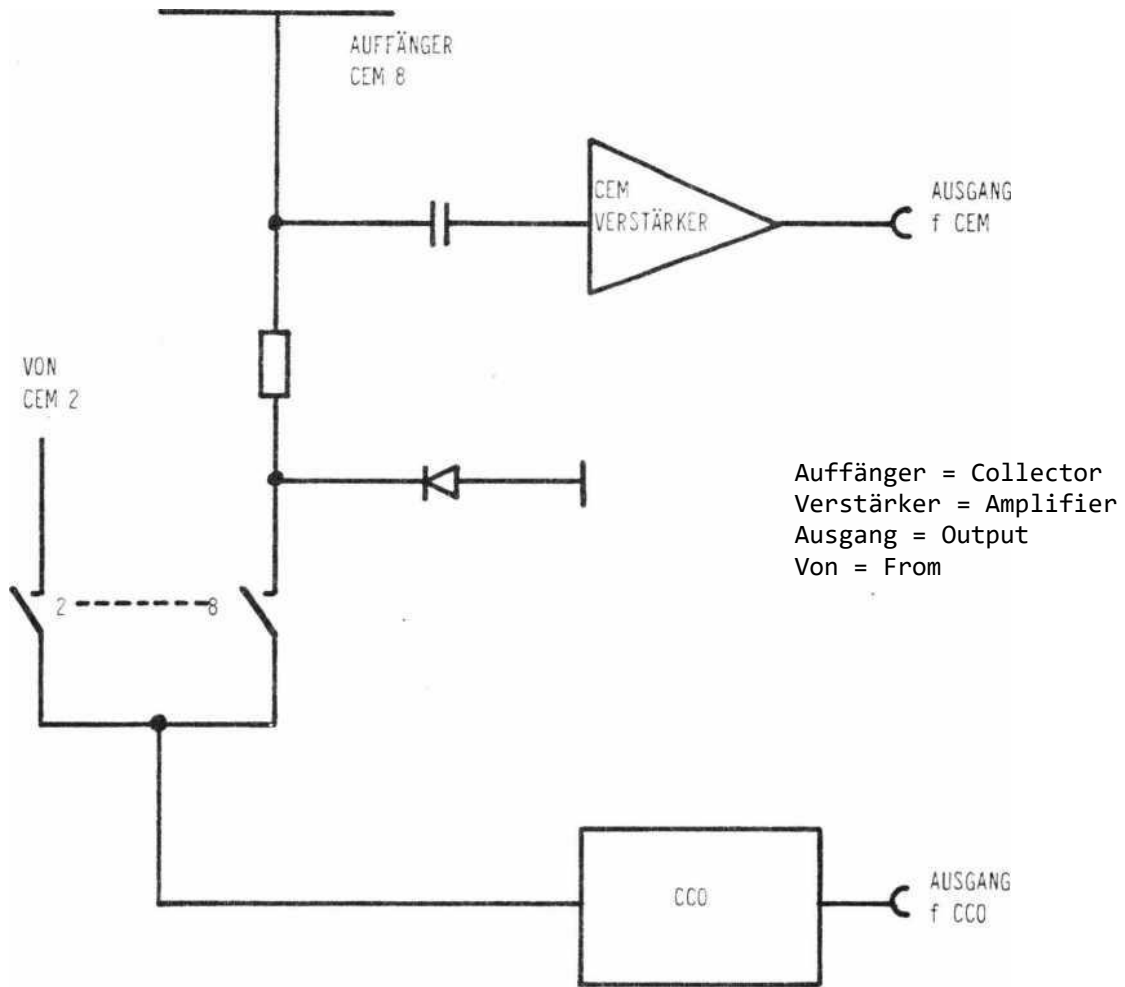


Fig. 30: Amplification measurement of channeltrons

Efforts to measure the Channeltron amplification on the fly have paid off greatly. For the first time this long time behavior of channeltrons in outer space could be directly and quantitatively tracked while previously only indirect methods for the quality control of the function were common. This data can certainly be considered an important independent result that is of great importance for future experiments.

High frequency generator

The operational principle of the high-frequency generator was already discussed in chapter I3. It should be entered here only on some important details.

The block diagram of the high-frequency generator is shown in Figure 31. You can see the two interlocking circuits in turn

- the amplitude control circuit and
- the frequency control circuit

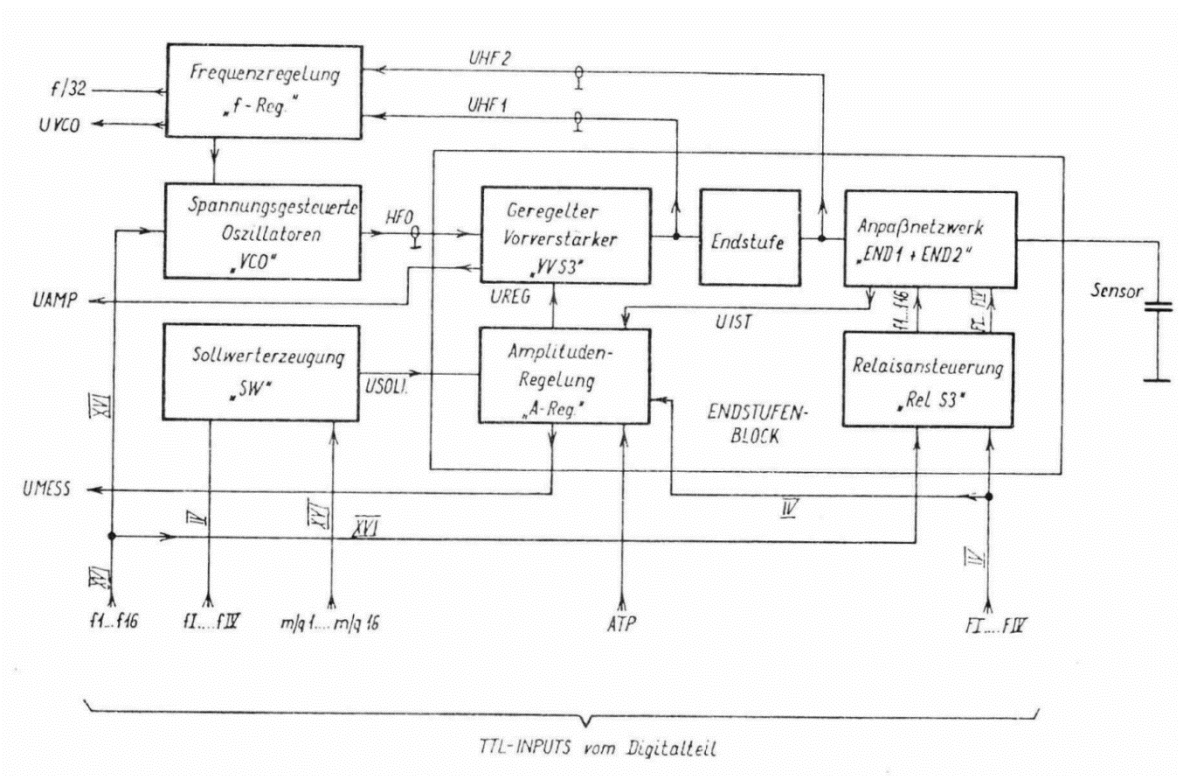


Figure 31: high frequency generator for I3, block diagram

- Frequenzregelung = frequency control
- Spannungsgesteuerte Oszillatoren = Voltage Controlled Oscillators
- Geregelter vorverstärker = Regulated preamp
- Endstufe = output stage / amplifier
- Anpaßnetzwerk = matching network
- Sollwertzeugung = Setpoint generation
- AmplitudenRegelung = amplitude regulation
- Endstufenblock = output stage block / amplifier block
- Relaisansteuerung = relay control
- vom Digitalteil = the digital part

The amplitude control circuit receives its reference from the set value generation and the controlled preamp, where a gain control by means of a FET is performed (AGC) as actuator. The frequency control circuit receives its reference from the resonance frequency of the amplifier and has as

Actuator 16 voltage controlled oscillators, where the frequency is returned by means of a capacity diode.

A waiver on the frequency control was not possible due to the requirement for extremely low power consumption and the required amplitude accuracy of $\pm 1\%$ (a slight variation of the control frequency compared to the resonance frequency of the amplifier increases power consumption at the high quality of the power amplifier circuit dramatically).

The use of 16 crystals were eliminated for the same reason. The use of only one VCO for all 16 frequencies was not possible because of the wide required frequency range and the required fast settling time of for each channel. Therefore, 16 single VCO were employed, which also have the advantage of a considerably higher reliability.

The amplifier circuit is series resonance circuit, controlled by the output stage transistor base, educated. Here a capacitor is used as a plate capacitor and the inductor is an air inductor which is located in a separately screened enclosure. This inductance, together with the disk capacity, the stray capacitance, the adjustment capacity and the load capacity of the capacitive part of output voltage, determines the highest frequency. To further explain of the frequency switch and the recovery of the control voltage for the frequency control circuit and the amplitude control circuit a principle diagram is specified in Fig. 32. From this it appears that the frequency is adjusted by 16 capacity, which the coil in parallel. This reduces the required performance of the power amplifier. The control voltage for the frequency control is created by 4 capacitive divider. This division into 4 groups is necessary to keep the output amplitude range of the control voltage within appropriate limits. The same division into 4 frequency group will also acquiring the control voltage for the amplitude control circuit. It a special capacitive divider with rectification is on each per group, whereas only a divider capacitor with the same relay is switched on in the frequency control. At the same time this relay sets the capacitors for determining the appropriate group of four frequency at the output. A relay is used to keep the capacitive load at the output through the deactivated divider, which sets the not activated groups to ground. Thus.

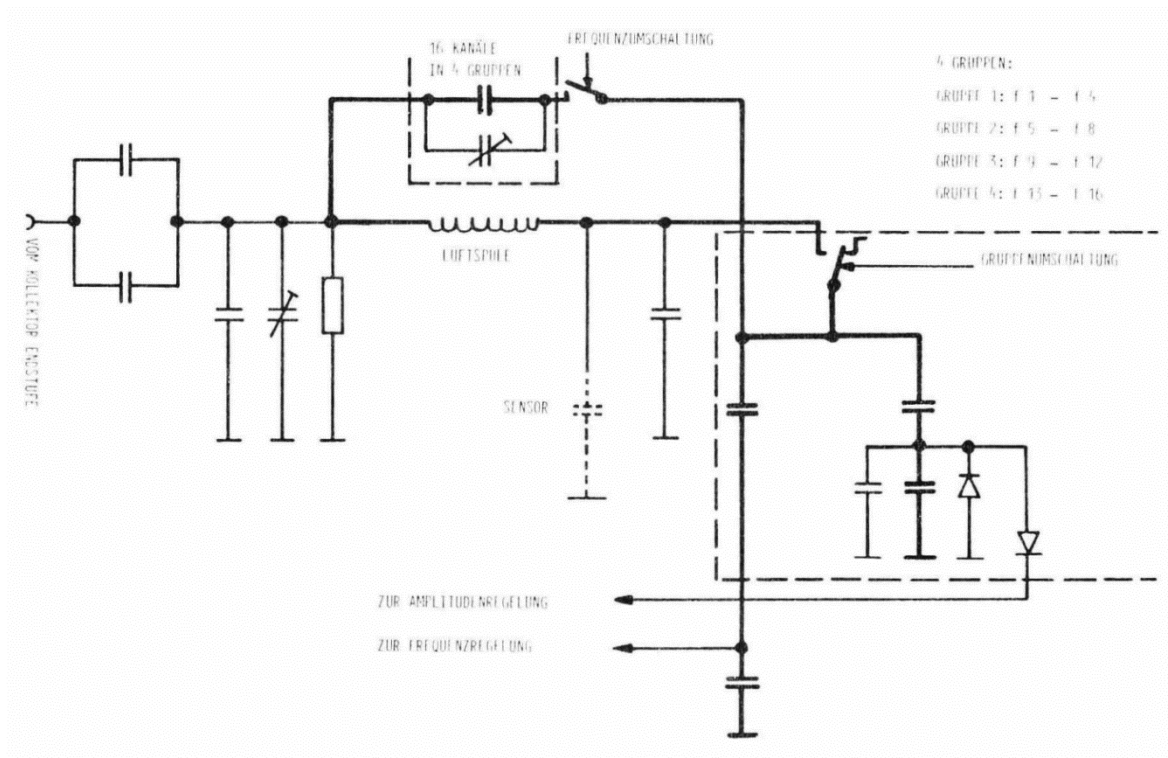


Figure 32: high frequency generator for I3, end circle

von kollektor endstufe = from collector output stage

Frequenzumschaltung = frequency switching

Luftspule = air coil

Gruppenumschaltung = group switchover

Zur = to

Amplitudenregelung = amplitude control

Frequenzregelung = frequency control

the at the same time the not switched capacitors for determining frequency also grounded. Here, the already mentioned mercury relays were also used. The thermal contact improved here with a normal Tin soldering because these relays are in the electronics section.

Yet none has failed so far.

Another important facility of the high-frequency generator, which is housed in the amplitude control is used to keep the output voltage during the frequency switch to zero. This is necessary to switch the relay off. At the same time ensured that the amplifier only works if it is also measured. This reflected positively on the average power consumption as well as on the EMC behavior. The release of the RF-generator is performed with ATP, with the release

takes place in sufficient time before the start of the first channel of the azimuth that the RF generator has settled, but switching the relay is guaranteed complete. To measure the frequency of the output voltage during the Inflight test, the frequency of from HF voltage by a factor of 32 is divided and led to a counter. To measure the amplitude of the output voltage during Inflight test the decoupled control voltage of the end circle is fed to an analog - to-digital converter. The release of amplitude control voltage in 4 frequency groups facilitates production of $16 \times 16 = 256$ nominal voltages (see table 8). First, the voltages corresponding to the 16 M/q ratios are generated from a reference voltage by means of 16 switches. Now turning to this reference voltage with the frequency to get the necessary combinations. It found only four switches are required, namely for the four frequencies within the groups of four, because the groups of four switching is done by switching the output voltage divider. To better understand the decoding of the energy channel counter is specified for the labels used in the block diagram of Fig. 31 table 33. This decoding worried yet another feature, namely the exclusion of certain frequency M/q combinations. The maximum power consumption is limited, voltage amplitudes specified in table 8 can not be exceeded. The institution now ensures that the each last permissible M/q channel remains switched on. Thereby, instead of carrying out measurements in the non-permitted channels, these are performed in those M/q channels where measurements were last permitted.

Some characteristics of the high-frequency generator

- Frequency range : 1 MHz ./ . 4 MHz
- Number of channels : 16
- Max. Output voltage (load = 75pF) : $720 V_{SS}$
- Number of voltage channels : $16 \times 16 = 256$

EN	m/q	f arab.	f röm.	F röm.	BEMERKUNGEN
1	3	1	I	I	<p>FREQUENZEN VON f 1 BIS f 16 BEI m/q-KANAL 3</p> <p>Frequencies of f 1 to f 16 in m/q channel 3</p>
2	3	2	II	I	
3	3	3	III	I	
4	3	4	IV	I	
5	3	5	I	II	
6	3	6	II	II	
7	3	7	III	II	
8	3	8	IV	II	
9	3	9	I	III	
10	3	10	II	III	
11	3	11	III	III	
12	3	12	IV	III	
13	3	13	I	IV	
14	3	14	II	IV	
15	3	15	III	IV	
16	3	16	IV	IV	
17	1	6	II	II	<p>FREQUENZ NACH MAXIMUM- REGISTER BEI NDM, NACH HDM-ZÄHLER BEI HDM (ANGENOMMEN f 6) m/q-KANAL VON 1 BIS 16</p> <p>Frquency to maximum register at NDM, according to HDM counter at HDM (adopted f 6) m/q channel from 1 to 16</p>
18	2	6	II	II	
19	3	6	II	II	
20	4	6	II	II	
21	5	6	II	II	
22	6	6	II	II	
23	7	6	II	II	
24	8	6	II	II	
25	9	6	II	II	
26	10	6	II	II	
27	11	6	II	II	
28	12	6	II	II	
29	13	6	II	II	
30	14	6	II	II	
31	15	6	II	II	
32	16	6	II	II	

Table 33: Decoding to the control of the high-frequency generator for I3

Bemerkunken = Remarks

- Settling Time : 30 ms
- Accuracy of output voltages : $\pm 1 \%$
- Temperature dependence of the output voltages : $\pm 1 \%$ (-25°C ./ . +55°C)
- Accuracy of frequencies : $\pm 0.5 \%$
- Temperature dependence of the frequencies : $\pm 0.5 \%$ (-25°C ./ . +55°C)
- Harmonic content of the output voltage : -34 dB compared to the fundamental wave

Counter

The meters are built as a 16-stage binary counter, whose opening time is determined by the control flow. It also controls the parallel transfer of the count results in a shift register which is read serially. This solution is selected for one to keep the wiring costs within limits, on the other hand, the serial transfer of counting results for the production of a quasi logarithmic compressed 8-bit representation is required.

The meters were not built to reduce the effort required and the power consumption as self-reducing meters, but it uses a central reduce plant for all 12 counter.

Reduce plant

The reduce plant has the task to carry over a binary counting result with 16-bit in a display with 4-bit exponent and 4-bit mantissa. As a result, the required data transfer rate is halved, with a minimal reduction in accuracy.

The exponent is determined by finding the number of zeros between the highest-value bit and the leading "L" in the 16-bit word that is to be reduced, not exceeding $16-4=12$. The mantissa consists of the 4 bits following the leading "L".

Decoding is performed by the formula

$$\text{Count rate} = \begin{cases} (M + 16) \cdot 2^{11-E} & \text{for } E \leq 11 \\ M & \text{for } E = 12 \\ \text{Faulty} & \text{for } E > 12 \end{cases}$$

The number 17 for example is represented as follows:

L 0 L L 0 0 0 L

Table 34 shows the appearance of all counting results can occur. You can see from the fact that when count rates from 32 which decoded values in the Middle will be lower than the original. E.g. the numbers are encoded 64, 65, 66, 67 all 64. During the evaluation we make the value 66, according to the center of the area. The maximum deviation from the true value is 3.1% in the worst case.

The technical implementation looks like this:

The counting process is completed in one sector, gets the core of reduce plant by the sequencing of the statement to evaluate a particular counter. To do this, the contents of the counter is applied to the Counter shift register (the counter can then be already put back and called again). Now, the information is moved as long as, until the leading "L" is found, or only 4 bit is not tested. It counts the number of shifts in the numerator of the exponent. There are now 2 cases to distinguish:

a) it became a "L" within the first 12-bit found:

The counter register is pushed on a bit, but not the exponent count. As a result, the leading "L" is eliminated; their existence and exact location has already registered the exponent count. Now the binary exponent counter state is taken parallel to the exponent register (4 bit). Exponent and counter registers are switched in series and this 8 bit is then pushed into the memory input register and stored. Then, the process can start it again if a group of counters will be reduced (at I1a or I3).

LLOOOOOO	0	LOLOOOOO	32
LLOOOOOL	1	LOLOOOOL	34
LLOOOOLO	2	LOLOOOLO	36
LLOOOOLL	3	LOLOOOLL	38
LLOOOLOO	4	LOLOOOL0	40
LLOOOLOL	5	LOLOOLOL	42
LLOOOLLO	6	LOLOOLLO	44
LLOOOLLL	7	LOLOOLLL	46
LLOCL000	8	LOLOLO00	48
LLOOLOCL	9	LOLOLOCL	50
LLOOLCLO	10	LOLOLOLO	52
LLOOLOLL	11	LOLOLOLL	54
LLOOLLOO	12	LOLOLLOO	56
LLOOLLOL	13	LOLOLLOL	58
LLOOLLLO	14	LOLOLLOO	60
LLOOLLLL	15	LOLOLLOL	62
LOLLOOOO	16	LOLOLOOO	64
LOLLOOOL	17	LOLOLOOL	68
LOLLOOLO	18	LOLOLOLO	72
LOLLOOLL	19	LOLOLOLL	76
LOLLOLOO	20	LOLOLLOO	80
LOLLOLOL	21	LOLOLLOL	84
LOLLOLLO	22	LOLOLLOO	88
LOLLOLLL	23	LOLOLLOL	92
LOLLOLOO	24	LOLOLLOO	96
LOLLOLOL	25	LOLOLLOL	100
LOLLOLOO	26	LOLOLLOL	104
LOLLOLOL	27	LOLOLLOL	108
LOLLOLOO	28	LOLOLLOO	112
LOLLOLOL	29	LOLOLLOL	116
LOLLOLLO	30	LOLOLLOO	120
LOLLOLLL	31	LOLOLLOL	124

Table 34: Quasi-logarithmic compression
(numbers 0 - 124)

L0000000	128	OLLO0000	512
L000000L	136	OLLO000L	544
L00000LO	144	OLLO00LO	576
L00000LL	152	OLLO00LL	608
L0000L00	160	OLLO0L00	640
L0000L0L	168	OLLO0L0L	672
L0000LLO	176	OLLO0LLO	704
L0000LLL	184	OLLO0LLL	736
L000L000	192	OLLO0L000	768
L000L00L	200	OLLO0L00L	800
L000L0LO	208	OLLO0L0LO	832
L000L0LL	216	OLLO0L0LL	864
L000LL00	224	OLLO0LL00	896
L000LL0L	232	OLLO0LL0L	928
L000LLLO	240	OLLO0LLLO	960
L000LLLL	248	OLLO0LLLL	992
OLLL0000	256	OLOLO0000	1024
OLLL000L	272	OLOLO000L	1088
OLLL00LO	288	OLOLO00LO	1152
OLLL00LL	304	OLOLO00LL	1216
OLLL0L00	320	OLOLO0L00	1280
OLLL0L0L	336	OLOLO0L0L	1344
OLLL0LLO	352	OLOLO0LLO	1408
OLLL0LLO	368	OLOLO0LLO	1472
OLLLLO00	384	OLOLLO00	1536
OLLLLO0L	400	OLOLLO0L	1600
OLLLLOLO	416	OLOLLOLO	1664
OLLLLOLL	432	OLOLLOLL	1728
OLLLLL00	448	OLOLLO00	1792
OLLLLL0L	464	OLOLLO0L	1856
OLLLLLLO	480	OLOLLOLO	1920
OLLLLLLL	496	OLOLLOLL	1984

Table 34 (Continued): Quasi-logarithmic compression (numbers 128 - 1984)

OL000000	2048	OOLO0000	8192
OL00000L	2176	OOLO000L	8704
OL0000LO	2304	OOLO00LO	9216
OL0000LL	2432	OOLO00LL	9728
OL000L00	2560	OOLO0L00	10240
OL000L0L	2688	OOLO0L0L	10752
OL000LLO	2816	OOLO0LLO	11264
OL000LLL	2944	OOLO0LLL	11776
OL00L000	3072	OOLOL000	12288
OL00L00L	3200	OOLOL00L	12800
OL00L0LO	3328	OOLOL0LO	13312
OL00L0LL	3456	OOLOL0LL	13824
OL00LL00	3584	OOLOLL00	14336
OL00LL0L	3712	OOLOLL0L	14848
OL00LLLO	3840	OOLOLLLO	15360
OL00LLLL	3968	OOLOLLLL	15872
OOLLO000	4096	OOOLO000	16384
OOLLO00L	4352	OOOLO00L	17408
OOLLO0LO	4608	OOOLO0LO	18432
OOLLO0LL	4864	OOOLO0LL	19456
OOLLOLO0	5120	OOOLOLO0	20480
OOLLOLOL	5376	OOOLOLOL	21504
OOLLOLLO	5632	OOOLOLLO	22528
OOLLOLLL	5888	OOOLOLLL	23552
OOLLLO00	6144	OOOLL000	24576
OOLLLO0L	6400	OOOLL00L	25600
OOLLLOLO	6656	OOOLL0LO	26624
OOLLLOLL	6912	OOOLL0LL	27648
OOLLLL00	7168	OOOLLLO0	28672
OOLLLL0L	7424	OOOLLLOL	29696
OOLLLLLO	7680	OOOLLLLO	30720
OOLLLLLL	7936	OOOLLLLL	31744

Table 34 (Continued): Quasi-logarithmic compression (numbers 2048 - 31744)

00000000	32768
0000000L	34816
000000LO	36864
000000LL	38912
00000L00	40960
00000LOL	43008
00000LLO	45056
00000LLL	47104
0000L000	49152
0000LOOL	51200
0000LOLO	53248
0000LOLL	55296
0000LLOO	57344
0000LLOL	59392
0000LLLO	61440
0000LLLL	63488

Table 34 (Continued): Quasi-logarithmic compression (numbers 32768 - 63488)

(b) there has been found no "L":

Then, only four unverified bits are in the counter register. Now becomes the State of Exponent counters (binary 12) taken in the exponent register. Analog then becomes a) procedures.

Due to the serial reduction, which is useful for reasons of simpler wiring and the simple structure of the counter, a bottleneck is created with regard to the reliability. This problem was solved because the counter as well as the reducer are built in redundancy.

The maximum possible result of the count of 63488 proved to be just enough. Only in some cases in the perihelion achieved by I2 values of over 50000, but never over 63488. the full dynamic range of I2 of over 10^5 (high counting rates the amp dead time is already a significant part) was thus fully exploited.

memory

The measuring cycle of the sensors and thus of the experiment is spin synchronous, the transfer of the measurement results to the telemetry, however, time-synchronous. This resulting in a continuous shift of measuring cycles within the time grid of telemetry. The two experiment stores that take per a whole block of data are used to compensate for this delay. The amount of memory is by the boundary conditions of the telemetry system i.e. set the length of a data frame:

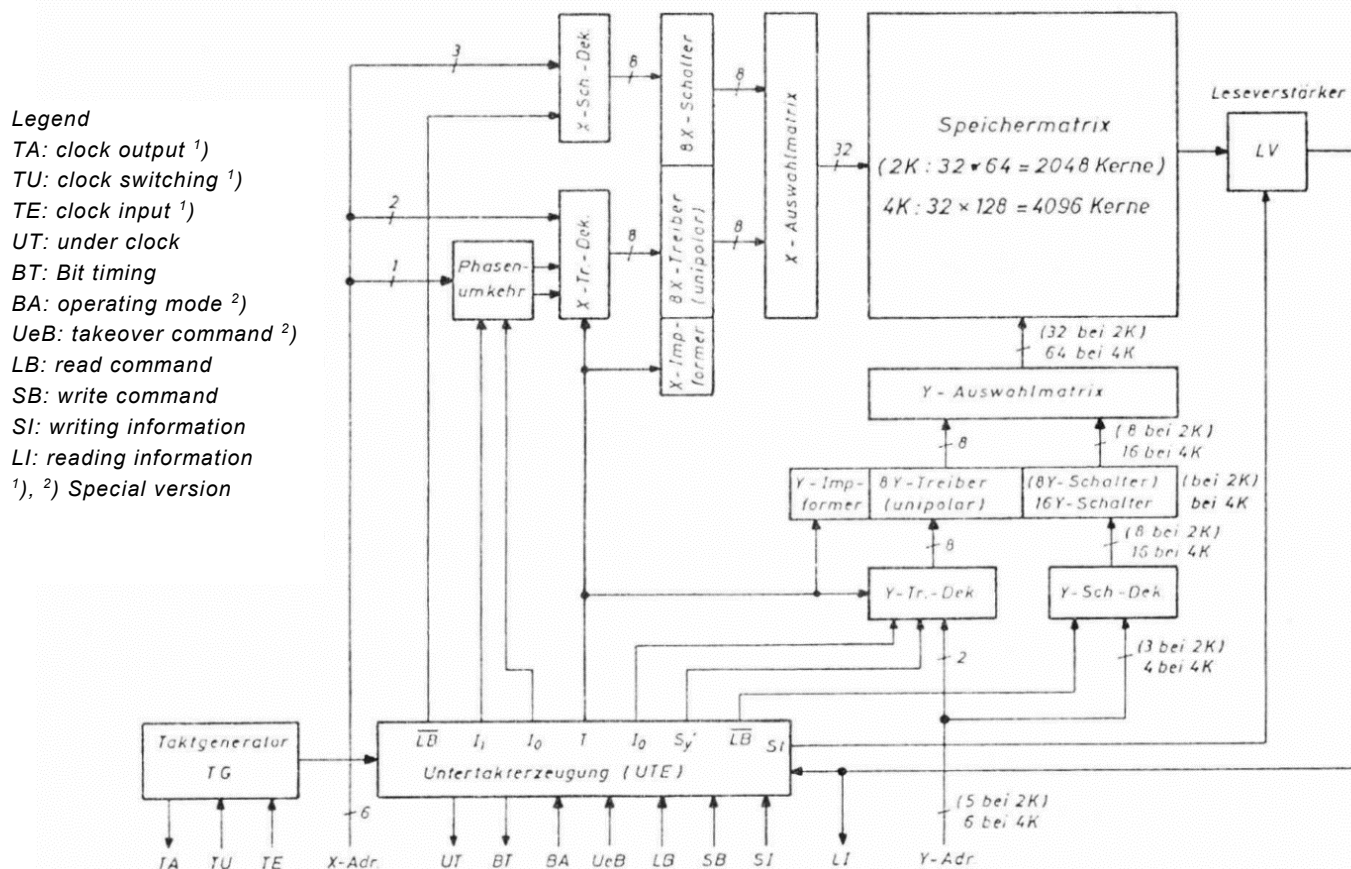
- Normal data mode: 432 words = 3456 bit
- High Data mode: 504 words = 4032 bit

Therefore, a memory size of 4096 bits per memory selected.

While data are inscribed in a store, the other memory is read by the telemetry. Semiconductor memory originally scheduled for COSMOS engineering, which are characterized by extremely low power consumption. At the time, appointment reasons, the execution had to be set, as the qualification procedure for the detection of airworthiness for the building blocks of the COSMOS was not yet completed. From project management COSMOS logic was decided completely excluded from use. This made us see considerable additional costs to switch to core memory, as well as low-power TTL technology. This caused also the power consumption of the plasma experiment increased by approx. 6 W.

*That turned out to be unexpectedly view advantage Later in the mission:
If at 1 AU available power is no longer enough to to operate of the heating
mats in the central part of HELIOS, E1 is greatly appreciated in his
capacity as a stove and enjoys high priority...*

The inner structure of the memory for the block diagram is shown in Fig. 33. As in any current coincidence core memory, the information from a core of memory matrix is read using each one half stream on an X and a Y-range line in temporal coincidence. At the same time, this operation is equivalent to writing a '0'. To write a "1" in the same core the same selection lines with each a half power of opposite polarity must be excited at the same time. When reading the selected memory core is switched to it's "0"-State. Depending on the stored information, the core produces a different reading signal being queried in the read amplifiers according to amplitude and temporal location. The digitised signal is provided to flip flop which comes after the input sensor amplifier and is available until the next cycle in the memory on data output LI. If the information read is to be saved further, this is performed immediately after the reading process by writing it into the same memory cell. Instead of the read information, the information on the data in the SI can be written either.



Legend
 TA: clock output ¹⁾
 TU: clock switching ¹⁾
 TE: clock input ¹⁾
 UT: under clock
 BT: Bit timing
 BA: operating mode ²⁾
 UeB: takeover command ²⁾
 LB: read command
 SB: write command
 SI: writing information
 LI: reading information
^{1), 2)} Special version

Schalter = Switch
 Phasenumkehr = phase reversal
 Treiber = Driver
 Auswahlmatrix = selection matrix
 Speichermatrix = memory matrix
 Kerne = cores
 Leseverstärker = read amplifier
 Bei = at
 Taktgenerator = clock generator
 Untertakterzeugung = Under clock generation

Figure 33: Block diagram of the core memory

The required current pulses are generated for each coordinate of the storage matrix from one of 8 unipolar power drivers, which are logically grouped together for 4 pairs of bipolar driver and with the help of 8 or 16 existing switch across the related selection matrix on the storage matrix selection lines. The selection matrices are specially adapted decoding circuits, that guide the driver current with the specified polarity in the corresponding selection wire of the memory matrix to each driver-switch combination power control.

The control of the driver and switch is done via a decoding of the address with Lp TTL gates. Also the impulses came from the lower clock generation are fed into this decoding, which cause the correct timing of the memory cycle. To reduce the number of inputs by selecting lines on the half in a coordinate, the store works on the principle of the phase reversal, the

later explained. The phase reverse control is the X-driver - decoding is placed in position.

Two memory can be operated synchronously to a clock generator and the entire data processing (data transfer, reducing plant, storage control), output the output signal of the clock generator.

With the help of the clock switch TU can be toggled between internal and external clock. Details on this are in the technical description of the core memory with operating and handling instructions.

Memory Controller

During the writing of data to the memory clock, the memory controller has the following tasks:

- Formatting the data in memory
- Calling the appropriate memory locations
- Providing data to the store

While reading out a store by the telemetry, the memory controller has the following tasks:

- Serial selection control of individual memory locations
- Control by the telemetry clock
- Submission of data to the telemetry.

Memory formatting was shown in figures 21 and 22 for the two data formats. These formats, as well as the importance of individual data have been explained already in detail. The writing of the "first runnings" - General data about the status of the instruments are, time information, as well as code words - is carried out parallel data transfer and serial output of the memory in the memory clock. This, the value will be held in the registers, in which the advance is made, which is when the first channel of a measurement cycle is turned on.

This also applies to the S/C-time. A counter is intended for selecting the memory locations, which is one of the 15 words.

Concerning the data, the control flow together with program control Announces originate from which sensor the currently available data. Each instrument and the integration counter is associated with a counter, from whose state the corresponding space selected.

The counter is advanced after writing of each word, with each counter being assigned a specific memory location. The distribution of the memory slots on the individual instruments is also shown in figures 21 and 22. The number of words is different in the two modes of data. The required counter length and set of the Word numbers range is performed by the program control.

When reading the memory the individual counters are connected in series now, and with each so called "Word transfer control pulse" (WTC) is forwarded this total counter by a Word. So the memory is read serially. The following signals are used to control readout of the satellite telemetry:

- BTC (block transfer control signal)

It says when the telemetry begins reading from a store, and when she's done.

- WTC (Word transfer control signal)

It says the same thing as above, only based on a single 8-bit word. With this, the memory controller is switched.

- BSP (bit shift pulse)

This is the data transfer clock, with which also the timing of the store takes place.

Maximum viewfinder and data control

The maximum viewfinder is a part of the program control for the most data-intensive tools I1a or I3.

- Finding the channel with the highest count rate
- Save the address of this channel
- Selecting the next measuring cycle according to this address to be memorized data

If all 4608 count rates (9 elevation channels, 16 channels of azimuth, 32 energy) a measurement of I1A or I3 to earth should be delivered, a totally inadequate temporal resolution would be achieved at the specified rate of telemetry. Therefore, only a specific selection of data is transferred, which contains the most important parts of a spectrum. This will be explained later. Initially only the technique.

During a measuring cycle of the sensor 1a or 3 the highest result of the count and the corresponding address is determined from all counting results first. This address is then used in the next measuring cycle, in which of course the address of the channel with the highest count rate determined for the selection of to be memorized data. Are the three coordinates of the maximum address EL (ξ), AZ (β) and EN (α), so then the channels with the following addresses stored:

EL ($\xi - 2$), EL ($\xi - 1$), EL (ξ), EL ($\xi + 1$), EL ($\xi + 2$),
So 5 elevation channels

AZ ($\beta - 2$), AZ ($\beta - 1$), AZ (β), AZ ($\beta + 1$), AZ ($\beta + 2$),
So 5 azimuth channels

EN ($\alpha - 2$), AZ ($\alpha - 1$), AZ (α), , AZ ($\alpha + 6$)
So 9 energy channels.

[Please note: The line beginning with EN has been written as it appears in the original report, however it is believed that the AZ on this line should be replaced with EN.]

That's a total of only $5 \times 5 \times 9 = 225$ words from the original 4608. For those cases in which the maximum address is close to the edge of the measuring range, that not the entire frequency range in the measuring range would fall, the block is moved so that its edge to fall along with the edge of the measuring range. The address of the channel of the highest count rate is calculated with a binary comparator. The counting result, which has been identified so far as largest is located in a register. The new result is loaded in a second register. This is greater, the comparator shall inform. Then loaded the status of the three channel counter (EL, AZ and EN) into the so called Address register (EL, AZ and EN). At the end of a measurement cycle, the status of this search register is loaded in the work register and the search register deleted. This latter is looking for the address of the maximum channel again in the next cycle. The work register is counting backwards now to 2 cycles and can control the storage of the data. It starts so two channels before the maximum. The respective end of transmission (5 bars at EL, 5 bars in AZ and 8 bars in EN) are hard-coded. The addresses to close on the edge (see above) so is, if they are at the end, as long as back clocked until the last channel can be transmitted, If they are at the beginning, is only to register status 0000..., which corresponds to the first channel. The data control is done now so that the maximum-working register is compared with the elevation channel counter, azimuth channel counter and energy channel counter. The channel number of the maximum of work register in EL, AZ and EN is reached, which is determined by the default as a starting point for the data storage, the registry runs with with the channel counters. A data storage is done whenever the register level is within the programmed range.

Flow Control

The control has the following tasks:

- Generation of the angle grid (open and close the counter)
- Production of the grid to read and reset of the counter
- Production of the channel grid (EN)
- Production of the measuring cycle times
- Creation of all necessary pulses to control the sensors

They essentially used the spin-synchronous pulse chain offered by the probe system from 512 pulses per revolution. Thus, a part of the control of flow consists of a counter that counts this 512 pulses per revolution. It decodes all sectors (AZ), also all impulses that are required to control the sensors. In table 9 all important angles were represented for HELIOS 1, (in table 10 for HELIOS 2). After a measurement on an azimuth channel nine counters must be read at sensor 1a and 3. This is done by means of the lower clock of the memory clock. The latter is the transmission of serial data, while the lower clock synchronously gets each single counter.

The second part of the control of flow consists of 3 counters:

- the elevation channel counter
- the azimuth channel counter
- the energy channel counter

The elevation channel counter is a modulo 9-counter, which is timed by the memory sub clock after each azimuth channel of each energy channel.

The azimuth counter is a modulo-16 counter that is clocked by the azimuth sector impulses and counts once per each energy channel.

The energy channel counter counts up to 32 and thus indicates the end of a cycle. This is clocked by the solar impulse "see sun pulse", which increases the counter per satellite revolution by one.

Construction technology

The basic construction technology of electronics is based on using bi layers with plated version with arrangement of elements on a page. Figure 34 shows such a version with digital components (integrated circuits), while Figure 35 shows a design with discrete components.

The following should be entered only on some special solutions of construction technology.

This one is first so called "Motherboard" plug-in to mention, which was used in the construction of nine Channeltron amplifier. It was a motherboard used here, which includes all inputs, outputs and connectors and the wiring of the individual boards with each other. At the same time, this Board is carrier of the nine CEM amplifier, ten shields, as well as of the CCO. These boards are plugged with plugs into the motherboard. On the individual boards, appropriate spacer rollers are applied to the intervals so that the installation of the entire "Channeltron amplifier block" in the sensor electronics housing by means of bolts can be performed. Figure 36 shows this block.

Another special form of the building represents the electrometer that was housed in a cavity created by the hemispherical plates to ensure minimum distance between catcher and electronics. The building had to be so round and semi-spherical. Figure 37 shows this structure.

A special building technique was to apply when the high-voltage equipment in the interests of weight savings and the required safety of high-voltage equipment. Compared to the conventional encapsulation technique of the Cascades and the high-voltage transformer, following solution was chosen:

- Transformer with maximum 350 V peak voltage
- Ceramic thick film circuits with soldered concentrated components for the Cascades

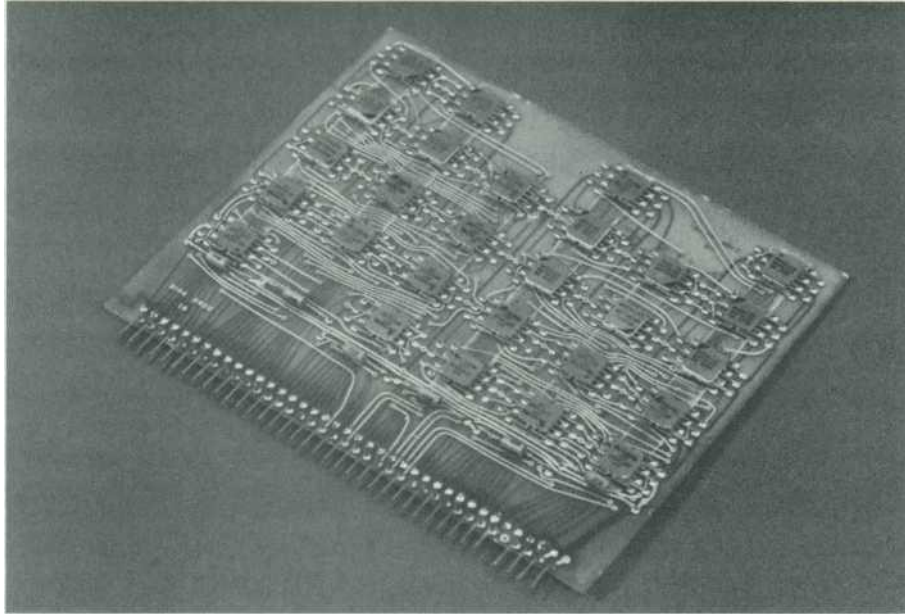


Figure 34: digital Board

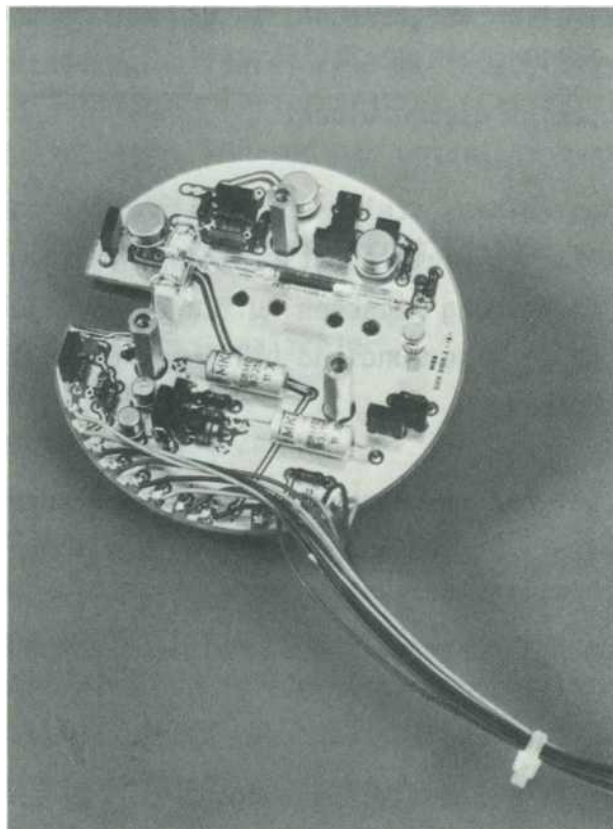


Figure 35: Analogue Board

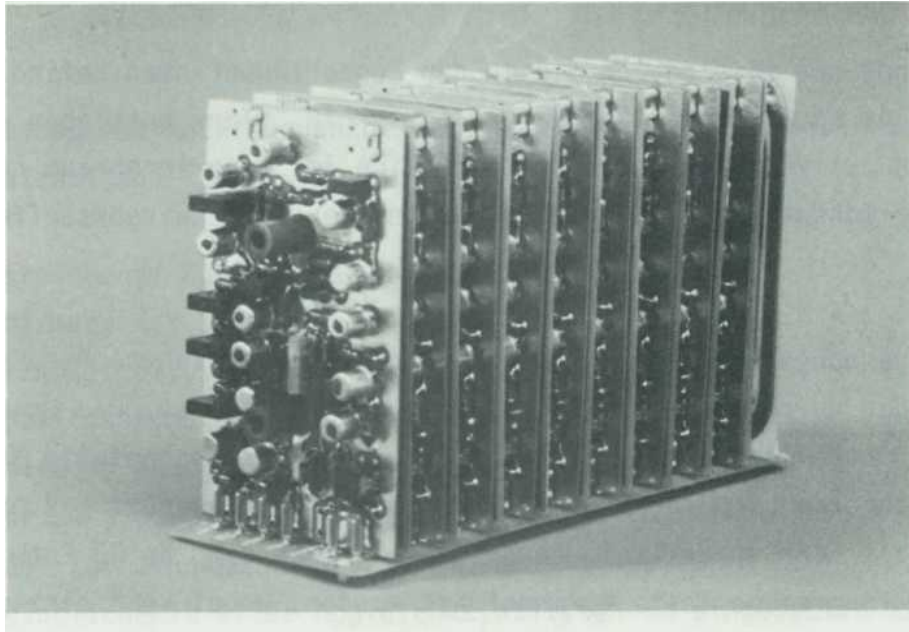


Figure 36: Channeltron amplifier block

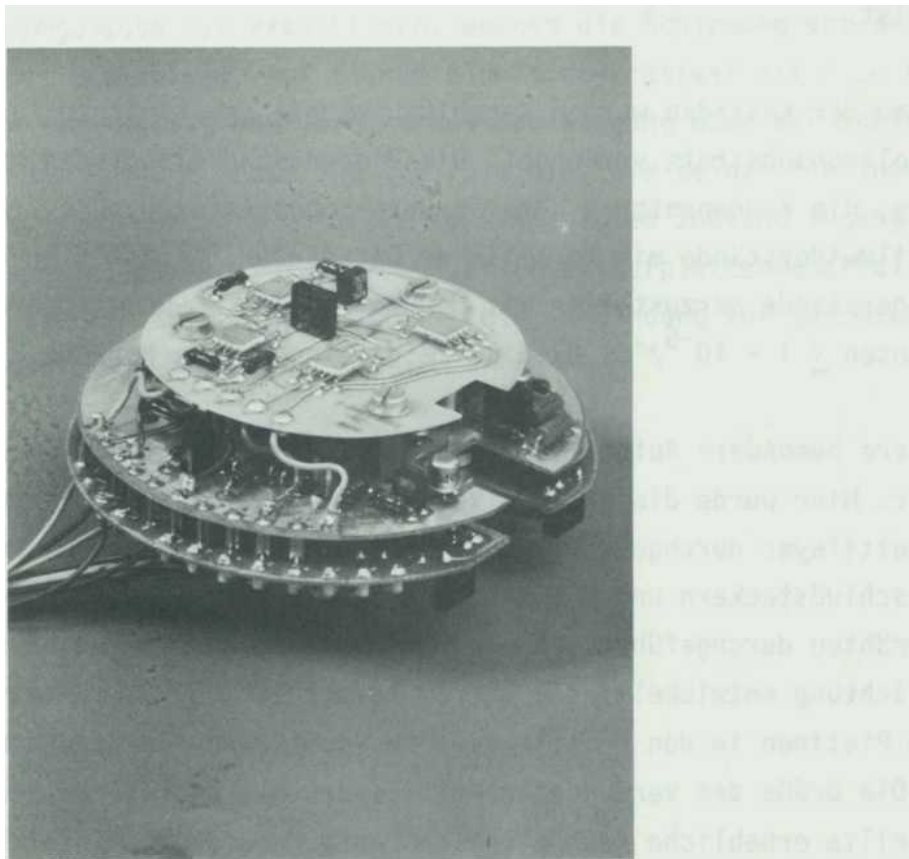


Figure 37: Electromechanical meter

- Accommodation of the Cascades in the Interior of the sensor
- Unforgotten vented high-voltage transformer

This solution is offered here in the Interior of the sensor located Channeltrons can only be operated in a vacuum by better 10^{-6} Torr and contamination inside the sensor uses only materials to avoid any hydrocarbons evaporating.

The high-voltage transformer were carried out unshed. The ferrite cores are sufficiently vented through the center hole. The wire insulation is double silk, the layer of insulation is performed with Kapton film, where the location voltage is only 20 V. This type of construction has proven very reliable. Extensive tests, carried 20 development patterns where there was not a single failure. 36 transformer were installed in each model, where is also still not a single failure.

Ceramic substrate of the same shape were used in the construction of the Cascades as the Channeltron substrate. The diodes are glass diodes without varnish, the capacitors are ceramic chip capacitors without seal, the thick film resistors are with thick covering glazing. Here, succeeded high ohm resistors to produce values of $180\text{ m}\Omega$ and Temperature coefficients $\leq 1 \cdot 10^{-6} / ^\circ\text{C}$. Figure 38 shows such a cascade.

Another special building technique is the wiring of the electronic box. Here, the entire wiring of the boards was conducted with each other on the multilayer. Only the wiring of the multilayer to the connectors and the wiring of the power supply was carried out using wires. In this context, a special connector equipment was developed, which is extremely light and allows us to insert the individual boards in the multilayer without use of plugs. The size of the used multi layers with five levels of wiring was significant technological development and production requirements. The size and complexity is shown in Fig. 39. The installation in the electronics box is shown in figs. 40 (from below) and 41 (from above).

There were following aspects be taken into account in the development of the high-frequency generator:

- sufficient cooling of the power transistor
- Shielding of the coil
- shortest lines in the end circle
- Capacity-poorest construction of the end circle
- Screening of the entire amplifier compared to the other electronics
- Arrangement of mercury relay in a particular location
(perpendicular to the z axis and parallel to the Y-axis)
- Accessibility of all adjustment capacity in the installed condition

This has led to a building, which is shown in Figure 42. The separate housing of the screen is shown, as the shield before the two boards of the final circuit. On this part of aluminum milling also the final transistor for cooling is mounted, the input is on the screen plate and the output down to towards the end circle. The two circuit boards of the final circuit, of which the bottom in the installed state is accessible, are made from our special low-capacity Teflon head plate material. The plug at the side represents the connection to the entire box wiring.

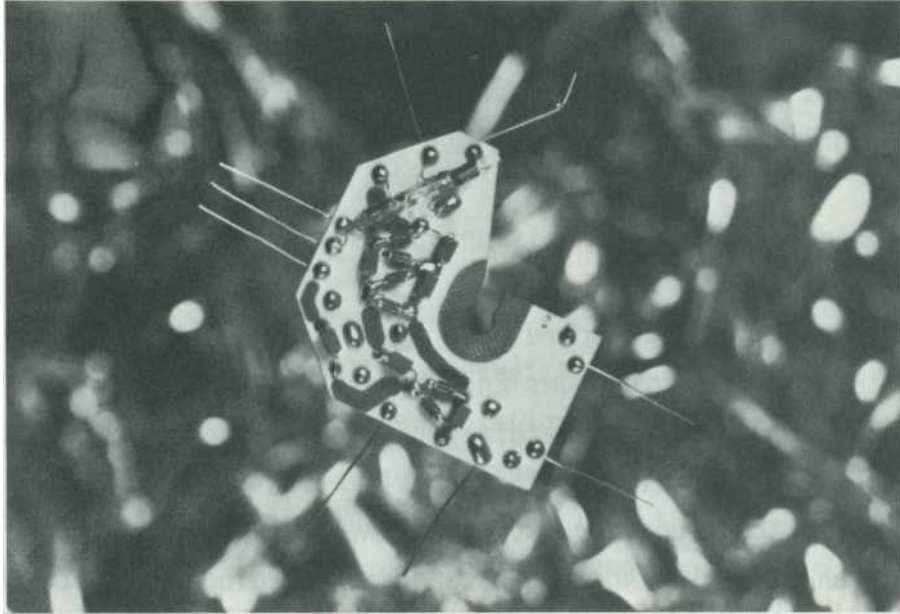


Figure 38: high voltage cascade in ceramic thick-film technology

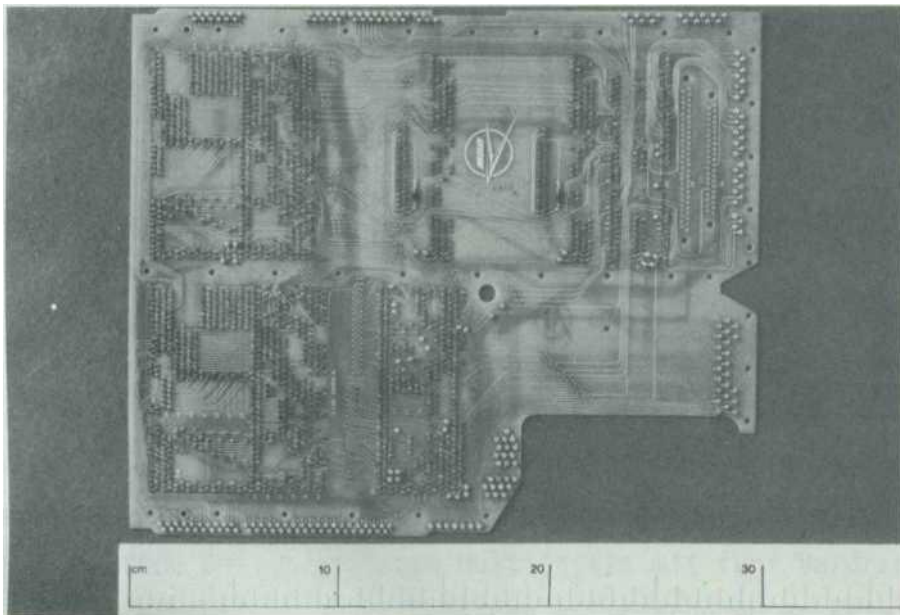


Figure 39: multilayer

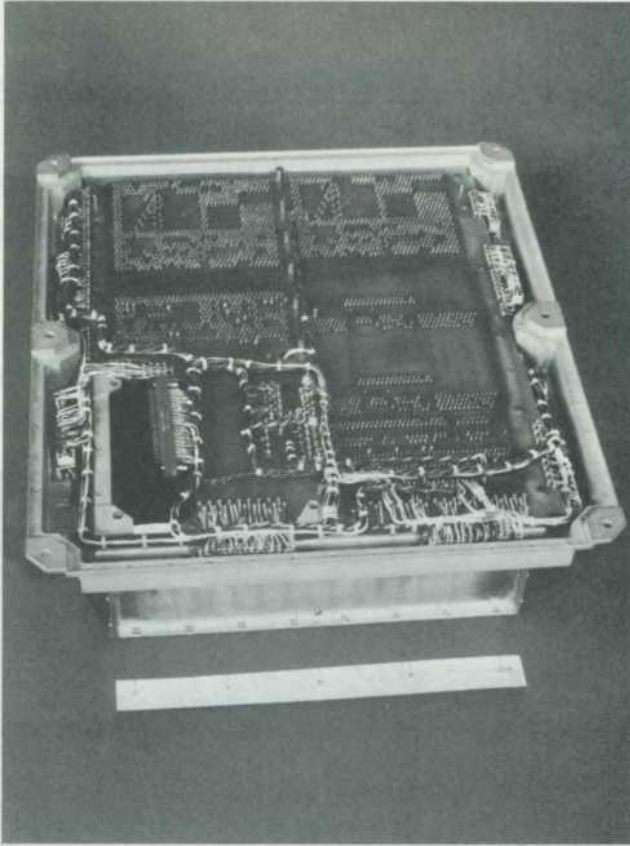


Figure 40: Electronics box (from the bottom)

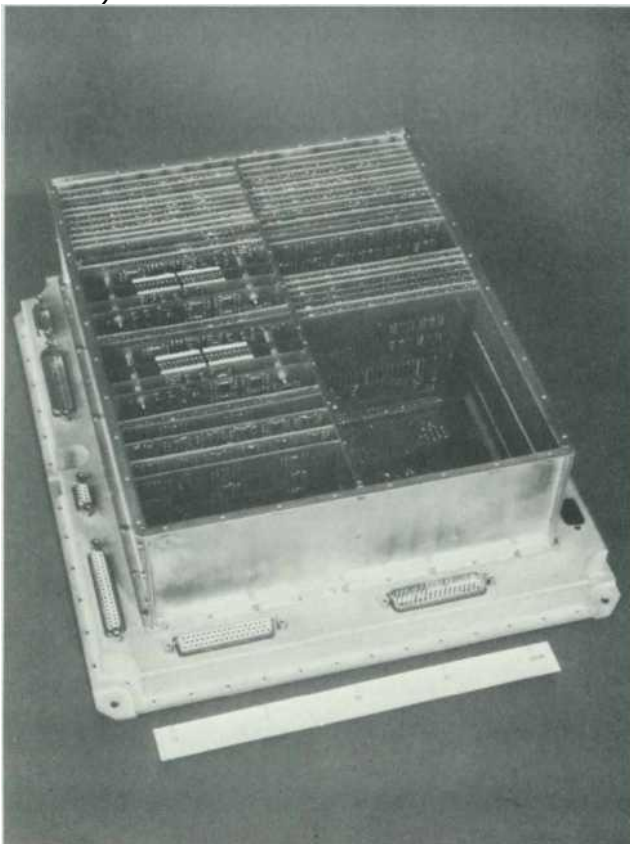


Figure 41: Electronics box (from above)

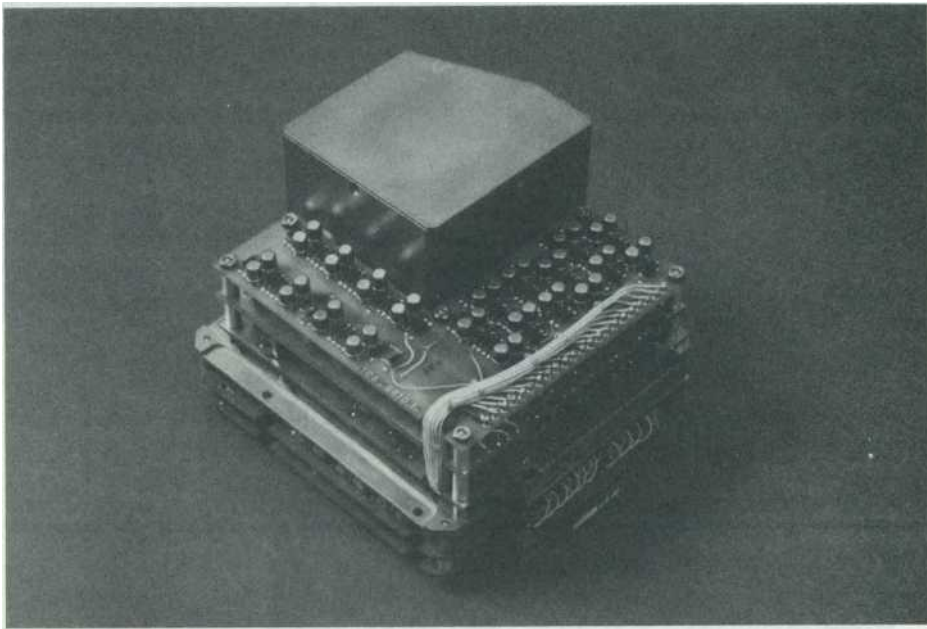


Figure 42: RF generator

Electromagnetic compatibility

That all known rules to achieve the required electromagnetic compatibility were applied in the construction of the experiment, such as

- Twisting of power supplies
- Shielding of HF sources
- Shielding of sensitive analog lines
- galvanic separation of "power ground" and "signal ground"
- HF-leakage of the boxes
- Special training of the cover flanges
- Gilding the box surfaces

may be assumed as known and need no further explanation.

Channeltrons

The channeltrons (CEM) were purchased by the MPE for a division of the Bendix company, then later as "Galileo Optics" became self-employed. After appropriate selection tests at MPE, they were then passed to MBB for installation.

A protocol was created for each CEM that reveals the individual steps.

1. Incoming inspection at MPE.

First, each CEM was examined for visible defects or impurities with magnifying glass or microscope.

2. First test.

Then began the preparation for the first duration test. 12 CEM were individually fitted with springs made of V4A on brackets. A small electron source (a Glow lamp with separate glass) faces each CEM funnel. The power supply for all 12 CEM is common, but pulse releases and the heater power supplies of the electron sources are individually accessible. The whole test arrangement is initially at least 10 hours in an oil-free UHV vacuum system at approx. 150° heated. Then begins the constant load rest pressure from $\sim 10^{-8}$ Torr. After applying the HV (3.0 kV) the zero count rate of all CEM is first of all measured. Then is the electron source of every single CEM so high regulated, that an output current I of usually 3×10^{-7} A (other values can be selected) is kept constant. Which according to the average gain \bar{G} is adjusting count rate is regularly registered and plotted as a function of the charge $Q = I \cdot t$ from the CEM. The test is terminated when $Q \approx 0.05$ Cb is reached, so after about two days. Usually in $Q \approx 0.01$ Cb the initial steep drop by \bar{G} has come to a standstill. After, a weak increase of \bar{G} occurs in good CEM, with bad a further drop.

Before the venting of the test Chamber, yet pulse height analysis (PHA) of CEM pulses at different HV between 3.0 and 4.1 kV be made and the dependency of \bar{G} examined by the count rate. Before and after the test the ohmic resistance of the CEM is measured and recorded.

3. Soldered onto Ceramic substrates

The CEM passed the sub-contractor by MBB, the company Lewicki microelectronics to be soldered. The soldering is carried out under protective atmosphere and without any flux with a particularly low melting solder. The prepared ceramic substrate and the CEM be slowly brought to a temperature just a few degrees below the melting point of the solder. A fine hot air allows then a fast, clean and almost completely stress-free soldering to the three gold-plated contact surfaces of the CEM as well as also the ceramic tube with a metal plate serving as electron collector.

4. Another stress test

This test is similar to the first test under point 2, but usually shorter, because the still in the running CEM here mostly achieve a stable end state at 0.02 Cb. The final PHA measurements are used as criteria for the final selection.

5. Shake test

At MBB, the CEM on a shaking device be mounted and shaken with the strength required for the qualification. There was initially so much break, that we had to ask for to minimize the amount of stress. This was fortunately possible.

Here would very much effort to nerves, work and money can be saved if the project would be in time determined by itself to the rectification of the claims, instead of always only on urgent request and much too late.

6. Installation

The now leftover CEM were selected according to their qualities of the individual instruments and finally installed. It was off not without soldering fluxes. Therefore the entire sensor area with freon was flushed at the end of the Assembly firmly, to remove all residues.

7. Tests in installed state

Each system test \bar{G} was measured with the help of the automatic Inflight tests. When the calibration at MPE was again each PHA and HV-

Dependency is recorded. For this purpose, the CEM outputs of the instruments from the outside are accessible and can be separated from the built-in amplifiers. This process was repeated a few days before starting the "final test" once again even the instruments integrated in the probe.

In the course of the work, we gained a lot of experience and often changed the procedure. So, steps 4 and 5 were often reversed, step 2 do not even have time pressure. Step 4 has been repeated several times for many CEM, however, for various reasons.

Behavior CEM in laboratory tests and in flight should be illustrated by a typical example from I1a Helios 1. Figure 43 shows the time-dependence of \bar{G} in the stress test (step 4) for the CEM No. C 163, measured on 27.8.1973. At $Q \approx 0.01 Cb$ a "plateau" is reached. It is with $\bar{G} = 2 \times 10^7$ for 3,0 kV relatively low. This was similar for all CEM of this delivery. The resistance was relatively low at all this CEM: $8.2 \times 10^8 \Omega$ (before the test $8.55 \times 10^8 \Omega$), while in the CEM from other Deliveries usually higher values have been achieved (up to $1.5 \times 10^9 \Omega$). But, low resistance favor the ratio at high count rates: the drop in \bar{G} is only noticeable at $n > 50 kHz$. In Figure 44, we see the HV - dependence of amplification of the CEM No. 163. Here, even G_m , the maximum gain due to the PHA as well as the half-width of the PHA is applied (in % of G_m) except \bar{G} . The curves show the typical rise of \bar{G} and G_m by about a factor of 2 per 300 V voltage boost; also occur a minimum of half-width of $\approx 25\%$ at $\approx 3.5 kV$ can be regarded as typical for a "good" CEM.

The behavior is interesting now this (and other) CEM after launching. In Fig. 45, \bar{G} measurements of CEM by I1a are shown on HELIOS 1 (with the exception of the two outermost). Place L6 the previously described CEM no. 163 is located on. The rapidly changing \bar{G} values before the start the CEM stemming probably differences in the times of the pump and the responsive during various system testing. After the start but you can see the usual "curing behavior" of all CEM.

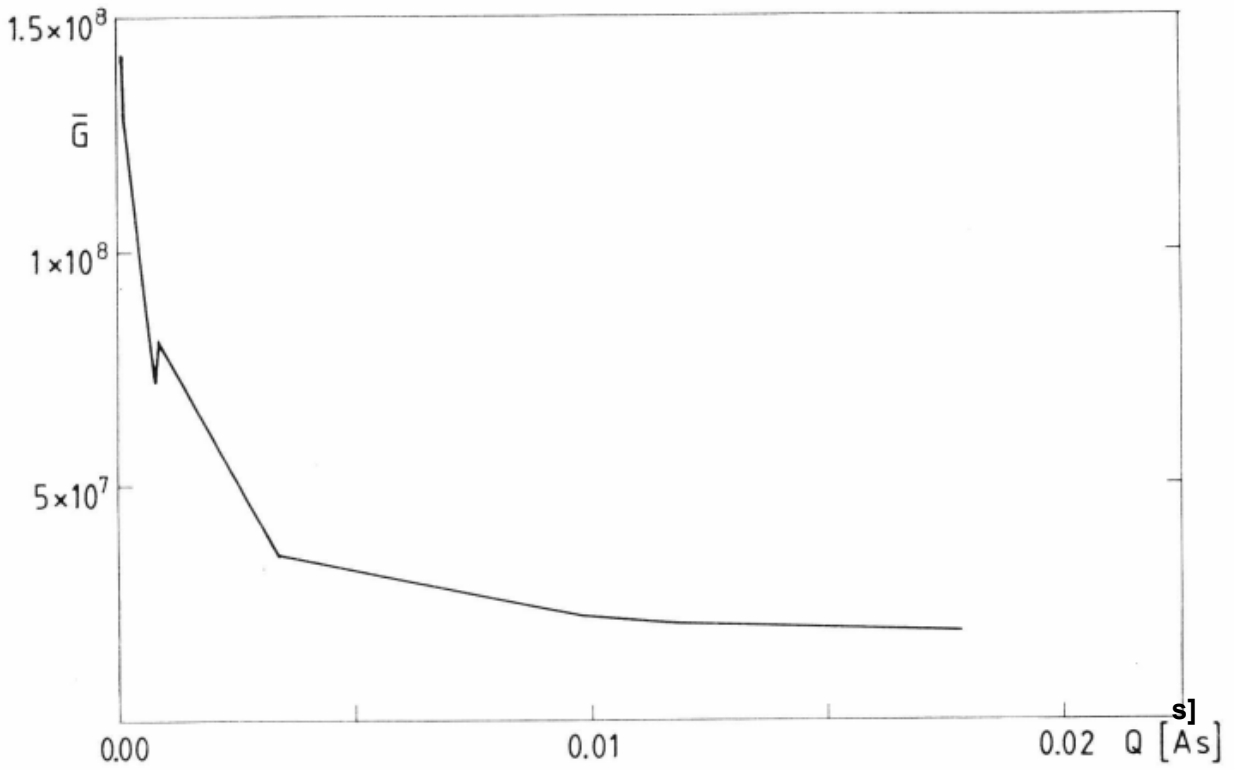


Figure 43: The dependence of the average gain \bar{G} of the total charge Q flowed through the CEM No.163.

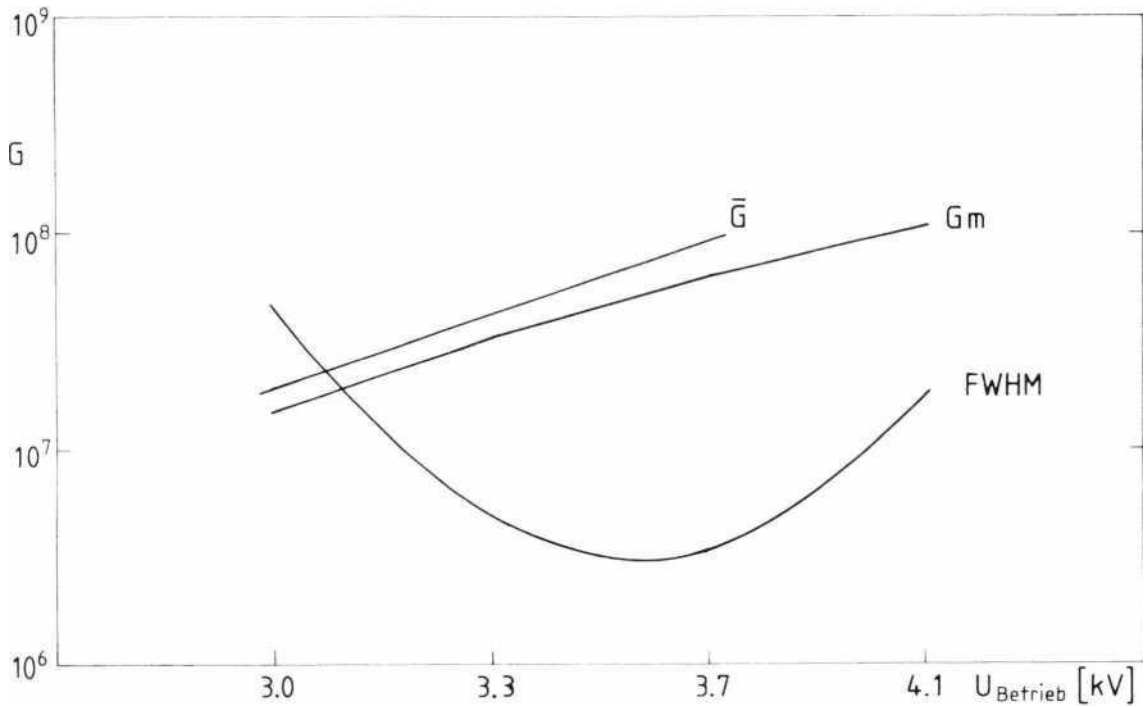


Figure 44: Depending on medium-gain \bar{G} , maximum gain G_m , as well as the half-width of pulse height distribution of the operating voltage. The recorded measurement on CEM No.163 after permanent load.

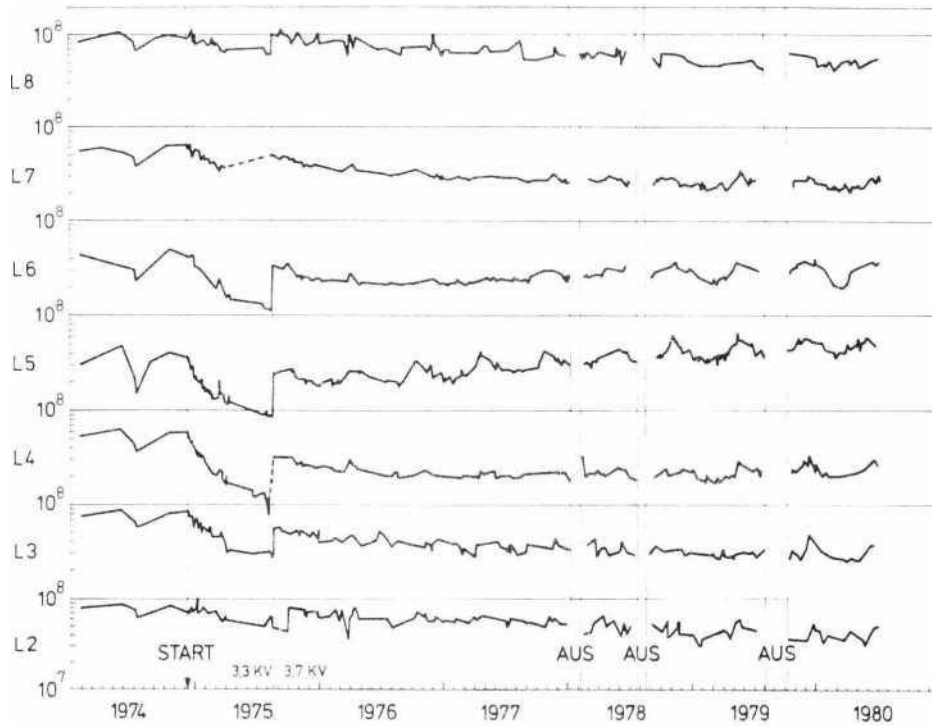


Figure 45: The average amplification \bar{G} the CEM in I1a Helios 1 from 1974 to 1980, L5 is the average CEM, looking in the ecliptic

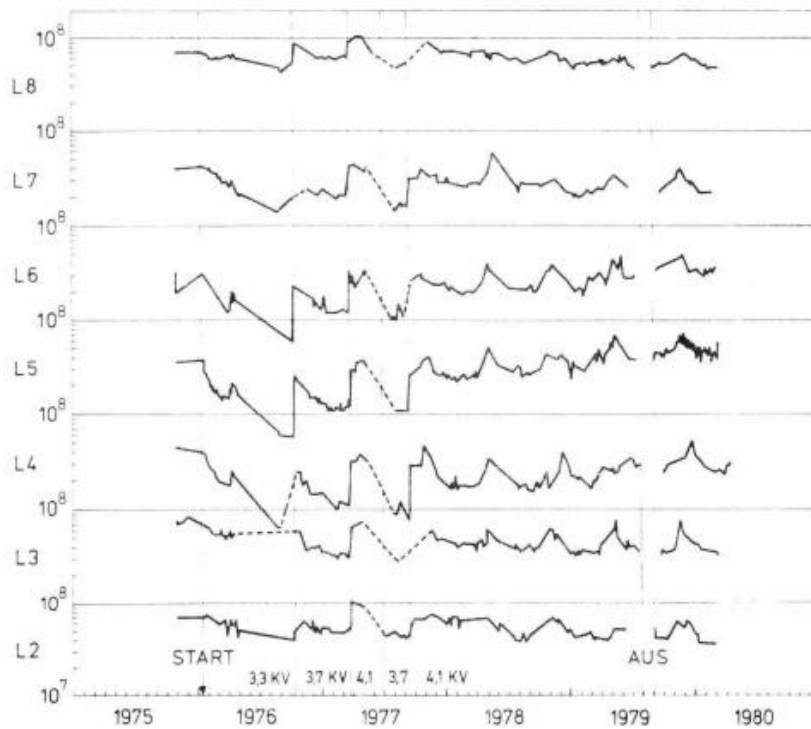


Figure 46: As picture 45 however for I1a Helios 2

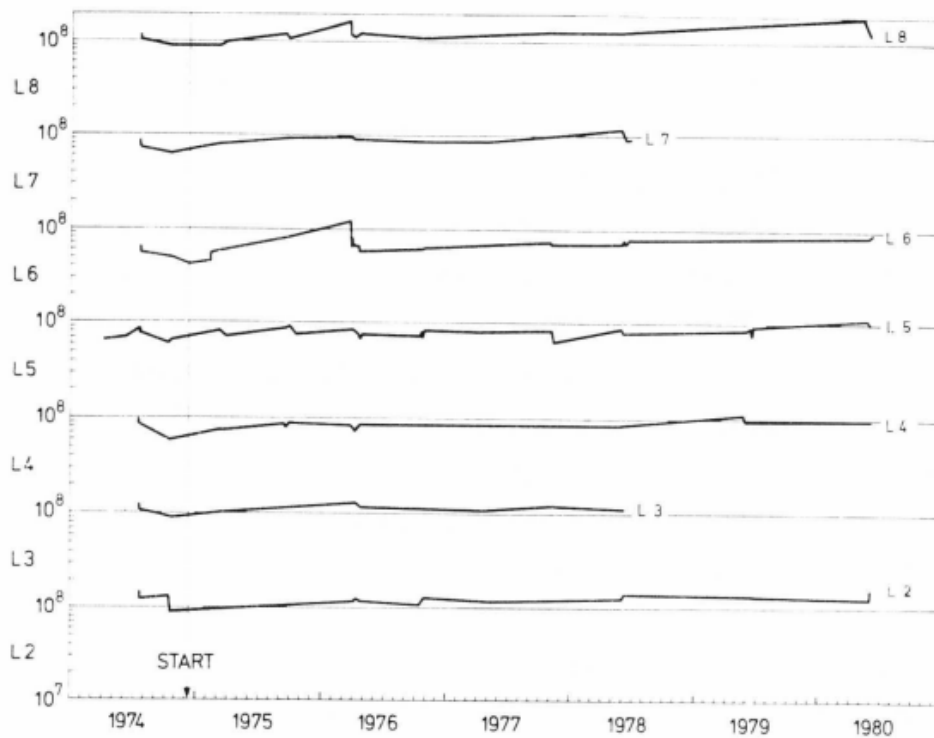


Figure 47: As picture 45, but for I3 of the HELIOS 1

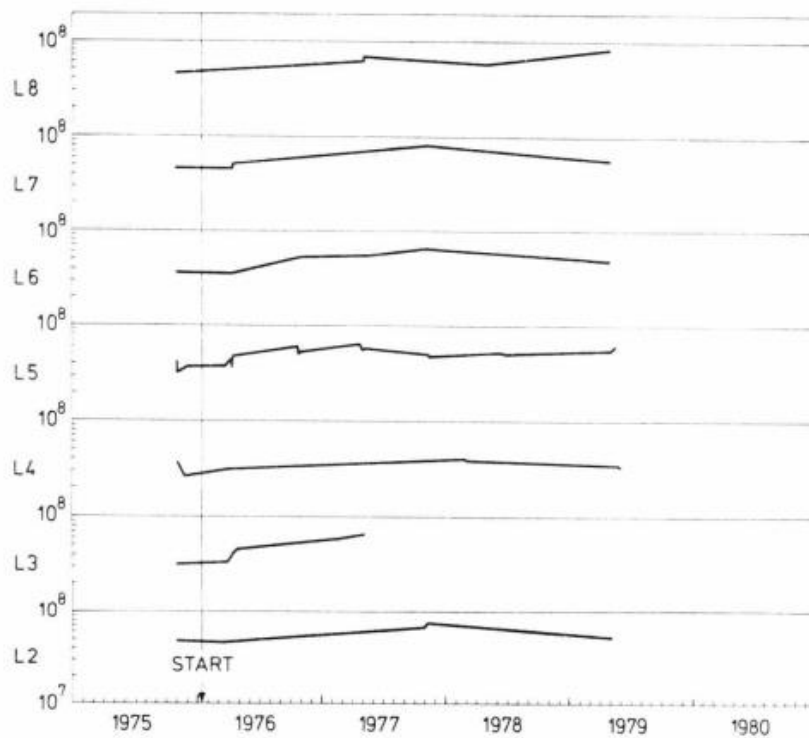


Figure 48: As picture 45, but for I3 of the HELIOS 2

Of course, \bar{G} decreases at L5, the Cem, which looks to the ecliptic, and the great majority of particles counts, the fastest off a bit slower on its neighbours L4 and L6. The CEM on the edge of L2 and L8 have not yet reached the "plateau" because of low stress today. Especially at L5, a clear upward trend can be observed already since 1976. The plateau of L6 $\bar{G} \approx 2.5 \times 10^7$ in the summer of 1976 is significantly lower than in the endurance test (fig. 43). Similar was observed in all CEM on HELIOS 1 and HELIOS 2. The reason for this is unclear; Perhaps the different residual gas atmosphere in sensor and test facility plays a role. Also the periodic fluctuations are striking by \bar{G} , especially clearly visible at L5. The maxima of \bar{G} coincide fairly well with the Periheidurch-courses, can be so close to a temperature effect. Appropriate laboratory tests are pending.

Figure 46 shows for the CEM in I1a on HELIOS 2 very similar behavior. Here \bar{G} declined however more after the launch, and the HV had to be set to 4.1 kV (3.7 kV for HELIOS 1). With the I3-CEM, yet nothing has changed due to the extremely low load: \bar{G} remained anywhere about at 10^8 (figures 47 and 48). Due to these images no doubt, that the lifetime of E1 at least should not be restricted by the degradation of the CEM.

This can be not so self-evident for the CEM built in I2.

Here is \bar{G} not measured directly, but qualitatively ensured only through comparison of the count rates at different amplifier thresholds, that \bar{G} still is sufficient. Two probes we have switched up the HV now to 4.1 kV, because the mentioned difference was increased slightly. The much more sensitive test, we occasionally conduct comparison of electron count rates with different HV, which would not require this increasing, but we know so that the measurements are guaranteed unaffected with 4.1 kV.

The zero count rates (NZR) CEM show a few characteristics. In the integration counter by I1a we find as NZR at HELIOS 2 average 1 count; that means 16 AZ x 9 EL channels with 10 ms measuring time a NZR less than 1 s^{-1} . At HELIOS 1, the NZR is about 2 s^{-1} .

It is striking that after some particularly strong flares the NZR sharply rises to the Sun, in individual cases to over 200 s^{-1} . The reason for this are high-energy particles, may be electrons with several MeV energy. The drop to normal levels takes usually from several hours up to several days. On 13th February 1978, went after such an event, the NZR not quite returned but is since approximately 2 s^{-1} . An investigation about whether this increase is based on only a CEM or more, was still not carried out.

6. Calibration of the instruments

The instruments I1a, I1b, and I3 have been calibrated at MPE system built specifically for this purpose. This procedure and the necessary evaluations are described in detail in a separate report, containing all technical data. Here will be outlined only the principle and the results listed.

The calibration system

Figure 49 shows a glimpse of the heart of the plant, which is in a container that is converted to the cleanroom. The upper end of the approx. 3 m-long vacuum system (with an ion getter pump) contains an ion source. Electrons from a hot cathode, on approximately 200 eV accelerates, ionize flowing through hydrogen gas in a field-free-held space. Result in particular H_2^+ ions, but also H_2O^+ and H^+ ions. They are sucked by a few volts from the effective area by a voltage of draw out and then accelerated to the desired just energy. Thus arises a very largely mono-energetic flow of ions, which energy per charge can be varied from 100 V up to 20 kV.

At the bottom of calibrating instrument is by means of a metal bellows moving in both directions. The suspension can unfortunately be no gimbal design reasons, i.e. the two axes of rotation and the inlet are not in the same plane. In turns, the instrument moves thus to the side. Possible Inhomogeneities of the particle beam must be compensated so carefully. These serve two channeltrons, that are brought 50 cm in front of the instrument from both sides up to approx. 1 cm on the beam path. Registered here count rates are converted into a voltage and supplied via a control unit of the heaters of the ion source. So, the radiant intensity over hours can be kept over very exactly stable. Lateral movements of the instruments in both directions, the control channeltrons run with, so the radiant intensity is also spatially constant.

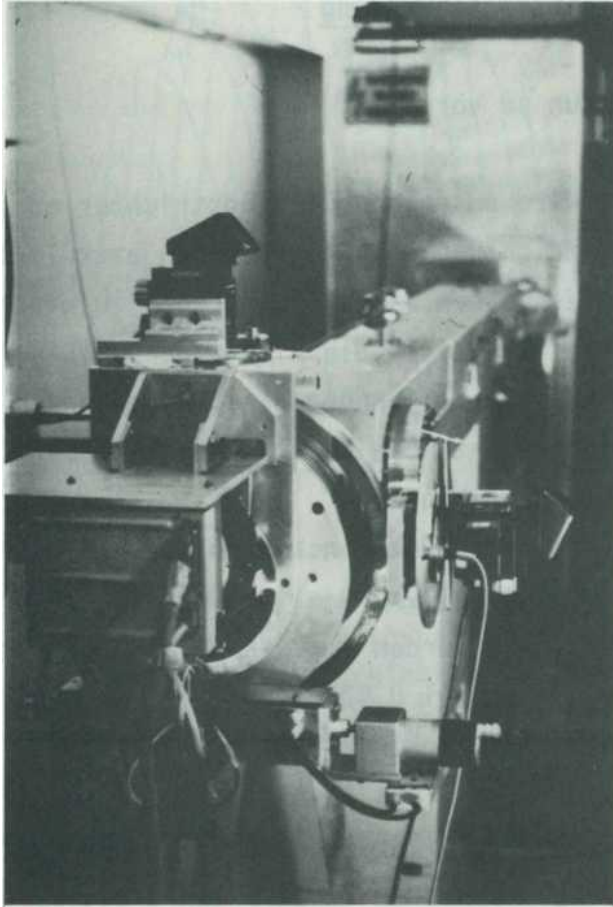


Figure 49: The calibration system for the ion instruments. Left you can see the box F1-E1A which is bolted on a portable system of bellows to a 3 m-long vacuum system. At the front end, this contains an ion source that provides Mono-energetic ions with E/q values from 100 V up to 20 kV.

The angle can be read with a accuracy of 15" and also reproducibly adjusted. Actuators that are controlled by the "green step machine" developed by M. Bechly serve.

Trace of an instrument calibration

a calibration is going now so on:

- 1.) The instrument is at its entrance funnel system flanged (Indium seal), then thoroughly evacuated. At the same time, already the necessary cables are manufactured connections to a specific interface plate, replaced the electronics box E1D. So get the necessary operating voltages, pulse frequency, and command information in the instrument; the standard pulse outputs the CEM are connected with electronic meters.
- 2.) Thorough electrical function test of the instrument.
- 3.) Turn on the ion source and all circuits.
The most calibrations were carried in the EN Channel 13 so in particle energies of nominally 0.978 kV.
- 4.) Is the so-called relative calibration for the determination of the relative Response probability of the instrument as a function of particle energy and both directions of incidence. In a fully automatic running measurement program, the corresponding counting rates Z (EN, AZ, EL) recorded in the entire three-dimensional measuring range (EN, AZ, EL) and registered along with their addresses on a data tape. Figure 50 shows a series of measurements for a single value of EL, i.e. $\epsilon = 5.07^\circ$. The entire EN range in steps of 3 V was driving for a detained each azimuth angle. The azimuth angle is in increments of approx. $0,3^\circ$ changed. Measuring ranges and increments can be varied. That often emerges naturally count rate zero on. To save time, count rates were noted at all only then when Z in a first "search period" of 0.1 sec exceeded a limit (adjustable). Nevertheless, such a verification takes a long time. $10 \times 25 \times 20$ (EN x AZ x EL) significant values will on average be recorded per CEM; these 5000 sec comes around again the same time for many

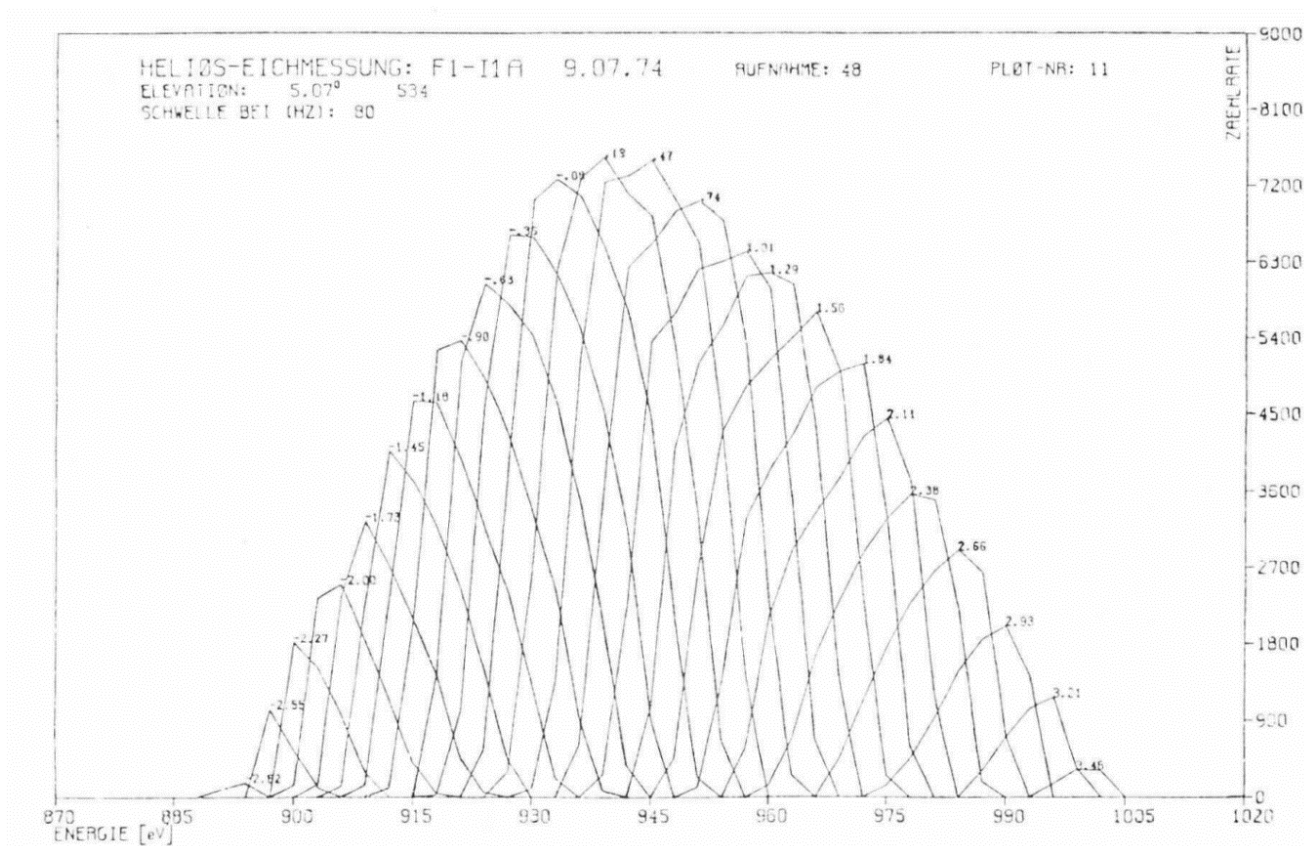


Figure 50: A series of measurements from the relative calibration of F1-I1A. The entire energy sector will pass for a detained each azimuth angle. Until then, the elevation angle - here 5.07° - is changed.

Search phase, the motor running times, belt change etc. So $9 \times 2 \times 5000$ sec takes this most important step of the complete calibration of instrument I1a or I3, just 25 hours, with 45000 significant count rates are to record.

5.) The so-called absolute calibration.

With unchanged is running on ion beam, the absolute intensity of the beam used for the relative calibration is now measured. This is a precisely calibrated electrometer, which directly measures the ion current true on a special collector. This collector is mounted by means of a swivel arm in the beam path of the instrument, immediately behind the two Stabilisation channeltrons. The ion current measured is a measure of the flow of particles falling on the inlet opening of the instrument.

Thus, the actual calibration is finished.

- 6.) Determination of dead time. For each CEM of the instrument is the count rate as Function of the incoming stream of particles measured. To do this, the ion beam in a very wide range needs to be changed. This caused problems, on the one hand with the CEM often stabilizing, whose amplifier have also finite dead times, the other source with the ion, which was often overloaded as a result. The HELIOS instruments I1a this measurement has never led to satisfactory results, and finally then the nominal value was used for the data analysis of 500 ns, of which the electronically certain values only marginally different ($\leq 10\%$).
- 7.) Some special function checks of the instruments operating in the Mission-like State, i.e. When exposed to particles. This includes a careful control of excessive coupling properties of CEM: when a CEM is under fire, none of them may say something.

This simple-sounding requirement caused much trouble during the course of the project. Already at the EM by I1a, there was over coupling effects. Then the CEM were sealed the exits completely. P-I1a there was over coupling again, this time apparently electronically. Then the pulse lines were that of the CEM lead through ducts in the sensor housing to the Preamps in the electronics section, modified. When the problem occurred again at F1-I1a, only a vigorous bailout helped literally last-minute: A detailed analysis showed that the CEM-pulse capacitively coupled to the common HV-supply and from there turn on the other pulse lines. This disorder of course strongly depends on flanking slope (rise times of ~ 1 ns) and amplitude of CEM-pulse. These properties were especially good in the F1-CEM, easily understanding reasons; the "tired" CEM of EM and also at P such effects were not more achieved. The pulse releases were changed again to the remedy; also, shielding plates have been inserted between the relatively densely stacked substrates of CEM. The story of this issue illustrates lot significantly, as necessary thorough tests under realistic conditions are, because in the Laboratory and with simulated CEM pulses were not to uncover problems.

More functional tests concerned mainly the CEM. Besides the usual measurements of amplification and pulse height distribution was among othersexamines whether in constant flux of particles the count rates may change with the CEM-HV. This can't be happening naturally. Nevertheless, it was, especially when new CEM with particularly strong and long pulses. Here, the CEM amplifier tended to overload, which is expressed in the distribution of double pulses. Also this error was to be found only through realistic operation.

At I2 this weakness of the amplifier, which is slightly different than that of I1A and I3, was particularly tough, not to say: tricky, and this has led even after the launch of HELIOS 1 be a radical change for F2. Double pulse occurred only in a specific counting rates range between approx. 1 to 5 kHz, and were therefore on the usual function checks with approx. 20 kHz not been discovered. The adulteration of the count rates was 10% to 20%, and was similar in all remaining copies of this amplifier, in principle, probably even with the already flying F1 model. The amplifier of F2 and P were in an unusual Act of force, especially by H. Rosenbauer and the electronics by MBB, yet redeveloped and repaired. Comparative measurements between HELIOS 1 and HELIOS 2 show fortunately that distortions in the unamended F1-I2 are not recognizable.

- 8.) Before removing the calibrated instrument, yet its location must be determined relative to the calibration system. The smooth polished surface of the instrument rests completely flat on the attachment flange. On the same front surface a solid lid is later screwed flat, a mirror cube is glued on the front.

The cover is by Dowel pins secured against twisting. The location of the instrument in the probe can be determined, so that ultimately a more accurate relationship between calibration system and viewing direction of the probe can be made with the mirror. For technical reasons, when mounting the sensor on the calibration system, minimal distortion of the instrument to the surface normal can not be excluded. Therefore, the position of the instrument over the dowel pins that secure the cover later, is measured with a special ruler.

9.) Finally, even the exact direction of the calibration beam must be determined relative to the normal to the flange. To do this, a kind of "Scope" was built. It consists of a 20 cm-long tube that is closed-ends with flat plates on both. In both plates centers, fine 0.5 mm diameter holes are drilled. Particles that pass through both holes, are registered in a CEM. The telescope is mounted instead of the instrument and into the beam path. With the help of the turning device it is panned as long as until a maximum of particles through; the direction of the then reached will be recorded. Then the scope is removed by 180 ° around its axis rotated and mounted again. Then again determines the direction. The average of two measurements give exactly the desired direction of the beam to the mounting level of scope (and instrument). Usually, the beam direction deviated by only a few arcseconds from the direction of the axis.

The duration of the whole procedure was per instrument per one week where some night shifts were required.

Calibration data

In the following we the main calibration data summarize without further explanation in some tables, how they are used for the data analysis. We evaluate all data according to moment process where only the zero and first moments of the device function enter $G(\vec{v})$

Thus arises E.g. for the density

$$n = \int G(\vec{v}) \cdot f(\vec{v}) d\vec{v}$$

the proximity

$$n = C \cdot \int f(\vec{v}) d\vec{v}.$$

It is

$$C = \frac{DELEL \cdot DELAZ}{DELZ} \cdot \frac{1}{G_0} \quad \text{with the 1D analysis, or}$$

$$C = \frac{1}{DELZ} \cdot \frac{1}{G_0} \quad \text{with the 3D-analysis}$$

C is as it were a measure of the ISO setting of the instrument. The verification has revealed the following values:

$$G_0 = 4 \cdot 10^{-7}$$

$$DELEL = 0,08727$$

$$DELAZ = 0,09774$$

$$DELZ = 0,01$$

They apply to the I1a instruments by F1, F2 and P. G_0 must be each corrected inversely proportional to the deviation of the spin rate of the nominal value of 60.1 per minute.

The 1D analysis of the proton density of the measured individual counting Z_i of the integration counter of I1a or I3 is then e.g. according to the formula

$$n = C \cdot \sum_{i=1}^{N-1} \frac{1}{2} \left(\frac{Z_i}{v_i} + \frac{Z_{i+1}}{v_{i+1}} \right) \cdot (v_{i+1} - v_i).$$

The v_i are the centres of the speed channel are also determined by the calibration (see below).

The sum must span only the count rates, really stemming from protons. The distinction of different types of ion from the measured data represents a fundamental evaluation problem, on which we can here no further go. The other parameters such as speeds, temperatures, etc., and also the 3D-data capture is calculated after basically similar formulas. There are other procedures, E.g. where analytic functions are adjusted to the measured count rates. All of this may be not the subject of this report.

The instruments I1b and I3 have different values for G_o , with same values of DELEL, DELAZ, DAKTARI:

$$\begin{array}{ll} \text{I3} & G_o = 0,1628 \times 10^{-7} \\ \text{I1b} & G_o = 0,877 \times 10^{-7} \end{array}$$

For the 3D-evaluations, the slightly different "sensitivities" of individual CEM are taken into account. You can express themselves through corrections of G_o , are specified in table 35.

	HELIOS 1		HELIOS 2	
	I1a	I3	I1a	I3
CEM 1	4,626	0,151	4,039	0,163
2	4,956	0,159	4,540	0,159
3	4,687	0,174	4,622	0,168
4	4,527	0,172	4,673	0,162
5	4,393	0,156	4,876	0,162
6	4,588	0,171	4,748	0,162
7	4,730	0,180	4,768	0,166
8	4,591	0,153	4,609	0,163
9	4,915	0,147	4,532	0,161

Table 35: The G_o values of the CEM in I1A and I3.
All values are 10^{-7} to multiply by.

The layers of the measuring channels are given by the 1st moments of the function. All values are summarized in table 36 (for F1) and 37 (for F2).

There are two further points should be noted: as already mentioned, the verification was limited to the E/q-Channel 13. Immediately before the start of the final test, we measured more closely again all plate voltages. The relative position of the E/q channels was then calculated from the ratio of plates voltages to which channel 13. The azimuth channels are given solely by the calibration measurement, as well as the electronic set channel spacing. Here is to be observed that at HELIOS 2 the situation of all azimuth channels of all 4 instruments can be shifted command 130-1AVL by 7.03° (see table 10).

KANAELF FUER INSTRUMENT 1A * HOS1 *										
GESCHWINDIGKEITSKANAEL OHNE SHIFT:										
	177.4205	190.8127	205.2966	221.0240	237.4854	255.4281	275.0674	295.9394	317.7335	
341.7998	367.6467	395.6724	425.2297	457.3389	492.6294	529.9421	569.2461	612.1265	658.5171	
KANAELF FUER INSTRUMENT 1A * HOS1 * GESCHWINDIGKEITSKANAEL OHNE SHIFT:										
	177.4205	190.8127	205.2966	221.0240	237.4854	255.4281	275.0674	295.9394	317.7335	6
14	341.7998	367.6467	395.6724	425.2297	457.3389	492.6294	529.9421	569.2461	612.1265	658.5171
GESCH	708.8071	761.7083	819.1196	882.2610	948.7708	1021.8484	1098.7119	1181.7590	1271.2358	1365.5386
	1463.4738	1580.5919	16° 9.9663							5
GESCHWIMIGKF ITSKANAELF WITH SH I CT:										
	171.0150	183.9177	197.80E89	2. 2.9468	228.9476	246.1972	265.2112	285.3137	306.3555	7
14	329.4919	354.5015	311.4312	409.9836	440.8940	474.9219	510.9014	548.8286	590.1736	634.9353
AZIML	683.5317	734.4736	789.7634	830.4597	914.9817	985.1646	1059.4478	1139.4680	1225.8027	1317.2397
	1416.1432	1524.6316	1639.36° 6							4
AZI MUTH CHANNEL WITHOUT SHL ^ T:										
AZIML	-54.56A	-48.939	4 3.314	-37.689	-32.064	-26.439	-20.814	-15.189	-9.564	
	-3.93°	1.606	7.31 1	12.936	18.561	24.186	29.811			2
AZI MOTH CHANNEL SHIFT:										
ELEV	-1.127	-51.751 4.498	-46.126 10.123	-40.501 15.748	-34.876 21.373	-29.251 26.998	-23.627 32.623	-13.002	-12.377	-b. 752
11 DAD CMS CHANNEL:										
	20.76	15.69	10.6 1	5.56	0.52 4.	57-9.	65-14.	72-19.75		
KANAELF FUER INSTRUMENT 3 * HOS1 *										
GESCHWINDIGKEITSKANAEL :										
KANAELF DRIVING TOOL 3 ' - HT'SL '										
G'-SfH'rtIndigkfitskanafle:										
AZIML	192.9609	211.0055	230.8934	252.8186	276.6838	302.7808	331.3999	362.6384	396.8343	3
	4P4.2315 475.1746	519.9051	569.0342	622.7327	681.4263	745.6497				1
AZI MUTH CHANNEL OHME SHIFT:										
AZIML	-54.7439	-49.1190	-43.4940	-37.8690	-12.2440	-26.6190	20.9940	-15.3691	-9.7441	6
	-4.1191 1.5058	7.1308	12.7558	18.3008	24.0057	29.6307				
AZI MUTH-KANAL WITH SHIFT:										
ELEV	-51.9314	-46.3065	-40.68] 5	-35.0565	-29.4315	-23.8065	18.1815	-12.5566	-6.9316	
	-1.3066 4.3183	9.9433	15.5683	21.1 9 33	26.8182	32.4432				
ELFVAMCNS CHANNEL :										
	20.913	1 5.843	10.823	5.793	0.823-4.	267 - 9.297 - 14.377		-19.457		
KANAELF FUER INSTRUMENT 1B * HOS1 *										
GESCHWINDIGKEITSKANAEL OHNE SHIFT:										
	171.7435	185.2370	198.7062	214.0882	230.3004	247.0319	265.6782	286.6697	307.5935	
	331.8147	355.5197	383.5547	412.4998	442.4983	477.6255	513.3958	551.4827	594.7793	637.9971
	647.3989	739.4260	793.0391	856.0723	920.1711	988.0325	1066.0488	1143.4380	1231.6724	1324.6543
	1420.3792	1532.9949	1647.4070							
GESCHWINDIGKEITSKANAELF MIT SHIFT:										
	165.4039	178.4133	191.4100	206.2247	221.8374	237.9380	255.8806	276.1287	295.1597	
	319.4558	342.7881	369.2900	397.1763	426.0525	459.9438	494.3591	530.9666	572.7212	614.2681
	661.8203	711.9856	763.5676	824.2412	885.9976	951.3602	1026.1824	1100.6946	1185.9590	1275.3406
	1347.6501	1476.1721	1586.4722							

Table 36: The location the measuring channels for the ion instruments on HELIOS 1 taking into account the calibrations.

Kanäle = channels
 Geschwindigkeit = speed
 Mit = with
 Ohne = without

HCS 2 KANAEL FUER INSTRUMENT 1A									
GESCHWINDIGKEITSKANAEL OHNE SHIFT:									
	178.1586	191.4310	205.6029	221.1543	237.8146	254.8014	274.9546	295.6865	317.5559
341.4294	366.8901	394.7362	424.3289	455.3274	491.4431	528.6404	569.4856	611.1689	657.0156
707.2450	760.2402	815.8066	880.4482	947.2307	1019.8423	1096.6001	1178.5918	1268.6731	1363.6038
1463.2292	1578.9460	1671.5481							
GESCHWINDIGKEITSKANAEL MIT SHIFT:									
	171.8321	194.6332	198.3019	213.3009	229.3697	245.7532	265.1907	285.1865	306.2891
329.3052	353.9618	380.7192	409.2607	439.1584	473.9915	509.8679	548.2983	589.4661	633.6853
682.1343	733.2437	785.8369	849.1931	913.5937	983.6270	1057.6594	1136.7397	1223.6218	1315.1814
1411.2692	1522.8767	1638.2312							
AZIMUTH-KANAL OHNE SHIFT 0 v.:									
	39.756	34.136	28.516	22.896	17.276	11.656	6.036	0.416	-5.204
-10.824	-16.444	-22.064	-27.684	-33.304	-38.924	-44.544			
AZIMUTH-KANAL MIT SHIFT 0 v.:									
	42.566	36.946	31.326	25.706	20.086	14.466	8.846	3.226	-2.394
-8.014	-13.634	-19.254	-24.874	-30.494	-36.114	-41.734			
ELEVATIONS-KANAL:									
	-20.78	-15.70	-10.59	-5.55	-0.51	4.52	9.63	14.69	19.71
HCS 2 KANAEL FUER INSTRUMENT 3									
GESCHWINDIGKEITSKANAEL :									
	191.5390	209.4506	229.1920	250.9557	274.6450	300.5496	328.9578	359.9661	393.9597
421.1311	471.6731	516.1533	564.8909	618.1440	676.4050	740.1553			
AZIMUTH-KANAL OHNE SHIFT 0 v.:									
	39.5938	34.3638	28.7438	23.1238	17.5038	11.8838	6.2638	0.6438	-4.9752
-10.5962	-16.2762	-21.8362	-27.4562	-33.0762	-38.6962	-44.3161			
AZIMUTH-KANAL MIT SHIFT 0 v.:									
	42.7938	37.1738	31.5538	25.9338	20.3138	14.6938	9.0738	3.4538	-2.1552
-7.7862	-13.4062	-19.0262	-24.6461	-30.2661	-35.8861	-41.5061			
ELEVATIONS-KANAL:									
	-20.548	-15.473	-10.443	-5.413	-0.395	4.694	9.777	14.837	19.924
HCS 2 KANAEL FUER INSTRUMENT 1B									
GESCHWINDIGKEITSKANAEL OHNE SHIFT:									
	174.2491	187.9659	201.7763	216.9383	234.0746	250.5906	270.4561	290.6262	311.4346
335.7917	360.7571	388.2131	417.5998	448.1162	483.3787	519.7019	557.7451	601.4404	645.8123
655.0132	748.5520	802.6470	865.6333	930.7544	1000.0188	1078.4387	1157.9849	1246.2710	1342.2422
1429.1455	1552.1416	1668.6924							
GESCHWINDIGKEITSKANAEL MIT SHIFT:									
	168.1129	181.3466	194.6706	209.2987	225.8315	241.7659	260.9319	280.3916	300.5156
323.9666	348.0527	374.5420	403.2793	432.3352	466.3560	501.4004	538.1040	580.2603	623.0596
670.5378	722.1914	774.3813	835.1978	877.9775	964.8027	1040.4609	1117.2056	1202.3831	1294.9744
1388.4652	1457.4817	1609.9287							

Table 37: The location of the measuring channels for the ion instruments on HELIOS 2, involving the calibrations.

Kanäle = channels
Geschwindigkeits = speed
Mit = with
Ohne = without

Calibration of I2

The calibration of I2 was on the one hand difficult because to a mono-energetic beam of electrons with low energies of exactly known direction was needed. This required special measures due to the deflection of electrons by the Earth's magnetic field and other fields. On the other hand, only one-dimensional, pretty rough direction resolution is required.

To do this, we built a separate facility: the instrument is hung up as a whole pivots in a large vacuum vessel. An electron beam from a specially developed source runs from there through a screening tube μ -metal up in the inlet. Also here there are again stabilisation and control electronics.

In these measurements, there was e.g. especially on the following points to:

By changing the ratio of two plates voltages on plate and sphere analyser had to ensure that the field of view of the instrument as possible perpendicular to the spin axis and thus almost parallel to the ecliptic is located. The necessary to trimming resistor was only afterwards still attached.

Measurements with very low-energy electrons had to prove that the relative flow characteristics are independent of particle energy, as usual in all electrostatic analyzers. At I2 local charges of the baffle plates of the magnitude of mV might cause but in principle already distortions. Fortunately, this was not the case.

The insensitivity of I2 compared with UV light had to be checked.

During the flight, the count rates $Z(i, k)$ as functions of energy (index i) and the azimuth angle (index k) are measured. From this we calculate the values for the speed distribution function $f(i, k)$ according to the following

Formula:

$$f(i, k) = CR \cdot \frac{Z(i, k)}{v^4(i)}$$

Where v_i is the value of the electron velocity corresponding to the i -th energy channel. CR describes the device constant, which was determined by the calibration. It is

$$CR = 1 / (\text{AREA} \cdot \text{EK} \cdot \text{DELEPS} \cdot \text{DELPHI} \cdot \text{EFFABS} \cdot \text{TAU})$$

The individual sizes are

AREA	= 0,3744	}	Entrance surface
EK	= 0,03035		determined from the relative calibration
DELEPS	= 0,117		
DELPHI	= 0,094		
EFFABS	= 0,9		
TAU	= 0,078 (HELIOS 1) = 0,031 (HELIOS 2)		Fraction of the measurement time, per full rotation.

Still the amp dead time must be considered in the count rates. It is $0.55 \times 10^{-7} s$ at HELIOS 1 and HELIOS 2.

The values measured at the calibration for the positions of the measuring channels are summarized in table 38.

For Table 38a is also to be noted that due to the Special Assembly of I2 in the probe the Middle direction of I2 from the radial direction differs by 11.25° . Therefore must be deducted from all values for HELIOS 1 still 11.25° , for HELIOS 2 11.25° added.

A more detailed description of this setting, a discussion of the problems it encountered, as well as details of appropriate transmission characteristics are discussed in a separate publication.

Energiekanal	Programm A	Programm B
1	0,00039	10,69
2	0,468	14,93
3	1,150	20,94
4	1,726	29,26
5	2,317	40,96
6	3,116	57,75
7	3,914	75,80
8	4,723	112,38
9	5,518	157,82
10	6,687	220,56
11	7,835	309,30
12	9,012	432,11
13	10,151	604,68
14	11,882	852,47
15	13,586	1186,06
16	15,457	1657,94

Table 38a: Location of the energy channels of I2; all information in keV.

Azimutkanal	HELIOS 1		HELIOS 2	
	NS	WS	NS	WS
1	168,75	171,55	167,345	189,845
2	213,75	216,55	122,345	144,845
3	258,75	261,55	77,345	99,845
4	303,75	306,55	32,345	54,845
5	348,75	351,55	- 12,655	9,845
6	33,75	36,55	- 57,655	- 35,155
7	78,75	81,55	-102,655	- 80,155
8	123,75	126,55	-147,655	-125,155

Table 38b: location of Azimuth channels of I2; all data in degrees, relative to the see-sun-pulse. At HELIOS 2 all channels by 7.03 ° towards negative values can be moved by command 130-1AVL (knowable to DHK Word B0.. bit 4 in position "PEHEL" instead of "APHEL").

7. Tests

Were at all stages of the project and be tested again and again:

- Design and development: Testing of components, sub-assemblies, circuits
- Manufacturing phase: Ongoing functional and environmental testing of components, assemblies and the integrated instruments. After qualification tests of the prototype instruments (P type) or Acceptance testing of the flight instruments (F type).
- Integration phase: Running functional tests in the integrated system of HELIOS, in the framework of the qualification and acceptance tests of the probe
- Phase of flight: Detailed function tests after the first turn and for future special occasions, in addition to daily regular test cycles (Inflight-tests).

Here will be given only on tests of the finished instruments. Inflight-tests have been described.

Test device

The experiment is so extensive in its entirety and complicated that a relatively costly test device is necessary to test the functionality of the entire experiment sufficiently after environmental testing as well as against the total integration.

The task of the test device is, in simple design and ease of use, the supply voltage and all signals supplied by the probe on the experiment to replicate (S/C-Simulator), to record all the data of the experiment and to evaluate such that a statement about the proper or improper function of the experiment can be made. In all operating conditions must be examined successively. Both the control of the instruments as well as the

Test data evaluation is carried out by a small computer (HP 2100).

The test set should perform this function tests under laboratory conditions, with nominal voltage, nominal-TTL data etc.

All cables between test equipment and experiment are guided over interrupting jacks that allow an interruption of lines feeding of additional or other signals, current and voltage measurements, etc.

The tester has to simulate the automatic test cycle (Inflight test), built into the experiment and evaluate. Also, it must allow also hand-controlled testing.

Each of the four boxes of the experiment has, in addition to the interface connectors, a test plug, to which the most important voltages are introduced. The individual pins of the test plug are listed in appropriate adapter bushings on the test device. These test plugs are not used in flight and were covered so shortly before the start with special caps. All test analog voltages occurring in are also fed to the computer via an extensive interface (multiplexing).

The power supply of the entire test device including the peripheral is designed so that the power is distributed to all devices requiring mains power via a switchable between 115 V and 220 V isolation transformer. In the actual power supply, the DC voltages required for S/C Simulator and the special test units, as well as special - test units are produced.

The block diagram of the test device in connection with the experiment is shown in Figure 51. Figure 52 shows a photographic representation of the test device. The test device is housed in a total of 6 Kayser racks, which also serve as transport boxes. A complete set was stationed in the final phase (integration and last function test before the start) at the Kennedy Space Center (KSC), an identical set remained in Germany for simultaneous testing of the other models. A further description of the test unit should, abandoning here since a detailed "description of the test device for experiment 1/HELIOS part A, B and C" already exists.

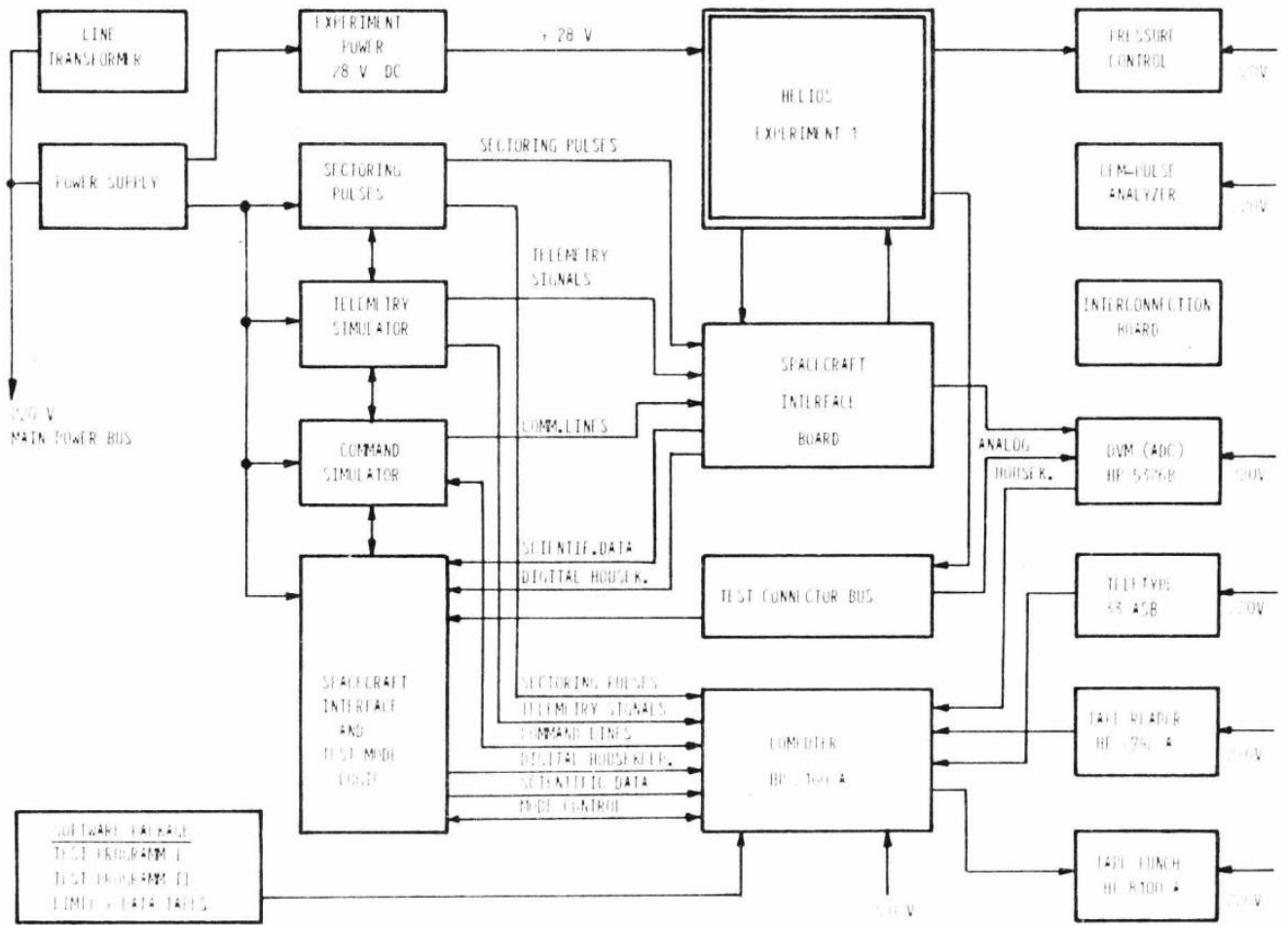


Figure 51: Test device, Block diagram

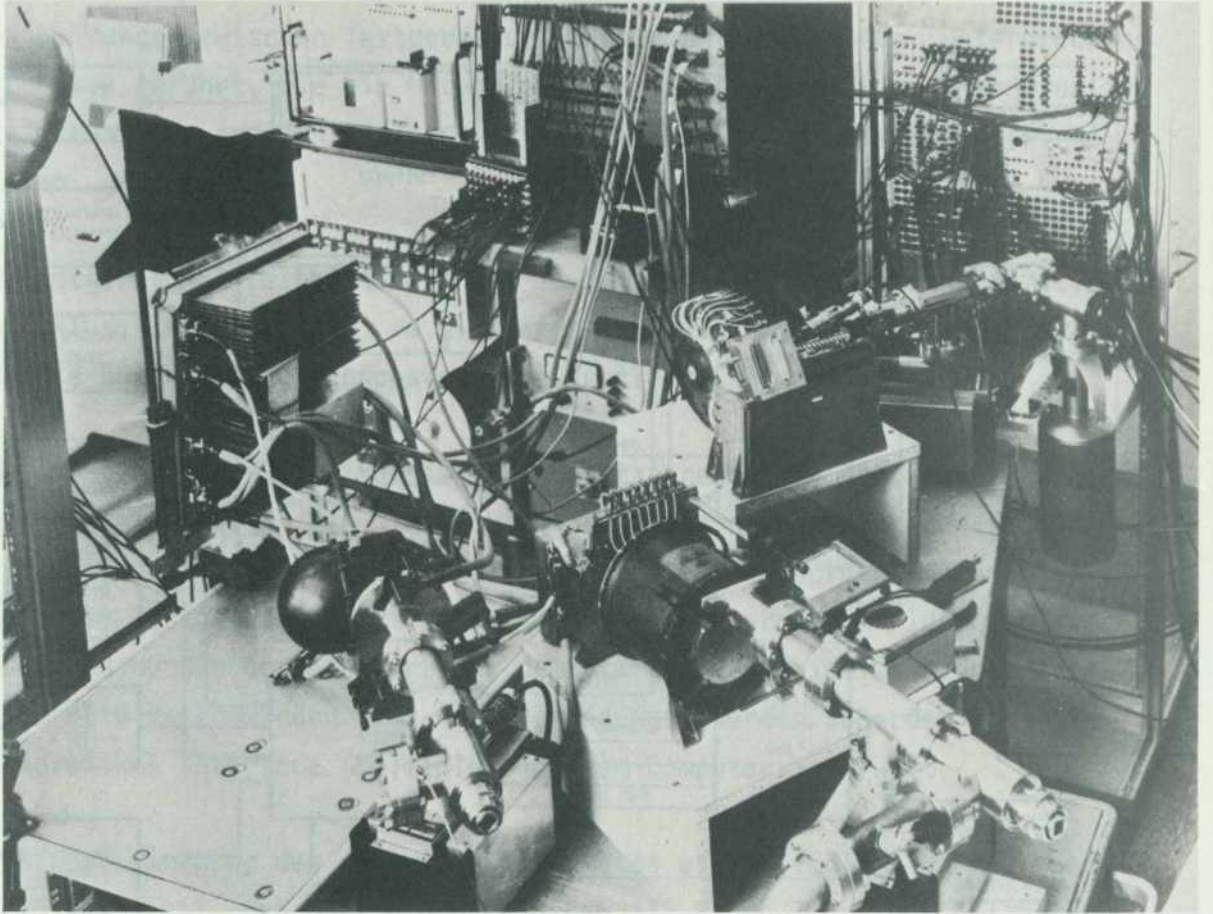


Figure 52: The test device at one of the first total tests of the engineering model of E1. Far left above the teletype for control and data output, in addition the process computer (HP 2100). Top center the "breakout box" for all instrument cables. Right the unit for "hand-controlled" special tests.

Qualification and acceptance tests

The environmental test facilities of the IABG in Ottobrunn were used for the qualification and acceptance tests of all HELIOS experiments, which were rented by the GfW for these purposes.

The engineering model (EM) was used primarily for development testing individual modules. The findings inspire in the construction of subsequent proto - and flying types.

Unfortunately that's true only conditionally because the schedule was too tight and the EM "necessarily" had to be ready for the integration into the probes EM. There were long waiting times, where our EM unused lying around. We would learn much in other tests can and must. Today we would attach this stage much more importance.

The qualification tests of the prototype instruments (P type), the test requirements were higher than for acceptance tests of the aircraft (F type).

Here, too, there was virtually no repercussions on the construction of the F-types due to time constraints. So it was possible that some errors only or even after the acceptance tests were discovered and then often only in "Night and fog action" could be eliminated.

The environmental tests of E1-HELIOS were conducted upon the test regulation PV-E1-100. After orduring environmental testing, a complete functional test of the experiment with the computer-controlled test device was carried after test specification "E1-HELIOS test program 1".

The experiment boxes were mounted to in a special test rack in the configuration in which they are located also in the probe. On the funnel of the sensors an adsorption pump system was flange mounted.

The interiors of the sensors were evacuated ($< 10^{-6}$ Torr), so that the high voltages and the function of the Channelmultiplier could be tested. This oil-free vacuum was needed to avoid contamination of the channeltrons.

In many cases, the evacuation was not possible due to time constraints. Then, special test plug were used where, suitable jumpers made for the artificial suppression of high voltages. So, then at least the electronic function of the experiment could be tested.

The test procedures are given in table 39.

The errors occurred during the qualification and acceptance tests are summarized in the following tables of 40-42.

The P-type was converted after the start of F1 with HELIOS 1 to the flight spare unit F2 on HELIOS-B and is therefore identical to F2. To do this, P had to pass also again acceptance tests.

Qualification (with prototype instruments)

- Function test
- Mass properties
- 1st magnetic measurement
- Functional testing
- Vibration (sine and random)
- Function test
- Linear acceleration
- Function test
- Temperature test and functional test
- Thermovakuum and function test
- EMV test and functional test
- 2nd Magnetic survey *
- Function test

Acceptance (with the flight and flight spare units)

- Function test
- Mass properties
- Vibration
- Function test
- Thermovakuum and function test
- EMV test and functional test
- Magnetic survey*.
- Functional testing

* experiment is turned, but not a function test.

Table 39: test procedure
Qualification and acceptance

Test	Disorder	Remedial measure
1st Magn. surveying	Short circuit in box E1C	improved isolation of the RF generator block against housing
Temperature test	Threshold exceedance of the sensor data at -20 °, + 55°	Exchange of Electr.Components and 1 card.Repetition of the temperature test, degradation of test temperature on + 50 °
Vibration test	Fracture of connections in box E1C	Improvement in support of the electronic block, repeat the test only with E1C
Repeat temperature test	Faulty switching time of the mercury relay	No. Improvements for model aircraft
TV test	Faulty mercury relays in E1A	Exchange
	Border crossings at -20 °, -30 ° for E1C	No
	Clipping in the A/D converter	circuit modification
EMV test	Local exceedances	No, as not critical

Table 40: Errors during the qualification prototype

Test	Disorder	Remedy
Vibration	Loosen the screws in E1C	tightened, secured
	Broken bolt in E1C	replaced
TV test	voltage converter in E1D does not turn on at -20 °	no error in the experiment, an inappropriate external power supply
Magn. Surveying	Exceeding of the permissible Magn.Field after magnetisation	Waiver approved.No change.

Table 41: Errors during the acceptance, F1 type

Test	Disorder	Remedial Measure
TV-Test	Screw on the funnel canceled E1C through handling errors	Replacement
	Failure of the power supply in the E1B	Replacement of faulty components Repetition of the test
EMC-Test	Interference by radiation electric fields in the range of 2-10 MHz	missing ground connection made (also in the F1, P) repetition of the test

Table 42: Errors during the acceptance, F2 type

Integration of E1 in the probe and system tests

After successfully completed qualification or acceptance and verification, the relevant model officially in the responsibility of the project manager and from this to the prime contractor (MBB) for integration into the probe was handed over. The most important part of the incoming inspection was a spacecraft Simulator test for the direct examination of all interface cables. After installation in the probe, E1 could be operated and tested like all other experiments only on the probe systems. These integrated system tests (IST) were now at probe level the function tests after each individual qualification and acceptance steps. Similarly as the E1 Tester was also the HELIOS test set (HTS) commands to E1, launched test cycles, evaluated the data and examined one at a time about 25 different operating States of E1. After the most important environmental tests, the E1 instruments were evacuated for the IST, with the help of the pump flange mounted on the front of the funnel (fig. 53).

Before the final completion of the probe there is still a special test, the so-called final test, for E1 at KSC. The speakers built into the probe were again separated from the probe systems and associated with the test device. Then all voltages were tested on the evacuated instruments in manual mode again progressively measured, the amplification of channeltrons with the lot channel Analyzer etc. Analyzer voltages measured in this final test serve as reference data for the calibration of the energy channels. Then came the final Assembly of the whole probe.

Immediately before countries impose the rocket top on the finished probe the airtight lid screwed on the E1 funnels were removed and replaced by lightweight dust cover held by spring-loaded. After putting the top together with the HELIOS on the rocket this lid with a gripping tool were removed only 20 hours before the start through again through a special opening in the top of the rocket. In this way we could the risky blasting off the lid or other

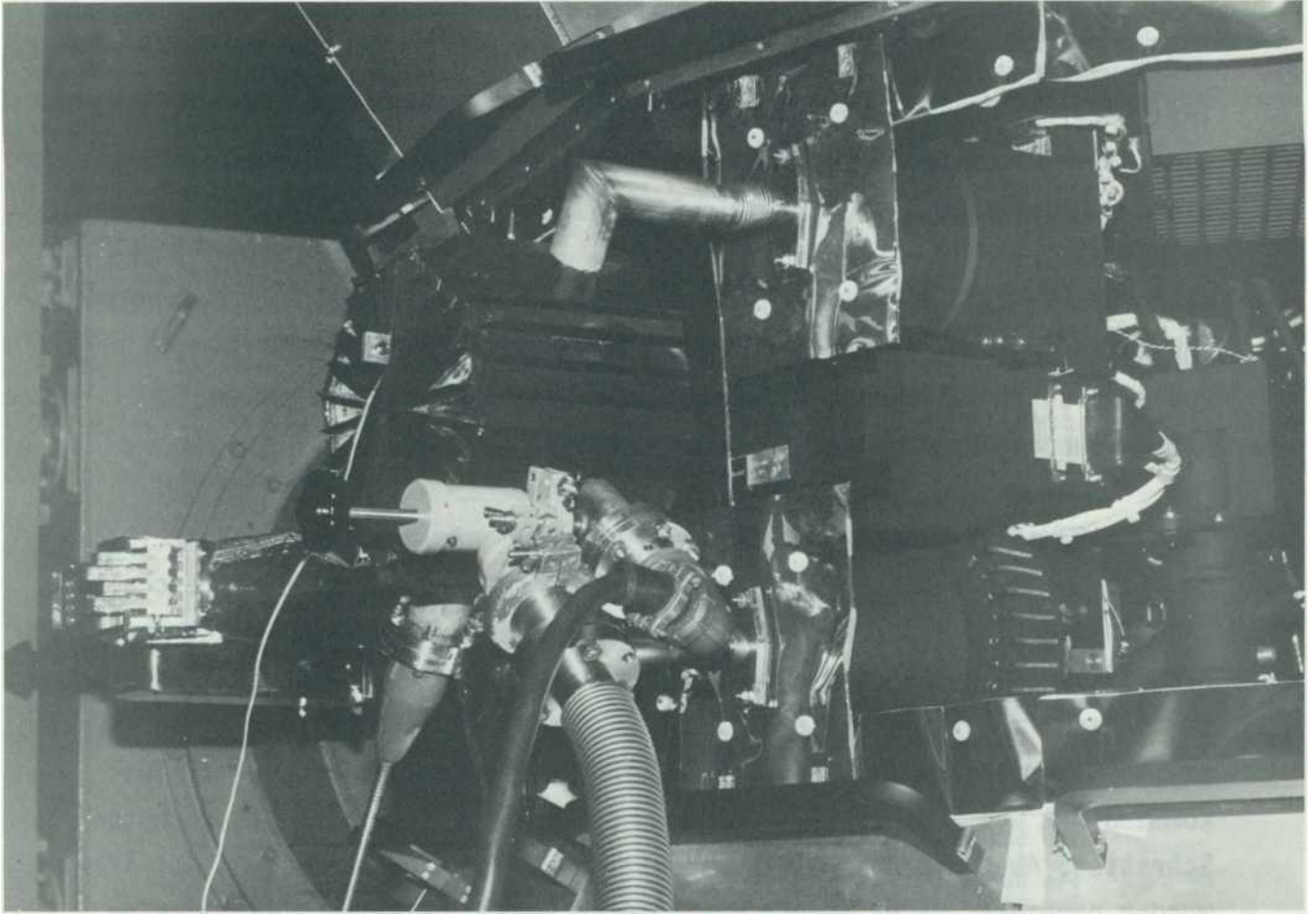


Figure 53: The vacuum pump to the test of the instruments built into the probe of E1.

avoid complicated actions in flight and yet the instruments protect quite well from contamination and dust.

On the other hand, the enforcement of this whole procedure the development of the cover and the gripping tool, the training of the gripper (with replacement), study of interface requirements, as well as the NASA-safety regulations and last but not least, the negotiations and the paperwork with all stakeholders has requires some grotesque efforts. Perhaps there is yet easier techniques...

First turn on the instruments

Two days after the launch of HELIOS 1 on the 10.12.1974 the involvement of the E1 instruments started. Until then, all sensors and electronics were evacuated safely enough. The power-up sequence was established long before in detail. Parts of it were tested during the "end to end test" of spacecraft (at that time still at the KSC) and mission control (at the JPL) and later during the "operational demonstration test" already and were used mainly to teach the participants (K. Müller and R. Schwenn) in dealing with the mission control systems.

Table 43 shows an excerpt from the command log book of the 12.12.1974. At 0115 GMT, the power supply of E1 was connected with CMD 004-E10N. This is followed by the actual E1 command. Each instrument was examined first individually exactly, namely the AHK and DHK channels on the screen were tracks (see Figure 31), and the scientific data directly to the quick printer. After each change a test cycle was each commanded and waited, then only carried out the release of the next step. Also the shut-off commands for the high voltage (E.g. 151-1V1R) have been tried, but not the higher voltage levels. Although no sufficient count rates were to be expected, we investigated also I3 and switching between I1a and I3. Then came still switching between NDM and HDM and the Digital electronics. There were no anomalies during the entire procedure, everything was exactly the last ground tests, with the exception of the last visible solar wind particles. Until recently all instruments were turned on, and the actual mission operation could begin at 0255 GMT.

S/C ID	CMD CTR	STATUS TIME	SPACECRAFT TIME	COMMAND	STATUS	CMD MES	FMT
90	0	0- 0	00/00/00	000/00/00/00.0	MANUAL V	940	601
90	0	0- 0	00/00/00	000/00/00/00.0	MANUAL V	970	601
90	0	0- 0	00/00/00	000/00/00/00.0	MANUAL V	980	601
90	50	346-74	01/15/00	000/16/48/49.5	004-E10N		120 601
90	51	346-74	01/15/00	000/16/48/12.8	004-E10N	V	120 601
90	51	346-74	01/16/10	000/16/48/10.8	374-ISOF		130 601
90	51	346-74	01/16/28	000/16/49/21.4	374-ISOF	V	130 601
90	51	346-74	01/17/50	000/16/49/21.4	066-IDE1		140 601
90	52	346-74	01/18/09	000/16/51/01.5	066-IDE1	V	140 601
90	0	0- 0	00/00/00	000/00/00/00.0	MANUAL N	970	601
90	0	0- 0	00/00/00	000/00/00/00.0	MANUAL N	980	601

S/C ID	CMD CTR	STATUS TIME	SPACECRAFT TIME	COMMAND	STATUS	CMD MES	FMT
90	0	0- 0	00/00/00	000/00/00/00.0	MANUAL N	70	601
90	0	0- 0	00/00/00	000/00/00/00.0	MANUAL N	80	601
90	0	0- 0	00/00/00	000/00/00/00.0	MANUAL V	70	601
90	0	0- 0	00/00/00	000/00/00/00.0	MANUAL V	80	601
90	52	346-74	01/20/20	000/16/51/01.5	122-1HDM		150 601
90	54	346-74	01/20/51	000/16/53/43.5	122-1HDM	V	150 601
90	54	346-74	01/22/00	000/16/53/43.5	024-1S1B		160 601
90	55	346-74	01/22/32	000/16/55/24.8	024-1S1B	V	160 601
90	55	346-74	01/23/40	000/16/55/24.8	332-ITCY		170 601
90	56	346-74	01/24/13	000/16/57/06.0	332-ITCY	V	170 601
90	56	346-74	01/27/20	000/16/57/06.0	374-ISOF		180 601
90	57	346-74	01/27/56	000/17/00/48.8	374-ISOF	V	180 601
90	57	346-74	01/29/00	000/17/00/48.8	066-IDE1		190 601
90	58	346-74	01/29/37	000/17/02/30.0	066-IDE1	V	190 601
90	58	346-74	01/31/30	000/17/02/30.0	122-1HDM		200 601
90	59	346-74	01/31/59	000/17/04/52.9	122-1HDM	V	200 601
90	59	346-74	01/33/10	000/17/04/52.9	003-1S1A		210 601
90	60	346-74	01/33/40	000/17/06/33.0	003-1S1A	V	210 601
90	60	346-74	01/34/50	000/17/06/33.0	332-ITCY		220 601
90	61	346-74	01/35/21	000/17/08/14.3	332-ITCY	V	220 601
90	61	346-74	01/38/30	000/17/08/14.3	107-1V11		230 601
90	62	346-74	01/39/04	000/17/11/57.0	107-1V11	V	230 601
90	62	346-74	01/42/10	000/17/11/57.0	332-ITCY		240 601
90	63	346-74	01/40/45	000/17/13/38.3	332-ITCY	V	240 601
90	63	346-74	01/42/20	000/17/13/38.3	151-1V1R		250 601

S/C ID	CMD CTR	STATUS TIME	SPACECRAFT TIME	COMMAND	STATUS	CMD MES	FMT
90	64	346-74	01/42/27	000/17/15/39.8	151-1V1R	V	250 601
90	64	346-74	01/44/00	000/17/15/39.8	374-ISOF		260 601
90	65	346-74	01/44/28	000/17/17/21.0	374-ISOF	V	260 601
90	65	346-74	01/45/40	000/17/17/21.0	066-IDE1		270 601
90	66	346-74	01/46/09	000/17/19/02.3	066-IDE1	V	270 601
90	66	346-74	01/48/10	000/17/19/03.4	122-1HDM		280 601
90	66	346-74	01/48/31	000/17/21/24.0	122-1HDM	V	280 601
90	66	346-74	01/49/50	000/17/21/24.0	353-1SE2		290 601
90	67	346-74	01/50/12	000/17/23/05.3	353-1SE2	V	290 601
90	67	346-74	01/51/30	000/17/23/05.3	332-ITCY		300 601
90	68	346-74	01/51/53	000/17/24/46.5	332-ITCY	V	300 601
90	68	346-74	00/10/59	000/17/24/46.5	U		1 601
90	69	346-74	01/54/29	000/17/27/01.8	U	N	1 601
90	69	346-74	01/54/40	000/17/27/24.0	172-1V21		310 601
90	69	346-74	00/10/59	000/17/27/58.9	U		1 601
90	70	346-74	01/55/16	000/17/28/09.0	172-1V21	V	310 601
90	70	346-74	00/03/35	000/17/28/20.3	U		1 601
90	70	346-74	01/55/30	000/17/28/22.5	U	N	1 601
90	70	346-74	01/55/43	000/17/28/42.8	U		1 601
90	70	346-74	01/56/20	000/17/29/18.8	332-ITCY		320 601
90	71	346-74	01/56/57	000/17/29/50.3	332-ITCY	V	320 601
90	71	346-74	01/59/30	000/17/32/28.9	234-1PGA		330 601
90	72	346-74	01/59/59	000/17/32/52.5	234-1PGA	V	330 601
90	72	346-74	02/01/10	000/17/34/07.9	332-ITCY		340 601
90	73	346-74	02/01/41	000/17/34/33.8	332-ITCY	V	340 601

Table 43: This snippet from the command log by HELIOS 1 shows of the 12.12.1974 power up for the E1 instruments.

S/C ID	CMD CTR	STATUS TIME	SPACECRAFT TIME	COMMAND	STATUS	CMD MES	FMT
90	73	346-74 02/04/20	000/17/37/20.3	247-1PGB		350	601
90	73	346-74 02/04/44	000/17/37/37.2	247-1PGB	V	350	601
90	74	346-74 02/06/00	000/17/38/58.2	226-1V2R		360	601
90	75	346-74 02/06/26	000/17/39/18.4	226-1V2R	V	360	601
90	75	346-74 02/07/40	000/17/40/39.4	374-1SOF		370	601
90	76	346-74 02/08/06	000/17/40/58.5	374-1SOF	V	370	601
90	76	346-74 00/03/35	000/17/41/27.8	U	I	601	
90	76	346-74 02/09/20	000/17/42/18.4	066-1DE1		380	601
90	77	346-74 02/09/47	000/17/42/39.8	066-1DE1	V	380	601
90	77	346-74 02/11/50	000/17/44/48.0	122-1HDM		390	601
90	77	346-74 02/12/10	000/17/45/02.7	122-1HDM	V	390	601
90	78	346-74 02/12/55	000/17/45/55.5	U	I	601	
90	78	346-74 02/13/30	000/17/46/28.2	045-1SE3		400	601
90	78	346-74 02/13/50	000/17/46/42.8	045-1SE3	V	400	601
90	79	346-74 02/15/10	000/17/48/09.4	532-1TCY		410	601
90	79	346-74 02/15/31	000/17/48/24.0	532-1TCY	V	410	601
90	80	346-74 02/18/20	000/17/51/20.7	107-1V11		420	601
90	80	346-74 00/10/59	000/17/51/20.7	U DTV OVER	I	601	
90	81	346-74 02/18/54	000/17/51/46.5	107-1V11	V	420	601
90	81	346-74 02/20/00	000/17/52/58.5	532-1TCY		430	601
90	82	346-74 02/20/36	000/17/53/28.9	532-1TCY	V	430	601
90	82	346-74 02/23/10	000/17/56/08.7	151-1VIR		440	601
90	82	346-74 01/55/43	000/17/56/08.7	U DTV OVER	I	601	
90	83	346-74 02/23/37	000/17/56/30.0	151-1VIR	V	440	601
90	83	346-74 02/24/50	000/17/57/48.8	374-1SOF		450	601
90	84	346-74 02/25/18	000/17/58/11.3	374-1SOF	V	450	601
90	84	346-74 02/26/30	000/17/59/30.0	066-1DE1		460	601
90	85	346-74 02/27/01	000/17/59/53.7	066-1DE1	V	460	601
90	85	346-74 02/28/10	000/18/01/07.9	311-1DE2		470	601
90	86	346-74 02/29/20	000/18/01/34.9	311-1DE2	V	470	601
90	86	346-74 01/55/43	000/18/03/34.2	U	I	601	
90	86	346-74 02/30/40	000/18/03/39.8	122-1HDM		480	601
90	86	346-74 02/31/23	000/18/03/55.5	122-1HDM	V	480	601
90	87	346-74 02/32/20	000/18/05/18.8	024-1S1B		490	601
90	87	346-74 02/32/44	000/18/05/36.8	024-1S1B	V	490	601
90	88	346-74 02/34/00	000/18/06/58.9	003-1S1A		500	601
90	88	346-74 00/03/35	000/18/06/58.9	U DTV OVER	I	601	
90	89	346-74 02/34/25	000/18/07/18.0	003-1S1A	V	500	601
90	89	346-74 02/35/40	000/18/08/40.2	107-1V11		510	601
90	90	346-74 02/36/08	000/18/09/00.4	107-1V11	V	510	601
90	90	346-74 02/37/20	000/18/10/18.0	553-1SE2		520	601
90	91	346-74 02/37/49	000/18/10/41.7	553-1SE2	V	520	601
90	91	346-74 02/39/00	000/18/11/58.2	172-1V21		530	601
90	91	346-74 02/12/55	000/18/11/58.2	U DTV OVER	I	601	
90	92	346-74 02/39/29	000/18/12/21.8	172-1V21	V	530	601
90	92	346-74 02/40/40	000/18/13/39.4	532-1TCY		540	601
90	93	346-74 02/41/10	000/18/14/03.0	532-1TCY	V	540	601
90	93	346-74 02/44/20	000/18/17/18.8	213-1NDM		550	601
90	94	346-74 02/44/53	000/18/17/45.8	213-1NDM	V	550	601
90	94	346-74 02/46/00	000/18/18/58.9	532-1TCY		560	601
90	94	346-74 00/10/59	000/18/18/58.9	U TBL OVER	I	601	
90	95	346-74 02/46/34	000/18/19/27.0	532-1TCY	V	560	601
90	95	346-74 02/47/10	000/18/20/09.8	066-1DE1		570	601
90	96	346-74 02/47/35	000/18/20/27.8	066-1DE1	V	570	601
90	96	346-74 02/48/50	000/18/21/49.9	532-1TCY		580	601
90	96	346-74 01/55/43	000/18/21/49.9	U TBL OVER	I	601	
90	97	346-74 02/49/16	000/18/22/09.0	532-1TCY	V	580	601
90	97	346-74 02/51/15	000/18/24/13.9	U	I	601	
90	97	346-74 02/52/00	000/18/24/57.8	122-1HDM		590	601
90	97	346-74 02/52/19	000/18/25/11.3	122-1HDM	V	590	601
90	98	346-74 02/54/50	000/18/27/48.8	532-1TCY		600	601
90	99	346-74 02/55/22	000/18/28/14.7	532-1TCY	V	600	601
90	99	346-74 02/59/02	000/18/32/00.8	201-0TST		610	601
90	99	346-74 01/55/43	000/18/32/00.8	U DTV OVER	I	601	
90	100	346-74 03/00/00	000/18/32/52.5	201-0TST	N	610	601

Table 43: Continuation

Subsequent special tests

Completely trouble-free working of the instruments made virtually unnecessary special tests during the mission. We have changed the channeltrons due to the accurate measurement of gain at the regular conducted daily Inflight test - of which we get each paper prints - safely under control. Nevertheless, we have occasionally commanded test sequences, in which we examined the individual instruments with different Channeltron high voltages. By direct comparison of the measured particle count rates and spreads, we can ensure that at no time to distort the measured particles fluxes entered through changes of channeltrons.

8. Flight experiences with E1 instruments

In this last chapter, we want to report much about our experience with the instruments during the mission. Much has been discussed already at the description of the instruments in the form of comments in detail.

The technology of instruments now only much: apart from the failure of the relay in I2 (S.133) there have been no problems so far. The extremes are verified by testing the temperatures were essentially being respected; There have been few exceedances (to -34° I1a/b, in operation and -42° when switched off). The thermal design of the I2 had concerned about much before the start because of the large inlet, so still relatively late a large comb-like finned had to be applied (see Figure 1). The temperature of I2 held indeed within the framework and reached values in the Perihelia of $32,10^{\circ}$ to $44,44^{\circ}$ (HELIOS 1) and $36,6^{\circ}$ to $49,28^{\circ}$ (HELIOS 2).

Finally illustrate some metrics, what is with these instruments and also where their boundaries lie.

The data collected during the mission are of an extraordinary variety, and even after over five years of mission, there are still new surprises in the form of data, no one could expect. Of course, the solar wind in most cases behaves "normally", and the interpretation of the instruments proves this as excellent. Examples of 'normal' measurements are shown in figs. 54 and 55. Much more interesting but, of course, are those events that deviate from the norm and so far observed in many cases by no one.

It turned out that most of the various extremes our instruments can keep up still and let quite some room for the unexpected. Only been two events our measurement ranges really are no longer sufficient, because in one case the solar winds speed under 170 kms^{-1} (fig. 56) fell, went in the other well over 1700 kms^{-1} (fig. 57).

The selected energy resolution was slightly more painful. It happened occasionally that at extremely low temperatures virtually the entire proton distribution in a single measuring channel fell (fig. 58) or even through the grate fell (fig. 59). Such data are useful only with restrictions.

Well as amazing, however, has the dimensions of sensitivities turned out. So far, the plasma densities varied between 0.1 (fig. 60) and 1500 cm^{-3} (fig. 61), i.e. by a factor of 1.5×10^4 . To in all cases still sufficiently accurately to measure, a dynamic range of at least 10^5 required. Here, the compilation of several instruments made to a 'Package' really paid. I1a covered mainly the area of low particle flows with its high sensitivity at the same time very low NZR. Even such low counting rates in the Proton peak of 10 counts (Figure 60) can yet be evaluated, because the NZR at ≈ 2 is located. I3 was particularly suited to the high flows close to the perihelion. The highest count rate previously measured by I3 of 6656 counts (picture 61) corresponds to I1a a count rate 200 000 counts (measured in 10 ms, i.e. the real count rate would be 20 MHz, which of course the CEM amplifiers with their dead time of approximately 500 ns according to 2 MHz were no longer grown). The simultaneously working in all cases instrument I1b is located approximately in the middle with his sensitivity and enabled precise cross calibrations of instruments on the fly.

Also I2 proved excellent. It can be seen in several of the examples that harmonized the selected sensitivity with the selected energy range: the 1-count level was only reached in the two top channels, while the core of the distribution count rates at the same time delivered up to 50 000 counts (fig. 62). Also I2 so covered a dynamic range of almost 10^5 . by the way, the maximum count rate of 63 488 counts (see table 34 on p. 143 ff) was never exceeded, but in many cases only just missed (61 image).

63 to 68 images show some more eye-catching features in the data, which are each described in the captions.

The shown examples illustrate the diversity of data, which surprised us in the course of the Mission again and again on the new. The expert viewer of these samples is able to avoid hardly the huge stimulus that emanates from them. What does this all mean? Are there "Holes" in the solar wind? Or even solar wind without electrons? Unknown ion? It is tempting to pounce immediately on the evaluation. So far us even today, after almost six years of mission. And therefore we look forward to further work with this experiment and its data, which will keep some more years in breath.

DFVLR-GS0C 8031 OBERPFÄFFENHOFEN GERMAN SPACE OPERATION CENTER 29, 2.80 GMT 4H 46M 54S 428MS PAGE-NO. 3
MISSION HELIOS-5 ***AUSGABE GEPUFFERT***
H-91 DSS--11 80 59 21:02:05 B/R 512 FM 1 DM 2-0 FMT 34; EXP1-NOR
SCTIME 26 00:22:39.468 FB/FF= 0/ 1
STATUS: PLA NDM TIME 0 00:51:49.500 MEM2 D1-ON D2-OFF I1A-ON I2-ON I1B-ON WS I3-OFF APHEL
INITIAL DATA W1-8 11110000 11000010 01011000 11110000 10001000 01010111 11110000 00001110
CW: 5 W9-15 11101011 11110000 10001000 01010111 11110000 11110000 11110000

I1B	EN1-16	23	24	23	24	22	24	25	31	84	240	40	25	25	32	24	25
	EN17-32	23	23	24	23	24	24	23	23	23	25	24	24	24	25	24	25
I1A INTEGR.	EN1-16	0	3	2	3	3	7	10	62	496	832	32	4	8	32	4	3
	EN17-32	3	0	3	5	1	3	5	2	1	2	3	1	0	2	0	3
I2A	AZ1	0	1	1	1	7	6	6	6	13	19	15	17	18	21	18	21
	AZ2	0	0	1	1	2	8	6	10	12	14	16	15	12	15	15	17
	AZ3	0	0	1	2	4	8	14	16	26	24	32	22	24	36	29	38
	AZ4	0	44	124	136	34	60	42	32	50	48	60	54	58	64	76	52
	AZ5	0	112	384	352	240	120	64	54	50	72	72	76	88	96	104	88
	AZ6	0	124	464	416	256	120	68	60	46	42	62	58	72	62	80	60
	AZ7	0	0	1	5	9	11	18	21	27	36	27	40	52	42	44	34
	AZ8	0	0	0	5	4	8	9	13	19	17	30	19	29	26	28	32

I1A/3 MAX AT: EN9 EL5 AZ8
EN7
EL3 EL4 EL5 EL6 EL7 EL3 EL4 EL5 EL6 EL7 EL3 EL4 EL5 EL6 EL7

AZ6	0	0	0	0	0	0	0	0	0	0	0	0	0	0	0	0
AZ7	0	0	0	0	0	1	0	0	0	0	0	0	0	0	0	0
AZ8	0	0	1	0	0	0	4	6	1	0	4	13	115	21	0	0
AZ9	0	1	2	0	0	3	13	19	3	0	1	34	216	36	2	0
AZ10	1	1	1	1	0	2	1	6	1	0	4	18	16	1	0	0
			EN10					EN11					EN12			
AZ6	0	0	0	0	0	0	0	0	0	0	0	0	0	0	0	0
AZ7	1	0	0	0	1	0	0	0	0	0	0	0	0	0	0	0
AZ8	1	7	144	24	0	0	0	2	0	0	0	0	0	1	0	0
AZ9	2	32	464	100	0	2	3	10	3	0	0	0	0	0	2	0
AZ10	0	10	26	5	0	1	2	3	1	0	0	0	0	0	0	0
			EN13					EN14					EN15			
AZ6	0	0	0	0	0	0	0	0	0	0	0	0	0	0	0	0
AZ7	0	0	1	0	0	0	0	0	0	0	0	0	0	0	0	0
AZ8	1	0	2	0	0	0	2	10	0	0	0	0	0	0	0	0
AZ9	0	0	1	0	0	0	1	10	3	0	0	0	0	4	0	0
AZ10	0	0	0	0	0	0	1	1	0	0	0	0	0	0	0	0

HELIOS 2
 $r = 0,954 \text{ AU}$
 $v_p = 312 \text{ kms}^{-1}$
 $n_p = 6,5 \text{ cm}^{-3}$
 $T_p = 22 \text{ 000 K}$

Figure 54: "Normal" slow solar wind, away from the Sun.
(1) The photo-peak in the A-programme of I2.
(2) The NZR by I1b varies only to ± 1 count (in HELIOS 2).
(3) The integral NZR by I1a lies at approx.2-3 counts.
(4) The maximum of the distribution has jumped from EN9/EL5/AZ8 to EN10/EL5/AZ9.
The stirring that often comes from the alternate channel shift.

UFVLR-GSUC 8031 OBERPFAFFENHOFEN GERMAN SPACE OPERATION CENTER 28. 4.79 GMT 19H 40M 28s 199MS PAGE-NO.
 MISSION HELIOS-A ***AUSGABE GEPUFFERT***
 H-90 DSS--67 79 118 16:04:02 B/R 512 Fi: 2 DM 3-0 FIIT 34; EXP1-HIGH
 SCTJME190 18:05:00,718 FN: 99 FB/FF= 1/ 47
 STATUS: PLA HDM2 MCP TIME 0 00:47:54.875 MEM2 01-04 28.4.79 G T 19 40 3 S 19 (<)k> NS PAGE NOFF
 UPvis GSUC d '31 OBEKPPAF FENHÜFE ^ GERM SPACE SURGERY CENTER
 INITIAL MISSION HELIOS-A ***AUSGABE GEPUFFERT***
 CW: 5 H pSS * 90 - 67 79118 16 : 0 A: 0 n/R 512 Fi: 2 DM 30 FHT34; E a H
 SCTJME190 : 0,718 F * J; 99 F9/FFs 1
 STATUS: ? LA H0>2 M C 9 TIME 0 00:47: 54.875 MEM2 01 -ON D2-OFF [1A-O N I 2 - 11H-ON NS I 5 C FF
 11B
 11A INTE INITIAL DATA W1-8 11110000 10110011 10101110 11110000 00101011 00110101 11110uOO 00011000
 CW: 5 wv - 15 1 1 1 01 01 0 1 1 1 00101011 00110101 11110000 1111 oooo m 10000
 12B
 11B EN 1-6 25 32 62 400 128 1 4C 8 i 66 64
 X 1 A INTEGR.CN1-o 5 76 4 9 6 3072 691 4608 736 1 00
 12B AZ 1 1 08 8 1-A72 1728 21 7 243 2 0 1 6 34 56 35 * 4
 AZ? 1 068 U72 1 728 2043 243 2 94 3328 3 * 40
 A-Z 3 1 < 72 1856 24 3 2 2 94 345 4096 4ü (6 53 7
 AZA ? ÜAä 7 6 3 3328 3963 < 5632 6o 56 7424
 AZS 2176 3072 78 A 0 4608 537 64-1 7680 8704
 AZ6 2 0 A 8 2688 3 A so 3963 460 5888 6 6 56 7 6 6
 11A / 3 A Z 7 1 66 4 204 * 26 3200 3 8 4 6 0 5376 58KO
 AZ8 1216 1728 2 0 4 8 2 294 35 34 4 0 96 4352
 11A / 11 C. 9 MAX A T; I m6L3
 11 A / 3

	EL?	EL3	S N1 ELA	6 L5	EL6	E L 7	5 L 2	EL3	EN 2 E L 4	E L 5	EIO EI7
AZ5	0	0	0	0	0	0	Q	0	0	0	0
AZo	0	0	0	0	0	0	1)	0	0	u
AZ?	0	0	1	0	1	0	0	0	0	1	0
A Z 8	0	0	0	0	0	0	1	3	10	6	4
A-Z 9	0	1	0	1	c	0	c	2	5	15	5
AZ 1 NC	0	0	UE	1	0	0	FJ	2	5	4	j
A-Z 1 1	0	0	0	0	0	0	i	0	0	1	0
AZ 5	1	0	0	0	0	0	0	0	1	3)
AZ6	1	0	0	1	0	0	c	1	2	<*	3
• 5 AU; L7	1	6	1 0	13	5	1	2	1 5	76	8 j	2 6
1 A-Z 9	2	21	56	5 0	20	5	6	6	366	432	152
• 5 kms * 210	7	12 64	1 4	104	27	5	6	62	416	6 B 19?	288
^ 3	2	5	32	10	4	4	2	20	136	6 8	7
• cm * 75	1	1	2	5	7	0	1	1	1 1	ü	;
AZc < 75	0	0	0	0	0	0	0	7	0	0	0
IO 000 K %	0	2	6	4	1	1	C	0	1	5	1
AZ 9	1	2 4	104	123	24	3	0	10	6 4	1 ^	23
AZ10	12	136	832	1024	256	26	5	6 *	576	672	152
A-Z 1 1	9	1 60	1024	1 53	608	24	8	9 o	7 0	1	400
A-Z 1 1	2	26	? «3»	6 ° 8	2	2 0	6	34	1 76	336	112
AZ 5	0	0	1	1	0	1	0	1	0	UE	0
AZf	0	0	0	1	2	0	0	0	0	0	0
A Z 7	0	2	1 0	20	1	0	0	1	3	6	4
A Zó	z	6	96	108	24	5	2	<	14	11	2
A-Z 9	ε	9	92	192	48	5	0	1	8	20	7
A-2 1 0	0	7	58	30	1 0	1	0	1	5	u	3
A-Z 1 1	0	2	1	1	5	1	0	0	0	0	1

HELIOS 1

$r = 0,45 \text{ AU}$

$v_p = 395 \text{ kms}^{-1}$

$n_p = 54 \text{ pcm}^{-3}$

$T_p = 160 \text{ p000 l}$

RP

Figure 55: "Normal" slow solar wind, close to the Sun.

Sample HDM2-block small block length (p.89), where the EL8 data be omitted. Still, the distribution of Proton is captured well.

INITIAL DATA
CW: 5

11B	EN1-16	176	116	60	42	40	32	29	29	28	28	27	25	27	27	27	27
	EN17-32	27	27	27	27	26	25	26	26	26	26	27	25	26	26	25	25
11A INTEGR.	EN1-16	832	448	152	62	44	10	10	2	5	1	3	0	1	3	1	0
	EN17-32	3	2	0	3	7	5	3	2	4	4	1	4	1	5	2	1
12A	A21	0	112	512	992	2816	432	640	864	1024	1280	1664	1984	2304	2944	3328	3712
	A22	0	112	432	1088	3200	704	608	800	1024	1344	1664	2048	2432	2816	3456	3712
	A23	0	192	736	1216	3840	3584	672	832	1088	1408	1728	2048	2304	3072	3456	3968
	A24	0	3584	5888	4608	4352	3840	1024	1024	1216	1600	1920	2432	2816	3328	3840	4096
	A25	0	2944	4352	3712	3456	3200	864	992	1216	1536	1984	2304	2688	3200	3584	3968
	A26	0	304	736	1280	4864	1344	672	864	1088	1536	1920	2176	2560	3072	3584	3840
	A27	0	136	544	2432	4352	1856	640	864	1088	1344	1792	2048	2432	2944	3456	3840
	A28	0	136	496	928	1856	1536	640	896	1088	1344	1664	1984	2304	2816	3200	3584

11A/3

	EN1	EL3	EL4	EN1	EL5	EL6	EL7	EN2	EL3	EL4	EL5	EL6	EL7	EN3	EL3	EL4	EL5	EL6	EL7
A26		1	8	18	12	17		4	0	2	4	9	5	1	1	1	2		0
A27		3	28	68	72	54		32	3	15	44	24	24	3	3	8	13		6
A28		9	46	112	112	64		76	5	27	76	42	42	3	8	21	27		8
A29		4	17	42	64	38		28	2	11	27	28	14	1	3	21	12		5
A210		0	1	7	8	4		4	0	2	3	4	2	0	1	1	1		1
				EN4				EN5						EN6					
A26		0	0	0	0	0		0	0	0	2	0	0	0	0	0	0		0
A27		1	4	0	1	0		1	0	2	1	0	1	0	0	0	0		0
A28		0	5	5	5	3		7	0	5	7	4	1	1	0	1	1		1
A29		3	4	8	0	3		5	0	4	5	3	0	0	2	0	2		0
A210		1	1	5	3	0		3	0	2	3	0	0	0	0	0	0		0
				EN7				EN8						EN9					
A26		0	0	1	0	0		0	0	0	0	0	0	0	0	0	0		0
A27		0	0	0	0	2		0	0	0	0	0	0	0	0	0	0		0
A28		0	0	0	0	0		0	0	0	0	0	1	0	0	0	0		0
A29		1	1	1	0	1		0	0	0	0	0	0	0	0	0	0		0
A210		0	1	0	0	0		0	0	1	0	0	0	0	1	1	0		0

HELIOS 2
 $r = 0,308 \text{ AU}$
 $v < 170 \text{ kms}^{-1}$

Figure 56: The slowest so far solar wind.

(1) Here v_p has become so low, that even the maximum of the distribution is still below EN1. v_p is likely much less than 170 kms^{-1} amount. This phase lasts several hours.

```

**HELIOS/A** MPE-PRINTOUT DLX EDF*2 WOM SORTED DATA TAPE
GRT 254 3:22:29.732 SCT 254 3: 7:14.648 B/R 8 FM 3 DM 7 MISSING EI DATA: 24
GRTEF 4: 5:41.638 JSTEF 3:50:26.654 NUM WS BIT ERROR RATE: 0
INITL.TIME: 1921 SITEF 3: 7:14.648
INITIAL DATA WL- B 11110000 00000101 11110001 11110000 10011110 01010111 11110000 00001110
W9-15 11101911 11110000 10011110 01010111 11110000 11110000 11110000
ALLGEM. QW 00000111 11111110
11A QW 00000000 11111111
12 QW 00000011 11111111
13 QW 00000000 00001111
11b QW 00000011 11111111

```

F 2 I ID

HA InftuR.

11A INT

J 2 A

I 1A / J

HELIOS 1

r = 0,884 AU

v > 1700 kms⁻¹

ED	23	23	2 4	2 2	23	23	2 3	2 3	2 3	2 3	24	21	22	2 3	2 3	2 2
ENI 16	23	2 3	2 4	2 2	23	23	2 3	2 3	2 3	2 3	24	21	22	2 3	2 3	2 2
ENI 7-32	23	2 2	2.L	24	2 4	22	2 4	23	24	2 3	28	^ 3	2 3	2 4	2 4	121 6
ENI 16	2 J	15	20	ID	12	16	16 / NVI 7	15	15	10	15	10	1 6	1 4	7	7
ENI 7-32	14	13	11	8	14	16	17 (±) 1 3	1 1	1 2	10	1 3	12	1 6	G 4 3	32 0	23
AZI	2	3	7	7	7	3	6	2	8	3	4	1 4	0	i 3	*	1 6
A-22	3	7	10	16	5	7	3	8	5	1 1	1 J	12	12	L 1	1 7	1 J
AZ 3	3	10	7	0	7	1 7	i 5	1 d	1 3	1 7	25	1 6	22	1 6	1 7	2 3
AZ 4	5	J 4	172	1 0 c	144	invit	tCr 13t		1 6 0	176	2 4 0	2» d	J 4	3 D 4	3 3 4 k >	192 0
AZ 5	3	224	5 76	■+7	3 32 2 0 b	2 72 30 n	512	640	8 0 J	1024	128 0	133 6	17 2 3	192 0	100 4	192 0
A Z 6	1	30 4	6 C J	54 4	4 00 24 d	272 32C.	4 0 0	34 4	672	b	10 24	128 0	14 7 2 1 OL)	192		192
A L 7	2	4	(3	19	32	36	5 6	64	DD 1 VJ 4	116	16 d	L2d	1 60	2 0 3	9 1 2	12
UL 8	3	4	6	6	5	*	7	12	15	10	d	d	2 4	1 2	1 8	1 2

Figure 57: Extremely faster solar wind.

- (1) After a strong shock v_p has grown so much, that our range is no longer sufficient. For several hours, the distribution had disappeared completely, i.e. v_p was larger than 1700 kms⁻¹. This happened only once.
- (2) The high values of the NZR stemming from high energy, presumably electrons, particles generated by a flare.
- (3) Here is missing a data frame. The illegible values are marked with -1. According to the tab. 11 on p. 84 a data frame at FM3 comprises 24 words. The absence of two bits in the quality Word indicates the absence of this framework and the decoding problem. In this case, only the affected 3D data would be excluded from evaluation.

STATES: PIA NDM TIME 001 : 03: 37.250 H E M 2 0 1 0 N D 2 0 F F I 1 A- ON 12 UN I 1 B-O w s I3-UFF

INITIAL DATA W1 FE CH: >.. W9-1 5 11110000 11101110 10010100 11110000 10010000 01011001 11110000 00001000

11 8	N1 - 1 E 6 EN17-32	18 20 28A-3 2	32 A0	1 5 38	1 5 20	19 28	21 152 ©	AA 36	38 28	21 34	30 3 A	32 36	32 21	30 25	23 i 7	1 5 18
I1A I N T E G R.	ENI - 1 NC EM 7-3 2	2 0 5 61440)	5 3	A 3	1 1	1 A	1 3	2 < D	3 3	2 1	1 A	0 2	3 1	0 1	2 A	2 0
128	AZ1 A 2 2	26 / 0 ' AA	26 30	26 32	25 36	1 0 1 8	9 1 1	6 7	io) 5	A 3	2 1	A 2	0 0	0 2	0 1	1 0
	A-Z 3	0 26	28	29	24	5	A	3	0	0	0	1	0	0	0	0
	AZA	v J 00 / 92	6 A	76	38	20	8	3	1	0	0	0	0	0	0	0
	AZ5	2 36 2 A 8	2 2 A	160	152	8 A	A0	21	6	5	2	1	1	1	0	0
	AZA	192-200	200	1 6 8	12A	96	5A	27	8	7	5	2	1	1	0	0
	AZ7	96 72	76	58	38	1 7	7	1	0	1	0	0	0	0	1	0
	AZ 8	3A 36	20	20	1 0	3	A	1	0	0	0	0	0	0	0	0

I 1 A / 4	MAX A T	: E N 17 EL5	AZ1 0 EM 5					E \ 1 6							ENI 7		
		EL3 ELA	EL5	E L 6 EL7	EL ₂	EL _A	EL 5	EL 6	EL 7	EL 3	ELA	EL 5	EL6	p L 7			
	AZ8	0 0	0	0 0 0	0	u	0	0	0	0	0	0	0	0	0	0	0
	A-Z 9	0 0	0	0 0	0	0	1	0	0	0	0	0	0	0	0	0	0
	A-Z 1 0	0 0	0	0 0	0	0	0	0	0	0	0	1	2	0	0	0	0
	A-Z 1 1	0 0	0	1 0	0	0	0	0	0	0	0	0	0	0	0	0	0
	A-Z 1 2	0 0	0	0 0	0	0	0	0	0	0	0	0	0	0	0	0	0
			EN18				EN 19								EN 2 0		
	A ZF		0	0	0	0	0	0	0	0	0	0	0	0	0	0	0
	AZQ	0 0 0 0	0	0	0	0	0	0	0	0	0	0	0	0	0	0	0
	A-Z 1 0	0 1	61AA	@ 2	0	0	1	0	0	0	0	0	0	0	0	0	0
	A-Z 1 1	0 1	6	0 0	0	0	0	0	0	0	0	0	0	0	0	0	0
	A-Z 1 2	0 0	0	0 0	0	0	0	0	0	0	0	0	0	0	0	1	.1
			EN 21				EN 22								EN23		
	A Z 8	1 0	0	0 0	0	0	0	0	0	0	0	0	0	0	0	0	0
	AZ9	0 0	0	0 0	0	0	0	0	0	0	0	0	0	0	0	0	0
	A-Z 1 C.	0 0	0	0 0	0	0	0	0	0	0	0	0	0	1	0	0	0
	AZ1 1	0 0	0	0 0	0	0	0	0	0	0	0	0	0	0	0	0	0
	A-Z 1 2	0 0	0	0 0	0	0	0	0	0	0	0	0	0	0	0	0	0

HEL HELIOS 1
r = r = 0,952 AU
v_p
n_p v 600 kms 1 P 3
T_p n «P 5».
P T «10 000 K».

Figure 58: Extreme cold solar wind.
(1) The entire distribution of Proton is in a single 3D-measuring channel.
(2) The extremely cold α particles fall at I1a through the grate.

STATUS: PLA NDM TIME 0 00:02:11.187 MEM2 D1-ON D2-OFF I1A-ON I2-ON I1B-ON WS I3-OFF PEHEL

INITIAL DATA W1-8 11110000 00001000 00110011 11110000 10010001 01100110 11110000 00001110
CW: 5 W9-15 11101001 11110000 10010001 01100110 11110000 11110000 11110000

I1B	EN1-16	24	23	24	24	23	24	24	24	24	24	23	23	23	24	24	23
	EN17-32	23	32	88 (1)	24	25	24	48 (2)	25	25	24	25	24	25	25	25	23
I1A INTEGR.	EN1-16	1	0	0	0	1	1	0	1	0	0	0	0	0	0	1	1
	EN17-32	4	42 (1)	3	1	2	0	4 (2)	0	3	0	0	1	0	0	2	0
I2A	AZ1	0	0	1	1	1	1	2	5	2	7	7	5	8	9	16	14
	AZ2	0	0	0	2	2	1	3	2	1	5	2	4	3	7	3	4
	AZ3	0	0	1	1	2	3	7	9	5	5	6	5	9	6	10	10
	AZ4	0	128	208	176	112	64	80	54	64	60	50	52	38	46	25	26
	AZ5	0	224	336	256	160	116	76	108	104	120	104	112	112	104	76	80
	AZ6	0	232	416	320	176	84	64	68	58	50	72	50	68	60	64	76
	AZ7	0	2	7	5	6	7	11	22	15	23	25	22	27	36	52	44
	AZ8	0	0	3	5	3	6	6	6	6	10	9	11	19	18	20	29

I1A/3 MAX AT: EN18 EL6 AZ7

	EL4	EL5	EL6	EL7	EL8	EL4	EL5	EL6	EL7	EL8	EL4	EL5	EL6	EL7	EL8
AZ5	0	0	0	0	0	0	0	0	0	0	0	0	0	0	0
AZ6	0	0	0	0	0	0	0	0	0	0	0	0	0	0	0
AZ7	0	0	0	0	0	0	0	0	0	0	1	0	14	21	1
AZ8	0	0	0	0	0	0	0	0	0	0	0	0	2	1	0
AZ9	0	0	0	0	0	0	0	0	0	0	0	0	0	0	0
AZ5	0	0	0	0	0	0	0	0	0	0	0	0	0	0	0
AZ6	0	0	0	0	0	0	0	0	0	0	0	0	0	0	0
AZ7	0	0	0	0	0	0	0	0	0	0	0	0	0	0	0
AZ8	0	0	1	0	1	0	0	0	0	0	0	0	0	0	0
AZ9	0	0	0	0	0	0	0	0	0	0	0	0	0	0	1
AZ5	0	0	0	0	0	0	0	0	0	0	0	0	0	0	0
AZ6	0	0	0	0	0	0	0	0	0	0	0	0	0	0	0
AZ7	0	0	0	0	0	0	0	0	0	0	0	0	0	0	0
AZ8	0	0	0	0	0	0	0	0	1	0	0	0	0	0	0
AZ9	0	0	0	0	0	0	0	0	0	0	0	0	0	0	0

HELIOS 2
 $r = 0,98 \text{ AU}$
 $v_p \approx 600 \text{ kms}^{-1}$

Figure 59: Extreme cold solar wind, not be evaluated.
(1) These 42 counts represent only a fraction of the real proton distribution. Even I1b, which is approx. five times less sensitive, counts already (88-24) = 64 counts. The proton distribution is apparently so narrow that most protons have fallen through the grate at I1a.
(2) Also I1a does not see the α -particles.

DFVLA-GS0C 8031 OBERPFAFFENHOFEN GERMAN SPACE OPERATION CENTER 19.12.78 GMT 12H 12M 43S 2d3MS PAGE-NO. 3
MISSION HELIOS-A ***AUSGABE GEPUFFERT***
H-90 DSS- 44 78 353 09:16:23 B/R 512 FM 1 DM 2-0 FMT 34: EXP1-NOR
SCTIME 60-11:17:51.468 FN : 162 FR/FF= 0/ 13
STATUS: PLA NDM TIME 0 00:37:10.062 MEM1 01-ON D2-OFF I1A-ON 12-ON I1B-ON WS I3-OFF

INITIAL DATA W1-8 11110000 10001011 01100001 11110000 10001000 01101010 11110000 10001000
CW: 5 W9-15 11101010 11110000 10001000 01101010 11110000 11110000 11110000

I1B	EN1-16	21	24	24	26	22	27	21	25	22	24	26	19	21	28	20	26
	EN17-32	25	26	21	22	24	22	19	18	23	28	22	19	27	26	28	23
I1A INTEGR.	EN1-16	0	1	0	5	2	4	1	6	10	13	10	9	4	10	4	8
	EN17-32	6	7	4	4	2	2	2	1	2	1	3	1	3	2	1	3
I2B	AZ1	0	108	184	336	640	736	224	48	168	6	7	2	1	0	0	0
	AZ2	2	88	76	96	96	64	44	19	10	6	5	0	1	1	0	0
	AZ3	2	96	64	36	36	22	5	2	2	2	0	0	0	0	0	0
	AZ4	480	176	184	116	96	68	36	20	13	3	3	3	0	0	0	0
	AZ5	116	248	336	608	896	1216	1344	1344	1088	736	544	288	92	27	6	2
	AZ6	108	152	152	136	92	52	21	11	7	5	3	2	0	0	1	0
	AZ7	112	128	96	60	58	42	15	7	5	1	0	0	1	0	0	0
	AZ8	104	128	136	200	232	240	124	42	12	17	6	0	0	0	0	0

I1A/S MAX AT: EN9 EL6 AZ11

	EL4	EL5	EL6	EL7	EL8	EL4	EL5	EL6	EL7	EL8	EL4	EL5	EL6	EL7	EL8
AZ9	0	0	0	0	0	0	1	1	0	0	0	0	2	0	2
AZ10	0	0	0	0	0	1	1	0	0	0	0	0	1	0	0
AZ11	0	0	0	0	0	0	0	0	0	0	0	0	1	0	0
AZ12	0	0	0	0	0	0	0	0	0	0	0	0	1	0	0
AZ13	0	0	0	0	0	0	0	0	0	0	0	0	0	0	0
	EN10			EN11			EN12								
AZ9	0	2	1	1	1	1	0	0	0	0	0	0	0	0	0
AZ10	0	0	1	1	1	0	0	0	0	0	0	0	0	0	0
AZ11	0	0	2	1	0	0	0	0	0	0	1	0	0	0	0
AZ12	0	0	0	0	0	1	0	1	0	0	0	0	0	1	1
AZ13	0	0	0	0	1	0	0	0	0	0	0	0	0	0	0
	EN13			EN14			EN15								
AZ9	0	0	0	0	0	0	1	1	1	1	0	0	0	0	0
AZ10	0	0	0	0	0	0	0	2	0	1	0	0	0	0	0
AZ11	0	0	0	0	1	0	0	0	1	0	0	0	1	0	0
AZ12	0	1	0	0	0	0	0	0	0	0	0	0	0	0	0
AZ13	0	0	0	0	0	0	0	0	0	0	0	0	0	0	0

MIN DQ=4

HELIOS 1
 $r = 0,771 \text{ AU}$
 $n < 0,1 \text{ cm}^{-3}$

Figure 60: A "hole" in the solar wind.
(1) Since 1977 we see occasionally Plasmas with extremely low densities, to less than 0.1 cm^{-3} . This manifests itself in the conspicuously low count rates, which reach up to the lower level of the significance level.
(2) The distribution in the noise of the NZR has sunk at I1b.

```

**HELIOS/A** MPE-PRINTOUT DER EDF'2 VOM SORTED DATA TAPE
GRT 150 12:20:13.387 SCT 150 12:14:15.687 B/R 512 FM 1 DM 2 MISSING E1 DATA: 0
CRTEF 12:20:53.890 SCTEF 12:14:56.187 NOM WS BIT ERRCK RATE: 0
INITL TIME: 14701 SDTEF 12:14:16.405
INITIAL DATA W1- 8 11110000 00111001 01101101 11110000 10001100 01011000 11110000 00001111
W9-15 01111010 11110000 10001100 01011000 11110000 11110000 11110000
ALLGEM. QW 00000111 11111110
I1A QW 00000000 00001111
I2 QW 00000011 11111100
I3 QW 00000011 11111111
I1B QW 00000011 11111111

```

E2 X: -33(198) Y: 50(93) Z: -349(124) NR.CF VALUE IN AVERAGE:160

I1B	EN1 -16	7	12	18	20	12	8	18	17	25	23	36	30	52	96	320	1984
	EN17-32	10752	29656	27648	6656	960	4864	21504	4096	256	128	60	18	7	3	9	10
I1A INTEGR.	EN1 -16	0	3	0	1	0	0	1	0	10	25	208	2176	6656	4352	464	1
	EN17-32	1520	11	6456	208	4	152	6	6	6	3	7	6	7	10	7	2
J2B	AZ1	1	36864	43008	47104	45056	38912	23552	9216	14848	1024	640	480	256	168	80	64
	AZ2	7536	38912	45056	49152	49152	43008	27648	11264	3968	1088	672	448	288	152	100	58
	AZ3	1344	47104	53248	55296	55296	53248	43008	21504	6144	1472	800	576	320	184	116	72
	AZ4	36864	55296	55296	55296	55296	55296	55296	40960	12288	2698	1088	736	416	224	124	64
	AZ5	51200	55296	55296	55296	55296	55296	55296	49152	17408	4096	1536	704	480	256	128	100
	AZ6	47104	55296	55296	55296	55296	55296	55296	45056	15360	3200	1280	736	432	240	124	60
	AZ7	38912	49152	53248	55296	55296	55296	49152	26624	7936	1664	928	576	368	184	112	52
	AZ8	31744	40960	49152	51200	51200	47104	32768	13312	3456	1152	672	416	272	160	76	64

I1A/3 MAX ADR: EN13 EL5 AZ9 MASS CHNL.NR.: 16

	EL3	EL4	EN11	EL6	EL7	EL3	EL4	EN12	EL6	EL7	EL3	EL4	EN13	EL6	EL7	
AZ7	5	13	11	5	3	28	108	124	27	10	60	272	368	144	14	
AZ8	13	30	28	14	1	84	336	400	163	30	272	1098	1280	544	32	
AZ9	5	17	13	10	3	50	256	272	152	16	208	736	992	400	36	
AZ10	1	8	3	3	1	4	36	48	22	8	22	112	152	64	4	
AZ11	2	0	0	1	1	1	4	2	3	0	2	6	6	3	1	
AZ7	21	192	EN14	88	9	7	11	EN15	8	1	0	0	EN16	0	0	
AZ8	108	672	560	352	30	13	42	84	30	3	0	0	0	0	0	
AZ9	88	512	736	288	16	12	46	80	36	5	0	0	0	0	0	
AZ10	9	64	104	26	5	3	6	15	4	1	0	0	0	0	0	
AZ11	1	1	7	3	1	1	0	3	1	1	0	0	0	0	0	
AZ7	2	14	EN17	1	0	0	0	EN18	0	1	0	84	EN19	336	116	8
AZ8	19	576	736	26	2	0	1	2	0	0	288	1152	1344	544	46	
AZ9	6	176	320	32	3	0	2	0	1	0	152	736	1024	368	34	
AZ10	1	2	6	2	1	1	0	0	0	0	21	88	128	42	9	
AZ11	0	0	0	0	0	0	0	1	0	0	1	5	8	4	2	

HELIOS 1

$r = 0,31 \text{ AU}$

$v_p = 574 \text{ kms}^{-1}$

$n_p > 1500 \text{ cm}^{-3}$

$T_p = 210 \text{ 000 K}$

$\frac{n}{n_p} > 10 \%$

Figure 61: Extreme plasma density

After a shock the density rose to a record of over 1500 cm^{-3} .

(1) Such counting rates in I1b and I3 are ten times larger than the 'normal' counting rates in perihelion. The low sensitivity of I3 here proved to be a great advantage.

(2) The count rates from I2 approach the possible maximum of 63 488, but never exceed it.

MISSION HELIUS-A ***AUSGARE GEPUFFERT***
 H-90 DSS--67 RO 144 08:02:29 B/R 512 FM 1 DM 3-0 FMT 34: EXP1-NUR
 SCTIME102 12:53:08.218 FN : 72 FB/FF= 0/ 1
 STATUS: PLA NDM TIME 0 00:59:54.125 MEM1 D1-ON D2-OFF I1A-OFF I2-ON I1B-ON NS I3-UN

INITIAL DATA	W1-8	11110000	11100000	10100010	11110000	00000111	01101000	11110000	10001111								
CW: 5	W9-15	01111010	11110000	00000111	01101000	11110000	11110000	11110000	11110000								
I1B	EN1-16	18	23	22	23	22	24	40	80	232	640	1024	800	136	68	96	152
	EN17-32	136	62	44	44	32	27	29	21	17	28	25	19	19	23	24	21
I1A INTEGR.	EN1-16	0	0	1	2	5	36	120	256	124	9	20	9	3	0	0	2
	EN17-32	11	1	256	8	0	5	2	0	0	0	0	1	1	0	1	0
I2B	AZ1	0	7936	11776	15360	17408	17408	12800	5888	8192	512	192	58	18	4	3	0
	AZ2	144	7936	11776	14848	16384	15360	11264	5376	2432	672	184	68	28	8	4	0
	AZ3	152	8192	12288	15872	17408	15360	9728	4096	1344	496	216	84	42	13	2	0
	AZ4	4608	9728	14336	17408	20480	21504	18432	9728	3072	640	216	68	32	8	5	0
	AZ5	6144	9728	13824	18432	22528	27648	30720	32768	34816	30720	25600	12800	5120	2304	304	12
	AZ6	6400	9216	13824	18432	21504	23552	20480	13824	6656	1792	256	100	32	6	2	1
	AZ7	5888	9216	13824	17408	20480	18432	12288	5376	1536	496	208	96	29	9	0	2
	AZ8	5120	8192	12288	15872	17408	16384	12288	5632	2048	672	248	100	32	6	1	0

I1A/3	MAX AT:	EN8	EL6	AZ9	EN6	EN7	EN8	EN9	EN10	EN11	EN12	EN13	EN14			
		EL4	EL5	EL6	EL7	EL8	EL4	EL5	EL6	EL7	EL8	EL4	EL5	EL6	EL7	EL8
AZ7	1	0	0	0	0	1	0	0	0	1	0	0	0	0	0	0
AZ8	0	2	0	2	2	0	10	8	3	0	1	19	8	1	1	1
AZ9	2	2	2	5	0	2	20	26	8	1	12	68	50	11	0	0
AZ10	1	3	3	0	1	4	8	11	5	0	4	40	32	6	0	0
AZ11	0	2	2	0	0	3	2	2	3	1	2	1	1	1	0	0
AZ7	0	0	0	0	0	0	0	0	1	0	0	0	1	0	0	0
AZ8	1	3	5	0	0	2	1	0	0	0	0	0	5	1	0	0
AZ9	5	36	29	5	1	0	1	0	0	0	0	11	1	0	0	0
AZ10	2	14	17	1	0	0	1	0	0	1	0	0	0	0	0	0
AZ11	0	0	1	1	0	0	1	0	0	0	0	0	0	0	0	0
AZ7	0	0	0	0	0	0	0	0	0	0	0	0	0	0	0	0
AZ8	1	2	0	0	0	0	0	0	0	0	0	0	0	0	0	0
AZ9	1	2	0	0	0	0	0	0	0	0	0	0	0	0	0	0
AZ10	0	1	0	0	0	0	0	0	1	0	0	0	0	0	0	0
AZ11	0	0	0	0	0	0	0	0	0	0	0	0	0	0	0	0

HELIOS 1
 $r = 0,333 \text{ AU}$
 $v_p = 340 \text{ kms}^{-1}$
 $n_p = 82 \text{ cm}^{-3}$
 $T_p = 180 \text{ 000 K}$

Figure 62: A measurement with I3 instead of I1a.
 (1) Here the significantly reduced count rate stands out, in comparison to I1b.
 (2) In a measurement with I1b alone, this secondary maximum would be been interpreted as α -particle. I3 but also sees this peak in the proton cycle and proves that this is a second proton component.
 (3) These are the real α -particles (comp.Tab.7 on p. 61).
 (4) A strong beam in the electron distribution.

MISSION HELIOS-A ***AUSGABE GEPUFFERT***

H-90 DSS- 44 . 79 1 08:12:50 B/R 512 FH 1 DM 3-0 FMT 34; EXP1-NUR

SCTIME 73 10:14:03.468 FB/FF# 0/ 33

STATUS: PLA NDM TIME 0 00:56:33.687 MEH2 D1-ON D2-OFF I1A-ON I2-ON I1B-ON NS I3-OFF

INITIAL DATA W1-8 11110000 11010100 00011011 11110000 00001100 01001010 11110000 00001000
 CW: 5 W9-15 11101010 11110000 00001100 01001010 11110000 11110000 11110000

I1B	EN1-16	19	15	19	22	21	19	21	20	25	22	22	63	160	128	72	32
	EN17-32	27	25	27	26	21	23	26	22	25	27	28	15	19	22	27	26
I1A INTEGR.	EN1-16	3	5	1	0	2	3	1	0	3	9	84	400	640	320	128	26
	EN17-32	15	32	13	12	10	15	17	13	17	5	3	4	3	1	3	3
I2B	AZ1	0	168	64	60	40	27	29	32	27	15	9	11	3	0	0	0
	AZ2	1	124	44	44	34	22	25	12	13	25	19	8	7	1	1	0
	AZ3	0	272	240	84	36	23	30	6	31	15	18	7	6	4	0	1
	AZ4	384	496	608	544	144	46	14	68	34	38	22	15	3	3	2	1
	AZ5	576	736	800	736	544	144	168	60	60	42	25	12	3	3	4	2
	AZ6	800	768	992	832	480	216	160	25	40	108	19	8	7	3	2	1
	AZ7	544	480	400	320	58	58	12	26	34	15	17	13	5	1	1	0
	AZ8	384	224	192	63	36	12	40	36	32	27	15	4	7	1	3	0

I1A/3 MAX AT:

	EN13	EL4	AZ11	EN11	EL5	EL6	EL2	EL3	EN12	EL5	EL6	EL2	EL3	EN13	EL5	EL6
	EL2	EL3	EL4	EL4					EL4					EL4		
AZ9	0	0	16	8	0	1	38	76	10	0	7	152	44	11	3	
AZ10	0	2	25	23	0	2	80	116	10	0	18	232	96	16	1	
AZ11	0	0	1	7	0	1	17	21	3	4	2	50	11	1	0	
AZ12	0	0	0	2	0	0	0	0	3	1	0	1	0	1	0	
AZ13	0	0	0	0	0	0	0	0	0	0	0	0	0	1	0	
			EN14	EN15	EN16									EN17	EN18	EN19
AZ0	0	6	12	12	4	0	0	8	17	2	0	1	1	1	1	0
AZ10	7	31	76	48	3	1	4	20	40	2	0	2	3	2	0	
AZ11	4	56	32	18	0	0	1	10	11	2	0	1	6	2	0	
AZ12	1	5	2	0	0	1	1	1	2	1	0	1	0	0	1	
AZ13	0	0	0	0	0	0	0	0	0	0	0	0	0	0	0	
AZ0	0	0	0	0	0	0	0	0	0	1	0	0	0	2	1	1
AZ10	0	0	5	3	0	0	3	1	2	1	0	0	2	0	1	
AZ11	0	0	3	2	1	0	2	6	7	2	0	0	2	0	2	
AZ12	0	0	0	0	0	0	0	2	2	1	0	0	0	0	0	
AZ13	0	0	0	0	0	0	0	1	0	0	0	0	0	0	0	

HELIOS 1
 $r = 0,866 \text{ AU}$
 $v_p = 435 \text{ kms}^{-1}$
 $n_p = 5,9 \text{ cm}^{-3}$
 $T_p = 123 \text{ 000 K}$

Figure 63: Quiet solar wind immediately before a shock, just before picture 64.

MISSION HELIOS-A ***AUSGABE BEENDEET***
 H=90 HSS= 44 SQTINE 73 10:13:50 87R 512 FI 1 OM 3=0 FMT 34; EXP1=NR
 FB/FF= 07/33

STATUS: PLA RDM TIME 0 00:57:14.687 D1-ON D2-OFF I1A-ON I2-ON I1B-ON WS I3-OFF

INITIAL DATA W1=8 11110000 11010110 10101011 11110000 10001100 00111001 11110000 10001000
 CW: 5 W9=15 11101010 11110000 10001100 00111001 11110000 11110000 11110000

11B	EN1-16	17	17	19	21	12	23	13	21	20	18	13	27	36	76	128	192
	EN17-32	272	232	240	120	68	56	42	57	36	28	22	29	24	26	29	26
11A INTEGR.	EN1-16	2	0	1	4	2	0	2	1	2	3	7	15	116	352	576	832
	EN17-32	1230	800	768	304	152	96	88	54	26	10	6	2	7	3	3	3
12B	A21	0	432	640	304	224	112	60	46	64	16	17	3	5	4	2	1
	A22	1	336	448	304	320	168	64	42	36	21	13	5	4	3	2	0
	A23	5	768	600	332	704	216	112	64	44	27	13	5	8	1	1	0
	A24	1024	1664	2304	2304	1600	512	216	128	72	58	23	12	6	2	1	0
	A25	1024	1984	2944	3536	3200	1536	544	192	80	52	30	9	7	0	1	0
	A26	1024	1408	2432	2560	1934	1408	464	160	64	46	24	16	9	1	2	0
	A27	1216	1152	1728	1728	1728	400	152	88	58	34	22	12	1	5	2	0
	A28	664	1216	1216	632	512	104	58	52	46	40	18	9	2	1	0	0

11A/3

MAX AT:	EN13	EL3	AZ10	EN11	EL4	EL5	EL1	EL2	EN12	EL4	EL5	EL1	EL2	EN13	EL4	EL5
AZ8	0	0	0	0	0	0	0	0	0	0	1	0	1	1	1	1
AZ9	0	0	0	0	0	1	1	1	0	0	0	0	1	3	7	2
AZ10	0	0	0	0	0	2	1	0	0	1	1	0	1	8	12	18
AZ11	0	0	0	0	0	2	0	0	1	0	0	0	2	10	12	10
AZ12	0	0	0	0	0	0	0	0	0	0	2	0	1	0	3	2
AZ8	0	3	3	7	4	7	6	10	13	10	1	3	5	2	4	4
AZ9	0	3	9	10	5	4	8	10	14	9	2	5	10	17	16	
AZ10	1	12	19	25	13	5	7	18	15	15	3	9	20	32	26	
AZ11	2	12	38	33	28	3	21	46	44	46	0	8	25	32	50	
AZ12	0	2	2	23	17	3	12	32	46	38	1	14	40	56	38	
AZ8	0	5	5	0	8	0	4	7	5	13	2	1	7	7	15	
AZ9	1	6	15	36	22	2	5	29	34	27	1	4	11	31	29	
AZ10	4	7	15	46	44	2	3	21	34	34	4	8	32	42	40	
AZ11	2	9	48	76	58	2	14	18	36	36	0	12	32	46	55	
AZ12	2	13	96	133	120	2	4	8	18	64	0	5	9	34	40	

HELIOS 1
 $r = 0,866 \text{ AU}$
 $v_p = 560 \text{ kms}^{-1}$
 $n_p = 14,7 \text{ cm}^{-3}$
 $T_p = 570 \text{ 000 K}$

Figure 64: First spectrum after the shock, only 40 seconds after image 63 recorded.

- (1) The maximum is now moved after EN17 (previously at EN13).
 The location of the 3D-Measurement range depends however on the old maximum so that poorly fits the new distribution.
- (2) The electron flows are here four times larger than before.

SCTIME124 15:42:13.968 FN : 18 FB/FF= 1/ 5
 STATUS: PLA NDM TIME 0 00:27:47.562 MEM1 D1-ON D2-OFF I1A-ON I2-ON I1B-ON WS I3-OFF

INITIAL DATA W1-8 11110000 01101000 00111001 11110000 10001111 01011001 11110000 10001000
 CW: 5 W9-15 11101010 11110000 10001111 01011001 11110000 11110000 11110000

I1B	EN1-16	22	18	10	19	12	22	21	20	14	20	17	11	13	13	38	128
	EN17-32	136	58	50	29	17	20	19	11	31	18	18	18	21	27	32	10
I1A INTEGR.	EN1-16	2	3	2	0	0	3	1	1	0	3	4	3	4	11	184	672
	EN17-32	304	100	64	27	10	7	6	5	1	2	1	1	0	1	2	1
I2B	AZ1	0	288	320	352	184	56	19	11	17	3	0	2	1	1	1	0
	AZ2	0	176	152	152	104	42	22	10	5	4	1	0	0	0	0	0
	AZ3	0	184	160	96	50	13	7	8	4	5	1	1	0	0	0	0
	AZ4	320	544	608	480	288	100	31	20	12	7	2	1	0	0	0	0
	AZ5	544	736	992	1152	1472	2176	2816	3072	2432	1920	1088	496	208	76	32	14
	AZ6	544	768	864	704	384	168	44	20	12	12	4	4	1	1	0	0
	AZ7	384	496	416	256	136	64	21	15	4	10	3	3	0	0	0	0
	AZ8	304	368	384	336	248	100	23	17	5	6	2	1	0	0	0	0

I1A/3 MAX AT:

	EN16	EL5	AZ10	EN14	EL6	EL7	EL3	EL4	EN15	EL6	EL7	EL3	EL4	EN16	EL6	EL7
AZ8	0	1	0	0	0	0	0	10	11	4	0	2	15	23	16	2
AZ9	0	1	2	4	0	0	6	38	30	19	2	21	84	128	48	6
AZ10	0	0	0	1	0	0	3	13	29	10	1	13	80	112	38	5
AZ11	0	0	0	0	0	0	0	1	0	2	0	0	19	26	11	0
AZ12	0	0	0	0	0	0	0	0	1	0	0	0	1	0	1	0
AZ8	4	3	12	5	1	1	2	9	1	1	0	1	7	6	3	0
AZ9	5	22	19	8	1	2	11	21	6	1	1	1	11	13	7	0
AZ10	8	58	56	24	4	1	10	17	4	0	1	1	5	6	1	0
AZ11	5	18	44	11	0	0	3	2	2	2	0	0	0	0	0	0
AZ12	0	0	0	0	0	0	1	0	0	0	0	0	0	0	0	0
AZ8	2	1	4	1	0	0	0	1	0	0	0	0	0	0	0	0
AZ9	2	5	3	2	0	1	2	3	0	0	0	0	0	2	1	0
AZ10	0	0	3	1	0	0	1	1	0	0	0	0	2	0	1	0
AZ11	0	1	0	0	0	0	0	0	0	0	0	0	0	0	0	0
AZ12	0	0	0	0	0	0	0	0	0	0	0	0	0	0	0	0

HELIOS 1
 $r = 0,97 \text{ AU}$
 $v_p = 525 \text{ kms}^{-1}$
 $n_p = 3,9 \text{ cm}^{-3}$
 $T_p = 180 \text{ 000 K}$

Figure 65: Extreme beam in the electron distribution.
 (1) In AZ5 greatly appear inflated count rates, a note on a focused component in the electron distribution. This "beam" was discovered with our instrument.
 (2) The selected count rates are not valid (p.117).
 (3) The NZR by I1b varies with HELIOS 1 typical to ± 5 counts.

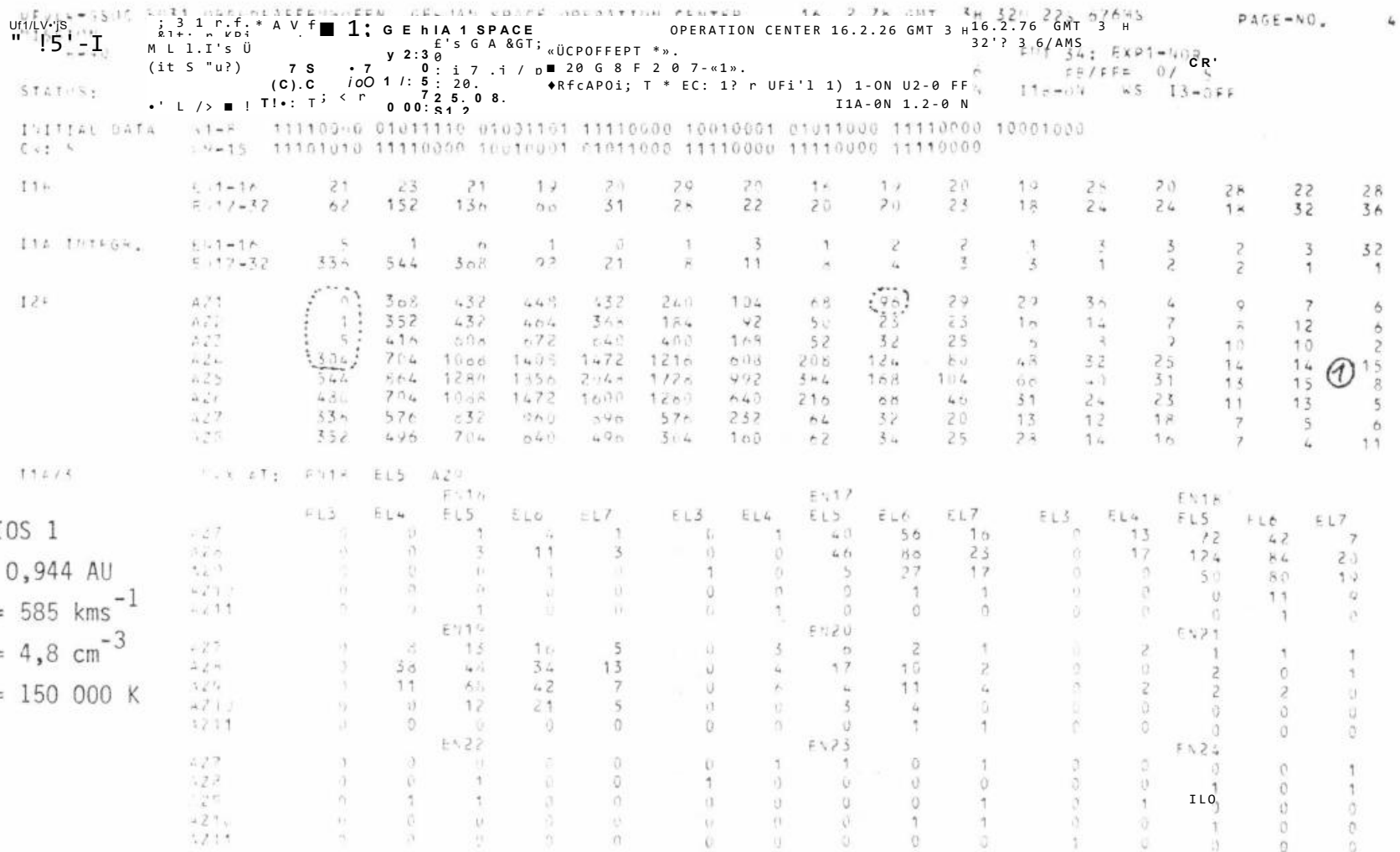


Figure 66: High-energy electrons.

(1) after strong flares on the Sun, I2 count rates increased in the upper energy-channels occasionally observed for some time. This seems to be the low-energy end of the spectrum of flare generated solar electrons. Such electrons cause type III radio bursts. Here we would have liked an extension of range to higher energies.

```

**HELICS/A** MPE-PRINTOUT DER EDF*2 VCM SORTED DATA TAPE
GRT 29 10:39:13.356 SCT 29 10:34: 7.572 B/R 512 FM 1 DM 3 MISSING E1 DATA: 0
GRTEF 10:39:13.356 SCTEF 10:34: 7.572 NDM NS BIT ERROR RATE: 0
INITL.TIME: 12731 SDTEF 10:33:27.790
INITIAL DATA W1- 8 11110000 00110001 10111011 11110000 00091110 01011001 11110000 10001000
W9-15 11101010 11110000 00001110 01011001 11110000 11110000 11110000
ALLCEM. QW C0000111 11111110
11A QW C0000011 11111111
12 QW C0000011 11111100
13 QW C0000000 00001111
11B QW C0000011 11111111

```

E2 X: 83(13) Y: 111(11) Z: 256(2) NR.OF VALUE IN AVERAGE:163

11B	EN1 -16	14	17	30	20	20	22	20	14	24	22	17	27	24	32	3584	128
	EN17-32	20	34	20	224	15	26	20	21	50	25	28	27	24	26	28	24
11A INTEGR.	EN1 -16	2	3	9	0	2	5	2	1	0	2	2	3	5	1024	8704	40
	EN17-32	7	1	38	6	5	5	5	64	3	3	0	3	0	2	1	0
J2B	AZ1	0	56	50	46	32	44	20	28	38	19	13	6	2	0	0	0
	AZ2	2	38	44	46	34	40	28	28	37	11	12	6	1	1	0	0
	AZ3	0	144	112	94	44	44	40	40	40	31	9	3	2	0	0	0
	AZ4	416	464	416	216	104	88	84	62	44	24	11	5	3	1	0	0
	AZ5	1024	1024	800	464	232	144	88	76	46	28	15	8	3	0	0	0
	AZ6	768	876	640	448	200	128	104	90	68	42	19	6	1	3	1	1
	AZ7	400	336	256	134	100	62	68	58	31	25	15	6	2	1	0	1
	AZ8	136	136	116	34	48	52	60	46	15	30	10	7	1	0	1	0

11A/3 MAX ACR: EN15 EL5 AZ10 MASS CHNL.NR.: 9

	EL3	EL4	EN13 EL5	EL6	EL7	EL3	EL4	EN14 EL5	EL6	EL7	EL3	EL4	EN15 EL5	EL6	EL7
AZ8	0	0	0	0	0	0	0	0	0	0	0	0	0	0	0
AZ9	0	1	0	0	0	2	1	38	3	0	4	8	34	2	0
AZ10	0	0	0	0	1	1	58	928	11	4	4	1280	7936	18	3
AZ11	0	0	1	1	0	0	1	2	6	1	2	16	208	0	2
AZ12	0	0	1	0	0	0	1	0	0	0	1	0	0	0	0
	EN16					EN17					EN18				
AZ8	0	0	0	0	0	0	0	0	0	0	0	0	0	0	0
AZ9	1	2	0	0	0	0	1	0	0	0	0	0	0	0	0
AZ10	3	7	11	1	0	0	1	1	0	0	0	0	0	0	0
AZ11	4	2	5	1	1	0	1	0	0	0	0	0	0	0	0
AZ12	0	0	0	1	0	0	0	1	0	0	1	0	0	0	0
	EN19					EN20					EN21				
AZ8	0	0	0	0	0	0	0	0	0	0	0	0	0	0	0
AZ9	0	0	0	0	0	0	0	0	0	0	0	0	0	0	1
AZ10	3	0	34	0	0	0	0	5	1	0	0	0	0	0	0
AZ11	0	0	0	0	0	0	0	0	0	0	0	0	0	1	0
AZ12	0	0	0	0	0	0	0	0	0	0	0	0	0	0	0

HELIOS 1

$r = 0,95 \text{ AU}$

$v_p = 475 \text{ kms}^{-1}$

$n_p = 15 \text{ cm}^{-3}$

$T_p = 17 \text{ 000 K}$

Figure 67: Discovery of singly ionized Helium

(1) this unusual third peak could be attributed to singly ionized helium. The distribution of protons and α -particles are extremely narrow, i.e. "cold". It's "Piston gas" in the wake of an interplanetary shock wave.

STATUS: PLA NDM TIME 0 01:02:32.500 MEM1 D1-ON D2-OFF I1A-ON I2-ON I1B-ON WS I3-OFF

INITIAL DATA W1-8 11110000 11101010 10001000 11110000 10001011 01011001 11110000 10001000
CW: 5 W9-15 11101010 11110000 10001011 01011001 11110000 11110000 11110000

I1B	EN1-16	19	19	26	7	10	22	30	22	6	18	15	512	1984	128	15	7
	EN17-32	168	58	30	12	21	14	11	27	31	26	26	22	30	11	34	9

I1A INTEGR.	EN1-16	1	4	1	1	1	2	0	0	2	5	192	5376	3712	31	5	7
	EN17-32	1024	10	8	4	6	1	1	1	3	0	2	1	0	0	3	0

I2B	AZ1	0	2	2	3	3	4	2	11	6	2	4	1	2	1	1	1
	AZ2	0	0	2	5	4	6	5	7	1	6	4	3	2	3	2	2
	AZ3	0	2	3	7	6	8	8	9	8	4	3	1	2	0	2	2
	AZ4	2	2	7	3	2	17	9	10	12	7	9	3	3	2	0	0
	AZ5	4	4	4	8	7	9	11	14	11	12	10	4	1	1	1	0
	AZ6	4	3	5	0	11	11	21	11	10	11	9	1	2	2	1	0
	AZ7	5	2	5	6	12	11	3	9	10	9	6	1	3	3	0	0
	AZ8	3	2	5	3	10	4	9	10	6	5	0	2	1	1	1	1

I1A/3	MAX AT:		EN12	EL5	AZ10			EN11			EN12			EN12		
	EL3	EL4	EL5	EL6	EL7	EL3	EL4	EL5	EL6	EL7	EL3	EL4	EL5	EL6	EL7	
AZ8	0	0	0	0	0	0	0	1	0	0	0	0	12	0	0	
AZ9	0	1	1	0	0	0	9	108	10	0	0	160	2432	184	1	
AZ10	0	0	0	0	1	0	0	52	6	0	1	100	2432	248	0	
AZ11	0	0	0	0	0	0	0	1	1	0	0	0	6	2	0	
AZ12	0	0	0	0	0	0	0	0	0	0	0	1	0	0	0	
			EN13					EN14					EN15			
AZ8	0	2	0	0	0	0	0	0	0	0	0	0	0	0	0	
AZ9	0	48	1152	54	0	0	0	7	0	0	0	0	1	0	0	
AZ10	0	64	2176	208	0	0	4	17	1	0	1	1	1	0	0	
AZ11	0	0	12	3	0	0	1	0	0	0	0	0	0	0	0	
AZ12	0	0	0	0	0	0	0	1	0	0	0	0	0	0	0	
			EN16					EN17					EN18			
AZ8	0	0	0	0	0	0	0	0	0	0	0	0	0	0	0	
AZ9	0	0	3	0	0	0	0	432	0	0	0	0	2	0	0	
AZ10	0	0	0	0	0	0	0	576	0	0	0	0	6	0	1	
AZ11	0	0	1	0	0	0	0	0	0	0	0	0	0	0	0	
AZ12	0	0	0	0	0	0	0	1	0	0	0	0	0	0	0	

HELIOS 1
 $r = 0,869 \text{ AU}$
 $v_p = 381 \text{ kms}^{-1}$
 $n_p = 42 \text{ cm}^{-3}$
 $T_p = 20 \text{ 000 K}$

Figure 68: The electron-less solar wind.
This strange phenomenon occurred during the whole mission only once for several hours, after 5 1/4 years!
(1) it seems as if the main part of the electron distribution, which is usually seen is gone. At the same time, the Proton distribution is absolutely normal. Could be the probe have so highly negatively charged, that the plasma electrons are shielded? We have so far no explanation.

FINAL WORD

With the completion of this report, the hardware-phase of the plasma experiment takes its final conclusion. Not only, because he was so long overdue, it is located the famous "Annex A" to the contract between the MPE and MBB in worthy succession to a similar work. which was however right at the beginning of the project, namely. Why this time thus came and a lot more about the fate of the project now running thirteen years, is described in further forward detail. This report comes late, simply because he had to be stopped because of the constantly bubbling abundance always again aside new exciting results. This wealth of data will occupy us for many years; us - soon also some who can apply their knowledge about the instruments of this report include. On the other hand is not to be forgotten: the instruments still to run and provide data unchanged quality, but now from a very different phase of the solar cycle, as we they had at the start.

This unexpectedly rich blessing of the data can be regarded as special success of ambitious, elaborate and often laborious project. So many individuals, companies and organizations have contributed to its success, that it is difficult for us to see any, if we want to go because here again, expressing our gratitude to all of them.

The HELIOS project was a joint undertaking of the Federal Republic of Germany and the United States. We don't want to miss, to thank particularly the German taxpayers that have applied over 450 million DM for HELIOS, about 13 million directly for our experiment. Under permit WRS 10/7 we got this money from the Federal Ministry for research and technology, funded at the time even our data analysis. For this we thank in particular the German program scientist Dr Otterbein and the program manager Mr. Käsmeier.

The German part of the project was led by Dr Ants Kutzer and his representative Dr Unz (in the DFVLR-BPT, the former GfW), the American Gil Ousley (NASA - Goddard Space Flight Center). We emphasize especially the good, even if a tough struggle often regulating cooperation with the members of the project team, who dealt directly with the experiments: Dr. Kasten, Dr. Wodsak, Dr. Dodeck, Dr. Kempe and H. Galle and of course our direct partners, Dr. Stampfl.

We are particularly pleased that this group - and they may also project management - it became gradually clear how passionate we were fighting for the success of the mission and our experiments; that alone was the reason that we measured in not always the number one priority works on paper...Here we thank also the project scientists, the gentlemen Porsche, Meredith and Trainor for their tireless efforts, to bring the interests of experimenters and project teams under one hat.

Our instruments have been developed to flight readiness and also manufactured by the company MBB, the sub-contracting of the company Lewicki, Zeiss and awarded Dornier System. The project manager Dr. Brauer together with his representative, H. Wagner and to H. Jochimsen was responsible for design and manufacturing of mechanics. The gentlemen Stiller, Friedrich and Nogai and their colleagues developed the complicated electronics. The skill, the extreme care and also the unusual personal commitment of this MBB team it is, that our instruments are today still with to the most modern, there is and that they work up today still error free. We also thank the MBB-HELIOS team, especially in the gentlemen Grün, Schuran and Ziegler for understanding, we always found them. The NASA crew at KSC provided two trouble-free startup of the first, by the mission control at the JPL or GSOC continue then were controlled. Still, we say thanks to H. Heftman at the JPL for his constant help in the fight to ground stations, as well as also Prof. Hachenberg and his colleagues at the MPI for radio astronomy for the possibility to use the 100 m radio telescope in Effelsberg for HELIOS data reception.

The DFVLR team in the GSOC - for many years headed by H. Panitz - sought from the outset very carefully to mission control, headed the HELIOS-2-start even on their own. Later, only H. led sweeping the HELIOS mission, then H. Hiendlmayer. He and his colleagues

have become true virtuoso in the optimum benefits of all options, in particular of the on-board storage system when it comes to bypass Station gaps. We thank also H. Wiegand, H. Piotrowski and wife Dusl and their colleagues for their careful work in the definition and production of our data tapes.

At MPE the experiment lasted more than ten years by Professor Lüst and Prof. Pinkau was been promoted continuously. H. Pellkofer, the first project managers, the gentlemen Ludwig, Müller, Kaiser, Fischer, still miss Kusser and Miss Wantosch and finally H. Mühlhäuser wore the brunt during development, testing, and calibration for many years. H. Antrack, H. Kipp and Miss Lipp concerned the treatment of the data tapes at MPE or run even today.

Our most gracious thanks to all these people and the many, that names should be mentioned here actually still.

The author and editor of this report, Rainer Schwenn, would not fail to thank their previous reports and other documents he could work here personally even when all those ("Annex A", "Final report", etc.), and - last not least - when Mrs. Spilker, who brought the slow-growing manuscript with amazing patience to the print-ready.

LITERATURE

- Bechly, M., design and construction of a control unit for automatic calibration of solar wind measuring devices, TU Munich, diploma thesis, 1974.
- Burlaga, l.f., N.F..Ness, John F. Mariani, B. Bavassano, U. Villante, H. Rosenbauer, R. Schwenn and j. Harvey, Magnetic Fields and flows between 1 and 0.3 AU during the primary mission of HELIOS-1, J. Geophys.Res.83, 5167, 1978.
- Burlaga, l.f., R. Lepping, R. Weber, T. Armstrong, C. Goodrich, J. Elwood - van, D. Gurnett, P. Kellogg, E. Keppler, John F. Mariani, F. Neubauer and R. Schwenn, interplanetary particles and fields, November 22 - Decem of ber 6, 1977: Helios, Voyager, and IMP observations between 0.6 AU and 1.6 AU, J. Geophys.Res.85, 2227, 1980.
- Cuperman, S., B. Levush, M. dryer, H. Rosenbauer and R. Saleem, on the radial expansion of the solar wind plasma between 0.3 and 1.0 Astro nomical units, Astrophys.J. 226, 1120, 1978.
- Dum, C.T., E. Marsh, W. Emma and D.A.Gurnett, ion sound turbulence in the solar wind, to be published in lecture notes in physics, Springer - Verlag, Berlin, 1979.
- Gurnett, D.A, M.M. tree back and H. Rosenbauer, stereoscopic direction finding analysis of a type III solar radio burst: evidence for emission at 2 f, J. Geophys.Res.83, 616, 1978.
P
- Gurnett, D.A, F.M. Neubauer and R. Schwenn, plasma wave turbulence associated with of interplanetary shock, J. Geophys.Res.84, 541, 1979.
- Gurnett, D.A a., E. Marsh, W. Emma, R. Schwenn and H. Rosenbauer, ion acoustic waves and related plasma observations in the solar wind. (J).Geophys.Res.84, 2029, 1979.
- Lamb, G., absolute measurement of response probability of channel - Tron,

Technical University of Munich, diploma thesis, 1972.

March, E., k-H.Mühlhäuser, W. Emma, R. Schwenn and H. Rosenbauer, initial results on solar wind alpha particle distributions as measured by Helios between 0.3 and 1 AU, to be published in lecture notes in physics, Springer-Verlag, Berlin, 1979.

March, E., W.G..Emma, and R. Schwenn, some characteristics of Proton velocity of distribution in the solar wind as observed by the Helios solar probes, to be published in lecture notes in physics, Springer - Verlag, Berlin, 1979.

Mühlhäuser, k.-H., R. Schwenn and H. Rosenbauer, the Helios-plasma experiments-ment.An example of the production and processing of large amounts of data, Kleinheubacher ber.2J_, 475, 1978.

Emma, w.g., R. Schwenn, E. March, k-H.Mühlhäuser and H. Rosenbauer, electron characteristics in the solar wind as deduced from Helios observations, to be published in lecture notes in physics, Springer - Verlag, Berlin, 1979.

Rosenbauer, H., the solar wind; Theories, measurements, measurement problems, space research XIII, 38, 1968.

Rosenbauer, H., measurements of interplanetary and magnetospheric plasma, industries Atomiques & spatiales, 1973.

Rosenbauer, H., possible effects of Photoelectrcn emission on a low-energy electron experiment in Photon and particle interactions with surfaces in space, R.J.L.Grad (ed.), D. Reidel publishing company, Dordrecht, Holland, 139, 1973.

- Rosenbauer, H., H. Miggenrieder, M. Montgomery and R. Schwenn, Preliminary results of the Helios plasma measurements, proc.of the International Symposium on solar-terrestrial physics, Boulder, June 1976, D.J.Williams (ed.), American Geophysical Union, 319, 1976.
- Rosenbauer, H., R. Schwenn, E., B. Meyer, H. Miggenrieder, M. Montgomery, k-H.Mühlhäuser, W. Pili pp, W. Voges and S.K.Zinc, A survey on initial results of the Helios plasma experiment, J. Geophys.42_, 561, 1977.
- Rosenbauer, H., R. Schwenn and S. Barne, the prediction of fast stream front arrivals at the Earth on the basis of solar wind measurements at smaller solar distances, proc.of AGARD Symposium on 'Operation modeling of the aerospace propagation environment', Ottawa, Canada 24.-28.4.1978, H. Soicher (ed.), AGARD-CP-238, 32-1, 1978.
- Schwenn, R., H. H. Miggenrieder, Rosenbauer, the plasma experiment on Helios (E1), space research 226, issue 5, 1975.
- Schwenn, R., H. Rosenbauer, H. Miggenrieder, and B. Meyer, preliminary results of the Helios plasma experiment, proceedings of the 18th plenary meeting of COSPAR, Varna, 1975, in space research XVI, M.J.. Rycraft (ed.), Akademie-Verlag Berlin, 671, 1976.
- Schwenn, R., H. Rosenbauer and k-H.Mühlhäuser, the solar wind during STIP II interval: stream structures, boundaries, shocks, and other features as observed on Helios 1 and Helios 2, proceedings of COSPAR Symposium B, study of travelling interplanetary phenomena, Tel Aviv, June 1977, M.A..Shea, D.F.Smart, S.T.Wu (ed.), air force Geophysics laboratory Rep.No.77-309, 351, 1977.
- Schwenn, R., M. Montgomery, H. Rosenbauer, H. Miggenrieder, k.-H.Mühlhäuser, S.J..Barne, W.C.2.Feldmann and R.T.1.Hansen, direct observations of the latitudinal extent of a high-speed stream in the solar wind. (J).Geophys.Res.83, 1011, 1978.
- Schwenn, R., k-H.Mühlhäuser and H. Rosenbauer, Two States of the solar wind at

the time of solar activity minimum, to be published in Lecture notes in physics, Springer-Verlag, Berlin, 1979.

Schwenn, R., K-H. Mühlhäuser, E. March and H. Rosenbauer, Two States of the solar wind at the time of solar activity minimum, II. Radial gradient of plasma parameter in fast and slow streams, to be published in lecture notes in physics, Springer-Verlag, Berlin, 1979.

Schwenn, R., H. Rosenbauer and K-H. Mühlhäuser, singly-ionized helium in the driver gas of an interplanetary shock wave, Geophys. Res. Lett. 7» 201, 1980.

LIST THE ABBREVIATIONS

AG	Contracting Authority
AHK	analog house-keeping data
AT	Contractor
BM	bitrate mode
BMFT	Federal Ministry for research and technology
BPS	Bits per second
BPT	Area for project funds in the DFVLR
BSP	bit shift pulse
BTC	block transfer clock pulse
CEM	channel electron multiplier ("Channeltron")
CMD	Telemetry command
CP	Amendment
DFVLR	German research - and Laboratory of air - and space travel e.V.
DHK	Digital house-keeping data
DM	distribution mode
E1	Experiment 1
E1A	Box containing I1a, I1b, and electronics
E1B	Box containing I2 and electronics
E1C	Box containing I3 and electronics
E1D	Box that contains digital electronics
EDF	experiment data frame
EM	Engineering model 1
F1	flight unit for HELIOS-1
F2	Flight unit for HELIOS 2
FM	format (telemetry format)
GB	large block length
GfW	Society for space research in the DFVLR
GMT	Greenwich mean time
HAN	Prime contractor (MBB)
HDM	high data mode
HP	Hewlett Packard
HTS	HELIOS test set

HV	High-voltage
I1a	3D-Ion instrument with CEMs
I1b	1D-Ion instrument with electrometer
I2	2D-Electron instrument
I3	3D-Ion instrument with CEMs, dynamic mass spectrometer
IABG	Industrial operating company in Ottobrunn
IST	integrated system test
JPL	Jet Propulsion Laboratory
KB	small block length
KSC	Kennedy Space Center, Florida, USA
KV	No shift (KV \equiv NS)
MBB	Messerschmitt-Bölkow-Blohm in Ottobrunn
MV	with shift (MV \equiv WS)
NDM	normal data mode
NS	without shift
NZR	Zero count rate
P	Prototype
PHA	Pulse height analysis
S/C	Spacecraft
UHV	Ultra high vacuum
UT	Universal time
UV	Ultraviolet (UV)
WS	with shift
WTC	Word transfer clock pulse

